SEISMIC STRUCTURAL RESPONSE OF STEAM GENERATORS AND THEIR SUPPORTING STRUCTURES*

Prepared by

T. Y. Yang, M. I. Baig and J. L. Bogdanoff
School of Aeronautics and Astronautics
Purdue University
West Lafayette, Indiana

Submitted to

THE NATIONAL SCIENCE FOUNDATION
April 1978

*Tennessee Valley Authority (TVA) Power Plant Unit #3 (1200 MW), at Paradise, Kentucky and Associated Electric Cooperative Power Plant (600 MW), at New Madrid, Missouri.

50272-101

REPORT DOCUMENTATION PAGE	1. REPORT NO. NSF/RA-780757	2.	3. Recipient's Accession No. PB80 216591

4. Title and Subtitle
Seismic Structural Response of Steam Generators and Their Supporting Structures

5. Report Date
April 1978

6.

7. Author(s)
T. Y. Yang, M. I. Baig, J. L. Bogdanoff

8. Performing Organization Rept. No.

9. Performing Organization Name and Address
Purdue University
School of Aeronautics and Astronautics
West Lafayette, IN 47907

10. Project/Task/Work Unit No.

11. Contract(C) or Grant(G) No.
(C)
(G) ENV7401575

12. Sponsoring Organization Name and Address
Engineering and Applied Science (EAS)
National Science Foundation
1800 G Street, N.W.
Washington, D.C. 20550

13. Type of Report & Period Covered

14.

15. Supplementary Notes

16. Abstract (Limit: 200 words)

Seismic response studies of two steam generators and their supporting structures were conducted using three-dimensional finite element models. Linear structural analyses of the two systems were performed in two phases. The first involved determining frequencies of free vibration and associated mode shapes. The second involved determining model responses of structural member stresses due to the El Centro Earthquake of May 18, 1940. Twelve natural frequencies and associated modal shapes were determined for each structural system. For the 1200 MW steam generator, torsional modes had to be included in the analysis. For the 600 MW steam generator structural system, the first and second natural modes were predominantly side-swaying motions in two orthogonal directions, while the third and higher natural modes contained torsional motion. Response spectrum analyses furnished quantitative information on shear forces, bending moments, and axial forces for each member of the structure. Maximum stresses and ratios of maximum normal stress to yield stress, and maximum shear stress to shearing yield stress, were obtained for each beam member. Vulnerable components of both models were identified.

17. Document Analysis a. Descriptors

Shear modulus
Vibration
Earthquake resistant structures
Seismic waves
Stress analysis
Structural analysis
Eigenvalues
Orthogonal functions

b. Identifiers/Open-Ended Terms

El Centro Earthquake (1940)
Seismic response

Earthquake Hazards Mitigation

c. COSATI Field/Group

18. Availability Statement	19. Security Class (This Report)	21. No. of Pages
NTIS	20. Security Class (This Page)	22. Price

(ANSI Z39.18) See Instructions on Reverse

OPTIONAL FORM 272 (4-77)
(Formerly NTIS-35)
Department of Commerce

TABLE OF CONTENTS

LIST OF TABLES

LIST OF FIGURES

Abstract

The seismic response studies of the steam generators and their supporting structures of a 1200 MW and a 600 MW fossil fuel steam generating plants have been carried out using finite element models. The 1200 MW steam generator has been modeled by 48 lumped masses connected by rigid massless bars and the columns, the beams and the girders of its supporting structure have been modeled by 878 three-dimensional beam finite elements. The bracings, the hanger rods and the horizontal tie bars have been modeled by 412 truss finite elements. The two concrete working floors have been modeled by plane finite elements. Five degrees-of-freedom have been assigned to each nodal point of the model. The 600 MW steam generator has been modeled by 66 lumped masses connected by rigid massless bars and its supporting structure has been modeled by 1607 three-dimensional truss finite elements. Three degrees-of-freedom have beed assinged to each nodal point of the model.

The seismic response analyses of the two systems have been carried out in two parts. The first part involves the determination of fundamental frequencies of free vibration and the associated mode shapes. The second part involves the determination of modal responses of structural member stresses due to El Centro earthquake of May 18, 1940.

Twelve natural frequencies and associated mode shapes have been determined for each structural system. It is observed that for 1200 NW steam generator structural system, the first and the third mode shapes contain predominantly torsional motion. The second and fourth mode shapes contain predominantly side-swaying motions in two orthogonal directions. The modal participation factors of the first three natural modes have been

observed to be much higher than those of the higher modes. This finding indicates that for dynamic analysis of structural systems similar to the 1200 MW steam generator-structural system, the torsional modes must be included in the analysis. This necessitates three dimensional modeling of the system. For the 600 MW steam generator-structural system, the first and second natural modes are predominantly side-swaying motions in the two orthogonal directions. The third and higher natural modes contain torsional motion. The modal participation factors corresponding to first and second modes are much higher than those corresponding to the higher modes.

The response spectrum analyses have been carried out. The spectrum of various response quantities such as the shear forces, the bending moments and the axial forces have been obtained for each member in the structure. The maximum stresses for each member have been obtained by using the root-mean-square value of the modal responses. The ratios of maximum normal stress to the yield stress and maximum shear stress to the shearing yield stress have been obtained for each beam member of both the structures. The ratio of axial stress to the Euler buckling stress has also been obtained for each truss member of both the structures.

It is observed that for the 1200 MW steam generator-structure system, 277 out of 1290 structural members exceed elastic limit while 85 structural members exceed the ultimate stress. The vulnerable components of this structural system are the horizontal tie bars and the columns supporting the airheater. For the 600 MW steam generator-structure system, 157 structural members out of 1607 exceed the elastic limit and 57 exceed the ultimate stress. The vulnerable components of this structural system are a few horizontal tie bars and the columns in the rear of the structure.

INTRODUCTION

Literature on the safety analysis of large fossil fuel steam generator and its supporting structure under earthquake loads is rare. In fact, the dynamic response of any large structure has seldom been studied using a realistic three dimensional model. Because of the complexity involved, various simplified approaches have been made to analyze such systems. For relatively small systems, Hardy Cross moment distribution method or Muto's D-value method has been used extensively. However, for larger systems these methods are discarded and finite element method is used because of its versatility and ease of use on large modern electronic computers. Computations for large fossil fuel steam generator and its supporting structure have been carried out with the help of extremely simplified models. Typical of what is available is referenced in [1-3]. In reference 1, three different kinds of plane models were used to analyze two steam generator systems. The three plane models included a Rahmen structure model, a truss model and a shear type frame model. In reference 2, a 600 MW steam generator and the supporting frame were studied by using a simple plane model. The model consisted of a plane portal frame and a 10-lumped mass steam generator. The portal frame included 22 lumped masses, 22 vertical shear members and three horizontal flexural members. The steam generator was connected to the portal frame by three horizontal ties and two hanger rods. In reference 3, a three dimensional simple model analysis was attempted for a 1000 MW steam generator and its supporting structure. The system was modeled by a simple 3-D rectangular box frame supporting 32-lumped masses. The box frame consisted only four vertical plane frames on the four sides. Thus far, no dynamic analysis has been made for the steam generator and its supporting structure by using a realistic three-dimensional model.

In this report, the dynamic response of two steam generators and the supporting structures under earthquake disturbances are studied with the use of realistic three-dimensional finite element models. The first system is the 1200 MW steam generator and its supporting structure of Tennessee Valley Authority (TVA) Power Plant Unit #3 at Paradise, Kentucky and the second system is the 600 MW steam generator and its supporting structure of Associated Electric Cooperative, Inc. at New Madrid, Missouri. The choice of these two power plants was made based upon their geographical location on the earthquake risk map. The Paradise Power Plant is located in zone I whereas the New Madrid Power Plant is located in zone III (Ref. 5). The Paradise plant is not seismically designed. It represents a conventional design without performing dynamic analysis. Because of the higher probability of occurrence of an earthquake in the region III, the New Madrid Power Plant has been designed seismically based on the Uniform Building Code. The earthquake response analysis of two power plants would, therefore, provide results for two different designs, one with and one without earthquake considerations.

The dynamic behavior of the system is studied in two parts. The first part involves the study of free vibration behavior of the system and the second part involves combining the fundamental vibration modes to study the response of the system when subjected to earthquake ground motion.

The free vibration behavior of the two systems is studied with the use of three dimensional finite element models. The finite element model of the Paradise Plant consists of 48 lumped masses interconnected by rigid weightless bars. The supporting structure is modeled by 3-dimensional beam finite elements for columns, shear beams and girders, 3-dimensional truss elements for bracings, tie rods and hanger rods, isotropic quadrilaterial plate elements for the concrete working decks and orthotropic quadrilateral plate elements for grid beams. The total model results in 1860 degrees-of-freedom. The half-bandwidth of the stiffness matrix for this model is 265. SAPIV Computer Program (Ref. 17) is used. In this program the eigenvalue equations are solved by 'subspace iteration technique'. As the solution time of eigenvalue problem depends mostly on the size of the half bandwidth of the stiffness matrix, a careful numbering of the nodes is necessary. Care must also be taken in preparing the data for the computer program. Ref. 6 describes various sources which may possibly cause error. In this work, every possible check has been made to avoid any error.

Because of the complexity of the system and because no prior computations have been made, a number of subsystems have been considered and analyzed prior to the analysis of the total system. The purpose of doing this has been to develop confidence in the computer program's capability to handle large complex problems and to check the consistency in the results of various subsystems. The various subsystem models have been constructed by adding or neglecting the stiffnesses and masses of certain portions of the total system. The fundamental natural frequencies and normal modes have been computed for these subsystems. The results show that the effect due to adding or neglecting certain portions of the stiffnesses and masses are consistent among the various subsystems. After the computation and evaluation of results for the subsystems have been performed, the total system is considered. Twelve natural frequencies and associated mode shapes have been obtained.

The New Madrid Plant was designed seismically by the Babcock and Wilcox Company at Barberton, Ohio. In order to transfer the lateral loads developed during the earthquake, the supporting structure was heavily braced. In the design and analysis by B&W Company, all the joints in the supporting structure were designed as hinged condition. This system is modeled by 66 lumped masses connected by rigid weightless bars. The support structure is modeled by 3-dimensional truss elements for columns, horizontal beams, tie rods and hanger rods. This model results in 1189 degrees-of-freedom with a half band-width of stiffness matrix equal to 235. Twelve natural frequencies and associated mode shapes are obtained for this model.

The two steam generators of the two plants are analyzed separately. The equations of motion for the steam generators are derived using the mechanics of rigid bodies. The fundamental frequencies and mode shapes of each steam generator obtained by such analytical analysis and those obtained by using finite element models are compared.

The response of the two systems described above to an earthquake ground motion is then studied. The ground acceleration data of one of the most severe earthquakes in the recorded history which took place on May 18, 1940 at El Centro, California, has been used to obtain the spectrum of various response quantities viz. displacement, shear force and bending moment. Using these spectrums, the maximum bending stress and maximum shearing stress are obtained for every beam and column member in the model. Also, the axial stresses in the truss members are obtained. The members which are stressed beyond the elastic limit are pointed out. The truss members that fail due to elastic buckling are also pointed out.

Chapter 1

THE STRUCTURAL SYSTEM

1.1 DESCRIPTION OF THE STRUCTURAL SYSTEMS

1.1.1 SYSTEM NO. 1 - Paradise Plant

The steam generator of system No. 1 is described by a vertical plane view in Fig. 1. It is also described by a rough three dimensional sketch (without the airheater) in Fig. 2. The walls are composed of closely spaced tubes for carrying hot circulating water. The walls are held in place horizontally by steel beams called buckstays. The steam generator is supported at the top by 277 steel rods which are connected to deep plate girders on top of the supporting structure. Such a hanging system allows the steam generator to expand downwards when subjected to operating temperature. The steam generator is also supported horizontally by 11 ties at the corners as shown in Fig. 2. Each tie is made of a pair of bars which connect the buckstay to the supporting column with pinned condition at both ends. In the event of an earthquake or other disturbances, the ties transmit the lateral inertia forces from the steam generator to the supporting structure. The steam generator weights approximately 24,000 kips. The distribution of weight for various components is listed in Table 1.

The airheater as shown in Fig. 1 is connected to the steam generator by an expansion joint which provides little bending or torsional rigidity. The airheater weighs approximately 15% of the steam generator. The supporting columns under the airheater rest on the concrete foundation with no rotational or torsional restraint at the bases. The airheater is stabilized from rocking motion by horizontal tie rods connected to the columns of the main frame.

Table 1

Weigth distribution of the structural components in the steam generator of the Paradise Plant.

No.	Structural Component	Weight (Kips)
1	Furnace Front Wall	1,400
2	Furnace Rear Wall	1,130
3	Furnace Side Walls (2)	820
4	Front Wind Box	1,400
5	Rear Wind Box	1,370
6	Pendant Side Walls (2)	164
7	Furnace Floor	1,400
8	Horizontal Convection Pass Side Walls (2)	330
9	Convection Pass Rear Wall	380
10	Convection Pass Front Wall	295
11	Risers	270
12	Economizer Enclosure	470
13	Pendant Floor	376
14	Secondary Super Heater	2,920
15	Furnace Roof	710
16	Pent-House	650
17	Pendant Reheat	1,154
18	Horizontal Reheater	1,400
19	Primary Super Heater	1,430
20	Economizer	3,400
21	Roof Outlet	250
22	Economizer Stringers	515
23	Supply Tubes	12
24	Secondary Super Heater Outlet	258
25	Primary Outlet	380
26	Secondary Super Heater Inlet	880
27	Economizer Inlet	340
	Total Weight	24,104 (Kips)

The steel framing structure is described in Fig. 3 by a three-dimensional sketch marked with overall dimensions. It is an all steel structure except at the planes at 42 feet and 169 feet above the ground level. At those levels are 5 and 4 concrete slabs, respectively, with 8 inches thickness and light reinforcements. The structure has a total of 1412 major beam and column members and 870 cross bracing members. All the cross bracing members are in the vertical frames. The stiffening of the horizontal frames is accomplished by closely spaced beams parallel to the major girders with rigid end conditions. There are 611 joints among which 66 are at the base. The largest girders are at the top of the frame hanging the steam generator. Such plate girders have flanges of 30 x 4 inch^2 and are 20 feet deep. The heaviest columns are at the lower level built with 14W730 wide flanges with two cover plates of 32 x $4\frac{3}{4}$ inch^2. The total weight of the whole steel framing structure is over 13,000 Kips which is approximately 50% of the combined weight of the steam generator and the air heater.

There are 23 coal silos extended from the levels of 101 to 175 feet. When the silos are filled with coal, the weight could be 6000 tons.

1.1.2 SYSTEM NO. 2 - New Madrid Plant:

The steam generator of system No. 2 is more or less similar to that of system No. 1 except that it weighs approximately 17,000 Kips. The distribution of weight for various components is listed in Table 2. Fig. 4 shows a rough outside view of the steam generator. It is supported at the top by 276 hanger rods which are connected to the deep plate girders at the top of the support structure.

The supporting structure of system No. 2 is different from that of system No. 1 in the sense that it is designed to resist lateral earthquake loads.

This is accomplished by providing various cross bracings in the lateral frame to resist the shear. The joints of this structure are designed for hinged conditions. There are 1607 major members. The top girders consist of deep plates and flanges of various sizes. The largest girder is $13\frac{1}{2}$ feet deep and has flange plates of 30 x 3 inch^2. The largest columns are adjacent to the steam generator. They are made of wide flange beam 14W370 with cover plates of 24 x 4 inch^2. The total weight of the whole steel framing structure is about 11,000 Kips which is approximately 65% of the weight of the steam generator.

Table 2

Weight distribution of the structural components in the steam generator of New Madrid Plant.

No.	Structural Component	Weight (Kips)
1	Steam Drum	886
2	Furnace Floor	996
3	Furnace Front Wall	453
4	Furnace Side Walls (2)	623
5	Furnace Rear Wall	242
6	Furnace Arch	115
7	Furnace Screen	29
8	Pendant Side Walls (2)	220
9	Pendant Super Heater Floor	151
10	Convection Pass Screen	69
11	Convection Pass Front Wall	193
12	Convection Pass Side Walls (2)	341
13	Convection Pass Rear Wall	293
14	Front Cyclones and Risers	1078
15	Rear Cyclones and Risers	1078
16	Middle Downcomer	224
17	Furnace Front Wall Supplies	48
18	Left End Downcomer	177
19	Furnace Supplies	138
20	Right End Downcomer	177
21	Front Cyclone Downcomer	357
22	Rear Cyclone Downcomer	402
23	Cyclone Risers	220
24	Roof Tube Supplied	69
25	Roof Tubes	269
26	Furnace Front Wall Risers	70
27	Furnace Side Wall Risers	89
28	Rear Screen Risers	130
29	Economizer	1240
30	Economizer Discharge Pipe	74
31	Primary Superheater	1328
32	Attemperator Pipe	104
33	Secondary Super Heater Inlet	571
34	Secondary Super Heater Outlet	575
35	Horizontal Reheat Superheat Outlet	1247
36	Pendant Reheat Superheat Outlet	892
37	Front Windbox	427
38	Rear Windbox	427
39	Side Wall Windbox (2)	281
40	Front Gas Recirculating Plenum	100
41	Rear Gas Recirculating Plenum	100
42	Economizer Encloser	129
43	Economizer Hopper	474
44	Penthouse	340
	Total Weight	17,200 Kips

1.2 BASIC ASSUMPTIONS MADE IN THE ANALYSIS

The following assumptions are made regarding the modeling of the two systems.

(1) The beams of the outside columns (far from the steam generator) were designed by using heavy anchor bolts to produce full capacity to resist bending moment. The bases of the inside columns were not designed to resist bending moment. The inside columns are under high initial compressive forces resulting from the dead weights of the steam generator and the steel frames. When the system is subjected to the overturning moment due to earthquake distrubances, the inside columns are subjected to lesser axial forces than the outside ones. Thus the initial compressions in the inside columns are likely to be higher than the tension produced by the overturning moment. It is felt that for these columns, the base conditions are closer to the fixed case than the hinged case. For this reasoning, all the column bases are assumed to be fixed. It is noted that the concrete footings and the base floor stabs are buried in the excavated limestone rock foundation.

(2) When a frame structure is full of cross bracing members such as the one shown in Ref. 1, the results of frequencies appear to be almost independent of joint conditions, either rigid or fixed. However, for systems No. 1 the frame consists of 1412 beam and column members, 370 cross bracings and 2 concrete floors. Examination of design of connections shows that all joints do generally provide sufficient moment resisting capacaties. All the joints are thus assumed as rigid for system No. 1. This assumption provides a stiffer structure than the hinged assumption. It also results in twice as many degrees of freedom per node.

(3) The steam generator may vibrate in two possible modes, a pendulum type swaying mode and a breathing mode. The later mode is not of primary interest in this study. Thus all the masses in the steam generator model are assumed to be connected by rigid bars.

In accordance with the "Earthquake-Resistant Design Criteria" (1963 Revision), the following assumptions are made regarding the response analyses of the two systems.

(1) Direction of Earthquake Forces: Only the horizontal component of earthquake forces has been considered in the calculation. Vertical components have been neglected. Also, the lateral forces have been assumed to act separately in the main directions (longitudinal and transverse) of the structure, and the case of both acting simultaneously has not been considered.

(2) Action of Earthquake Forces: The earthquake forces are generally considered to act concentratedly at slab locations. The base of the structure may thus be assumed to have uniform acceleration all over.

(3) Inelastic Deformation: The stress calculation of the structure has been based on linear elastic theory.

1.3 THE MODELING

1.3.1 The Modeling of the Steam Generator: Based on the distribution of the weight of the components of the steam generator as listed in Table 1 for system No. 1 and in Table 2 for system No. 2, the steam generators are modeled by lumped masses. Two considerations govern the locations of the lumped masses: (a) The bandwidth of the resulting stiffness matrix is as small as possible; (b) the model appropriately represents the distribution of the mass of the steam generator. System No. 1 is modeled by 48 lumped masses and system No. 2 by 66. Figs. 5 and 6 represent the two models graphically. Tables 3 and 4 list the location and magnitude of each lumped mass for the two systems, respectively.

1.3.2. The modeling of the supporting structure: The detail designs of the supporting structure, especially for system No. 1, involves enormous amounts of engineering drawings. It is difficult to visualize the total structure based on so many separate drawings. It is also difficult to prepare input data for the finite element model based on these drawings. To circumvent such difficulties, a small model of system No. 1 is built with balsa wood on a scale of $\frac{1}{64}$. The overall dimensions of the model is 5 x 3.27 square feet at the base. The height of this model is 3.72. A photograph of the model is shown in Fig. 7. Each member in the model is labeled with its dimensions and weight per unit longitudinal length. The finite element model is made based on the balsa wood model. A few nodes which are connected with less stiff member have been omitted. The stiffness and mass properties of the adjacent members have been modified to account for the effect of these omitted members. By doing so, the total number of resulting equations is 1860 with the half bandwidth of 265.

Table 3

Lumped mass modeling for the steam generator of the Paradise Plant

Mass No.	x-ordinate Measured from line (23)	y-ordinate Measured from line (Gv)	z-ordinate Measured from EL0.0	Mass kips-sec^2/ft
1	106.00'	0.00	422.0	25.031
2	10.34'	0.00	422.0	25.031
3	106.00'	54.00	422.0	25.031
4	10.34'	54.00	422.0	25.031
5	106.00'	0.00	461.5	16.429
6	10.34'	0.00	461.5	16.429
7	106.00'	54.00	461.5	16.429
8	10.34'	54.00	461.5	16.429
9	106.00'	10.45	494.0	3.292
10	10.34'	10.45	494.0	3.292
11	106.00'	43.55	494.0	3.292
12	10.34'	43.55	494.0	3.292
13	106.00'	10.45	512.0	4.161
14	10.34'	10.45	512.0	4.161
15	106.00'	43.55	512.0	4.161
16	10.34'	43.55	512.0	4.161
17	106.00'	10.45	535.0	6.149
18	10.34'	10.45	535.0	6.149
19	106.00'	43.55	535.0	11.640
20	10.34'	43.55	535.0	11.640
21	106.00'	10.45	568.5	3.804
22	10.34'	10.45	568.5	3.804
23	106.00'	43.55	568.5	16.227
24	10.34'	43.55	568.5	16.227
25	106.00'	10.45	582.0	9.916
26	10.34'	10.45	582.0	9.916
27	106.00'	43.55	582.0	36.587
28	10.34'	43.55	582.0	36.587
29	106.00'	79.65	582.0	37.565
30	10.34'	79.65	582.0	37.565
31	106.00'	79.65	553.0	35.025
32	10.34'	79.65	553.0	35.025
33	106.00'	79.65	535.0	12.829
34	10.34'	79.65	535.0	12.829
35	106.00'	79.65	505.0	32.363
36	10.34'	79.65	505.0	32.363
37	106.00'	91.96	481.6	1.441
38	10.34'	91.96	481.6	1.441
39	106.00'	121.67	481.6	1.441
40	10.34'	121.67	481.6	1.441
41	106.00'	121.67	505.0	32.363
42	10.34'	121.67	505.0	32.363
43	106.00'	111.15	535.0	29.941
44	10.34'	111.15	535.0	29.941
45	106.00'	111.15	568.5	1.042
46	10.34'	111.15	568.5	1.042
47	106.00'	111.15	582.0	9.792
48	10.34'	111.15	582.0	9.792

Table 4

Lumped mass modeling for the steam generator of New Madrid Plant

Mass No.	x-ordinate measured from line 5	y-ordinate measured from line H	z-ordinate measured from the base	Mass Kips-sec^2/ft
1	69.380	6.500	40.000	30.3120
2	126.630	6.500	40.000	30.3120
3	69.380	66.500	40.000	25.0840
4	126.630	66.500	40.000	25.0840
5	69.380	6.500	56.000	9.2830
6	98.010	6.500	56.000	18.5660
7	126.630	6.500	56.000	9.2830
8	69.380	66.500	56.000	8.3390
9	98.010	66.500	56.000	16.6780
10	126.630	66.500	56.000	8.3390
11	69.380	20.000	75.500	6.5170
12	126.630	20.000	75.500	6.5170
13	69.380	53.000	75.500	4.5230
14	126.630	53.000	75.500	4.5230
15	69.380	104.000	75.500	2.3410
16	126.630	104.000	75.500	2.3410
17	69.380	20.000	93.500	4.6990
18	126.630	20.000	93.500	4.6990
19	69.380	53.000	93.500	2.8110
20	126.630	53.000	93.500	2.8110
21	69.380	87.400	93.500	2.3410
22	126.630	87.400	93.500	2.3410
23	69.380	104.000	93.500	5.4920
24	126.630	104.000	93.500	5.4920
25	69.380	20.000	108.000	2.5290
26	98.010	20.000	108.000	5.0580
27	126.630	20.000	108.000	2.5290
28	69.380	53.000	108.000	1.5170
29	98.010	53.000	108.000	3.0340
30	126.630	53.000	108.000	1.5170
31	69.380	74.000	108.000	7.3430
32	98.010	74.000	108.000	14.6850
33	126.630	74.000	108.000	7.3430
34	69.380	104.000	108.000	7.4260
35	98.010	104.000	108.000	14.8520
36	126.630	104.000	108.000	7.4260
37	69.380	20.000	128.750	6.4830
38	126.630	20.000	128.750	6.4830
39	69.380	53.000	128.750	5.6670
40	126.630	53.000	128.750	5.6670
41	69.380	74.000	128.750	15.6740
42	126.630	74.000	128.750	15.6740
43	69.380	104.000	128.750	15.8900
44	126.630	104.000	128.750	15.8900
45	69.380	20.000	157.000	1.4050
46	108.000	20.000	157.000	2.8110
47	126.630	20.000	157.000	1.4050

48	69.380	53.000	157.000	21.1680
49	126.630	53.000	157.000	21.1680
50	69.380	74.000	157.000	9.3250
51	126.630	74.000	157.000	9.3250
52	69.380	104.000	157.000	1.2250
53	102.000	104.000	157.000	2.4530
54	126.630	104.000	157.000	1.2250
55	69.380	20.000	175.750	9.8310
56	98.010	20.000	175.750	19.6610
57	126.630	20.000	175.750	9.8310
58	69.380	53.000	175.750	2.0410
59	98.010	53.000	175.750	4.0830
60	126.630	53.000	175.750	2.0410
61	69.380	74.000	175.750	2.4950
62	98.010	74.000	175.750	4.9890
63	126.630	74.000	175.750	2.4950
64	69.380	104.000	175.750	.9470
65	98.010	104.000	175.750	1.8940
66	126.630	104.000	175.750	.9470

With the experience gained in reading the engineering drawings and making the model for the system No. 1, it was not necessary to make a balsa wood model of system No. 2. Rather the finite element model was constructed directly from the engineering drawings. The finite element model resulted in 1189 equations with the half bandwidth of the stiffness matrix equal to 235.

1.3.3 Connection between the steam generator model and the supporting structure model: The steam generator of both systems is supported at the top by hanger rods connected to the deep plate girders. In the finite element model of system No. 1 these rods are modeled by 4 equivalent truss elements with the hinge conditions at the top of the frame. The hanger rods of system No. 2 are also modeled by 4 equivalent truss elements with hinge conditions at the top.

The lateral supports to the steam generator are provided by horizontal tie rods. The tie rods connect the buckstays to the frame columns. System No. 1 has 11 elastic ties. The locations of these ties are shown in Fig. 2. These ties are modeled by three dimensional truss elements with the hinge conditions at the connection points between the ties and the frame, System No. 2 has 19 ties.

The following section describes the kinds of finite elements used to model the two systems.

1.4 FINITE ELEMENTS

The present mathematical models are constructed by the following kinds of finite elements - (1) Three dimensional beam element, (2) Three dimensional truss element, (3) Three dimensional isotropic quadrilateral element and (4) Three dimensional orthotropic quadrilateral element.

1.4.1 The Three Dimensional Beam Finite Element

The three dimensional beam finite element is shown in Fig. 8. The element is described by six section properties, viz., the axial area A, the shear area associated with local $\bar{y}$ axis $A\bar{y}$, the shear area associated with local $\bar{z}$ axis $A\bar{z}$, the torsional inertia associated with local $\bar{x}$ axis $I\bar{x}$, the flexural inertia associated with local $\bar{y}$ axis $I\bar{y}$ and the flexural inertia associated with local $\bar{z}$ axis. The element is assumed to have six degrees of freedom at each nodal point: three displacement $\bar{u}$, $\bar{v}$ and $\bar{w}$ along the local $\bar{x}$, $\bar{y}$ and $\bar{z}$ axes, respectively and three rotations $\theta\bar{x}$, $\theta\bar{y}$ and $\theta\bar{z}$ about the local $\bar{x}$, $\bar{y}$ and $\bar{z}$ axes, respectively. Corresponding to the six nodal degrees of freedom, there are three forces $F\bar{x}$, $F\bar{y}$ and $F\bar{z}$, one twisting moment $M\bar{x}$ and two bending moments $M\bar{y}$ and $M\bar{z}$, respectively.

The element formulation is derived in the form that the 12 nodal forces are related to 12 nodal displacements (in local coordinates) by the following relation.

$$\underset{12\times12}{[\,\bar{k}\,]}\ \underset{12\times1}{\{\,\bar{q}\,\}} - \omega^2 \underset{12\times12}{[\,\bar{m}\,]}\ \underset{12\times1}{\{\,\bar{q}\,\}} = \underset{12\times1}{\{\,\bar{f}\,\}} \tag{1.1}$$

where the bar is needed to associate the formulations to the local $\bar{x}$, $\bar{y}$, and $\bar{z}$ coordinates. Matrix $[\,\bar{k}\,]$ is the so-called stiffness matrix. It may be derived either by stress-strain equilibrium method or by the minimum strain energy method. Matrix $[\,\bar{m}\,]$ is known as the mass matrix. It is desired using the lumped mass approach. The rotatory inertia is neglected. Therefore, the mass matrix is a diagonal matrix with terms corresponding to rotations equal to zero. There are only six non-zero diagonal terms. Each term is equal to half of the total mass of the element i.e., $\rho AL/2$. Where, ρ is the mass density of the element. The vector $\{\bar{f}\}$ contains the generalized excitation forces and the vector $\{\bar{q}\}$ contains the generalized coordinates or degrees of freedom.

1.4.2 The Three Dimensional Truss Element

The three dimensional truss element is a special case of the three dimensional beam finite element described above. Since the truss element cannot carry bending and twisting moments, the number of degrees-of-freedom per node is three. To make the truss element compatible with the beam element, all the six degrees-of-freedom are retained. The rotation terms are taken to be zero. Thus, the local stiffness matrix for the three dimensional truss element is 12x12 in size. The local mass matrix for this element is identical to the one for beam element.

1.4.3 The Quadrilateral Plate Finite Element (Isotropic & Orthotropic)

The isotropic quadrilateral finite element used to model the concrete floor and orthotropic quadrilateral finite element used to model a group of relatively flexible parallel beams, have five degrees-of-freedom at each of the four corner nodal points: three displacement degrees-of-freedom along the three local Cartesian coordinate axes and two slope degrees-of-freedom about the two orthogonal axes in the plane of the plate. For reasons of computational efficiency, the quadrilateral element is composed of four triangular plate elements. The four triangles share a common central nodal point whose coordinate locations are the averages of those of the four corner nodal points. The five degrees-of-freedom of this central nodal point are eliminated at the element level prior to the assemblage. Thus the quadrilateral element effectively has a total of twenty degrees-of-freedom, five per nodal point.

The membrane stiffness of each sub-triangular element is based on the constant strain assumption with linear in-plane displacement function [Ref. 15]. The bending stiffness of each subtriangular element is represented by the HCT plate elements based on the lateral deflection function for each subtriangle which satisfies compatibility of normal slopes along the exterior edge. The orthotropic properties of the material of the plate element is taken into account by properly defining the modulus of elasticity along the local coordinate axes. The local mass matrix is formulated based on the lumped mass assumption. The rotatory inertia is neglected.

1.4.4 Transformation of Coordinates

Before the assembly of each individual element, the equations of motion for each element must be transformed from the local coordinates ($\bar{x}$, $\bar{y}$, $\bar{z}$) to the global coordinates (x, y, z) by using the nine direction cosines defined as follows:

$$\begin{aligned} \lambda_i &= \cos\theta_{xi} \\ \mu_i &= \cos\theta_{yi} \\ \nu_i &= \cos\theta_{zi} \qquad\qquad i = \bar{x}, \bar{y}, \bar{z} \end{aligned} \tag{1.2}$$

The equation of motion with reference to the global coordinates are in the form

$$\underset{12\times12}{[T]^T}\,[\underset{12\times12}{[k]} - \omega^2 \underset{12\times12}{[m]}]\,\underset{12\times12}{[T]}\,\underset{12\times1}{\{q\}} = \underset{12\times1}{\{f\}} \tag{1.3}$$

where the coordinate transformation matrix is defined as

$$[T] = \begin{bmatrix} \Lambda & 0 & 0 \\ 0 & \Lambda & 0 \\ 0 & 0 & \Lambda \end{bmatrix} \tag{1.4}$$

with

$$[\Lambda] = \begin{bmatrix} \lambda_{\bar{x}} & \mu_{\bar{x}} & \nu_{\bar{x}} \\ \lambda_{\bar{y}} & \mu_{\bar{y}} & \nu_{\bar{y}} \\ \lambda_{\bar{z}} & \mu_{\bar{z}} & \nu_{\bar{z}} \end{bmatrix} \tag{1.5}$$

The global element stiffness and mass matrices are formed as follows

$$[k] = [T]^T[\bar{k}][T] \tag{1.6}$$

$$[m] = [T]^T[\bar{m}][T] \tag{1.7}$$

1.4.5 Assembly of Structural Matrices:

The system equations are assembled by superposing the stiffness and mass contributions of the elements to each of the equations of motion. This is accomplished as follows: Let us assume that $\{Q\}$ is the displacement vector of the structural system. For n^{th} element the displacement vector may be written as:

$$\{Q\}^n = \{\delta_{i\underline{j}}\ q_{\underline{j}}\}^n \qquad i = 1, 2, \ldots\ldots, N \tag{1.8}$$

where, N is the total number of degrees-of-freedom and δ_{ij} is Kronecker's delta defined as

$$\left.\begin{aligned} \delta_{ij} &= 0 \\ &= 1 \end{aligned}\right\} \begin{aligned} &\text{whenever } i \neq j \\ &\qquad\qquad i = j \end{aligned} \tag{1.9}$$

also j's are those degrees-of-freedom pertinent to the n^{th} element. A bar under j i.e. $\underline{j}$ means that the indicial notation summation is not carried out.

The element stiffness and mass matrices are also arranges in the above fashion. Thus

$$[k]^n = [k_{ij}{}^n] \tag{1.10}$$

$$[m]^n = [m_{ij}{}^n] \tag{1.11}$$

The system matrices may, thus, be formed as

$$[K] = \sum_{n=1}^{NE} [k]^n = [\sum_{n-1}^{NE} k_{ij}{}^n] \tag{1.12}$$

$$[M] = \sum_{n=1}^{NE} [m]^n = [\sum_{n=1}^{NE} m_{ij}{}^n] \tag{1.13}$$

where NE is the total number of elements.

1.4.6 Treatment of Boundary Conditions:

If a displacement component at a node is zero, the corresponding equation is not retained in the structure equilibrium equations. The corresponding terms in the stiffness and mass matrices are disregarded. For example, if a nodal point is fixed in the space, the corresponding translations and rotations are discarded from the structure displacement vector. For a nodal point having hinged conditions, only the rotational degrees-of-freedom are discarded from the system displacement vector. The stiffness and mass matrices are modified everytime a degree-of-freedom is discarded.

If a non-zero displacement is to be specified for a particular degree-of-freedom, an artificially stiff spring either extensional or rotational is introduced on the diagonal term of the stiffness matrix corresponding to that degree-of-freedom. For example, let us assume that we want to specify a displacement d at the j^{th} degree-of-freedom q_j. i.e., $q_j = d$ then equation

$$Kq_j = Kd \tag{1.14}$$

is added to the structural system equations. If $K >> K_{jj}$ the displacement of the j^{th} degree-of-freedom is obtained equal to d. (Ref. 17)

Table 5 describes the summary of the finite element models of the two systems.

Table 5

Summary of the finite element modeling of the two structural systems

	System No. 1 Paradise Plant	System No. 2 New Madrid Plant
Number of Nodal Points	415	439
Number of degrees-of-freedom per node	5	3
Number of Truss Elements	412	522
Number of Beam Elements	878	1085
Number of Isotropic Plate Elements	38	-
Number of Orthotropic Plate Elements	150	-
Number of Lumped Masses	48	66
Number of Equations	1860	1189
Half Band Width	265	235
Number of Equations per block	93	25
Number of blocks	20	48
Central Processor time on CDC6500, per frequency	4962 sec.	964 sec.
Transfer Units, per frequency	750,000	201,740
Tracks needed, per frequency	438	265
Total estimated cost, per frequency	$ 316.47	$ 61.92

Chapter 2

2.1 Dynamic Analysis of the Structural System

The dynamic analysis of the structural system is performed in the following two sequences.

a. Determination of frequencies of free vibration and mode shapes of the multi-degree of freedom structural system.

b. Determination of modal response and evaluation of structural member stresses due to given earthquake ground acceleration.

2.1 Eigenvalue Analysis

To determine the frequencies and mode shape of the structural system, the following generalized eigenvalue problem must be solved:

$$\underset{N\times N}{[K]}\underset{N\times 1}{\{q\}} = \omega^2 \underset{N\times N}{[M]}\underset{N\times 1}{\{q\}} \tag{2.1}$$

where, N is the total number of degrees-of-freedom. The stiffness matrix [K] is a symmetric band matrix, i.e.,

$$\text{and,}\quad K_{ij} = K_{ji}$$

$$K_{ij} = 0 \qquad \text{for } j > i + b - 1 \tag{2.2}$$

where (2b - 1) is the bandwidth of the matrix. The lumped mass matrix [M] is a diagonal matrix.

2.1.1 Storage of Stiffness and Mass Matrices:

Because of the special properties of stiffness and mass matrices, it is not necessary to store every element of these matrices. As will be described later, special techniques are used for solving the eigenvalue problem. This requires that the two matrices be also stored in a special manner. The stiffness matrix is formed in blocks. The size of the block is determined depending upon the high speed storage available. If Ne represents the number of equations per block, then, the stiffness matrix is stored in the form of sub-matrices of size Nexb. The mass matrix is stored in the form of a column vector which is partitioned in sub-columns of rows Ne. Fig. 9 shows the storage scheme of these matrices (Ref. 17).

2.1.2 Solution Techniques:

The solution of generalized eigenvalue problem given by equation (2.1) can be obtained by different methods. Some of them are listed in Ref. 8-12. The choice of an algorithm for solving the problem mainly depends upon the size of the problem, number of eigenvalues required and amount of high speed storage available on the computer installation. In the present case where the number of degrees-of-freedom is enormous and a relatively small number of eigenvalues are of particular interest, two most popular algorithms suitable for these conditions are described below.

a. Determinant Search Solution:

The fact that the eigenvalues are the roots of the characteristic polynomial

$$p(\omega^2) = \det([K] - \omega^2[M]) \qquad (2.3)$$

is used in this algorithm. The algorithm uses triangular factorization and vector inverse iteration directly on the general problem and solves the required eigen pair in the order of dominance.

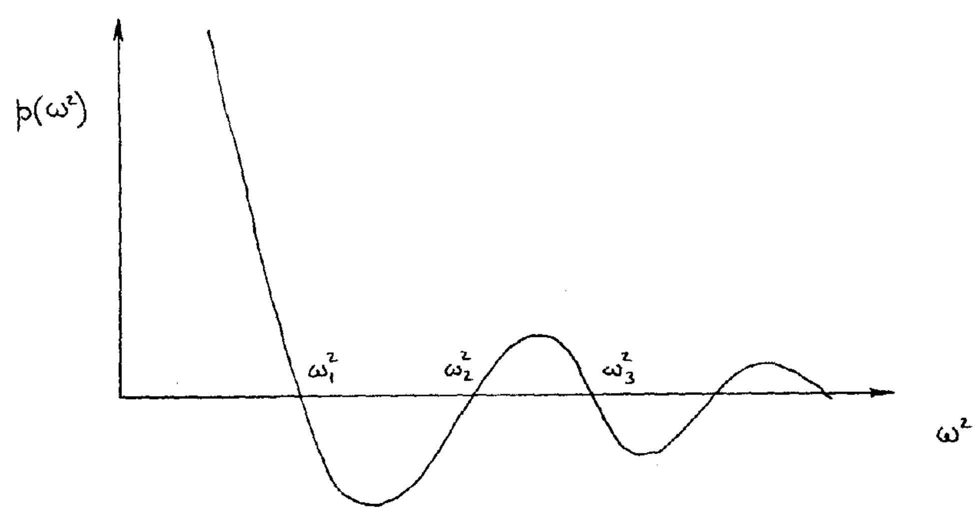

This algorithm is particularly useful and fast but a large dynamic storage is needed to implement it. If the total number of degrees-of-freedom is N and the half-bandwidth of the stiffness matrix b, the storage needed to implement the algorithm is N(b+1) + 10N. A more detailed description of this algorithm may be found in Ref. 10.

b. Subspace Iteration Solution:

In the subspace iteration solution, the aim is to solve the p lowest eigenvalues and associated eigenvector satisfying the equation

$$[K][\Phi] = [M][\Phi][\Omega^2]$$

where the columns in $[\Phi]$ are the p eigenvectors and $[\Omega^2]$ is a diagonal matrix with the corresponding eigenvalues.

The following flow chart describes the subspace iteration algorithm. The algorithm may be described in matrix notations as follows:

$$\underbrace{\underset{n\times n}{[K]}\underset{n\times p}{[\Phi]}}_{n\times p} = \underbrace{\underset{n\times n}{[M]}\underset{n\times p}{[\Phi]}}_{n\times p}\underset{p\times p}{[\Omega^2]} \qquad (2.4)$$

$$\underset{n\times n}{[K]}\underset{n\times p}{[\overline{X}_{k+1}]} = \underset{n\times n}{[M]}\underset{n\times p}{[X_k]} \qquad (2.5)$$

$$\underset{p\times p}{[K_{k+1}]} = \underset{p\times n}{[\overline{X}_{k+1}]^T}\underset{n\times n}{[K]}\underset{n\times p}{[\overline{X}_{k+1}]} \qquad (2.6)$$

$$\underset{p\times p}{[M_{k+1}]} = \underset{p\times n}{[\overline{X}_{k+1}]^T}\underset{n\times n}{[M]}\underset{n\times p}{[\overline{X}_{k+1}]} \qquad (2.7)$$

$$\underset{p\times p}{[K_{k+1}]}\underset{p\times p}{[Q_{k+1}]} = \underset{p\times p}{[M_{k+1}]}\underset{p\times p}{[Q_{k+1}]}\underset{p\times p}{[\Omega^2{}_{k+1}]} \qquad (2.8)$$

SUBSPACE ITERATION FLOW CHART

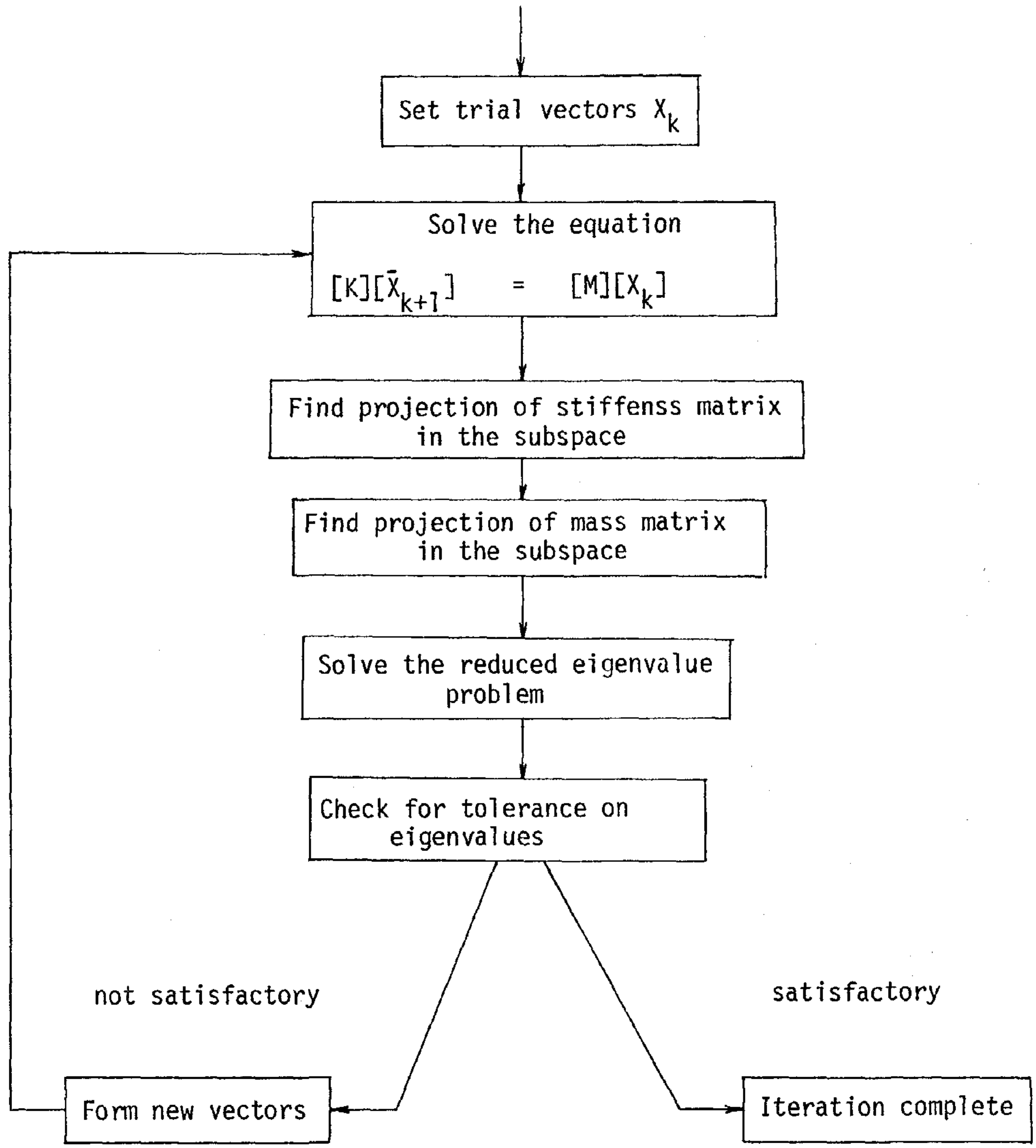

$$\underset{n\times p}{[X_{k+1}]} = \underset{n\times p}{[\bar{X}_{k+1}]}\underset{p\times p}{[Q_{k+1}]} \tag{2.9}$$

$$\text{as } k \to \infty \qquad [X_k] \to [\Phi]$$

Ref. 10 describes the algorithm in more detail. This algorithm solves the problem totally out-of-core. Therefore, there is no limitation on the size of the problem. However, the interaction between the central processor and peripheral devices requires additional time for solution.

2.2 Response Analysis

2.2.1 Formulation of Response Equations:

The dynamic equilibrium equations of a multi-degree-of-freedom system with an arbitrary ground acceleration $\ddot{x}_0(t)$ may be written as

$$[K]\{y(t)\} + [C]\{\dot{y}(t)\} + [M]\{\ddot{y}(t)\} = -[M]\{\ddot{x}_0(t)\} \tag{2.10}$$

where [K], [C] and [M] are the stiffness, damping and mass matrices, respectively. $\{y(t)\}$ is a column-vector of instantaneous relative displacements and $\{\ddot{x}_0(t)\}$ is a column-vector of instantaneous ground accelerations.

If the ground acceleration vector $\{\ddot{x}_0(t)\}$ is considered as a delta-function defined by

$$\{\ddot{x}_0(t)\} = \{v\}\delta(t-\tau)$$

where $\{v\}$ is a vector of constant value, the solution of eqn. (2.10) for undamped case may be obtained as

$$\{y(t)\} = \sum_n a_n\{u_n\}\sin \omega_n(t-t_n) \qquad \begin{matrix} t > \tau \\ t_n = \tau+ \end{matrix} \tag{2.11}$$

where a_n is a constant; ω_n is the nth natural circular frequency; and $\{u_n\}$ is the corresponding mode shape. The value of a_n is obtained using the derivation of Ref. 18 as

$$a_n = -\frac{\{u_n\}^T[M]\{v\}}{\omega_n\{u_n\}^T[M]\{u_n\}} \tag{2.12}$$

the eqn. (2.11) then becomes:

$$\{y(t)\} = -\sum_n \frac{1}{\omega_n} \frac{\{u_n\}\{u_n\}^T[M]}{\{u_n\}^T[M]\{u_n\}}\{v\} \sin \omega_n(t-\tau) \tag{2.13}$$

In order to consider an arbitrary ground acceleration $\{\ddot{x}_0(t)\}$ we take $\{\ddot{x}_0(\tau)d\tau\}$ for $\{v\}$ and integrate with respect to time. This is permissible because of linearity of the problem. The eqn. (2.13) will, then, take the form

$$\{y(t)\} = - \sum_n \frac{1}{\omega_n} \frac{\{u_n\}\{u_n\}^T[M]}{\{u_n\}^T[M]\{u_n\}} \int_0^t \{\ddot{x}_o(\tau)\}\sin[\omega_n(t-\tau)]d\tau \tag{2.14}$$

If the damping is taken into account, eqn. (2.13) takes the form: (Ref. 14)

$$\{y(t)\} = - \sum_n \frac{1}{\omega_n} \frac{\{u_n\}\{u_n\}^T[M]}{\{u_n\}^T[M]\{u_n\}} \int_0^t \{\ddot{x}_o(\tau)\}\exp[-\zeta_n\omega_n(t-\tau)]\sin[\omega_n(t-\tau)]d\tau \tag{2.15}$$

where, ζ_n is the ratio of damping coefficient to critical damping coefficient in the nth vibration mode. Eqn. (2.15) may be written as:

$$\{y(t)\} = - \sum_n Y_n(\omega_n)\ R_n(\omega_n\ ,\ \zeta_n,\ t) \tag{2.16}$$

where,

$$Y_n(\omega_n) = \frac{\{u_n\}\{u_n\}^T[M]}{\{u_n\}^T[M]\{u_n\}} \tag{2.17}$$

and

$$R_n(\omega_n,\ \zeta_n,\ t) = \frac{1}{\omega_n} \int_0^t \{\ddot{x}_o(\tau)\}\exp[-\zeta_n\omega_n(t-\tau)]\sin[\omega_n(t-\tau)]d\tau \tag{2.18}$$

It may be observed that $Y_n(\omega_n)$ is totally a structure property and $R_n(\omega_n,\ \zeta_n,\ t)$ is a function of earthquake ground acceleration. For both design purpose and safety analysis, our interest will be centered to the maximum value of $R_n(\omega_n,\ \zeta_n,\ t)$. It is, therefore, conventional to plot this maximum value versus the period of vibration $(\frac{2\pi}{\omega_n})$ for different values of ζ_n. This plot is referred to as Response Spectra. Response spectra for most major earthquakes have been analyzed by Housner et al. (Ref. 13).

It is convenient to rearrange eqn. (2.13) so as to get maximum advantage in computation. Let us assume that the ground motion $\{x_o(t)\}$ may be expressed in the following form.

$$\{x_o(t)\} = \sum_k \{i_k\}\ x_k(t) \tag{2.19}$$

where $\{i_k\}$ is a column vector whose i-th term represents the static displacement induced by a unit displacement in the k-th degree-of-freedom of the base and $x_k(t)$ is the displacement of the base in its k-th degree of freedom at time t. Suppose that the base has a displacement only in x direction, then $\{i_k\}$ is a column vector of size (Nx1), N being the total number of degrees-of-freedom, whose element corresponding to x displacement are unity and all other elements are zero. From eqn. (2.19)

$$\{\ddot{x}_0(t)\} = \sum_k \{i_k\} \ddot{x}_k(t) \tag{2.20}$$

eqn. (6) takes the form,

$$\{y(t)\} = - \sum_n\sum_k \frac{\{u_n\}\{u_n\}^T[M]\{i_k\}}{\{u_n\}^T[M]\{u_n\}} \frac{1}{\omega_n} \int_0^t \ddot{x}_k(\tau) \exp[-\zeta_n\omega_n(t-\tau)]\sin[\omega_n(t-\tau)]d\tau \tag{2.21}$$

$$= - \sum_n\sum_k \{u_n\} p_{nk} R_k(t, \omega_n) \tag{2.22}$$

where, $$p_{nk} = \frac{\{u_n\}^T[M]\{i_k\}}{\{u_n\}^T[M]\{u_n\}} \tag{2.23}$$

and $$R_k(t,\omega_n) = \frac{1}{\omega_n} \int_0^t \ddot{x}_k(\tau)\exp[-\zeta_n\omega_n(t-\tau)]\sin[\omega_n(t-\tau)]d\tau \tag{2.24}$$

p_{nk} is known as k-th participation factor of the n-th natural mode. $R_k(r, \omega_n)$ is known as the excitation coefficient for displacement.

2.2.2 Solution for Maximum Response:

One straightforward way to obtain the maximum value of displacements is to solve eqn. (2.10) for various times. This method is known as Time History Analysis. However, for a system with a large number of degrees-of-freedom this method, although exact, is very uneconomical. Various approximate methods have been employed to obtain the maximum response of the system. Two of these methods will be described here.

An inspection of eqn. (2.22) reveals that the response of the n-th vibration mode, depends directly upon the magnitude of the excitation coefficient $R_k(t, \omega_n)$. This coefficient has the dimension of displacement, its maximum value is called the Spectral Displacement.

$$s_{d_n} = [R(t,\omega_n,\zeta_n)]_{max}$$

$$= [\frac{1}{\omega_n} \int_0^t \ddot{x}_k(\tau) \exp[-\zeta_n\omega_n(t-\tau)] \sin[\omega_n(t-\tau)]d\tau]_{max} \qquad (2.25)$$

For a given earthquake motion, the spectral displacement s_{d_n} depends upon the natural frequency ω_n and the damping ratio ζ_n. A family of curves may be plotted for various values of ζ_n which may be used for evaluation of maximum response in a particular mode.

The modal response of the structure may be obtained using eqn. (2.22) as follows:

$$\{Y_n(\omega_n)\} = \sum_k \{u_n\} p_{nk} s_{d_n}(\omega_n) \qquad (2.26)$$

The absolute maximum displacement consists of the contributions from various modal responses. However, the maximum value of $s_{d_n}(\omega_n)$ for different natural frequencies does not occur at the same instant. Therefore, an algebraic sum of various modal responses would not give a satisfactory result. The following methods are known to give good approximation to the exact result.

Root-Mean-Square Method:

Goodman *et al*. (Ref. 19) have shown from probability considerations that the most probable value of any earthquake response quantity is given by the square root of the sum of the squares of various maximum modal responses. The modal response of the structure displacement can be obtained using eqn. (2.26). The root-mean-square (R.M.S.) value of the displacement may, thus, be obtained as:

$$\{y\}_{max} = \sqrt{\sum_n (\{Y_n(\omega_n)\})^2} \qquad (2.27)$$

The modal response of the structure nodal forces (and moments) may be obtained by substituting the modal response of structure displacements (and rotations) in the equation

$$\{F_n(\omega_n)\} = [K]\{Y_n(\omega_n)\} \qquad (2.28)$$

where $\{F_n(\omega_n)\}$ is a column vector of modal response of the structure nodal forces (and moments), $\{Y_n(\omega_n)\}$ is a column vector of modal response of structure displacements (and moments) and [K] is the stiffness matrix of the entire structure system. The modal response of the element (beam, truss, or plate) end forces (and moments) may, likewise, be obtained using the equation

$$\{f_n(\omega_n)\} = [k]\{y_n(\omega_n)\} \qquad (2.29)$$

where $\{f_n(\omega_n)\}$ and $\{y_n(\omega_n)\}$ are the modal response of element end forces and displacements, respectively.

The most probable value of the element end forces may, then, be obtained by using root-mean-square method. Thus, the maximum end forces of the element may be obtained using the equation:

$$\{f\}_{max} = \sqrt{\sum_n (\{f_n(\omega_n)\})^2} \qquad (2.30)$$

Spectrum Superposition Method:

The direct superposition of earthquake response quantities will always result in a higher value of maximum response. This is due to the fact that the spectral displacement defined by eqn. (2.25) attains maximum values at different instants for various modes. It may, therefore, be possible to obtain the maximum value of response quantities by superposing the modal responses in varying proportions. The lower modes, in general, contribute greater in the total response. Whereas the higher modes provide a correction to the lower mode effect. The maximum response of the structure displacement and element end forces may, thus, be obtained from the following equations:

$$\{y\}_{max} = \sum_{m=1}^{M} \gamma_m \{Y_m(\omega_m)\} \tag{2.31}$$

$$\{f\}_{max} = \sum_{m=1}^{m} \lambda_m \{f_m(\omega_m)\} \tag{2.32}$$

where γ_m and λ_m represent the proportion of m-th mode response of structure displacements and element forces respectively, contributing to the maximum response. M is the total number of modes which contribute to the maximum response.

For simple structure systems the values of γ_m and λ_m have been obtained by Clough (Ref. 14). However for a large three-dimensional system these constants are not known. Therefore, spectrum superposition analysis will not be performed for the present problem.

Chapter 3

ANALYTIC ANALYSIS OF STEAM GENERATORS CONSIDERED AS RIGID BODIES (Ref. 20)

Although the steam generator is not a rigid body, its stiffness may have little or no effect on the gross dynamic behavior of the total system of both the steam generator and the supporting structure. This assumption is especially true in the present case where the horizontal ties that connect the steam generator to the supporting structure are considerably less stiff than the steam generator itself. Based on this reasoning, the lumped masses in the present model are assumed as connect by rigid bars.

The dynamic behavior of the steam generator itself can be obtained using mechanics of rigid body. In this chapter we derive the equations of motion of the steam generator by considering it to be a rigid body. The results of finite element analysis and those obtained by analytic analysis are compared.

Fig. 10 illustrates the outside view of the steam generator. The top of the penthouse is slanted as shown in the figure. C is the center of gravity of the steam generator. Oxyz is the body axes system. OXYZ is the frameof reference fixed in space. Axis Z passes through the centroid. PA is the i^{th} hanger rod. A is the point where the rod is welded to the penthouse. C_j is the distance of point A from the xy plane. Z axis meets the penthouse at point B. Distance OB is defined as ℓ_o and distance CB as C_o.

To derive the equation of motion of the steam generator, the first step is to find the direction cosines of the unit vectors along the rotated body axes Cx'y'z'. If the steam generator is assumed to be rotated by an amount θ along x axis, ϕ along y axis and ψ along z axis, the direction cosines of the required vectors are evaluated by following coordinate transformation.

First, we rotate the frame by an amount θ. The unit vectors in this coordinate system are i_{x_1}, i_{y_1}, i_{z_1} which are connected to the original unit vectors by the following relations.

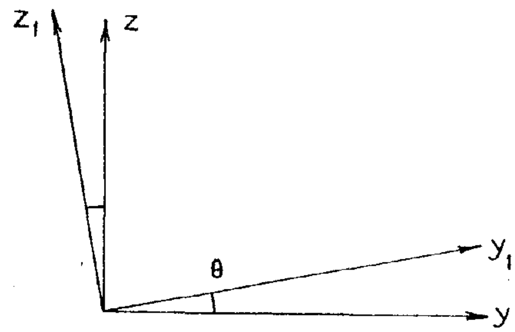

$$\left.\begin{aligned}\vec{i}_{x_1} &= \vec{i}_x \\ \vec{i}_{y_1} &= \vec{i}_y \cos\theta + \vec{i}_z \sin\theta \\ \vec{i}_{z_1} &= -\vec{i}_y \sin\theta + \vec{i}_z \cos\theta\end{aligned}\right\} \quad (3.1)$$

Next we rotate the coordinate frame by an amount Φ about the y_1 axis.

$$\left.\begin{aligned}\vec{i}_{x_{1'}} &= \vec{i}_{x_1} \cos\phi - \vec{i}_{z_1} \sin\phi \\ \vec{i}_{y_{1'}} &= \vec{i}_{y_1} \\ \vec{i}_{z_{1'}} &= \vec{i}_{x_1} \sin\phi + \vec{i}_{z_1} \cos\phi\end{aligned}\right\} \quad (3.2)$$

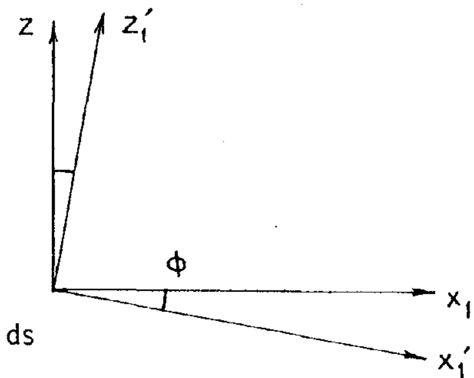

Substitution of eqns. (3.1) into eqns. (3.2) yields

$$\left.\begin{aligned}\vec{i}_{x_{1'}} &= \vec{i}_x \cos\phi + \vec{i}_y \sin\theta \sin\phi - \vec{i}_z \cos\theta \sin\phi \\ \vec{i}_{y_{1'}} &= \qquad\qquad \vec{i}_y \cos\theta \qquad + \vec{i}_z \sin\theta \\ \vec{i}_{z_{1'}} &= \vec{i}_x \sin\phi - \vec{i}_y \sin\theta \cos\phi + \vec{i}_z \cos\theta \cos\phi\end{aligned}\right\} \quad (3.3)$$

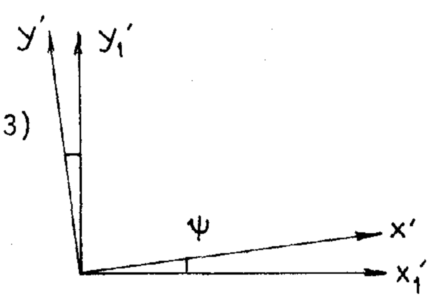

Finally, we rotate the previous coordinate frame by an amount ψ about z_1' axis. We thus obtain the new coordinate system x', y', z'. The unit vectors in this reference system are as follows:

$$\left.\begin{aligned}
\vec{i}_{x'} &= \vec{i}_{x_1'} \cos\psi + \vec{i}_{y_1'} \sin\psi \\
\vec{i}_{y'} &= -\vec{i}_{x_1'} \sin\psi + \vec{i}_{y_1'} \cos\psi \\
\vec{i}_{z'} &= i_{z_1'}
\end{aligned}\right\} \quad (3.4)$$

Substitution of eqns. (3.3) into (3.4) yields:

$$\left.\begin{aligned}
\vec{i}_{x'} &= \vec{i}_x(\cos\phi\cos\psi) + \vec{i}_y(\sin\theta\sin\phi\cos\psi + \cos\theta\sin\psi) + \vec{i}_z(\sin\theta\sin\psi \\
&\qquad - \cos\theta\sin\phi\cos\psi) \\
\vec{i}_{y'} &= \vec{i}_x(-\cos\phi\sin\psi) + \vec{i}_y(\cos\theta\cos\psi - \sin\theta\sin\phi\sin\psi) + \vec{i}_z(\sin\theta\cos\psi \\
&\qquad + \cos\theta\sin\phi\sin\psi)
\end{aligned}\right\} \quad (3.5)$$

$$\vec{i}_{z'} = \vec{i}_x(\sin\phi) - \vec{i}_y(\sin\theta\cos\phi) + \vec{i}_z(\cos\theta\cos\phi)$$

where θ, ϕ and ψ are small quantities. Therefore, eqns. (3.5) may be simplified to the accuracy of second order terms as follows:

$$\left.\begin{aligned}
\vec{i}_{x'} &= \vec{i}_x\left(1 - \frac{\phi^2+\psi^2}{2}\right) + \vec{i}_y(\theta\phi+\psi) + \vec{i}_z(\theta\psi-\phi) \\
\vec{i}_{y'} &= \vec{i}_x(-\psi) + \vec{i}_y\left(1 - \frac{\theta^2+\psi^2}{2}\right) + \vec{i}_z(\theta+\phi\psi) \\
\vec{i}_{z'} &= \vec{i}_x(\phi) + \vec{i}_y(-\theta) + \vec{i}_z\left(1 - \frac{\theta^2+\phi^2}{2}\right)
\end{aligned}\right\} \quad (3.6)$$

The above eqns. may also be written as:

$$\left.\begin{aligned}
\vec{i}_{x'} &= \vec{i}_x\, \ell_{11} + \vec{i}_y\, \ell_{12} + \vec{i}_z\, \ell_{13} \\
\vec{i}_{y'} &= \vec{i}_x\, \ell_{21} + \vec{i}_y\, \ell_{22} + \vec{i}_z\, \ell_{23} \\
\vec{i}_{z'} &= \vec{i}_x\, \ell_{31} + \vec{i}_y\, \ell_{32} + \vec{i}_z\, \ell_{33}
\end{aligned}\right\} \quad (3.7)$$

where the direction cosines ℓ_{ij} are defined as follows:

$$\left.\begin{aligned}
\ell_{11} &= 1 - \frac{\phi^2+\psi^2}{2} \\
\ell_{12} &= \theta\phi + \psi \\
\ell_{13} &= \theta\psi - \phi \\
\ell_{21} &= -\psi \\
\ell_{22} &= 1 - \frac{\theta^2+\psi^2}{2} \\
\ell_{23} &= \theta + \phi\psi \\
\ell_{31} &= \phi \\
\ell_{32} &= -\theta \\
\ell_{33} &= 1 - \frac{\theta^2+\phi^2}{2}
\end{aligned}\right\} \qquad (3.8)$$

3.1 Potential Energy of the Steam Generator

The potential energy of the system may be evaluated with the help of principle of virtual work. We will first evaluate the virtual work done by a generic hanger rod and then sum the work done by all the rods. When the center of gravity of the boiler translates by the amounts u, v, and w along X, Y and Z axes, respectively, with respect to the fixed axes system OXYZ, the connection point of j-th rod A moves to A'. Let us represent the j-th hanger rod by a vector $\vec{R}_j$, the displaced shape of this rod is represented by a vector $\vec{R}_j'$.

To obtain the displaced vector $\vec{R}_j'$ we use the position vectors of points A and A' and apply vector algebra as follows:

$$\left.\begin{aligned} \vec{R}_j &= \vec{P}A = \vec{P}O + \vec{O}C + \vec{C}A \\ &= -(x_j\vec{i}_x+y_j\vec{i}_y+\rho_j\vec{i}_z)+(\ell_o+C_o)\vec{i}_z+(x_j\vec{i}_x+y_j\vec{i}_y-c_j\vec{i}_z) \\ &= (\ell_o+C_o-\rho_j-C_j)\vec{i}_z \end{aligned}\right\} \quad (3.9)$$

$$\left.\begin{aligned} \vec{R}_j' &= \vec{P}A' = \vec{P}O + \vec{O}C + \vec{C}C' + \vec{C}'A' \\ &= -(x_j\vec{i}_x+y_j\vec{i}_y+\rho_j\vec{i}_z)+(\ell_o+C_o)\vec{i}_z+(u\vec{i}_x+v\vec{i}_y+w\vec{i}_z) \\ &\quad +(x_j\vec{i}_{x'}+y_j\vec{i}_{y'}-C_j\vec{i}_{z'}) \end{aligned}\right\} \quad (3.10)$$

Substitution of eqns (3.7) into eqns. (3.10) yields:

$$\left.\begin{aligned} \vec{R}_j' = \vec{i}_x\{u+x_j(\ell_{11}-1)+y_j(\ell_{21})-C_j(\ell_{31})\}+\vec{i}_y\{v+x_j(\ell_{12})+y_j(\ell_{22}-1) \\ -C_j(\ell_{32})\}+\vec{i}_z\{w-\rho_j+\ell_o+x_j+C_o(\ell_{13})+y_j(\ell_{23})+(-C_j\ell_{33})\} \end{aligned}\right\} \quad (3.11)$$

Substitution of eqns. (3.8) into eqn. (3.11) yields:

$$\left.\begin{aligned}\vec{R}_j' = \vec{i}_x\{u - \frac{\phi^2+\psi^2}{2} x_j - \psi y_j - \phi C_j\} + \vec{i}_y\{v + (\theta\phi+\psi)x_j - \frac{\theta^2+\psi^2}{2} y_j \\ + \theta C_j\} + \vec{i}_z\{w - \rho_j + \ell_o + C_o - C_j + (\theta\psi - \phi)x_j + (\theta+\phi\psi)y_j + \frac{\theta^2+\phi^2}{2} C_j\}\end{aligned}\right\} \quad (3.12)$$

but

$$\ell_o + C_o = \rho_j + \ell_j + C_j \qquad (3.13)$$

$$-\rho_j + \ell_o + C_o - C_j = \ell_j \qquad (3.14)$$

Substitution of eqn. (3.14) into eqn. (3.12) gives:

$$\begin{aligned}\vec{R}_j' = \vec{i}_x\{u - \frac{\phi^2+\psi^2}{2} x_j - \psi y_j - \phi C_j\} + \vec{i}_y\{v + (\theta\phi+\psi)x_j - \frac{\theta^2+\psi^2}{2} y_j + \theta C_j\} \\ + \vec{i}_z\{w + \ell_j + (\theta\psi - \phi)x_j + (\theta+\phi\psi)y_j + \frac{\theta^2+\phi^2}{2} C_j\}\end{aligned} \qquad (3.15)$$

Let e_j be the extension of the j-th rod due to the motion, then,

$$\ell_j + e_j = |\vec{R}_j'| \qquad (3.16)$$

$$(\ell_j + e_j)^2 = \vec{R}_j' \cdot \vec{R}_j' \qquad (3.17)$$

To the first order of approximation, eqn. (3.17) may be written as

$$\ell_j^2 + 2\ell_j e_j = \ell_j^2 + 2\ell_j w - 2\ell_j x_j \phi + 2\ell_j y_j \theta \qquad (3.18)$$

or $$e_j = w - x_j\phi + y_j\theta \qquad (3.19)$$

If the j-th rod carries a load t_j and the spring constant of this rod is k_j, then, the equilibrium equations are

$$\sum t_j = mg \quad , \quad \sum t_j x_j = 0 \quad \text{and} \quad \sum t_j y_j = 0 \qquad (3.20)$$

In the displaced position the load carried by j-th rod has the magnitude equal to $(t_j + k_j e_j)$ and the direction of this force is opposite to that of $\vec{R}_j'$, i.e.,

$$\vec{F}_j = -(t_j + k_j e_j)\,\frac{\vec{R}_j'}{\ell_j+e_j} \tag{3.21}$$

The virtual displacement of the j-th rod may be obtained by using eqn. (3.15) as:

$$\begin{aligned}\delta\vec{R}_j' = {} & \vec{i}_x\{\delta u-\phi\delta\phi x_j-\psi\delta\psi x_j-\delta\psi y_j-\delta\phi C_j\} \\ & +\vec{i}_y\{\delta v+\theta\delta\phi x_j+\phi\delta\theta x_j+\delta\psi x_j-\theta\delta\theta y_j-\psi\delta\psi y_j+\delta\theta C_j\} \\ & +\vec{i}_z\{\delta w+\theta\delta\psi x_j+\psi\delta\theta x_j-\delta\phi x_j+\delta\theta y_j+\phi\delta\psi y_j+\psi\delta\phi y_j \\ & \quad +\theta\delta\theta C_j+\phi\delta\phi C_j\}\end{aligned} \tag{3.22}$$

The virtual work δw_j of the force F_j acting on the body due to the j-th rod in the virtual displacement $\delta\vec{R}_j$ is:

$$\delta w_j = -(t_j + k_j e_j)\,\frac{\vec{R}_j'}{\ell_j+e_j} \cdot \vec{R}_j' \tag{3.23}$$

To the first order of approximation we may write

$$\frac{\vec{R}_j'}{\ell_j+e_j} = \frac{u-C_j\phi-y_j\psi}{\ell_j}\, i_x + \frac{v+C_j\theta+x_j\psi}{\ell_j}\,\vec{i}_y + \vec{i}_z \tag{3.24}$$

Eqn. (3.23) may thus be written as:

$$\begin{aligned}\delta w_j = {} & -\{(t_j+k_j w-k_j x_j\phi+k_j y_j\theta)[(\delta u-\phi\delta\phi x_j-\psi\delta\psi x_j-\delta\psi y_j-\delta\phi C_j) \\ & \left(\frac{u-C_j\phi-y_j\psi}{\ell_j}\right)+(\delta v+\theta\delta\phi x_j+\phi\delta\theta x_j+\delta\psi x_j-\theta\delta\theta y_j-\psi\delta\psi y_j+\delta\theta C_j) \\ & \left(\frac{v+C_j\theta+x_j\psi}{\ell_j}\right)+(\delta w+\theta\delta\psi x_j+\psi\delta\theta x_j-\delta\phi x_j+\delta\theta y_j+\phi\delta\psi y_j+\psi\delta\phi y_j \\ & \quad +\theta\delta\theta C_j+\phi\delta\phi C_j)]\}\end{aligned} \tag{3.25}$$

To the first order of approximation, the above eqn. may be written as:

$$\delta w_j = -\left[\frac{t_j}{\ell_j}u - \frac{t_jC_j}{\ell_j}\phi - \frac{t_jy_j}{\ell_j}\psi\right]\delta u + \left[\frac{t_j}{\ell_j}v + \frac{t_jC_j}{\ell_j}\theta + \frac{t_jx_j}{\ell_j}\psi\right]\delta v$$

$$+ [k_jw - k_jx_j\phi + k_jy_j\theta]\delta w$$

$$+ \left[\frac{t_jC_j}{\ell_j}v + k_jy_jw + (t_jC_j + \frac{t_jC_j^2}{\ell_j} + k_jy_j^2)\theta - k_jx_jy_j\phi + (t_jx_j + \frac{t_jC_jx_j}{\ell_j})\psi\right]\delta\theta$$

$$+ \left[-\frac{t_jC_j}{\ell_j}u - k_jx_jw - k_jx_jy_j\theta + (t_jC_j + \frac{t_jC_j^2}{\ell_j} + k_jx_j^2)\phi + (t_jy_j + \frac{t_jC_jy_j}{\ell_j})\psi\right]\delta\phi$$

$$+ \left[-\frac{t_jy_j}{\ell_j}u + \frac{t_jx_j}{\ell_j}v + (t_jx_j + \frac{t_jC_jx_j}{\ell_j})\theta + (t_jy_j + \frac{t_jC_jy_j}{\ell_j})\phi + (\frac{t_jx_j}{\ell_j} + \frac{t_jy_j}{\ell_j})\psi\right]d\psi\} \qquad (3.26)$$

The total virtual work w_t of the forces acting on the body in the virtual displacement is

$$\delta w_t = mg\ \delta w + \sum \delta w_j \qquad (3.27)$$

Using eqns. (3.20) and (3.26) may be written as:

$$\delta w_t = c_{11}u\delta u + c_{15}\phi\delta u + c_{16}\psi\delta u + c_{22}v\delta v + c_{24}\theta\delta v + c_{26}\psi\delta v$$
$$+ c_{33}w\delta w + c_{34}\theta\delta w + c_{35}\phi\delta w + c_{42}v\delta\theta + c_{43}w\delta\theta + c_{44}\theta\delta\theta$$
$$+ c_{45}\phi\delta\theta + c_{46}\psi\delta\theta + c_{51}u\delta\phi + c_{53}w\delta\phi + c_{54}\theta\delta\phi + c_{55}\phi\delta\phi$$
$$+ c_{56}\psi\delta\phi + c_{61}u\delta\psi + c_{62}v\delta\psi + c_{64}\theta\delta\psi + c_{65}\phi\delta\psi + c_{66}\psi\delta\psi \qquad (3.28)$$

where

$$c_{11} = c_{22} = \Sigma \frac{t_j}{\ell_j}$$

$$c_{15} = -c_{24} = -\Sigma \frac{t_j c_j}{\ell_j} = c_{51}$$

$$c_{16} = -\Sigma \frac{t_j y_j}{\ell_j}$$

$$c_{26} = \Sigma \frac{t_j x_j}{\ell_j}$$

$$c_{33} = \Sigma k_j \quad , \quad c_{34} = \Sigma k_j y_j \quad , \quad c_{35} = -\Sigma k_j x_j \tag{3.29}$$

$$c_{44} = \Sigma(t_j c_j + \frac{t_j c_j^2}{\ell_j} + k_j y_j^2) \qquad c_{45} = -\Sigma k_j x_j y_j$$

$$c_{46} = \Sigma \frac{t_j x_j c_j}{\ell_j} \qquad c_{55} = \Sigma(t_j c_j + \frac{t_j c_j^2}{\ell_j} + k_j x_j^2)$$

$$c_{56} = \Sigma \frac{t_j y_j c_j}{\ell_j} \qquad c_{66} = \Sigma(\frac{t_j x_j^2}{\ell_j} + \frac{t_j y_j^2}{\ell_j})$$

The potential energy of the system, may thus be defined as:

$$V = \frac{1}{2}(c_{11}u^2 + 2c_{15}u\phi + 2c_{16}u\psi + c_{22}v^2 + 2c_{24}v\theta + 2c_{26}v\psi + c_{33}w^2 + 2c_{34}w\theta + 2c_{35}w\phi + c_{44}\theta^2 + 2c_{45}\theta\phi + 2c_{46}\theta\psi + c_{55}\phi^2 + 2c_{56}\phi\psi + c_{66}\psi^2) \tag{3.30}$$

3.2 Kinetic Energy of the steam generator:

Let m_j be a generic mass particle of the steam generator and x_j, y_j, z_j be its coordinates with respect to the body axes c_{xyz}. If the principal moments and products of inertia of the steam generator are defined as:

$$A = \Sigma m_j(y_j^2 + z_j^2)$$

$$B = \Sigma m_j(z_j^2 + x_j^2)$$

$$C = \Sigma m_j(x_j^2 + y_j^2)$$

$$F = \Sigma\, m_j y_j z_j$$

$$G = \Sigma\, m_j z_j x_j$$

$$H = \Sigma\, m_j x_j y_j \tag{3.31}$$

the kinetic energy of the system is obtained as:

$$T = \frac{1}{2}\,[a_{11}\dot{u}^2 + a_{22}\dot{v}^2 + a_{33}\dot{w}^2 + a_{44}\dot{\theta}^2 + 2a_{45}\dot{\theta}\dot{\phi} + 2a_{46}\dot{\theta}\dot{\psi}$$

$$+ a_{55}\dot{\phi}^2 + 2a_{56}\dot{\phi}\dot{\psi} + a_{66}\dot{\psi}^2] \tag{3.32}$$

where

$$a_{11} = a_{22} = a_{33} = m$$

$$a_{44} = A$$

$$a_{55} = B$$

$$a_{66} = C$$

$$a_{45} = -H$$

$$a_{46} = -G$$

$$a_{56} = -F \tag{3.33}$$

3.3 Equations of Motion

The equations of motion for a multi-degree-of-freedom system may be obtained by performing partial differentiations on the kinetic and potential energy expressions based on the Lagrange's equation.

$$a_{11}\ddot{u} + c_{11}u + c_{15}\phi + c_{16}\psi = 0$$

$$a_{22}\ddot{v} + c_{22}v + c_{24}\theta + c_{26}\psi = 0$$

$$a_{33}\ddot{w} + c_{33}w + c_{34}\theta + c_{35}\phi = 0$$

$$a_{44}\ddot{\theta} + a_{45}\ddot{\phi} + a_{46}\ddot{\psi} + c_{24}v + c_{34}w + c_{44}\theta + c_{45}\phi + c_{46}\psi = 0$$

$$a_{45}\ddot{\theta} + a_{55}\ddot{\phi} + a_{56}\ddot{\psi} + c_{15}u + c_{35}w + c_{45}\theta + c_{55}\phi + c_{56}\psi = 0$$

$$a_{46}\ddot{\theta} + a_{56}\ddot{\phi} + a_{66}\ddot{\psi} + c_{16}u + c_{26}v + c_{46}\theta + c_{56}\phi + c_{66}\psi = 0 \qquad (3.34)$$

or in matrix form

$$[a_{ij}]\{\ddot{q}\} + [c_{ij}]\{q\} = \{0\} \qquad (3.35)$$

where a_{ij} and c_{ij} are as defined earlier and

$$\{q\}^T = [u, v, w, \theta, \phi, \psi] \qquad (3.36)$$

for a simple harmonic motion

$$\{\ddot{q}\} = -\omega^2\{q\}$$

Therefore, the equations of motion may be written in the form of the following eigenvalue equations.

$$[c_{ij}]\{q\} = \omega^2[a_{ij}]\{q\} \qquad (3.37)$$

The solution of eqns. (37) will give the natural frequencies of the steam generator and the corresponding mode shapes.

Eq. (3.1 - 3.37) are due to Lo and Bogdanoff (Ref. 20).

3.4 EIGENVALUE ANALYSIS OF THE STEAM GENERATOR OF PARADISE PLANT

To carry out an eigenvalue analysis of the steam generator, it is necessary to obtain the weight and location of individual components of the steam generator. Table 1 lists the components of the steam generator and their respective weights. The location of each component is obtained from Bobcock and Wilcox drawing no. 22790-F9. Based on the above information, the discrete mass model of the steam generator is made. This model is described graphically by Figure 5. The magnitude and location of each mass is listed in Table 3.

The top supports to the steam generator are provided by 277 hanger rods, 54 of which are spring supported. The figure shows the mechanics by which the spring is bolted to the hanger rod. For this combination, the equivalent stiffness may be obtained from the following formula:

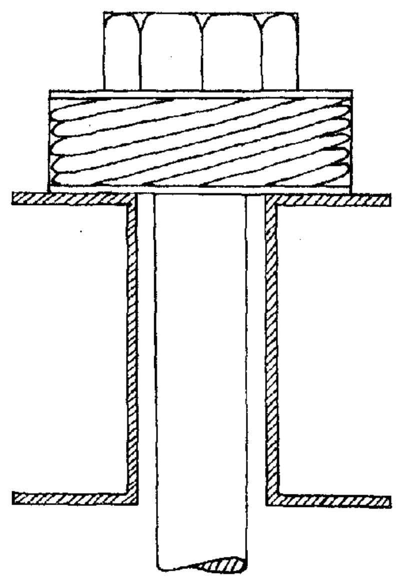

$$K_{eq} = \frac{K_{spring} \times K_{rod}}{K_{spring} + K_{rod}} \qquad (3.33)$$

where K_{spring} = stiffness of the spring

= 20 Kips/in

K_{rod} = stiffness of the hanger rod.

Table 6 lists the location and properties of each hanger rod. The location of each rod is also shown in a plan view in Fig. 11.

The constants defined by eqn. (3.29) are as follows:

$c_{11} = c_{22} = 1.31 \times 10^3$ K/ft

$c_{15} = -c_{24} = 1.12 \times 10^9$ K

$c_{16} = 1.38 \times 10^4$ K

TABLE 6
THE LOACATIONS AND PROPERTIES OF THE HANGER RODS OF THE PARADISE STEAM GENERATOR

ROD NO.	X- ORDINATE (FT.)	Y- ORDINATE (FT.)	DIAMETER (IN.)	LENGTH (FT.)	TENSION (KIPS)	STIFFNESS (KIPS/FT)	ROD NO.	X- ORDINATE (FT.)	Y- ORDINATE (FT.)	DIAMETER (IN.)	LENGTH (FT.)	TENSION (KIPS)	STIFFNESS (KIPS/FT)
1	10.34	4.30	2.0	14.89	36.0	6330.70	41	96.74	6.81	3.5	14.83	108.0	19461.07
2	19.04	4.30	2.0	14.89	36.0	6330.70	42	99.83	6.81	3.5	14.83	108.0	19461.07
3	27.73	4.30	2.0	14.89	36.0	6330.70	43	102.91	6.81	3.5	14.83	108.0	19461.07
4	36.43	4.30	2.0	14.89	36.0	6330.70	44	106.00	6.81	3.5	14.83	108.0	19461.07
5	45.13	4.30	2.0	14.89	36.0	6330.70	45	10.34	18.00	2.5	14.58	40.0	10099.37
6	53.82	4.30	2.0	14.89	36.0	6330.70	46	17.70	18.00	2.5	14.58	40.0	10099.37
7	62.52	4.30	2.0	14.89	36.0	6330.70	47	25.06	18.00	2.5	14.58	40.0	10099.37
8	71.21	4.30	2.0	14.89	36.0	6330.70	48	32.42	18.00	2.5	14.58	40.0	10099.37
9	79.91	4.30	2.0	14.89	36.0	6330.70	49	39.77	18.00	2.5	14.58	40.0	10099.37
10	88.61	4.30	2.0	14.89	36.0	6330.70	50	47.13	18.00	2.5	14.58	40.0	10099.37
11	97.30	4.30	2.0	14.89	36.0	6330.70	51	54.49	18.00	2.5	14.58	40.0	10099.37
12	106.00	4.30	2.0	14.89	36.0	6330.70	52	61.85	18.00	2.5	14.58	40.0	10099.37
13	10.34	6.81	3.5	14.83	108.0	19461.07	53	69.21	18.00	2.5	14.58	40.0	10099.37
14	13.43	6.81	3.5	14.83	108.0	19461.07	54	76.57	18.00	2.5	14.58	40.0	10099.37
15	16.51	6.81	3.5	14.83	108.0	19461.07	55	83.92	18.00	2.5	14.58	40.0	10099.37
16	19.60	6.81	3.5	14.83	108.0	19461.07	56	91.28	18.00	2.5	14.58	40.0	10099.37
17	22.68	6.81	3.5	14.83	108.0	19461.07	57	98.64	18.00	2.5	14.58	40.0	10099.37
18	25.77	6.81	3.5	14.83	108.0	19461.07	58	106.00	18.00	2.5	14.58	40.0	10099.37
19	28.85	6.81	3.5	14.83	108.0	19461.07	59	10.34	24.80	3.5	14.43	120.0	20003.20
20	31.94	6.81	3.5	14.83	108.0	19461.07	60	13.43	24.80	3.5	14.43	120.0	20003.20
21	35.03	6.81	3.5	14.83	108.0	19461.07	61	16.51	24.80	3.5	14.43	120.0	20003.20
22	38.11	6.81	3.5	14.83	108.0	19461.07	62	19.60	24.80	3.5	14.43	120.0	20003.20
23	41.20	6.81	3.5	14.83	108.0	19461.07	63	22.68	24.80	3.5	14.43	120.0	20003.20
24	44.28	6.81	3.5	14.83	108.0	19461.07	64	25.77	24.80	3.5	14.43	120.0	20003.20
25	47.37	6.81	3.5	14.83	108.0	19461.07	65	28.85	24.80	3.5	14.43	120.0	20003.20
26	50.46	6.81	3.5	14.83	108.0	19461.07	66	31.94	24.80	3.5	14.43	120.0	20003.20
27	53.54	6.81	3.5	14.83	108.0	19461.07	67	35.03	24.80	3.5	14.43	120.0	20003.20
28	56.63	6.81	3.5	14.83	108.0	19461.07	68	38.11	24.80	3.5	14.43	120.0	20003.20
29	59.71	6.81	3.5	14.83	108.0	19461.07	69	41.20	24.80	3.5	14.43	120.0	20003.20
30	62.80	6.81	3.5	14.83	108.0	19461.07	70	44.28	24.80	3.5	14.43	120.0	20003.20
31	65.88	6.81	3.5	14.83	108.0	19461.07	71	47.37	24.80	3.5	14.43	120.0	20003.20
32	68.97	6.81	3.5	14.83	108.0	19461.07	72	50.46	24.80	3.5	14.43	120.0	20003.20
33	72.06	6.81	3.5	14.83	108.0	19461.07	73	53.54	24.80	3.5	14.43	120.0	20003.20
34	75.14	6.81	3.5	14.83	108.0	19461.07	74	56.63	24.80	3.5	14.43	120.0	20003.20
35	78.23	6.81	3.5	14.83	108.0	19461.07	75	59.71	24.80	3.5	14.43	120.0	20003.20
36	81.31	6.81	3.5	14.83	108.0	19461.07	76	62.80	24.80	3.5	14.43	120.0	20003.20
37	84.40	6.81	3.5	14.83	108.0	19461.07	77	65.88	24.80	3.5	14.43	120.0	20003.20
38	87.49	6.81	3.5	14.83	108.0	19461.07	78	68.97	24.80	3.5	14.43	120.0	20003.20
39	90.57	6.81	3.5	14.83	108.0	19461.07	79	72.06	24.80	3.5	14.43	120.0	20003.20
40	93.66	6.81	3.5	14.83	108.0	19461.07	80	75.14	24.80	3.5	14.43	120.0	20003.20

ROD NO.	X-ORDINATE (FT.)	Y-ORDINATE (FT.)	DIAMETER (IN.)	LENGTH (FT.)	TENSION (KIPS)	STIFFNESS (KIPS/FT)
81	78.23	24.80	3.5	14.43	120.0	20003.20
82	81.31	24.80	3.5	14.43	120.0	20003.20
83	84.40	24.80	3.5	14.43	120.0	20003.20
84	87.49	24.80	3.5	14.43	120.0	20003.20
85	90.57	24.80	3.5	14.43	120.0	20003.20
86	93.66	24.80	3.5	14.43	120.0	20003.20
87	96.74	24.80	3.5	14.43	120.0	20003.20
88	99.83	24.80	3.5	14.43	120.0	20003.20
89	102.91	24.80	3.5	14.43	120.0	20003.20
90	106.00	24.80	3.5	14.43	120.0	20003.20
91	10.34	31.70	2.5	14.28	48.0	234.54
92	14.90	31.70	2.5	14.28	48.0	234.54
93	19.45	31.70	2.5	14.28	48.0	234.54
94	24.01	31.70	2.5	14.28	48.0	234.54
95	28.56	31.70	2.5	14.28	48.0	234.54
96	33.12	31.70	2.5	14.28	48.0	234.54
97	37.67	31.70	2.5	14.28	48.0	234.54
98	42.23	31.70	2.5	14.28	48.0	234.54
99	46.78	31.70	2.5	14.28	48.0	234.54
100	51.34	31.70	2.5	14.28	48.0	234.54
101	55.89	31.70	2.5	14.28	48.0	234.54
102	60.45	31.70	2.5	14.28	48.0	234.54
103	65.00	31.70	2.5	14.28	48.0	234.54
104	69.56	31.70	2.5	14.28	48.0	234.54
105	74.11	31.70	2.5	14.28	48.0	234.54
106	78.67	31.70	2.5	14.28	48.0	234.54
107	83.22	31.70	2.5	14.28	48.0	234.54
108	87.78	31.70	2.5	14.28	48.0	234.54
109	92.33	31.70	2.5	14.28	48.0	234.54
110	96.89	31.70	2.5	14.28	48.0	234.54
111	101.44	31.70	2.5	14.28	48.0	234.54
112	106.00	31.70	2.5	14.28	48.0	234.54
113	10.34	33.20	2.0	14.24	26.0	6617.74
114	15.97	33.20	2.0	14.24	26.0	6617.74
115	21.59	33.20	2.0	14.24	26.0	6617.74
116	27.22	33.20	2.0	14.24	26.0	6617.74
117	32.85	33.20	2.0	14.24	26.0	6617.74
118	38.48	33.20	2.0	14.24	26.0	6617.74
119	44.10	33.20	2.0	14.24	26.0	6617.74
120	49.73	33.20	2.0	14.24	26.0	6617.74
121	55.36	33.20	2.0	14.24	26.0	6617.74
122	60.98	33.20	2.0	14.24	26.0	6617.74
123	66.61	33.20	2.0	14.24	26.0	6617.74
124	72.24	33.20	2.0	14.24	26.0	6617.74
125	77.86	33.20	2.0	14.24	26.0	6617.74
126	83.49	33.20	2.0	14.24	26.0	6617.74
127	89.12	33.20	2.0	14.24	26.0	6617.74
128	94.75	33.20	2.0	14.24	26.0	6617.74
129	100.37	33.20	2.0	14.24	26.0	6617.74
130	106.00	33.20	2.0	14.24	26.0	6617.74
131	10.34	45.20	2.5	13.97	51.0	10538.62
132	15.97	45.20	2.5	13.97	51.0	10538.62
133	21.59	45.20	2.5	13.97	51.0	10538.62
134	27.22	45.20	2.5	13.97	51.0	10538.62
135	32.85	45.20	2.5	13.97	51.0	10538.62
136	38.48	45.20	2.5	13.97	51.0	10538.62
137	44.10	45.20	2.5	13.97	51.0	10538.62
138	49.73	45.20	2.5	13.97	51.0	10538.62
139	55.36	45.20	2.5	13.97	51.0	10538.62
140	60.98	45.20	2.5	13.97	51.0	10538.62
141	66.61	45.20	2.5	13.97	51.0	10538.62
142	72.24	45.20	2.5	13.97	51.0	10538.62
143	77.86	45.20	2.5	13.97	51.0	10538.62
144	83.49	45.20	2.5	13.97	51.0	10538.62
145	89.12	45.20	2.5	13.97	51.0	10538.62
146	94.75	45.20	2.5	13.97	51.0	10538.62
147	100.37	45.20	2.5	13.97	51.0	10538.62
148	106.00	45.20	2.5	13.97	51.0	10538.62
149	10.34	47.00	2.5	13.93	47.5	10569.04
150	16.72	47.00	2.5	13.93	47.5	10569.04
151	23.09	47.00	2.5	13.93	47.5	10569.04
152	29.47	47.00	2.5	13.93	47.5	10569.04
153	35.85	47.00	2.5	13.93	47.5	10569.04
154	42.23	47.00	2.5	13.93	47.5	10569.04
155	48.60	47.00	2.5	13.93	47.5	10569.04
156	54.98	47.00	2.5	13.93	47.5	10569.04
157	61.36	47.00	2.5	13.93	47.5	10569.04
158	67.74	47.00	2.5	13.93	47.5	10569.04
159	74.11	47.00	2.5	13.93	47.5	10569.04
160	80.49	47.00	2.5	13.93	47.5	10569.04
161	86.87	47.00	2.5	13.93	47.5	10569.04
162	93.25	47.00	2.5	13.93	47.5	10569.04
163	99.62	47.00	2.5	13.93	47.5	10569.04
164	106.00	47.00	2.5	13.93	47.5	10569.04
165	10.34	51.20	2.5	13.84	47.0	10640.71
166	16.72	51.20	2.5	13.84	47.0	10640.71

ROD NO.	X- ORDINATE (FT.)	Y- ORDINATE (FT.)	DIAMETER (IN.)	LENGTH (FT.)	TENSION (KIPS)	STIFFNESS (KIPS/FT)	ROD NO.	X- ORDINATE (FT.)	Y- ORDINATE (FT.)	DIAMETER (IN.)	LENGTH (FT.)	TENSION (KIPS)	STIFFNESS (KIPS/FT)
167	23.09	51.20	2.5	13.84	47.0	10640.71	210	61.36	64.00	2.5	13.55	58.0	10865.24
168	29.47	51.20	2.5	13.84	47.0	10640.71	211	67.74	64.00	2.5	13.55	58.0	10865.24
169	35.85	51.20	2.5	13.84	47.0	10640.71	212	74.11	64.00	2.5	13.55	58.0	10865.24
170	42.23	51.20	2.5	13.84	47.0	10640.71	213	80.49	64.00	2.5	13.55	58.0	10865.24
171	48.60	51.20	2.5	13.84	47.0	10640.71	214	86.87	64.00	2.5	13.55	58.0	10865.24
172	54.98	51.20	2.5	13.84	47.0	10640.71	215	93.25	64.00	2.5	13.55	58.0	10865.24
173	61.36	51.20	2.5	13.84	47.0	10640.71	216	99.62	64.00	2.5	13.55	58.0	10865.24
174	67.74	51.20	2.5	13.84	47.0	10640.71	217	106.00	64.00	2.5	13.55	58.0	10865.24
175	74.11	51.20	2.5	13.84	47.0	10640.71	218	10.34	67.00	2.5	13.49	56.0	234.84
176	80.49	51.20	2.5	13.84	47.0	10640.71	219	13.43	67.00	2.5	13.49	56.0	234.84
177	86.87	51.20	2.5	13.84	47.0	10640.71	220	16.51	67.00	2.5	13.49	56.0	234.84
178	93.25	51.20	2.5	13.84	47.0	10640.71	221	19.60	67.00	2.5	13.49	56.0	234.84
179	99.62	51.20	2.5	13.84	47.0	10640.71	222	22.68	67.00	2.5	13.49	56.0	234.84
180	106.00	51.20	2.5	13.84	47.0	10640.71	223	25.77	67.00	2.5	13.49	56.0	234.84
181	10.34	51.50	2.5	13.83	415.0	10645.86	224	28.85	67.00	2.5	13.49	56.0	234.84
182	34.25	51.50	2.5	13.83	415.0	10645.86	225	31.94	67.00	2.5	13.49	56.0	234.84
183	58.17	51.50	2.5	13.83	415.0	10645.86	226	35.03	67.00	2.5	13.49	56.0	234.84
184	82.08	51.50	2.5	13.83	415.0	10645.86	227	38.11	67.00	2.5	13.49	56.0	234.84
185	106.00	51.50	2.5	13.83	415.0	10645.86	228	41.20	67.00	2.5	13.49	56.0	234.84
186	10.34	55.00	2.5	13.75	57.0	10706.39	229	44.28	67.00	2.5	13.49	56.0	234.84
187	16.72	55.00	2.5	13.75	57.0	10706.39	230	47.37	67.00	2.5	13.49	56.0	234.84
188	23.09	55.00	2.5	13.75	57.0	10706.39	231	50.46	67.00	2.5	13.49	56.0	234.84
189	29.47	55.00	2.5	13.75	57.0	10706.39	232	53.54	67.00	2.5	13.49	56.0	234.84
190	35.85	55.00	2.5	13.75	57.0	10706.39	233	56.63	67.00	2.5	13.49	56.0	234.84
191	42.23	55.00	2.5	13.75	57.0	10706.39	234	59.71	67.00	2.5	13.49	56.0	234.84
192	48.60	55.00	2.5	13.75	57.0	10706.39	235	62.80	67.00	2.5	13.49	56.0	234.84
193	54.98	55.00	2.5	13.75	57.0	10706.39	236	65.88	67.00	2.5	13.49	56.0	234.84
194	61.36	55.00	2.5	13.75	57.0	10706.39	237	68.97	67.00	2.5	13.49	56.0	234.84
195	67.74	55.00	2.5	13.75	57.0	10706.39	238	72.06	67.00	2.5	13.49	56.0	234.84
196	74.11	55.00	2.5	13.75	57.0	10706.39	239	75.14	67.00	2.5	13.49	56.0	234.84
197	80.49	55.00	2.5	13.75	57.0	10706.39	240	78.23	67.00	2.5	13.49	56.0	234.84
198	86.87	55.00	2.5	13.75	57.0	10706.39	241	81.31	67.00	2.5	13.49	56.0	234.84
199	93.25	55.00	2.5	13.75	57.0	10706.39	242	84.40	67.00	2.5	13.49	56.0	234.84
200	99.62	55.00	2.5	13.75	57.0	10706.39	243	87.49	67.00	2.5	13.49	56.0	234.84
201	106.00	55.00	2.5	13.75	57.0	10706.39	244	90.57	67.00	2.5	13.49	56.0	234.84
202	10.34	64.00	2.5	13.55	58.0	10865.24	245	93.66	67.00	2.5	13.49	56.0	234.84
203	16.72	64.00	2.5	13.55	58.0	10865.24	246	96.74	67.00	2.5	13.49	56.0	234.84
204	23.09	64.00	2.5	13.55	58.0	10865.24	247	99.83	67.00	2.5	13.49	56.0	234.84
205	29.47	64.00	2.5	13.55	58.0	10865.24	248	102.91	67.00	2.5	13.49	56.0	234.84
206	35.85	64.00	2.5	13.55	58.0	10865.24	249	106.00	67.00	2.5	13.49	56.0	234.84
207	42.23	64.00	2.5	13.55	58.0	10865.24	250	10.34	69.70	2.0	13.43	27.0	7019.72
208	48.60	64.00	2.5	13.55	58.0	10865.24	251	24.01	69.70	2.0	13.43	27.0	7019.72
209	54.98	64.00	2.5	13.55	58.0	10865.24	252	37.67	69.70	2.0	13.43	27.0	7019.72

ROD NO.	X-ORDINATE (FT.)	Y-ORDINATE (FT.)	DIAMETER (IN.)	LENGTH (FT.)	TENSION (KIPS)	STIFFNESS (KIPS/FT)
253	51.34	69.70	2.0	13.43	27.0	7019.72
254	65.00	69.70	2.0	13.43	27.0	7019.72
255	78.67	69.70	2.0	13.43	27.0	7019.72
256	92.33	69.70	2.0	13.43	27.0	7019.72
257	106.00	69.70	2.0	13.43	27.0	7019.72
258	10.34	72.00	1.0	13.37	4.0	1761.67
259	24.01	72.00	1.0	13.37	4.0	1761.67
260	37.67	72.00	1.0	13.37	4.0	1761.67
261	51.34	72.00	1.0	13.37	4.0	1761.67
262	65.00	72.00	1.0	13.37	4.0	1761.67
263	78.67	72.00	1.0	13.37	4.0	1761.67
264	92.33	72.00	1.0	13.37	4.0	1761.67
265	106.00	72.00	1.0	13.37	4.0	1761.67

ROD NO.	X-ORDINATE (FT.)	Y-ORDINATE (FT.)	DIAMETER (IN.)	LENGTH (FT.)	TENSION (KIPS)	STIFFNESS (KIPS/FT)
266	10.34	73.50	2.0	13.34	26.0	7064.39
267	42.23	73.50	2.0	13.34	26.0	7064.39
268	74.11	73.50	2.0	13.34	26.0	7064.39
269	106.00	73.50	2.0	13.34	26.0	7064.39
270	10.34	84.50	2.5	13.10	33.0	11245.28
271	42.23	84.50	2.5	13.10	33.0	11245.28
272	74.11	84.50	2.5	13.10	33.0	11245.28
273	106.00	84.50	2.5	13.10	33.0	11245.28
274	10.34	93.50	2.0	12.89	23.0	7309.22
275	42.23	93.50	2.0	12.89	23.0	7309.22
276	74.11	93.50	2.0	12.89	23.0	7309.22
277	106.00	93.50	2.0	12.89	23.0	7309.22

$$c_{26} = 0.0$$

$$c_{33} = 2.71 \times 10^{6} \text{ K/ft}$$

$$c_{34} = -40 \times 10^{6} \text{ K}$$

$$c_{35} = 0.0 \qquad (3.39)$$

$$c_{44} = 1.93 \times 10^{9} \text{ K-ft}$$

$$c_{45} = 0.0$$

$$c_{46} = 0.0$$

$$c_{55} = 2.35 \times 10^{9} \text{ K-ft}$$

$$c_{56} = -1.17 \times 10^{9} \text{ K-ft}$$

$$c_{66} = 1.91 \times 10^{6} \text{ K-ft}$$

Also, the constants defined by eqns. (3.33) are evaluated as follows:

$$a_{11} = a_{22} = a_{33} = 751.90 \text{ K-sec}^2\text{/ft}$$

$$a_{44} = 3.19 \times 10^{6} \text{ K-ft sec}^2$$

$$a_{55} = 3.87 \times 10^{6} \text{ K-ft-sec}^2$$

$$a_{66} = 2.75 \times 10^{6} \text{ K-ft-sec}^2 \qquad (3.40)$$

$$a_{45} = 0.0$$

$$a_{46} = 0.0$$

$$a_{56} = -0.44 \times 10^{6} \text{ K-ft-sec}^2$$

Substitution of the above constants in the eigenvalue eqn. (2.37) yields six natural frequencies and corresponding mode shapes. The result is presented in Table 7.

Table 7

Result of Analytic Analysis of Paradise Steam Generator

Mode No.	1	2	3	4	5	6
Natural Frequency	.12475	.20925	.21446	3.17420	3.95820	9.83010
u	1.0000	0.	1.0000	0.	-0.2400	0.
v	0.	1.0000	0.	-0.0225	0.	0.
w	0.	-0.0013	0.	1.0000	0.	1.0000
θ	0.	0.	0.	-0.0606	0.	-0.0039
ϕ	0.	0.	0.	0.	1.0000	0.
ψ	-0.0615	0.	0.0044	0.	0.152	0.

It may be observed from the above table that the first mode shape is a combination of translation along x-axis and torsion about z-axis. The second and third modes are predominantly translation along y and x axes respectively. Fourth, fifth and sixth modes have frequencies of 3.1742, 3.9582, and 9.8301 which are too high to be of interest to the present study. A plot of the first three modes is presented in Fig. 12.

A finite element model of the boiler consisting of lumped masses as listed in table 3 connected by rigid massless bars and supported at the top by four beam elements of finite section properties is then analyzed. The axial, bending, and torsional stiffness of the four equivalent hanger rods are obtained by systematically verying their values in order to match the resulting natural frequencies and mode shapes with those obtained by using the present alternative analytic approach. This is a tedious but practical process. The values that provide good matching are $A = 5{:}00\ ft^2$, $I_{xx} = 1.4\ ft^4$, $Ixy = 1.58\ ft^4$, $J = 1.0\ ft^4$ for two rods and $A = 5.0\ ft^2$, $I_{xx} = 1.4\ ft^4$, $I_{yy} = 1.34\ ft^4$, $J = 1.0\ ft^4$ for the other two rods. Table 8 compares the natural frequencies of the finite element model of the steam generator with the analytical results listed in Table 7.

Table 8

Comparison of Results of Two Analyses of Paradise Steam Generator

Mode No.	Natural Frequency of Finite Element Model	Natural Frequency obtained by analytical analysis	% difference
1	0.12622	0.12475	1.18
2	0.21074	0.20925	0.71
3	0.21583	0.21446	0.64

The mode shapes corresponding to the first three natural frequencies of the finite element model is shown in Fig. 13. All the three modes agree with the ones obtained by the analytical analysis.

3.5 EIGENVALUE ANALYSIS OF THE STEAM GENERATOR OF THE NEW MADRID PLANT

The steam generator of the New Madrid Plant is analyzed in the same way as the Paradise Plant described in the previous section. The weights of the components of the steam generator are listed in Table 2. The discrete mass model of the steam generator is made on the basis of Bobcock and Wilcox drawing No. 28115F-2, which describes the location of each element of the steam generator. Table 4 lists the locations and magnitudes of each discrete mass in the model. Fig. 6 represents these masses graphically.

The steam generator is supported at the top by 276 hanger rods, the location and size of each rod are listed in Table 9. Fig. 14 shows these rods in a plan view.

The elements of the matrices [c] and [a] described in eqn. (3.37) are evaluated as follows:

$c_{11} = c_{22} = 1.204 \times 10^3$ K/ft

$c_{15} = -c_{24} = -.1028 \times 10^6$ K

$c_{16} = -6.639 \times 10^3$ K

$c_{26} = 0.$

$c_{33} = 3.793 \times 10^6$ K/ft

$c_{34} = 20.62 \times 10^6$ K

$c_{35} = 18.963 \times 10^3$ K

$c_{44} = 3.214 \times 10^9$ K-ft

$c_{45} = .103 \times 10^6$ K-ft

$c_{46} = -.513 \times 10^3$ K-ft

$c_{55} = 1.834 \times 10^9$ K-ft

TABLE 9

THE LOCATIONS AND PROPERTIES OF THE HANGER RODS OF THE NEW MADRID STEAM GENERATOR

ROD NO.	X-ORDINATE (FT.)	Y-ORDINATE (FT.)	DIAMETER (IN.)	LENGTH (FT.)	TENSION (KIPS)	STIFFNESS (KIPS/FT)	ROD NO.	X-ORDINATE (FT.)	Y-ORDINATE (FT.)	DIAMETER (IN.)	LENGTH (FT.)	TENSION (KIPS)	STIFFNESS (KIPS/FT)
1	63.13	10.10	5.0	13.38	204.0	44023.15	41	69.38	30.75	4.5	13.81	153.0	34547.96
2	132.88	10.10	5.0	13.38	204.0	44023.15	42	126.63	30.75	4.5	13.81	153.0	34547.96
3	64.05	10.10	5.0	13.38	204.0	44023.15	43	69.38	35.50	4.5	13.91	153.0	34302.18
4	131.96	10.10	5.0	13.38	204.0	44023.15	44	126.63	35.50	4.5	13.91	153.0	34302.18
5	63.13	17.80	5.0	13.54	204.0	43501.62	45	69.38	38.25	4.5	13.97	153.0	34161.47
6	132.88	17.80	5.0	13.54	204.0	43501.62	46	126.63	38.25	4.5	13.97	153.0	34161.47
7	64.05	17.80	5.0	13.54	204.0	43501.62	47	73.23	40.50	2.5	14.01	40.0	10508.40
8	131.96	17.80	5.0	13.54	204.0	43501.62	48	77.73	40.50	2.5	14.01	40.0	10508.40
9	70.88	20.00	3.0	13.59	68.0	15607.75	49	82.24	40.50	2.5	14.01	40.0	10508.40
10	74.50	20.00	3.0	13.59	68.0	15607.75	50	86.74	40.50	2.5	14.01	40.0	10508.40
11	78.11	20.00	3.0	13.59	68.0	15607.75	51	91.25	40.50	2.5	14.01	40.0	10508.40
12	81.73	20.00	3.0	13.59	68.0	15607.75	52	95.75	40.50	2.5	14.01	40.0	10508.40
13	85.35	20.00	3.0	13.59	68.0	15607.75	53	100.26	40.50	2.5	14.01	40.0	10508.40
14	88.96	20.00	3.0	13.59	68.0	15607.75	54	104.76	40.50	2.5	14.01	40.0	10508.40
15	92.58	20.00	3.0	13.59	68.0	15607.75	55	109.27	40.50	2.5	14.01	40.0	10508.40
16	96.20	20.00	3.0	13.59	68.0	15607.75	56	113.77	40.50	2.5	14.01	40.0	10508.40
17	99.81	20.00	3.0	13.59	68.0	15607.75	57	118.28	40.50	2.5	14.01	40.0	10508.40
18	103.43	20.00	3.0	13.59	68.0	15607.75	58	122.78	40.50	2.5	14.01	40.0	10508.40
19	107.05	20.00	3.0	13.59	68.0	15607.75	59	73.23	41.50	1.5	14.03	12.0	3777.41
20	110.66	20.00	3.0	13.59	68.0	15607.75	60	83.14	41.50	1.5	14.03	12.0	3777.41
21	114.28	20.00	3.0	13.59	68.0	15607.75	61	93.05	41.50	1.5	14.03	12.0	3777.41
22	117.90	20.00	3.0	13.59	68.0	15607.75	62	102.96	41.50	1.5	14.03	12.0	3777.41
23	121.51	20.00	3.0	13.59	68.0	15607.75	63	112.87	41.50	1.5	14.03	12.0	3777.41
24	125.13	20.00	3.0	13.59	68.0	15607.75	64	122.78	41.50	1.5	14.03	12.0	3777.41
25	69.38	23.00	4.5	13.65	153.0	34956.64	65	69.38	42.25	4.5	14.05	153.0	33958.85
26	126.63	23.00	4.5	13.65	153.0	34956.64	66	126.63	42.25	4.5	14.05	153.0	33958.85
27	69.38	27.50	4.5	13.74	153.0	34718.17	67	72.51	44.75	2.5	14.10	38.0	10442.42
28	126.63	27.50	4.5	13.74	153.0	34718.17	68	78.18	44.75	2.5	14.10	38.0	10442.42
29	73.23	29.50	2.5	13.78	38.0	10683.10	69	83.84	44.75	2.5	14.10	38.0	10442.42
30	77.73	29.50	2.5	13.78	38.0	10683.10	70	89.51	44.75	2.5	14.10	38.0	10442.42
31	82.24	29.50	2.5	13.78	38.0	10683.10	71	95.17	44.75	2.5	14.10	38.0	10442.42
32	86.74	29.50	2.5	13.78	38.0	10683.10	72	100.84	44.75	2.5	14.10	38.0	10442.42
33	91.25	29.50	2.5	13.78	38.0	10683.10	73	106.50	44.75	2.5	14.10	38.0	10442.42
34	95.75	29.50	2.5	13.78	38.0	10683.10	74	112.17	44.75	2.5	14.10	38.0	10442.42
35	100.26	29.50	2.5	13.78	38.0	10683.10	75	117.83	44.75	2.5	14.10	38.0	10442.42
36	104.76	29.50	2.5	13.78	38.0	10683.10	76	123.50	44.75	2.5	14.10	38.0	10442.42
37	109.27	29.50	2.5	13.78	38.0	10683.10	77	69.38	46.00	4.5	14.13	153.0	33771.07
38	113.77	29.50	2.5	13.78	38.0	10683.10	78	126.63	46.00	4.5	14.13	153.0	33771.07
39	118.28	29.50	2.5	13.78	38.0	10683.10	79	69.38	49.00	3.0	14.19	83.0	14943.26
40	122.78	29.50	2.5	13.78	38.0	10683.10	80	77.56	49.00	3.0	14.19	83.0	14943.26

ROD NO.	X- ORDINATE (FT.)	Y- ORDINATE (FT.)	DIAMETER (IN.)	LENGTH (FT.)	TENSION (KIPS)	STIFFNESS (KIPS/FT)
81	85.74	49.00	3.0	14.19	83.0	14943.26
82	93.92	49.00	3.0	14.19	83.0	14943.26
83	102.09	49.00	3.0	14.19	83.0	14943.26
84	110.27	49.00	3.0	14.19	83.0	14943.26
85	118.45	49.00	3.0	14.19	83.0	14943.26
86	126.63	49.00	3.0	14.19	83.0	14943.26
87	69.38	52.00	3.0	14.25	77.0	14877.74
88	126.63	52.00	3.0	14.25	77.0	14877.74
89	72.38	53.00	2.5	14.27	46.0	10316.68
90	76.32	53.00	2.5	14.27	46.0	10316.68
91	80.26	53.00	2.5	14.27	46.0	10316.68
92	84.21	53.00	2.5	14.27	46.0	10316.68
93	88.15	53.00	2.5	14.27	46.0	10316.68
94	92.09	53.00	2.5	14.27	46.0	10316.68
95	96.03	53.00	2.5	14.27	46.0	10316.68
96	99.98	53.00	2.5	14.27	46.0	10316.68
97	103.92	53.00	2.5	14.27	46.0	10316.68
98	107.86	53.00	2.5	14.27	46.0	10316.68
99	111.80	53.00	2.5	14.27	46.0	10316.68
100	115.75	53.00	2.5	14.27	46.0	10316.68
101	119.69	53.00	2.5	14.27	46.0	10316.68
102	123.63	53.00	2.5	14.27	46.0	10316.68
103	69.38	54.50	3.0	14.31	66.0	14823.57
104	126.63	54.50	3.0	14.31	66.0	14823.57
105	72.18	55.25	2.5	14.32	40.0	10282.91
106	77.92	55.25	2.5	14.32	40.0	10282.91
107	83.66	55.25	2.5	14.32	40.0	10282.91
108	89.40	55.25	2.5	14.32	40.0	10282.91
109	95.14	55.25	2.5	14.32	40.0	10282.91
110	100.87	55.25	2.5	14.32	40.0	10282.91
111	106.61	55.25	2.5	14.32	40.0	10282.91
112	112.35	55.25	2.5	14.32	40.0	10282.91
113	118.09	55.25	2.5	14.32	40.0	10282.91
114	123.83	55.25	2.5	14.32	40.0	10282.91
115	72.18	59.25	2.5	14.40	40.0	10223.42
116	77.92	59.25	2.5	14.40	40.0	10223.42
117	83.66	59.25	2.5	14.40	40.0	10223.42
118	89.40	59.25	2.5	14.40	40.0	10223.42
119	95.14	59.25	2.5	14.40	40.0	10223.42
120	100.87	59.25	2.5	14.40	40.0	10223.42
121	106.61	59.25	2.5	14.40	40.0	10223.42
122	112.35	59.25	2.5	14.40	40.0	10223.42
123	118.09	59.25	2.5	14.40	40.0	10223.42

ROD NO.	X- ORDINATE (FT.)	Y- ORDINATE (FT.)	DIAMETER (IN.)	LENGTH (FT.)	TENSION (KIPS)	STIFFNESS (KIPS/FT)
124	123.83	59.25	2.5	14.40	40.0	10223.42
125	71.48	61.00	1.5	14.44	14.0	3671.14
126	77.37	61.00	1.5	14.44	14.0	3671.14
127	83.27	61.00	1.5	14.44	14.0	3671.14
128	89.16	61.00	1.5	14.44	14.0	3671.14
129	95.06	61.00	1.5	14.44	14.0	3671.14
130	100.95	61.00	1.5	14.44	14.0	3671.14
131	106.85	61.00	1.5	14.44	14.0	3671.14
132	112.74	61.00	1.5	14.44	14.0	3671.14
133	118.64	61.00	1.5	14.44	14.0	3671.14
134	124.53	61.00	1.5	14.44	14.0	3671.14
135	69.38	61.60	3.0	14.45	66.0	14671.86
136	126.63	61.60	3.0	14.45	66.0	14671.86
137	72.48	64.50	2.5	14.51	45.0	10146.38
138	78.15	64.50	2.5	14.51	45.0	10146.38
139	83.82	64.50	2.5	14.51	45.0	10146.38
140	89.50	64.50	2.5	14.51	45.0	10146.38
141	95.17	64.50	2.5	14.51	45.0	10146.38
142	100.84	64.50	2.5	14.51	45.0	10146.38
143	106.51	64.50	2.5	14.51	45.0	10146.38
144	112.19	64.50	2.5	14.51	45.0	10146.38
145	117.86	64.50	2.5	14.51	45.0	10146.38
146	123.53	64.50	2.5	14.51	45.0	10146.38
147	69.38	65.50	3.0	14.53	66.0	14589.85
148	126.63	65.50	3.0	14.53	66.0	14589.85
149	69.38	67.70	3.0	14.58	66.0	14543.98
150	126.63	67.70	3.0	14.58	66.0	14543.98
151	72.48	68.20	2.0	14.59	27.0	6459.38
152	78.15	68.20	2.0	14.59	27.0	6459.38
153	63.82	68.20	2.0	14.59	27.0	6459.38
154	89.50	68.20	2.0	14.59	27.0	6459.38
155	95.17	68.20	2.0	14.59	27.0	6459.38
156	100.84	68.20	2.0	14.59	27.0	6459.38
157	106.51	68.20	2.0	14.59	27.0	6459.38
158	112.19	68.20	2.0	14.59	27.0	6459.38
159	117.86	68.20	2.0	14.59	27.0	6459.38
160	123.53	68.20	2.0	14.59	27.0	6459.38
161	72.48	72.20	2.0	14.67	27.0	6422.70
162	78.15	72.20	2.0	14.67	27.0	6422.70
163	83.82	72.20	2.0	14.67	27.0	6422.70
164	89.50	72.20	2.0	14.67	27.0	6422.70
165	95.17	72.20	2.0	14.67	27.0	6422.70
166	100.84	72.20	2.0	14.67	27.0	6422.70

ROD NO.	X- ORDINATE (FT.)	Y- ORDINATE (FT.)	DIAMETER (IN.)	LENGTH (FT.)	TENSION (KIPS)	STIFFNESS (KIPS/FT)	ROD NO.	X- ORDINATE (FT.)	Y- ORDINATE (FT.)	DIAMETER (IN.)	LENGTH (FT.)	TENSION (KIPS)	STIFFNESS (KIPS/FT)
167	106.51	72.20	2.0	14.67	27.0	6422.70	210	125.03	81.10	3.5	14.86	109.0	19424.07
168	112.19	72.20	2.0	14.67	27.0	6422.70	211	69.38	81.45	3.0	14.87	61.0	14263.75
169	117.86	72.20	2.0	14.67	27.0	6422.70	212	126.63	81.45	3.0	14.87	61.0	14263.75
170	123.53	72.20	2.0	14.67	27.0	6422.70	213	72.48	83.95	1.5	14.92	17.0	3553.49
171	69.38	72.35	3.0	14.68	66.0	14447.99	214	78.15	83.95	1.5	14.92	17.0	3553.49
172	126.63	72.35	3.0	14.68	66.0	14447.99	215	83.82	83.95	1.5	14.92	17.0	3553.49
173	71.03	74.25	3.0	14.72	67.0	14409.13	216	89.50	83.95	1.5	14.92	17.0	3553.49
174	77.02	74.25	3.0	14.72	67.0	14409.13	217	95.17	83.95	1.5	14.92	17.0	3553.49
175	83.02	74.25	3.0	14.72	67.0	14409.13	218	100.84	83.95	1.5	14.92	17.0	3553.49
176	89.01	74.25	3.0	14.72	67.0	14409.13	219	106.51	83.95	1.5	14.92	17.0	3553.49
177	95.01	74.25	3.0	14.72	67.0	14409.13	220	112.19	83.95	1.5	14.92	17.0	3553.49
178	101.00	74.25	3.0	14.72	67.0	14409.13	221	117.86	83.95	1.5	14.92	17.0	3553.49
179	107.00	74.25	3.0	14.72	67.0	14409.13	222	123.53	83.95	1.5	14.92	17.0	3553.49
180	112.99	74.25	3.0	14.72	67.0	14409.13	223	69.38	86.15	3.0	14.96	61.0	14170.42
181	118.99	74.25	3.0	14.72	67.0	14409.13	224	126.63	86.15	3.0	14.96	61.0	14170.42
182	124.98	74.25	3.0	14.72	67.0	14409.13	225	71.76	88.20	2.0	15.01	32.0	6280.04
183	69.38	75.25	4.0	14.74	121.0	25580.01	226	79.26	88.20	2.0	15.01	32.0	6280.04
184	126.63	75.25	4.0	14.74	121.0	25580.01	227	86.76	88.20	2.0	15.01	32.0	6280.04
185	75.48	77.25	1.5	14.78	18.0	3587.05	228	94.26	88.20	2.0	15.01	32.0	6280.04
186	84.49	77.25	1.5	14.78	18.0	3587.05	229	101.75	88.20	2.0	15.01	32.0	6280.04
187	93.50	77.25	1.5	14.78	18.0	3587.05	230	109.25	88.20	2.0	15.01	32.0	6280.04
188	102.51	77.25	1.5	14.78	18.0	3587.05	231	116.75	88.20	2.0	15.01	32.0	6280.04
189	111.52	77.25	1.5	14.78	18.0	3587.05	232	124.25	88.20	2.0	15.01	32.0	6280.04
190	120.53	77.25	1.5	14.78	18.0	3587.05	233	69.38	93.85	4.0	15.13	121.0	24924.67
191	70.98	81.10	3.5	14.86	109.0	19424.07	234	126.63	93.85	4.0	15.13	121.0	24924.67
192	73.82	81.10	3.5	14.86	109.0	19424.07	235	70.98	97.60	3.5	15.20	89.0	18984.89
193	76.67	81.10	3.5	14.86	109.0	19424.07	236	73.82	97.60	3.5	15.20	89.0	18984.89
194	79.51	81.10	3.5	14.86	109.0	19424.07	237	76.67	97.60	3.5	15.20	89.0	18984.89
195	82.36	81.10	3.5	14.86	109.0	19424.07	238	79.51	97.60	3.5	15.20	89.0	18984.89
196	85.20	81.10	3.5	14.86	109.0	19424.07	239	82.36	97.60	3.5	15.20	89.0	18984.89
197	88.05	81.10	3.5	14.86	109.0	19424.07	240	85.20	97.60	3.5	15.20	89.0	18984.89
198	90.89	81.10	3.5	14.86	109.0	19424.07	241	88.05	97.60	3.5	15.20	89.0	18984.89
199	93.74	81.10	3.5	14.86	109.0	19424.07	242	90.89	97.60	3.5	15.20	89.0	18984.89
200	96.58	81.10	3.5	14.86	109.0	19424.07	243	93.74	97.60	3.5	15.20	89.0	18984.89
201	99.43	81.10	3.5	14.86	109.0	19424.07	244	96.58	97.60	3.5	15.20	89.0	18984.89
202	102.27	81.10	3.5	14.86	109.0	19424.07	245	99.43	97.60	3.5	15.20	89.0	18984.89
203	105.12	81.10	3.5	14.86	109.0	19424.07	246	102.27	97.60	3.5	15.20	89.0	18984.89
204	107.96	81.10	3.5	14.86	109.0	19424.07	247	105.12	97.60	3.5	15.20	89.0	18984.89
205	110.81	81.10	3.5	14.86	109.0	19424.07	248	107.96	97.60	3.5	15.20	89.0	18984.89
206	113.65	81.10	3.5	14.86	109.0	19424.07	249	110.81	97.60	3.5	15.20	89.0	18984.89
207	116.50	81.10	3.5	14.86	109.0	19424.07	250	113.65	97.60	3.5	15.20	89.0	18984.89
208	119.34	81.10	3.5	14.86	109.0	19424.07	251	116.50	97.60	3.5	15.20	89.0	18984.89
209	122.19	81.10	3.5	14.86	109.0	19424.07	252	119.34	97.60	3.5	15.20	89.0	18984.89

ROD NO.	X- ORDINATE (FT.)	Y- ORDINATE (FT.)	DIAMETER (IN.)	LENGTH (FT.)	TENSION (KIPS)	STIFFNESS (KIPS/FT)
253	122.19	97.60	3.5	15.20	89.0	18984.89
254	125.03	97.60	3.5	15.20	89.0	18984.89
255	69.38	102.35	4.0	15.30	121.0	24636.23
256	126.63	102.35	4.0	15.30	121.0	24636.23
257	70.98	104.00	2.5	15.34	45.0	9601.96
258	73.82	104.00	2.5	15.34	45.0	9601.96
259	76.67	104.00	2.5	15.34	45.0	9601.96
260	79.51	104.00	2.5	15.34	45.0	9601.96
261	82.36	104.00	2.5	15.34	45.0	9601.96
262	85.20	104.00	2.5	15.34	45.0	9601.96
263	88.05	104.00	2.5	15.34	45.0	9601.96
264	90.89	104.00	2.5	15.34	45.0	9601.96
265	93.74	104.00	2.5	15.34	45.0	9601.96

ROD NO.	X- ORDINATE (FT.)	Y- ORDINATE (FT.)	DIAMETER (IN.)	LENGTH (FT.)	TENSION (KIPS)	STIFFNESS (KIPS/FT)
266	96.58	104.00	2.5	15.34	45.0	9601.96
267	99.43	104.00	2.5	15.34	45.0	9601.96
268	102.27	104.00	2.5	15.34	45.0	9601.96
269	105.12	104.00	2.5	15.34	45.0	9601.96
270	107.96	104.00	2.5	15.34	45.0	9601.96
271	110.81	104.00	2.5	15.34	45.0	9601.96
272	113.65	104.00	2.5	15.34	45.0	9601.96
273	116.50	104.00	2.5	15.34	45.0	9601.96
274	119.34	104.00	2.5	15.34	45.0	9601.96
275	122.19	104.00	2.5	15.34	45.0	9601.96
276	125.03	104.00	2.5	15.34	45.0	9601.96

$c_{56} = .546 \times 10^6$ K-ft

$c_{66} = 1.623 \times 10^6$ K-ft

Also,

$a_{11} = a_{22} = a_{33} = 534.18$ K-sec^2/ft

$a_{44} = 1.804 \times 10^6$ K-sec^2-ft

$a_{55} = 1.559 \times 10^6$ K-sec^2-ft

$a_{66} = 0.9419 \times 10^6$ K-sec^2-ft

$a_{45} = 0.$

$a_{46} = 0.$

$a_{56} = -0.2125 \times 10^6$ K-sec^2-ft

The following table lists the results obtained by solving the eigenvalue eqns. (3.37).

Table 10

Results of Analytic Analysis of New Madrid Steam Generator

Mode No.	1	2	3	4	5	6
Natural Frequency	.20073	.23868	.24534	5.5455	6.5620	13.488
u	1.0000	-0.0094	1.0000	-0.1611	0.	0.
v	.0009	1.0000	.0009	0.	-0.0159	.0001
w	0.	0.0018	0.	-0.0067	1.0000	1.0000
θ	0.	-0.0003	0.	0.	-0.1399	0.0021
ϕ	0.	0.	.0001	1.0000	0.	0.
ψ	.0530	0.	-0.0107	.2264	0.	0.

A plot of mode shapes is presented in Fig. 15. It may be noticed that the torsional mode appears before the translational modes. After third frequency there is a considerable amount of jump to fourth frequency. Also, the fourth, fifth and sixth modes are associated with vertical translation. These frequencies are of no interest to us.

The natural frequencies of the discrete mass model connected by rigid massless bars and supported at the top by four equivalent beam members are also obtained. Table 11 compares the frequencies with those obtained by the analytical analysis. Fig. 16 shows the mode shapes of the finite element model.

Table 11

Comparison of Results of Two Analyses of New Madrid Steam Generator

Mode No.	Natural frequency of the finite element model	Natural frequency obtained by analytical analysis	% difference
1	0.21339	0.20073	6.30
2	0.23801	0.23868	-0.28
3	0.24507	0.24534	-0.11

Chapter 4

RESULTS AND OBSERVATIONS

4.1 System No. 1 - Paradise Steam Generator and its Supporting Structure

The system No. 1 is notoriously complex and no previous computation on the natural frequencies have been done for similar systems without severe simplifications. It appears that some analysis of the subsystems are needed before the total system could be considered. Such preliminary subsystem analyses are important for the following reasons. By carefully selecting and neglecting certain portions of the total system, the effects of those portions on the dynamic behaviors can be studied and the consistency among various sets of results can be checked. Such analyses not only provide with the insights to the problem but also the confidence in the computer program used.

Four subsystems, all related to the central portions of the system, had been analyzed before the total system was studied.

4.1.1 The central structure without both the steam generator and the bracing members

The central portion of the supporting frame structure as shown in Fig. 17 was first analyzed. The steam generator and the cross bracing members were neglected. This structure has 434 joints and 865 beam and column members. Among the 434 joints, 36 are at the base. This results in a total of 1968 equations. The way that the joints are numbered results in a matrix bandwidth of 426.

The first mode frequency was found to be 0.4299 Hz. The corresponding normal mode shape plotted in a three-dimensional view for the outside members is shown in Fig. 18. Because of the unsymmetrical arrangement of the members within the structure, the mode shape is seen to be a combination of strong side-swaying motion and slight torsional motion. The eigenvector output shows that the vertical displacements of all the joints are two-order of magnitude smaller than the horizontal displacements. Such degrees of freedom could have been suppressed in the analysis of the first few modes.

The central processing time for the CDC 6500 computer was 50 minutes. However, the transfer of information between the peripheral processor and the central processor required about eight hours.

4.1.2 The central structure without the steam generator but with the bracing members

There are a total of 147 cross bracing members in the central portion of the structure. They are all in the vertical planes. The bracing members have been known to have stiffening effect on the frame structure. They were included in the free vibration analyses of the central structure.

The fundamental natural frequency for this subsystem was found to be 0.5517 Hz. The bracing members are seen to stiffen the structure and increase the fundamental frequency by 28%. The corresponding normal mode shape in a three dimensional view is shown in Fig.19. Because the arrangement of the cross bracing members is quite irregular and nonsymmetrical, the torsional motion is more pronounced than that seen in the previous case. The computation for this case took virtually the same amount of time as the previous case.

4.1.3 The central structure with the steam generator but without the bracing members

The steam generator, without including the air heater, has a total weight of 24,000 kips. The central structure without bracing members has a total weight of 7400 kips. When the two subsystems are combined, the natural frequencies should be considerably less than those for the central structure alone.

The fundamental natural frequency was found to be 0.1556 Hz as compared with the 0.4299 Hz found for the central structure without the steam generator. A 64% drop in fundamental frequency is seen. The corresponding normal mode shape is shown in Fig. 20. The mode is seen to be predominantly in side-swaying motion with unnoticeable torsional motion. The swaying motion of the steam generator, which is symmetrical about one vertical plane, apparently overrides the slight torsional motion of the central structure.

Since the fundamental mode for this case contains only side-swaying motion with no torsional motion, the second mode was also found and shown in Fig. 21. The second mode shows a side-swaying motion in the direction perpendicular to that of the first mode. Again no torsional motion is seen. The second mode freqeuncy was found as 0.1987 Hz which is 28% higher than the first mode frequency.

It is noted that this subsystem is quite similar to (but with considerably more complexity in modeling) the simple three-dimensional box model used by Suehiro [Ref. 3] for the analysis of a 1000 MW steam generator structure. The first two normal modes found here agree well with the first two mode shapes found by Suehiro.

The system has a total of 2328 equations with a bandwidth of 474. The CDC 6500 central processing time was 96 minutes for the first mode and 104 minutes for both the first and the second modes.

4.1.4 The central structure with both the steam generator and the bracing members

With the inclusion of the 147 cross bracing members, the central frame structure is expected to be stiffer. The fundamental mode natural frequency is found to be 0.2060 Hz which is 32% higher than the structure without the bracings. The corresponding normal mode shape for the frame structure in a three dimensional view is shown in Fig. 22. A predominant side-swaying motion is seen. The corresponding normal mode shape for the steam generator is shown in Fig. 23. It is noted that the rigid-body translational motion in the direction of the frame motion is not shown. Only the pendulum type swining motion, which is in the same direction as the frame motion, is shown.

The CDC 6500 central processing time used was 101 minutes.

A summary of the results for the first natural frequencies for the four subsystems is given in Table 12. The results are seen to be consistent among the four cases.

After confidence had been gained through computation and evaluation of the results for the four subsystems, the total system was analyzed.

Table 12

THE FIRST MODE FREQUENCIES FOR THE ANALYSES OF CENTRAL STRUCTURE

Subsystem Number	Steam Generator	147 Bracing Members	Number of Degrees of freedom	Band Width	CDC 6500 CP Time (Minutes)	Frequency
1	No	No	1968	426	50	0.4299 Hz
2	No	Yes	1968	426	52	0.5517 Hz
3	Yes	No	2328	474	96	0.1556 Hz
4	Yes	Yes	2328	474	101	0.2060 Hz

4.2 The Total System No. 1 - The Paradise Plant

The total system contains the steam generator model and the supporting structure model, as described in the section of modelling, plus the airheater which has 15% of the mass of the steam generator. The supporting structure contains 1412 beam and column elements, 370 cross bracing members, two concrete floors and 611 joints. In the computation of the first few frequencies, all the vertical displacement degrees-of-freedom were found to be two orders of magnitude smaller than the lateral displacement degrees of freedom. Such displacements are customarily neglected. Excluding the zero degrees-of-freedom of the fixed joints, the total systems results in a set of 2715 equations. The present way of numbering of the joints results in a semi-bandwidth of 472. A system of this size needs over 8 hours of central processing time at CDC 6500 computer of Purdue University to evaluate one frequency. With the additional time required for data transfer between central processor and peripheral processor, a conservative estimate of the time required to compute one frequency and the corresponding mode shape is approximately 50 hours. Obviously, some slight modification of the model must be made to reduce the size of the problem so that the necessary computing time is not formidably long. An observation of the model (Fig. 7) shows that the columns in the side structure are connected by lesser members. They are less stiff and contain less mass. Therefore, some joints in the vertical plane 2l and fv are eliminated. All the masses and stiffnesses associated with these joints are redistributed to the adjacent joints and members. The redistribution of stiffnesses are done by a tedious static analysis to create members with equivalent stiffnesses. It is felt that for such a large system, such modification should not significantly affect the results. The final modified model consists of 415 nodal points, 878 beam elements, 412 truss elements, 38 isotropic plate elements and 150 orthotropic plate elements. This results in 1860 equtions. The semi-bandwidth of the stiffness matrix is 412.

To solve the eigenvalue problem resulting from the above model, subspace iteration algorithm as described in section 2.1.2 is used. To evaluate one natural frequency about 82 minutes of central processor time is needed. Another 10 to 12 hours is needed to transfer information between peripheral processor and the central processor. Twelve natural frequencies have been calculated. The program is written such that it evaluates one frequency and associated mode shape at a time. Information after evaluation of each frequency is stored at magnetic tape to be used for the evaluation of subsequent frequency. An average of eight iterations were performed to obtain convergence for each frequency. The convergence criteria was set that in the i-th iteration $|(\omega_i^2 - \omega_{i-1}^2)/\omega_i^2| \leq 0.00001$, where, ω_{i-1} is the circular frequency obtained in the (i-1)th iteration and ω_i is that obtained in the i-th iteration.

Table 13 lists the result obtained for the system No. 1 (the steam generator and its supporting structure at Paradise Plant). Figs. 24-67 illustrate the normal mode shapes associated with the various frequencies in different perspectives viz., three dimensional view, plan view at the top of the structure, elevation view on line Nz looking west, side view on line 20 looking south. The lines Nz and 20 are marked in Fig. 3. Views on various other sections have also been plotted and studied. However, these views are not presented in this report.

The normal mode shapes for the supporting structure corresponding to the first natural frequency is shown in a three dimensional view in Fig. 24. It is seen that the mode includes not only the side-swaying motion in both the north-south and east-west directions, but also torsional motion. A plan view of the top of the structural steel vibrating in first mode is shown in Fig. 25. This figure clearly describes the mixing of the two orthogonal side-swaying motions plus the torsional motion. The first mode motion of the vertical plane frames at the two sides Nz and 20 are shown in Figs. 26 and 27 respectively. The two figures show that none of them is stationary and each vibrates in the 'conventional' first mode of the plane frame.

Table 13

Natural Frequencies of Paradise Plant

Mode No.	Circular Frequency rad/sec	Frequency cycle/sec	Period sec
1	4.4837	.7136	1.4013
2	5.1812	.8246	1.2127
3	6.8978	1.0978	0.9109
4	7.2061	1.1469	0.8719
5	10.1120	1.6093	0.6214
6	10.7740	1.7147	0.5832
7	14.3530	2.2844	0.4378
8	15.4810	2.4638	0.4059
9	16.8060	2.6747	0.3739
10	17.6060	2.8021	0.3569
11	17.6390	2.8074	0.3562
12	19.4920	3.1023	0.3223

The normal mode shapes for the steam generator corresponding to the first mode is shown in a three-dimensional view in Fig. 28. The horizontal rigid-body motion, parallel to the motion of the top girders of the supporting structure are not shown in Fig. 28. Only the pendulum type of swinging motion is shown. The torsional motion seems to be quite pronounced. A top view of the motion of the horizontal cross-section at the top of the steam generator is shown in Fig. 29. It clearly describes the mixing of the translational and torsional modes. To give more description, a front view of the motion of the vertical wall of the steam generator along line AB is shown in Fig. 30 and a side view of the motion of the wall along line BC is shown in Fig. 31. Recalling from chapter 3 that the first natural mode shape of the suspended steam generator was predominantly torsional, it may be assumed that the steam generator has a dominating effect on the first natural mode shape of the combined system of the steam generator and its supporting structure.

Fig. 32 illustrates the second normal mode shape in a three-dimensional view. This mode is composed of side-swaying motion in both north-south and east-west direction. The magnitude of side-sway in east-west direction is much smaller than that in north-south direction. Fig. 33 shows the mode shape of the top plane of the system. The motion is seen to be translational with no twisting. Figs. 34-35 show that the side-swaying motions of the plane frames along lines Nz and 20 are in the 'conventional' first mode.

The system is found to be dominated by torsional motion in the third mode. A three-dimensional view of the system vibrating in the third mode is shown in Fig. 36. The elevation views of the vertical frame at line Nz and the vertical frame at line 20 vibrating in the third mode are shown in Figs. 38 and 39, respectively. The fourth mode is a combination of side-swaying motion in east-west direction and a torsional motion about the vertical axis. Fig. 40 shows this motion in a three-dimensional view. An elevation view along line Nz in Fig. 42 shows that the side-sway along north-south direction is much smaller than that along the east-west direction shown in side view along line 20 in Fig. 43.

Figs. 44-46 illustrate the fifth natural mode shape in various views. An inspection of Fig. 45 reveals that in the fifth mode the side-sway of the structural system in north-south direction takes the 'conventional' form of the second mode vibration of a plane structure. The nodal points appear on a horizontal plane about 120 feet above the bottom of the structural steel. The side-sway in east-west direction shown in Fig. 46 still remain the 'conventional' first mode for a plane structure. There is a torsional motion about the vertical axis also present in this mode of vibration.

The normal mode shapes associated with the sixth through twelfth frequencies are various combination of the fundamental modes of vibration of plane frame in both north-south and the east-west direction plus torsional motion about a vertical axis in various proportions. These mode shapes are represented in Figs. 47-67 in various views.

To visualize the mode shapes better, a computer program was written to plot the three-dimensional view of the structural system. These plots were used to animate the motion of the structure. A motion picture of the animated motion of the structure in the first four natural modes of vibration has been prepared.

RESULT OF RESPONSE SPECTRUM ANALYSIS: With the help of information obtained in the vibration analysis of the system, the response spectrum analysis of the system is carried out as described in chapter 2. The time history of ground acceleration of North-south component of El Centro earthquake of May 18, 1940 as shown in Fig. 68 has been used in eqn. (2.10) to carry out the analysis. The earthquake ground forces are assumed to act in the north-south direction and east-west direction separately.

Table 14 lists the modal participation factors p_{nk} as defined by eqn. (2.23) for the structural system of Paradise Plant. It may be observed from this table that the modal participation factors of the first three modes in both north-south and east-west directions are much greater than those for higher modes. Therefore, the contribution of these modes to the total response of the system is more significant than other modes. Displacement response of the total system is obtained by root-mean-square analysis as described in Chapter 2. Fig. 69 shows the maximum displacement of a column adjacent to the steam generator located at the intersection of planes 23 and Nz both along north-south (weak) and east-west (strong) directions. The lines 23 and Nz are defined in Fig. 3 . The maximum displacement along the weak direction is almost three times larger than that along the strong direction. The maximum displacement at the top of the steel structure is 11.98 inches which is comparable with the maximum deflection of a steel structure of the similar dimensions analysed in Ref. 4.

Response spectrum of the member forces and moments are obtained by substitution of the values of nodal displacements in the element stiffness equations. The maximum nodal forces and moments are obtained by taking the root-mean-square of the various modal responses. For each member in the structural system, the maximum direct stress and maximum shear stress has been obtained using the bi-axial stress formulae. The ratio of maximum direct stress to yield stress and maximum shear stress to elastic shearing strength of the material ASTM A36, of which all the steel members are composed of, has been obtained for each member. These values have been labeled for every member in Figs. 70-84. The numbers without parentheses correspond to direct stress ratio and those included in parentheses correspond to shear stress ratio. It is observed that out of 1290 beam elements in the model, 277 members are stressed beyond the elastic limit and 85 members are stressed to the ultimate strength. The maximum values of the stress ratio are found to be in the regions where the columns support the airheater.

The amount of stresses in the horizontal tie members is of great concern. These ties are the prime means of transferring the lateral inertia load of the steam generator developed during an earthquake to the supporting structure. Table 15 lists the ratio of stress developed in all the tie members to the elastic strength of the material. It is found that out of 11 tie members 2 remain within the elastic limits and 6 remain within the ultimate strength. If the tie members fail during the earthquake, as it is expected, the motion of the steam generator will be entirely different than what has been considered in this linear elastic study. Because of the impact of the steam generator on the support structure, the stress pattern in the structure members will also change.

When the earthquake ground acceleration was assumed to act in the east-west direction, the resulting displacements, and the nodal forces and moments were smaller than those obtained when the earthquake ground acceleration was acting in the north-south directon. The results for this case are therefore not presented in this report.

Table 14

Modal Participation Factors of Paradise Plant

Mode No.	North-South direction	East-West direction	Vertical direction
1	8.6759	31.1430	0.
2	32.8180	-9.3300	0.
3	2.2279	12.2180	0.
4	0.1435	1.2318	0.
5	-0.0149	0.0012	0.
6	1.2787	0.0001	0.
7	-0.1020	0.1540	0.
8	-2.4409	0.4613	0.
9	4.8151	-0.1064	0.
10	0.4126	0.3895	0.
11	0.4774	-0.5204	0.
12	7.7422	3.5222	0.

Table 15

Stress Ratio for Horizontal Ties of Paradise Plant

Tie Number	Elevator	Direction	Location	Stress Ratio
1	114'	F&A	N-W corner	1.475
2	114'	F&A	S-W corner	0.793
3	114'	S to S	S-W corner	1.235
4	132'	F&A	N-W corner	0.653
5	132'	F&A	S-W corner	2.395
6	132'	S to S	S-W corner	3.126
7	154'10"	S to S	S-E corner	5.720
8	188'5"	F&A	N-W corner	2.831
9	188'5"	F&A	S-W corner	1.293
10	188'5"	S to S	S-W corner	1.623
11	188'5"	S to S	S-E corner	2.443

4.3 System No. 2, The New Madrid Plant

The model of the steam generator of this system, as described in chapter 3, consists of 66 lumped masses. The supporting structure consists of 439 nodal points, 31 of which are located at the base. The structure is modelled by 1607 truss elements and 378 beam elements. The steam generator is connected to the supporting structure by 20 tie rods. Apart from the differences discussed earlier in Chapter 1, there is another difference in the supporting structure between system No. 1 and system No. 2. The structure of system No. 2 is symmetrical about a vertical east-west plane. The nodal points of this system are numbered in such a way that the semi-bandwidth of the stiffness matrix is 235. The model results in 1189 equations.

The eigenvalue analysis of this system is performed by subspace iteration technique. About 16 minutes of central processor time was needed to solve one frequency. The actual solution time including the time used to transfer information between the central processor and the peripheral processor was about 4 hours for each frequency. The computation was performed for 12 natural frequencies. Table 16 lists the results obtained and Figs. 85-122 show the normal mode shapes corresponding to these frequencies in various perspectives viz. three-dimensional view, plan view at the top of the structure, elevation view on Line (H) looking east and side view on Line (5) looking north. The Lines (H) and (5) are defined in Fig. 85. Views on various other sections have also been plotted and studied. However, in order to avoid lengthiness and tediousness of presentation they have not been presented in this report.

The normal mode shape of vibration of the supporting structure corresponding to the first natural frequency is shown in a three-dimensional view in Fig. 85. Figs. 86-88 illustrate this mode shape in a plan view looking down at the top of the structure, in an elevation view on line (H) looking east and in a side view on line (5) looking north, respectively. It is seen that the mode of vibration is predominantly of side swaying motion in the north-south direction. The elevation view shows that the side swaying motion along the line (H) is similar to the 'conventional' first mode of vibration of the plane frame. There is also a slight torsional motion associated with this mode which may be observed from the plan view.

The second normal mode, according to Figs. 89-92, comprises mainly a side swaying motion along the east-west direction. The absence of torsional motion from this mode may be noticed from Fig. 90. The side swaying motion along the east-west direction, according to Fig. 92, is similar to the 'conventional' first mode of vibration of the plane frame. The third normal mode of vibration consists of predominantly torsional motion about a vertical axis. This mode shape is illustrated in Figs. 93-95. The fourth and higher modes of vibration, as shown in Figs. 96-122, have motions comprising of the combination of the motions of the first, the second and the third natural modes of vibration of the structural system.

RESULT OF RESPONSE SPECTRUM ANALYSIS: The response spectrum analysis of system no. 2 has been carried out for north-south component of El Centro earthquake of May 18, 1940. The earthquake ground motion is assumed to take place only in north-south (weak) direction of the structural system.

Table 17 lists the modal participation factors p_{hk}. It is observed from this table that the modal participation factors of the first two modes are much greater than those of higher modes. Therefore, in the response spectrum of various quantities (displacements, axial forces, etc.) the contribution of these modes is more significant than other modes. Fig. 123 illustrates the root-mean-square displacement of a representative column located adjacent to the steam generator (H4) both in north-south and east-west directions for comparative purpose. The maximum displacement at the

Table 16

Natural Frequencies of New Madrid Plant

Mode No.	Circular Frequency	Frequency	Period
1	5.3049	.8443	1.1844
2	6.3359	1.0084	.9917
3	8.4312	1.3419	.7452
4	10.853	1.7274	.5789
5	11.047	1.7582	.5688
6	14.073	2.2397	.4465
7	14.713	2.3416	.4271
8	16.538	2.6322	.3799
9	16.583	2.6392	.3789
10	16.632	2.6471	.3778
11	17.738	2.8231	.3542
12	18.069	2.8758	.3477

Table 17

Modal Participation Factors of New Madrid Plant

Mode No.	North-south Direction	East-west Direction	Vertical Direction
1	28.3900	-1.0401	-0.0120
2	1.0499	28.8490	0.0217
3	-0.0862	-0.6611	1.5844
4	-0.0884	-0.3585	1.5383
5	0.0344	-0.2464	1.2053
6	3.8868	-0.1740	-0.0281
7	-0.1427	-0.1963	1.1710
8	-0.0796	0.3528	0.7162
9	-0.0767	0.2471	-1.9274
10	-0.0445	-0.0983	1.6638
11	0.0207	0.8239	0.0158
12	-0.2240	0.9844	-0.3435

Table 18

Stress Ratio for Horizontal Ties of New Madrid Plant

Tie No.	Elevation	Direction	Location	Stress Ratio
1	56'	F&A	West wall	0.01512
2	56'	S to S	NE corner	0.50577
3	56'	S to S	SE corner	0.42821
4	56'	F&A	E wall	0.12318
5	108'	F&A	W wall	0.03662
6	108'	F&A	West inside wall	0.05946
7	108'	F&A	West inside wall	0.00468
8	108'	F&A	West inside wall	0.02405
9	108'	F&A	East inside wall	0.02800
10	108'	F&A	East inside wall	0.04629
11	108'	F&A	East inside wall	0.01991
12	108'	F&A	East wall	0.16186
13	128'9"	S to S	North wall	1.65064
14	128'9"	S to S	NE corner	1.00032
15	128'9"	F&A	East inside wall	0.02348
16	128'9"	F&A	East inside wall	0.00715
17	157'	S to S	North wall	2.84081
18	157'	S to S	South wall	2.46261
19	157'	F&A	West wall	0.14690
20	157'	F&A	East wall	0.04272

top of steel structure is 15.30 inches.

Response spectrum of member axial force is obtained using the nodal displacements. Ratio of axial stress to the yield strength of the material, ASTM A36 steel, of which the truss members are made is calculated for every member. Ratio of axial stress to the critical buckling stress is also obtained for each member. These values for each member is labeled in Figs. 124-138. The number without parentheses represent stress ratio to elastic strength and those included within the parentheses represent stress ratio to critical buckling stress. It is observed that out of 1607 truss members, the stress exceeds elastic limit in 158 members and the ultimate stress in 57 members. The side column members in the rear of the structure in general attain higher stresses.

Because of the importance of horizontal tie member during an earthquake, the stresses developed in these members are listed in table 18. The stresses in only 4 out of 20 tie members cross the elastic limit. Only 2 members exceed the ultimate strength of the material.

The response analysis of system no. 2 is also carried out for 0.5, 1.0, 2.0 and 5.0 percent critical damping. Fig. 139 compares the magnitude of displacement of column H4 for different damping ratios. It is noticed that with the assumption of 0.5% critical damping, the displacements of this column are reduced, in general, by about 33%. This would cause an appreciable reduction in stresses. Since the amount of damping for this structure is not known, no further analysis is carried out for damped case.

SUMMARY AND CONCLUSIONS

The linear elastic structural analyses of two steam generators and their supporting structures have been performed by the use of three-dimensional finite element models. The analyses are performed in two phases. The first phase involves the determination of frequencies of free vibration and the corresponding mode shapes of the multi-degree-of-freedom structural systems and the second phase involves the determination of spectra of various response quantities (e.g. displacements, shear forces, bending moments etc.).

It appears in the literature that no vibration analysis has been performed for such large systems without severe simplifications. In this analysis the model is made as realistically as possible. Fundamental frequencies and corresponding mode shapes have first been found for various subsystems of the Paradise Plant which included or excluded certain portions of the system. The consistency among results for various subsystems has been examined. The steam generators of the two systems need special treatment because of their enormous mass and peculiar dynamic behavior. The analytical equations of motion for each generator treated as rigid body have been derived and the frequencies of free vibration have been calculated and compared with those obtained by finite element modeling.

It is customarily understood that for a symmetrical three-dimensional frame structure, the vibration modes are such that the structure may sway in one direction in the first mode and sway in the orthogonal direction in the second mode. This is true for the boiler-structure system of New Madrid plant which is symmetrical about a vertical east-west plane and consists of many bracing members to transfer the lateral loads. This is, however, not the case for the boiler-structure system of Paradise plant which is non-symmetric and has relatively fewer bracing members. For such a system, the first natural mode of vibration not only includes side-swaying motions in both orthogonal directions, it also includes a torsional motion about a vertical axis. It must be pointed that the torsional motion could not have been included in the simplified analysis with the use of two-dimensional models [Ref. (1-3)]. Three dimensional model must be used if the effect of torsional motions were to be included.

For the boiler-structure system of Paradise plant, 12 natural frequencies and corresponding mode shapes have been obtained. It is found that the first and third modes are predominantly in torsional motion, the second and the fourth modes are predominantly in side-swaying motion. The rest of the modes are dominated by the combination of the torsional and side-swaying motions.

For the boiler-structure system of New Madrid plant, also, 12 natural frequencies and corresponding mode shapes have been obtained. The first and the second modes consist of predominantly side-swaying motion in two orthogonal directions with very little torsional motion present in the first mode. The third mode of vibration comprises a predominantly torsional motion. The higher modes are dominated by the combination of the torsional and side-swaying motions.

The response spectrum analysis of the two structural systems is carried out based on the ground accelerations of El Centro earthquake of May 18, 1940. It is observed that for the Paradise plant the modal participation factors corresponding to first three natural frequencies are much larger than those corresponding to the higher modes. For the New Madrid plant, however, the modal participation factors corresponding to only the first two frequencies are significant. The maximum member forces and moments have been obtained by using the root-mean-square of the modal responses. The member stresses are compared with the elastic strength and the ultimate strength of the material. The stresses in the truss members are also compared with the Euler buckling stresses of the members.

For the boiler-structure system of Paradise plant it is observed that 277 out of 1290 beam members exceed the elastic limit while 85 beam members exceed the ultimate stress. The maximum values of stresses are found to be in the columns that support the airheater. The horizontal tie members connecting the steam generator and support structure of this system seem to be more vulnerable under the present earthquake disturbances. Out of 11 horizontal tie members, 9 exceed the elastic limit and 5 exceed the ultimate stress.

The boiler-structure system of the New Madrid plant has fewer members exceeding the elastic limit and ultimate stress. Out of 1607 truss members, 157 exceed the elastic limit and 57 exceed the ultimate stress of the material. The high stresses are found in the columns at the rear of the structure.

Although the study of two different kinds of structural systems may not provide a basis of generalization, it does give an insight into the structural analysis of complex steam generator structural system within the assumption of linear elastic analysis. Guidelines have been provided for the modeling of such systems for free vibration and response spectrum analysis. Results of natural frequencies, modes and root-mean-square stresses from spectrum analysis have been obtained for the two systems. Such results may be valuable to the structural analysts and designers for the design of large steam-generating power plants.

References

[1] Shiraki, K. and Nakazawa, S.; "Study on the Aseismic Design of Boilers and Structural Steels - Considerations on the Vibration Characteristics and Design Criteria for Boilers and Structural Steels", Mitsubishi Technical Review, Sept. 1968, pp. 184-195.

[2] Anderson, J. C., Srinirasan, R., and Small, R.J.; "Response of Suspended Boilers to Earthquake Motion", Electric Power and the Civil Engineer, ASCE Power Division Specialty Conference, Boulder, Colorado, Aug. 12-14, 1974, pp. 363-387.

[3] Suehiro, T; "Vibration Analysis of a 1000 MW Boiler Frame Structure", Report KBD 19012, Ishikawajima-Harima Heavy Industries Co., Ltd., March 1974 (In Japanese).

[4] An Evaluation of a Response Spectrum Approach to Seismic Design of Buildings, Applied Technology Council, San Francisco, California, Sept. 1974.

[5] Muto, Kiyoshi; Aseismic Design Analysis of Buildings, Maruzek Company, Ltd., Tokyo, 1974.

[6] Flower, W. R. and Schmidt, L. C.; "A Note on Data Checking for Large Framework Analysis", International Journal for Numerical Methods in Engineering, Vol. 4, 1972, pp. 175-179.

[7] Wright, G.C., and Miles, G. A.; "An Economical Method for Determining the smallest Eigenvalues of Large Linear Systems", International Journal for Numerical Methods in Engineering, Vol. 3, 1971, pp. 25-33.

[8] Jennings, A. and Orr, D. R. L.; "Application of the Simultaneous Iteration Method to Undamped Vibration Problems", International Journal of Numerical Methods in Engineering, Vol. 3, 1971, pp. 13-24.

[9] Dong, S. B., Wolf Jr., J. A. and Peterson, F. E.; "On a Direct-Iterative Eigensolution Technique", International Journal of Numerical Methods in Engineering, Vol. 4, 1972, pp. 155-161.

[10] Bathe, K. J. and Wilson, E. L.; "Solution Methods for Eigenvalue Problems in Structural Mechanics", International Journal for Numerical Methods in Engineering, Vol. 6, 1973, pp. 213-226.

[11] Yamamoto, Y. and Ohtsubo, H.; "Subspace Interation Accelerated by using Chebyshev Polynomials for Eigenvalue Problems with Symmetric Matrices", International Journal of Numerical Methods in Engineering, Vol. 10, 1976, pp. 935-944.

[12] Corr, R. B. and Jennings, A.; "A Simultaneous Iteration Algorithm for Symmetric Eigenvalue Problems", International Journal of Numerical Methods in Engineering", Vol. 10, 1976, pp. 647-663.

[13] Housner, G. W., Martel, R. R. and Alford, J. L.; "Spectrum Analysis of Strong-Motion Earthquakes", Bulletin of Seismological Society of America, Vol. 43, No. 2, April 1953, pp. 97-119.

[14] Clough, R. W.; "Earthquake Analysis by Response Spectrum Superposition", Bulletin of Seismological Society of America, Vol. 52, No. 3, July 1962, pp. 647-660.

[15] Turner, M. J. et al., "Stiffness and Deflection Analysis of Complex Structures", Journal of Aeronautical Sciences, Vol. 23, No. 9, Sept. 1956, pp. 805-823.

[16] Clough, R. W. and Tocher, J. L.; "Finite Element Stiffness Matrices for the Analysis of Plate Bending", Proceedings of the Conference of Matrix Methods in Structural Mechanics, Air Force Flight Dynamics Lab. Report TR-66-80, Dayton, Ohio, Oct. 1965, pp. 515-546.

[17] Bathe, K. J. et. al.; "Structural Analysis Program (SAPIV) Manual", University of California, Berkeley, Cal.

[18] Newmark, N. M. and Rosenblueth, E.; Fundamental of Earthquake Engineering, Prentice Hall, 1971.

[19] Goodman, L. E., Rosenblueth, E. and Newmark, N. M.; "Aseismic Design of Firmly Founded Elastic Structures", Trans ASCE 120, 1958, pp. 782-802.

[20] Lo, H. and Bogdanoff, J. L.; "Derivation of Equations of Motion of a Free Rigid Body Steam Generator Supported by Vertical Elastic Rods", Report submitted to the National Science Foundation, October 1977.

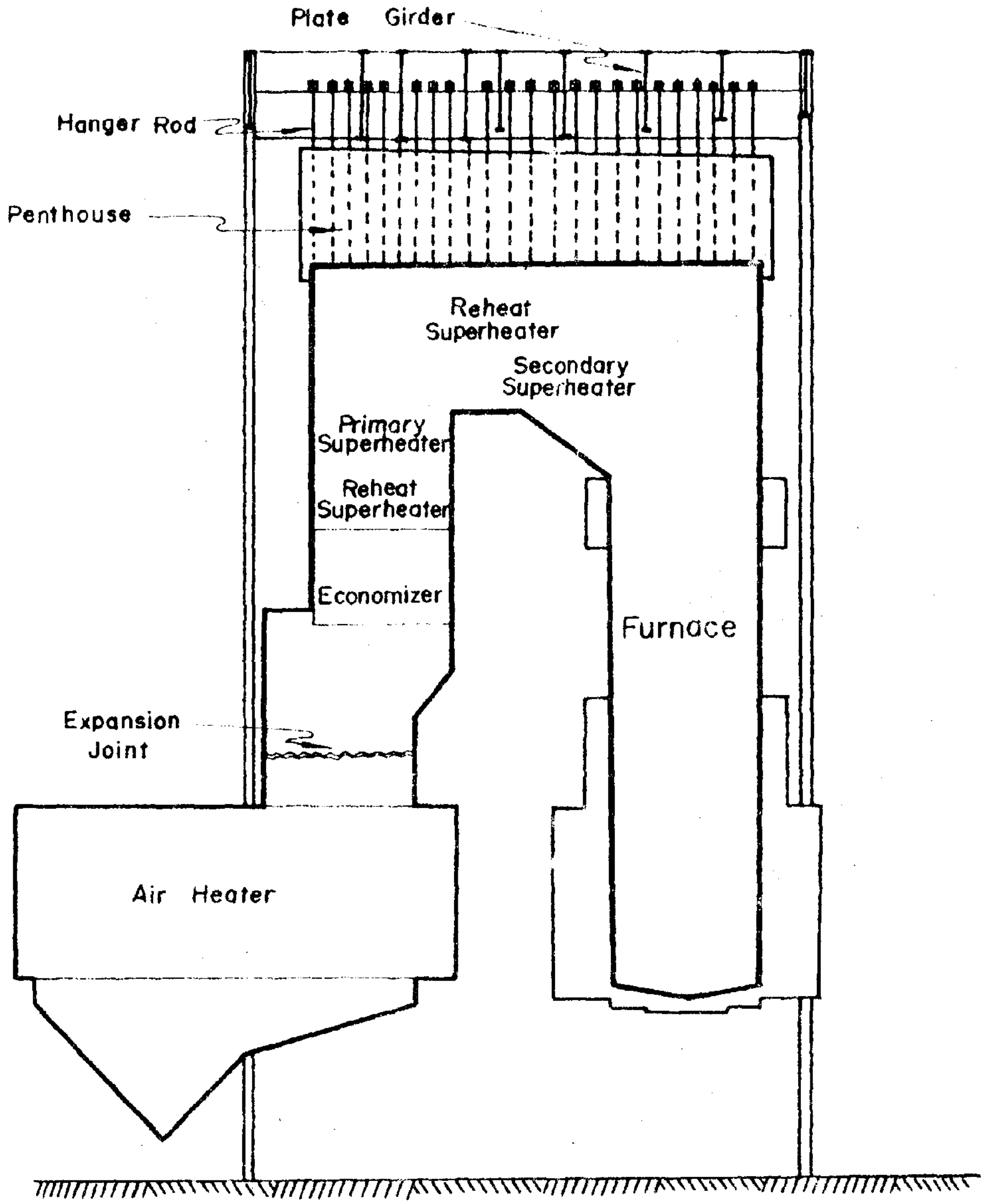

Figure 1

An elevation view of the steam generator of the Paradise plant

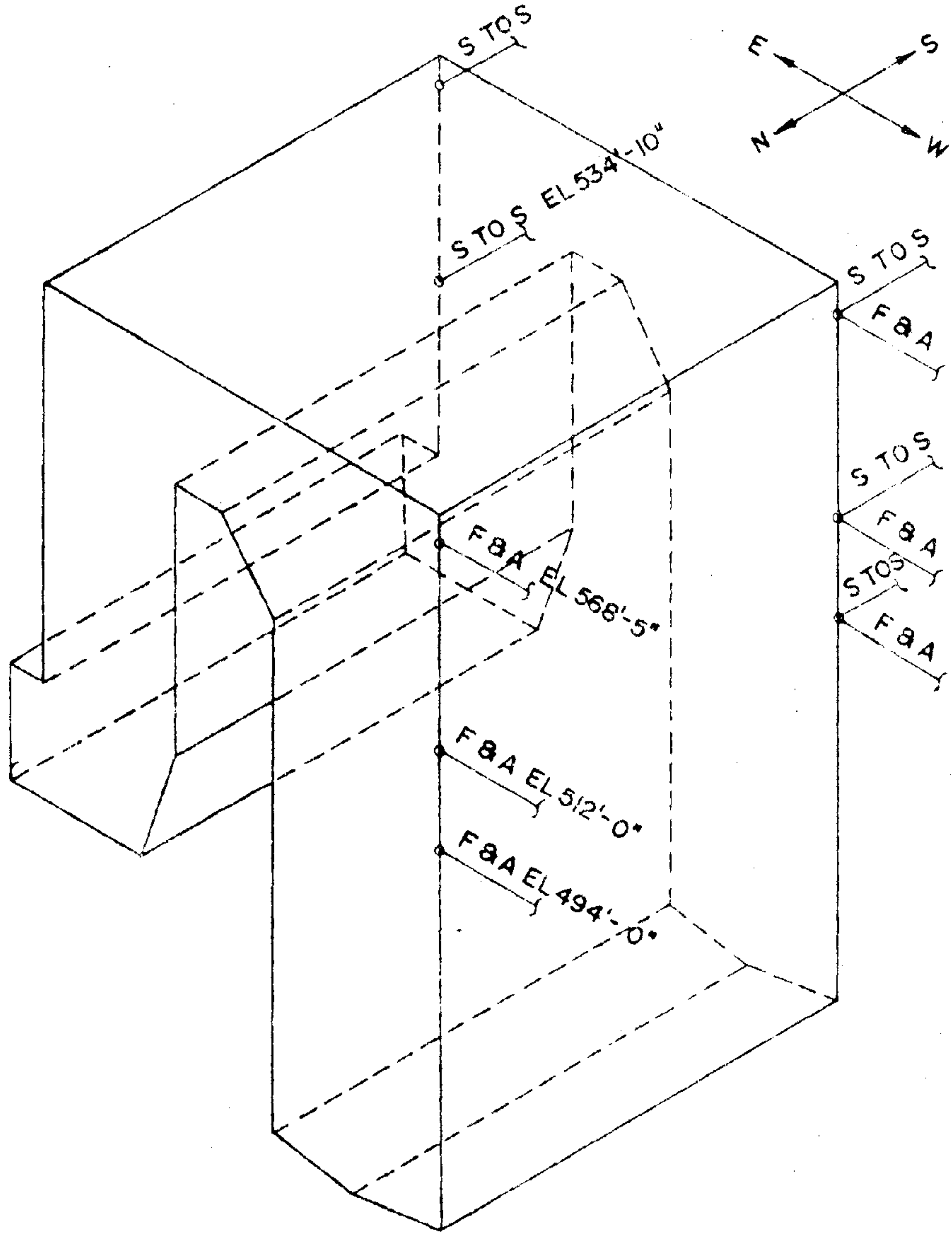

Figure 2

A rough three-dimensional sketch of the steam generator of the Paradise plant and its 11 ties.

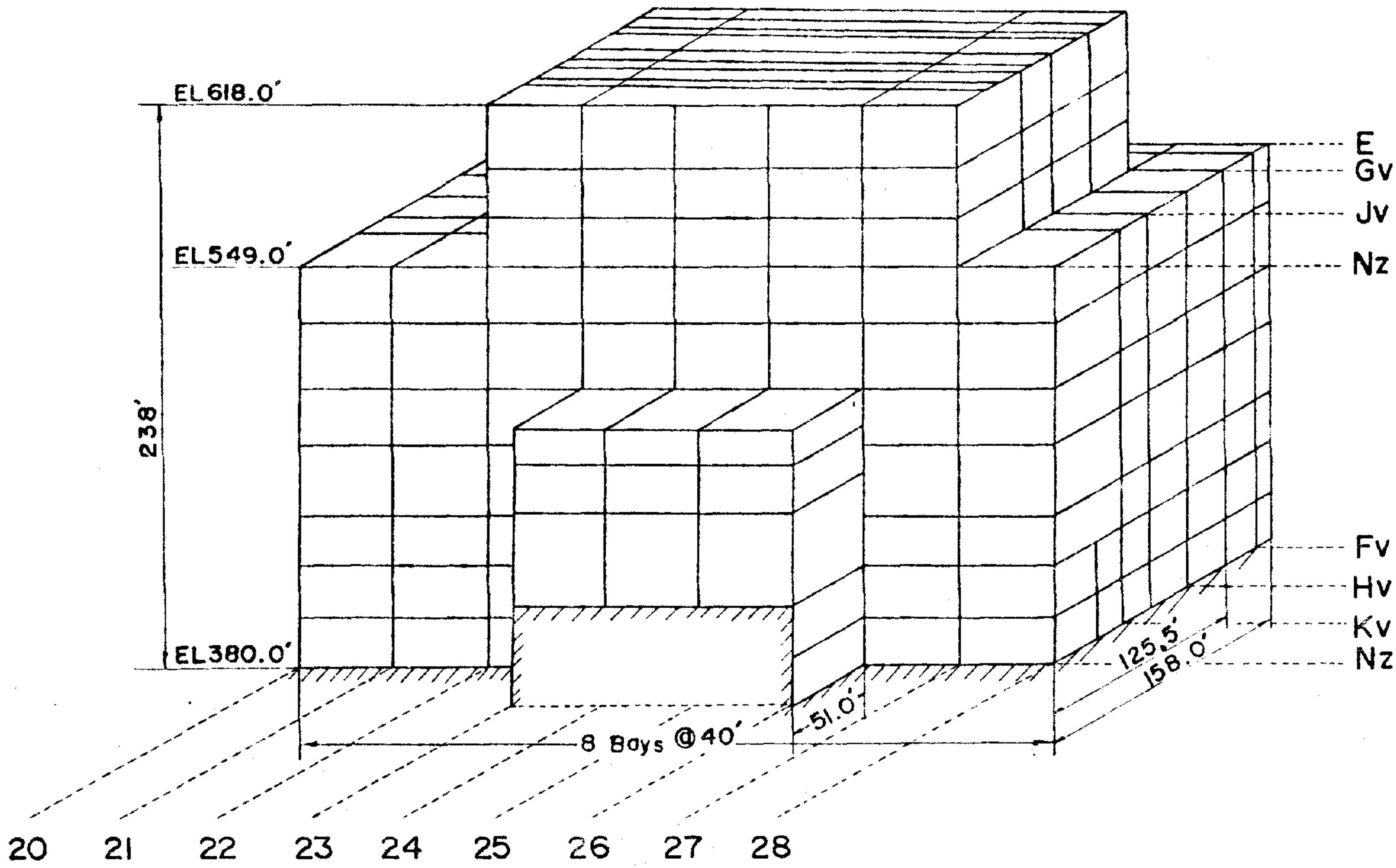

Figure 3

A three-dimensional outside view of the steel framing structure of the Paradise Plant

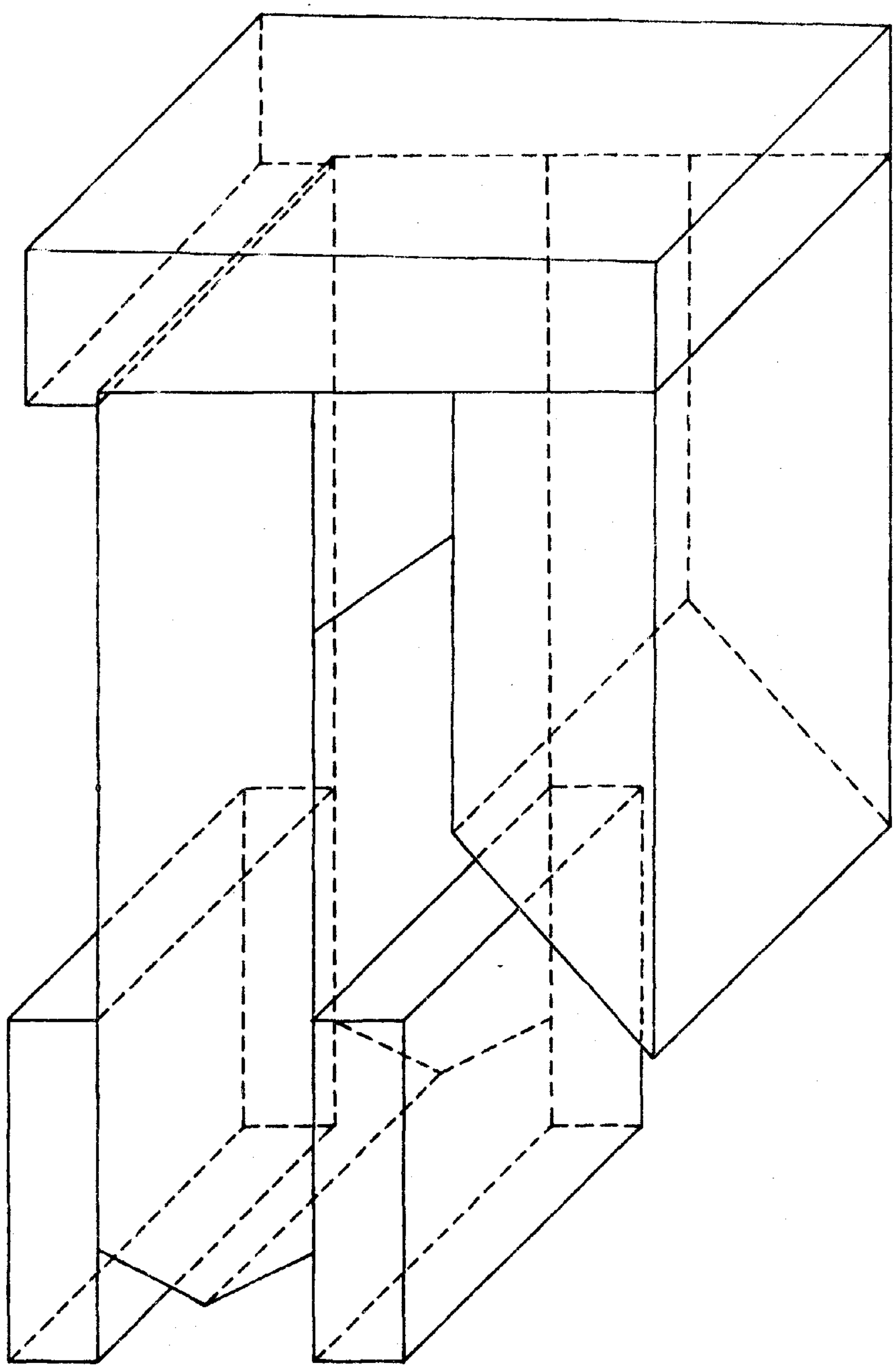

Figure 4

A rough three-dimensional sketch of the steam generator of the New Madrid Plant.

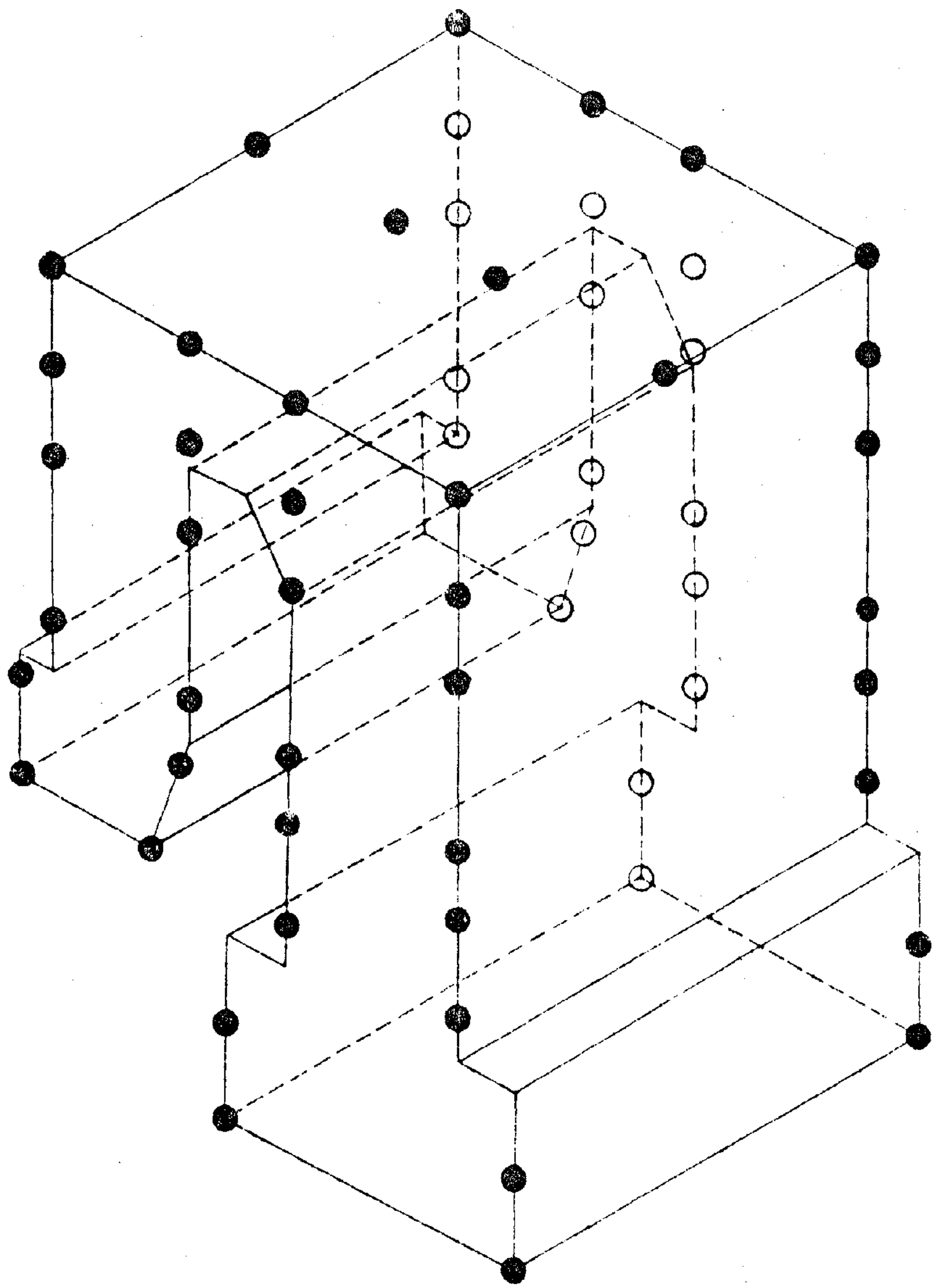

Figure 5

Lumped mass and rigid bar model of the steam generator of the Paradise plant.

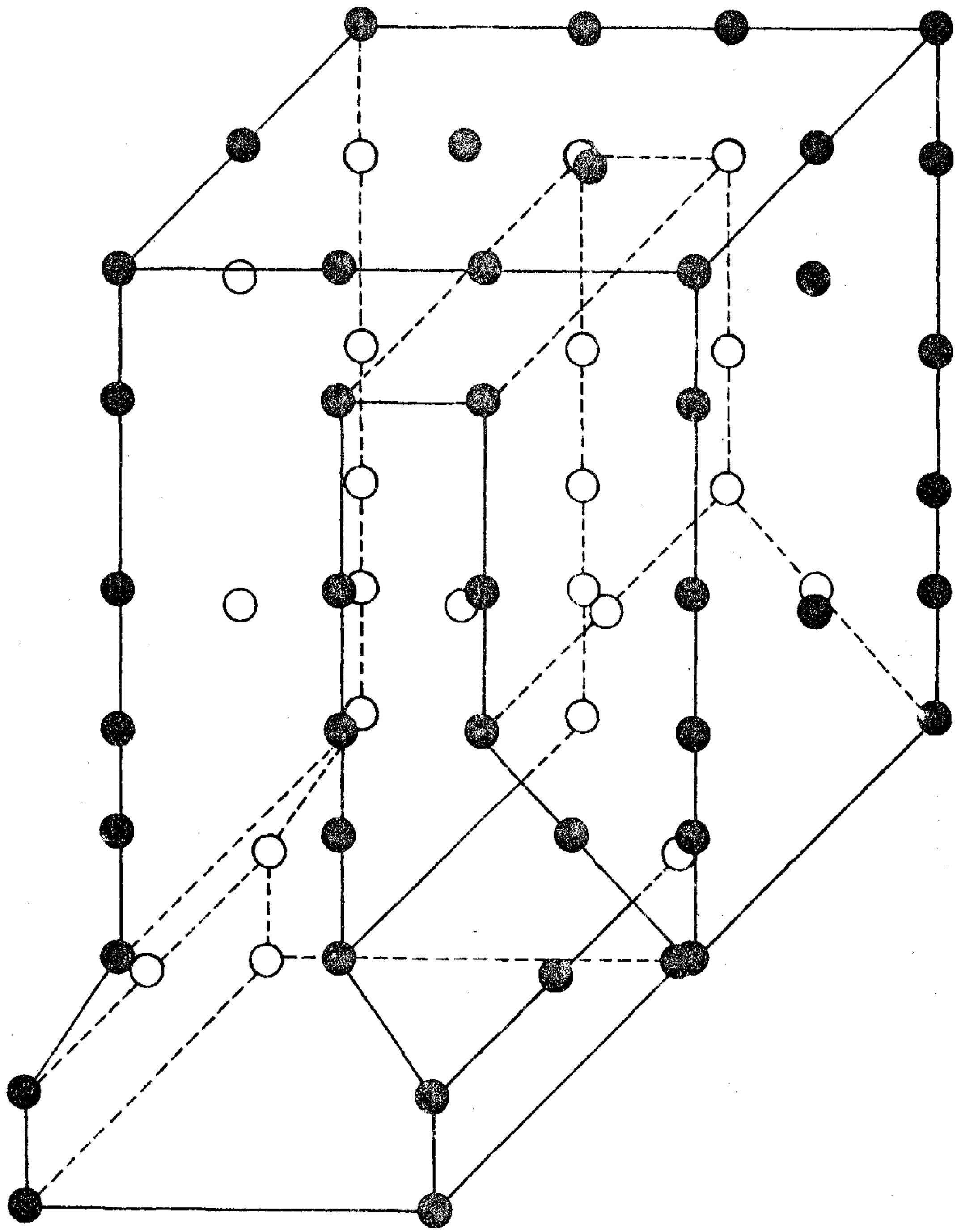

Figure 6

Lumped mass and rigid bar model of the steam generator of the New Madrid plant.

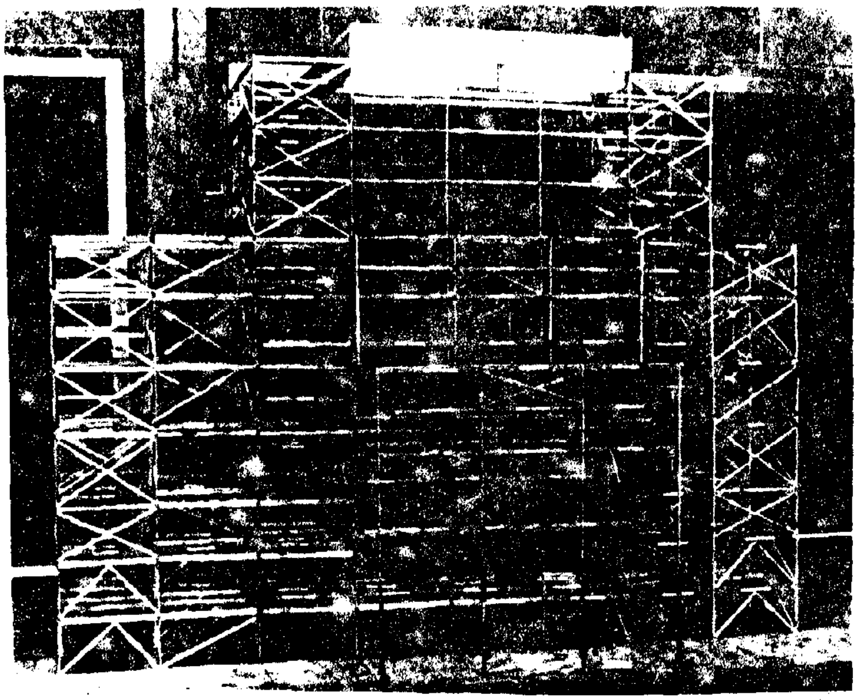

Figure 7

Balsa wood model of the supporting frame structure of the Paradise plant.

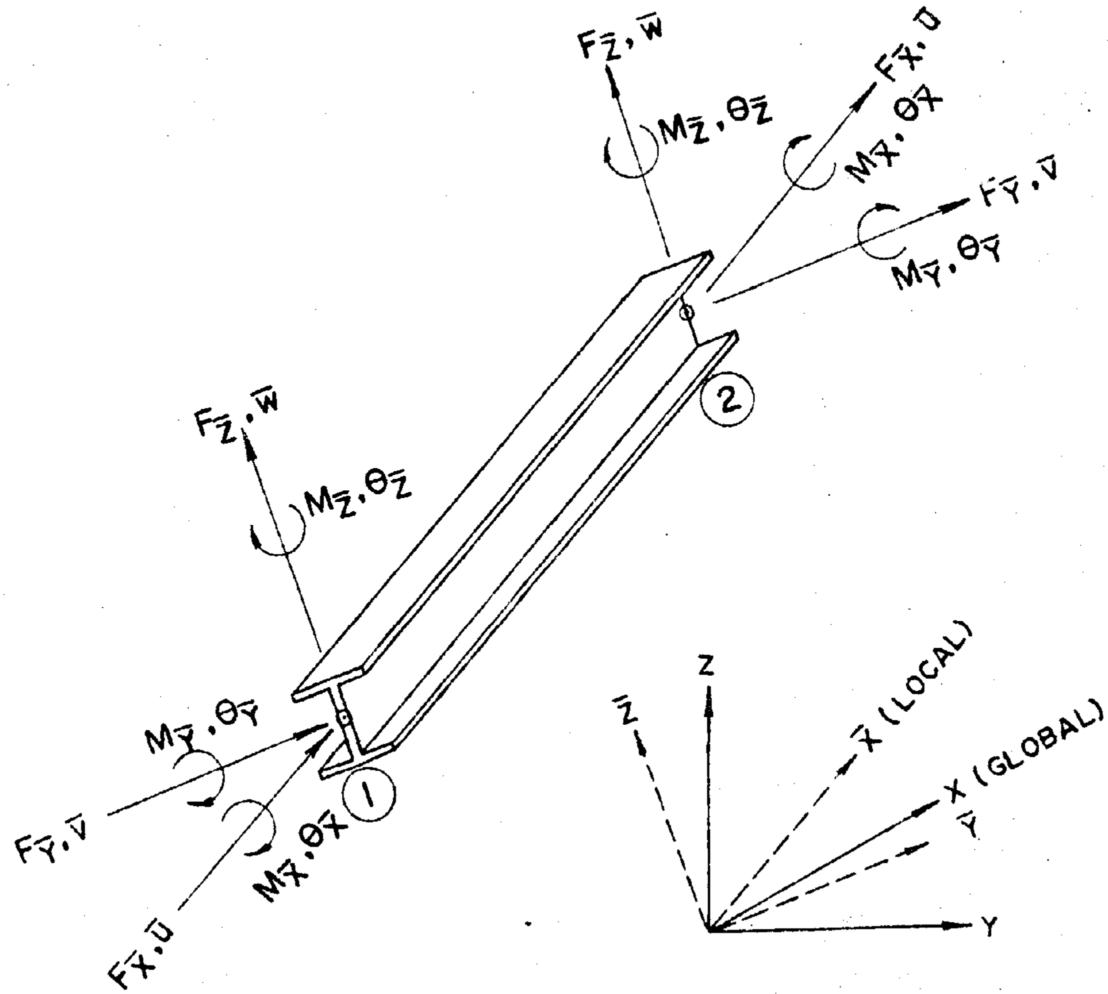

Figure 8

Description of a three-dimensional beam finite element

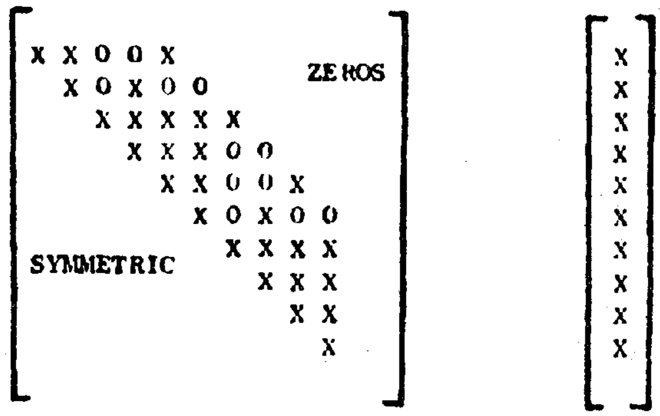

STIFFNESS MATRIX

MASS MATRIX

ACTUAL STRUCTURE MATRICES

O = ZERO ELEMENT

X = NONZERO ELEMENT

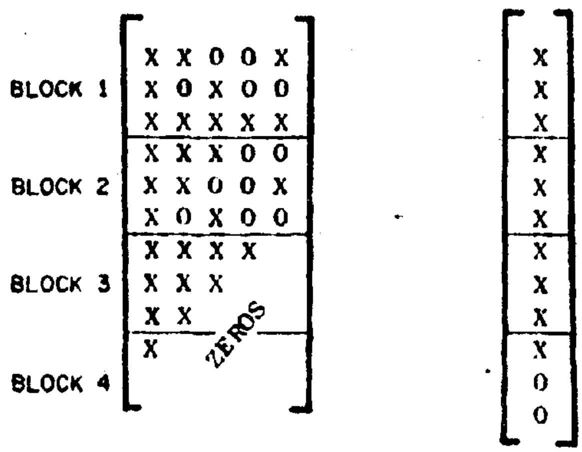

STIFFNESS MATRIX

MASS MATRIX

BLOCK STORAGE OF STRUCTURE MATRICES

Figure 9

Storage of stiffness matrix and mass matrix on the tape.

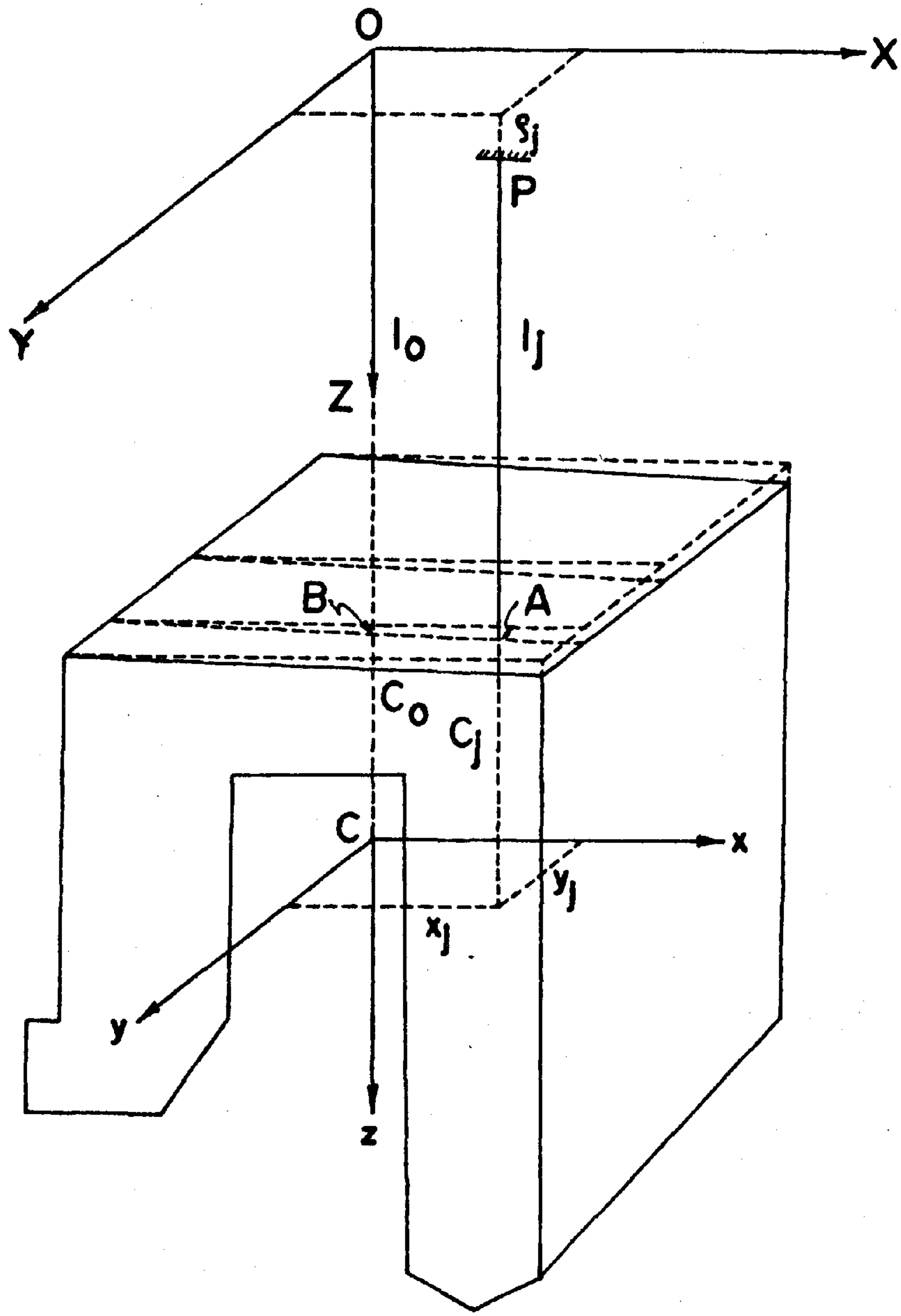

Figure 10

Axes system for the derivation of equations of motion for the steam generator considered as a rigid body.

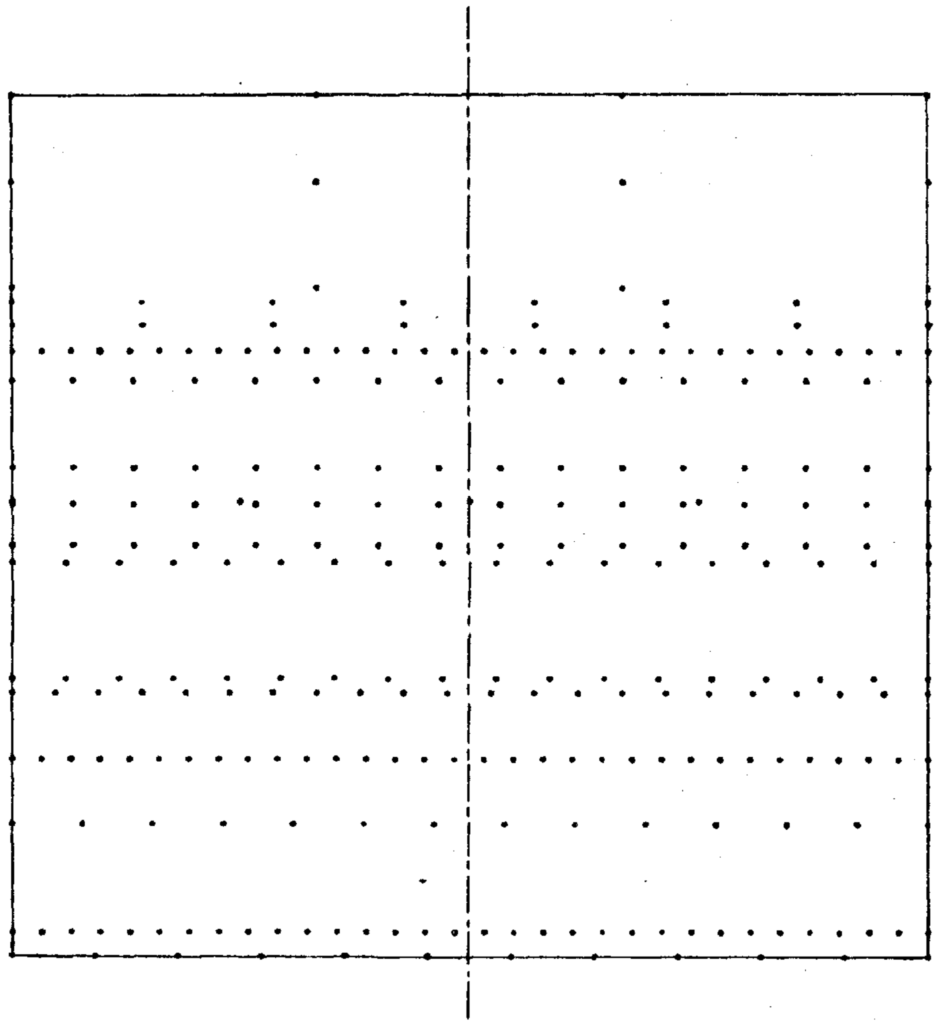

Figure 11

A plan view showing the locations of the hanger rods of the Paradise plant.

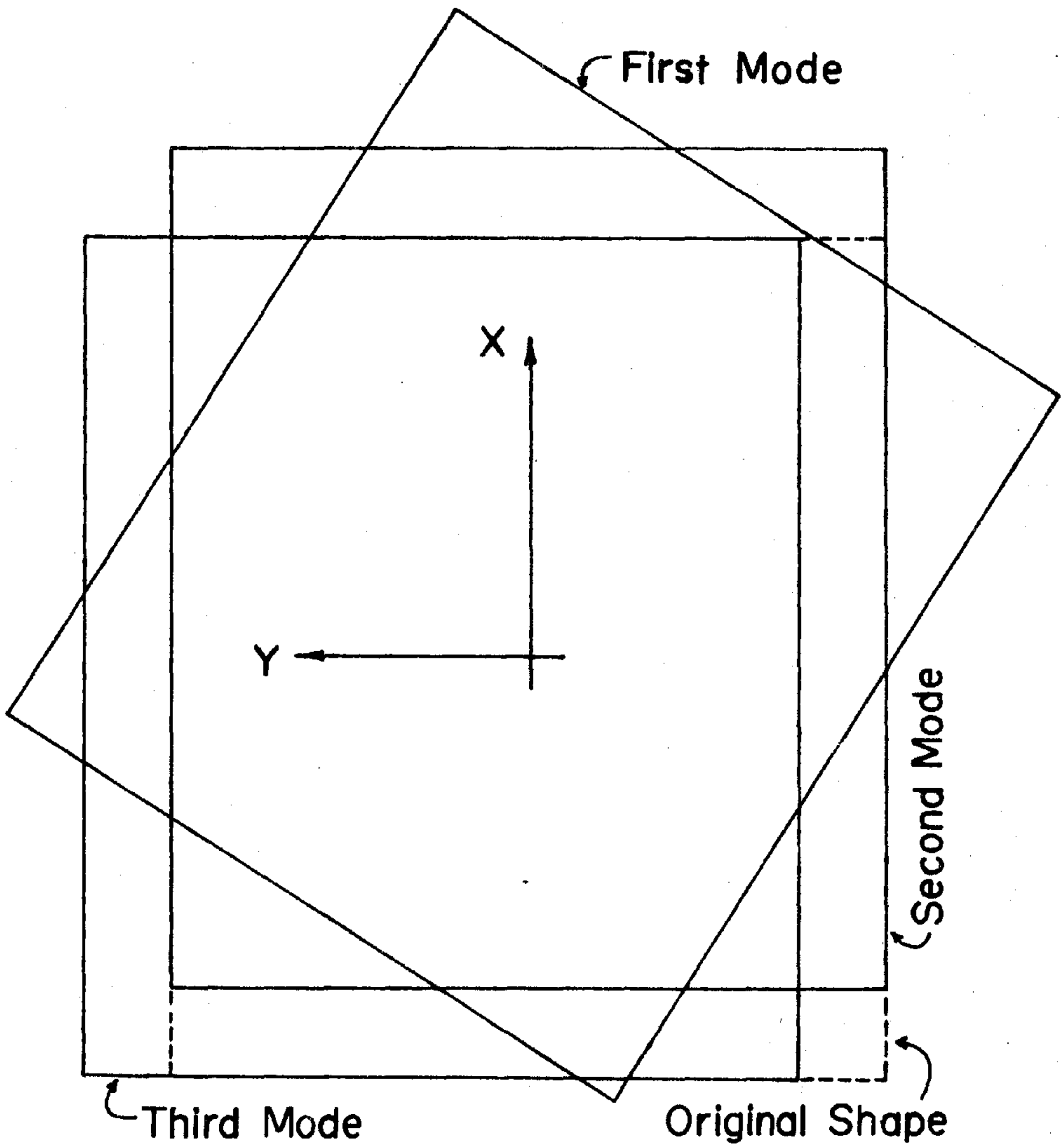

Figure 12

Mode shapes of the rigid steam generator of the Paradise plant obtained by the analytical analysis.

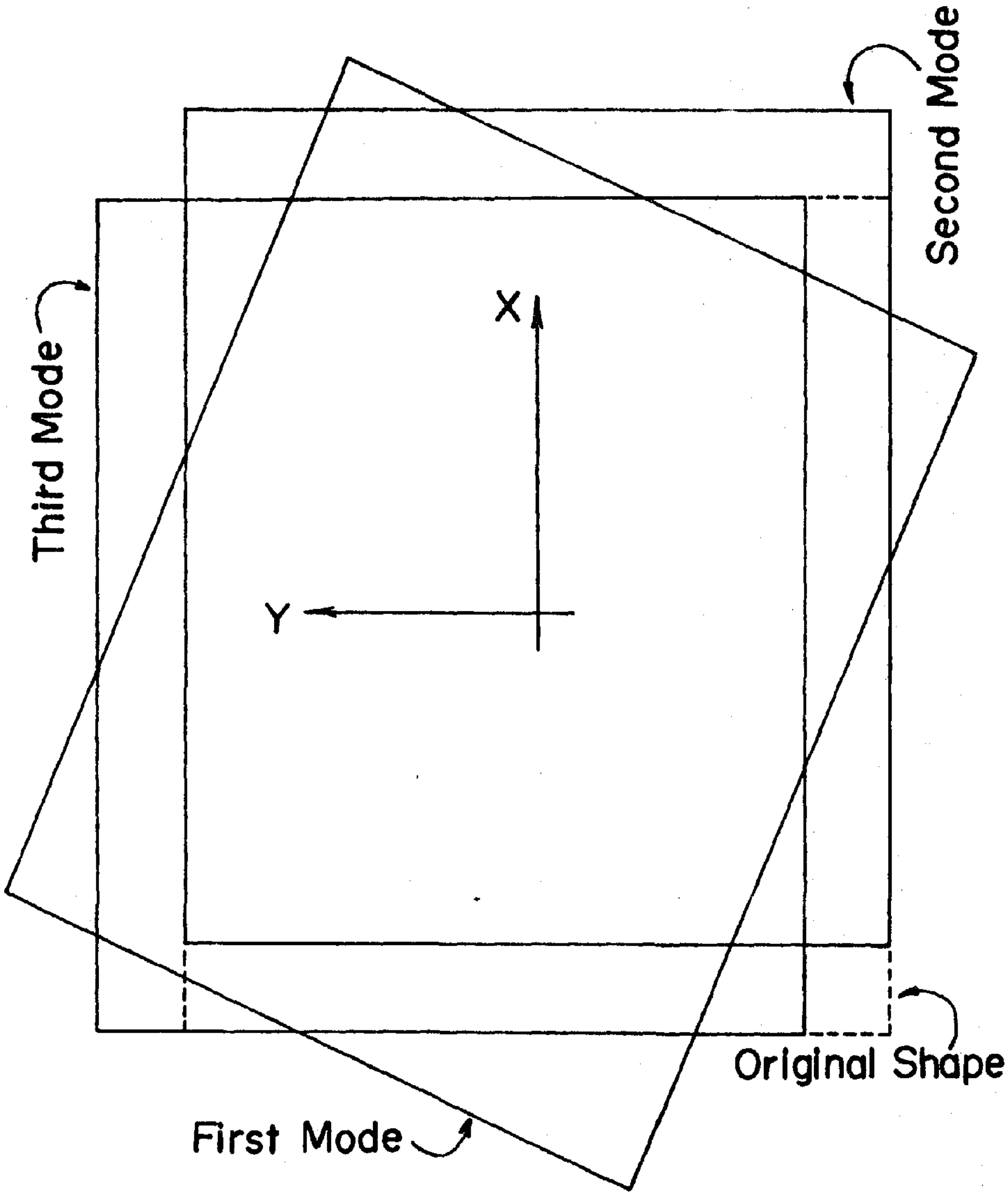

Figure 13

Mode shapes of the rigid steam generator of the Paradise plant obtained by the finite element analysis.

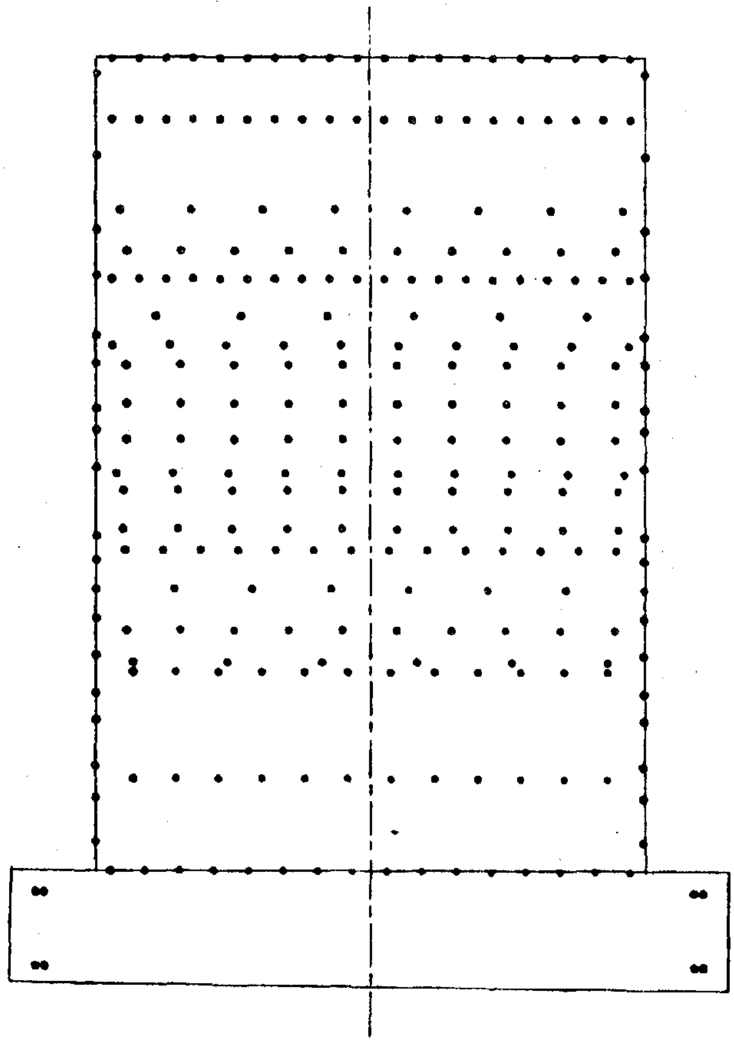

Figure 14

A plan view showing the locations of the hanger rods of the New Madrid plant.

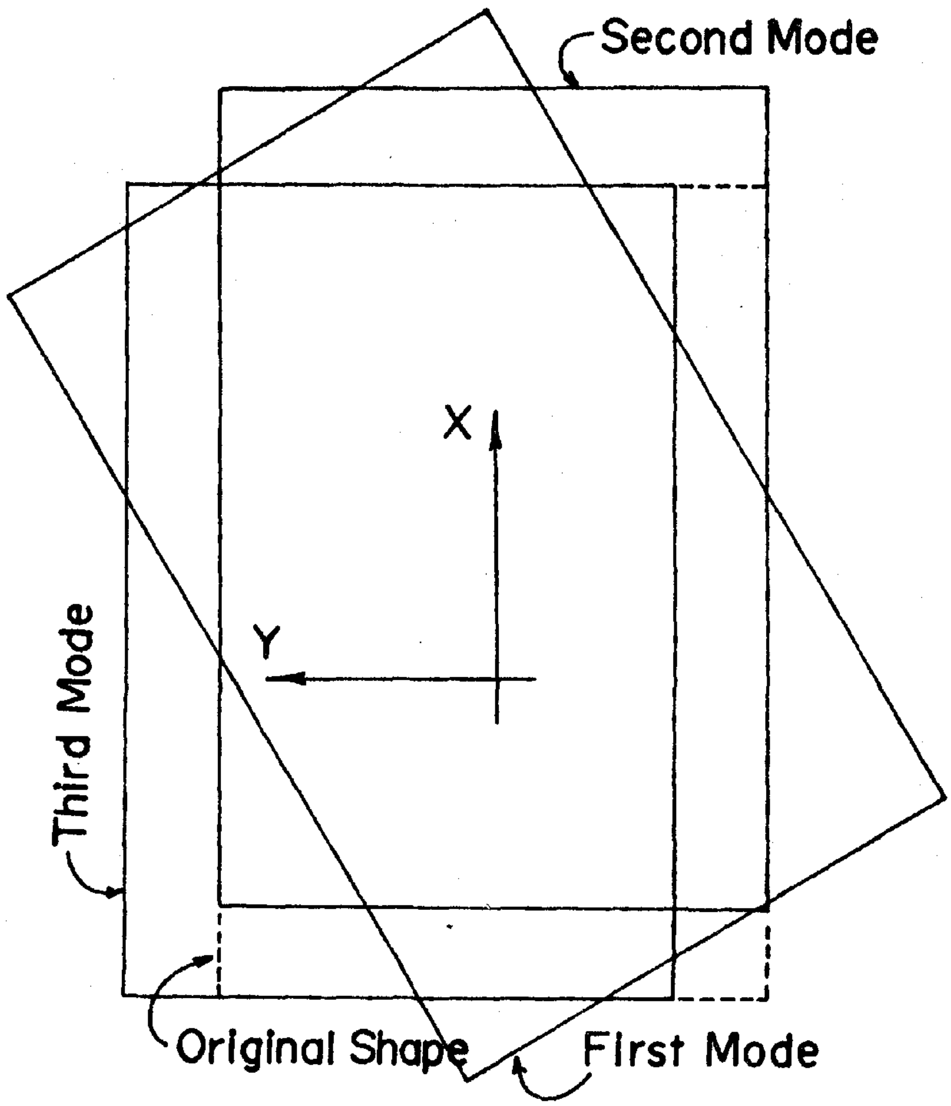

Figure 15

Mode shapes of the rigid steam generator of the New Madrid plant obtained by the analytical analysis.

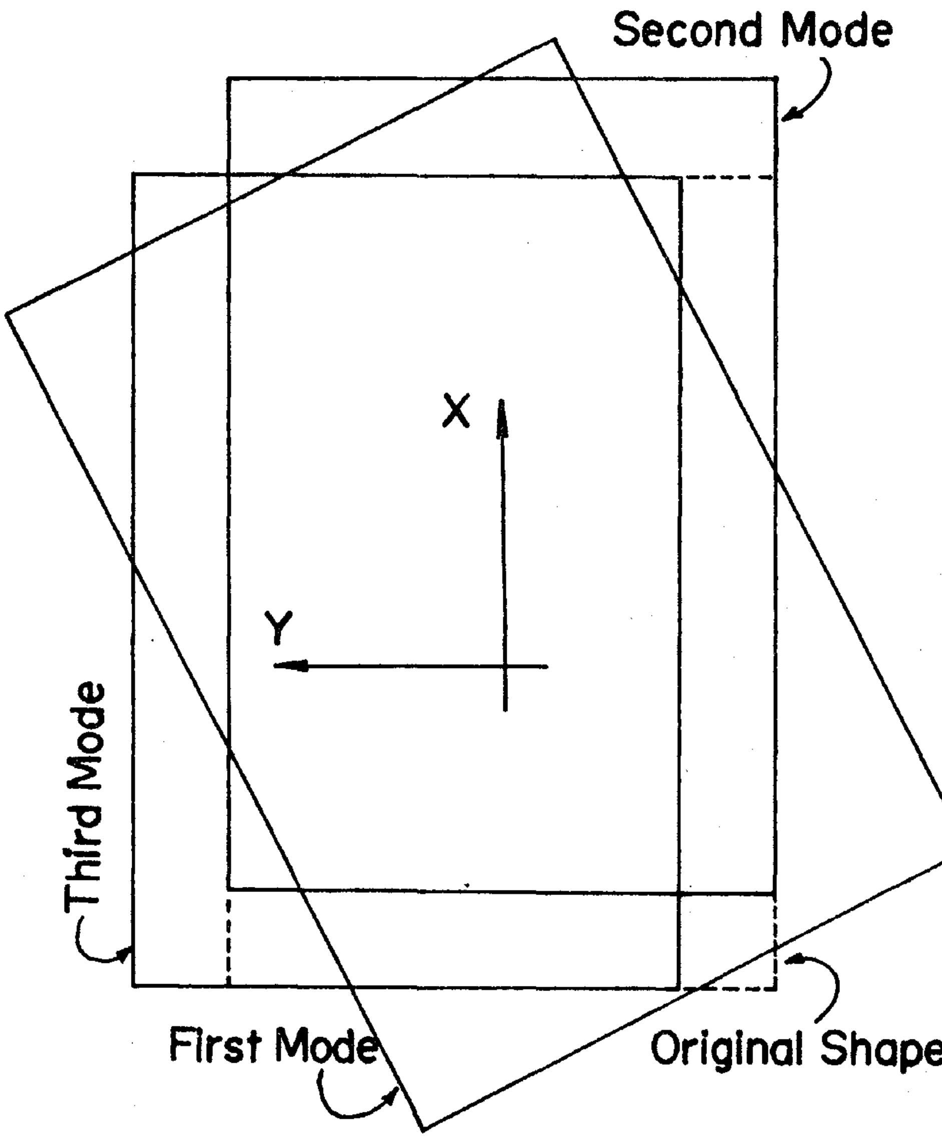

Figure 16

Mode shapes of the rigid steam generator of the New Madrid plant obtained by the finite element analysis.

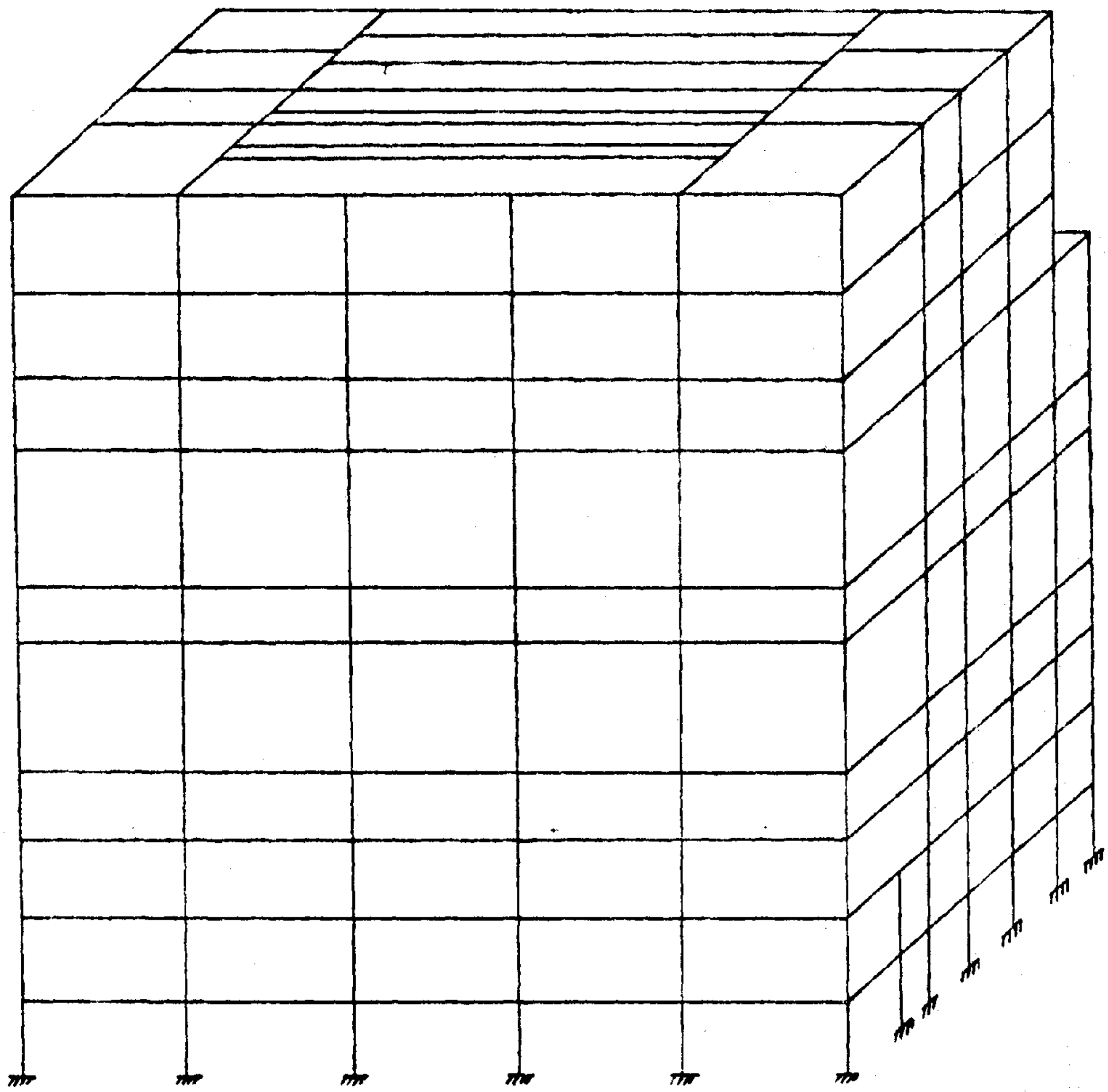

Figure 17

The central portion of the supporting structure of the Paradise plant for initial analysis.

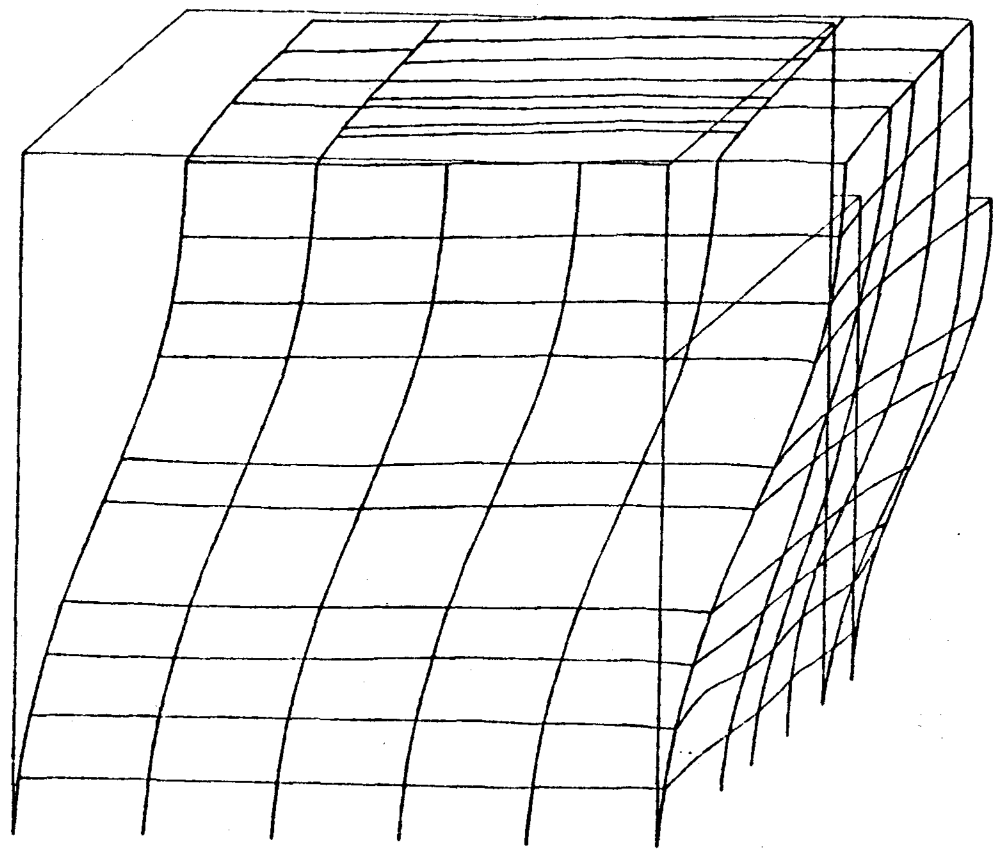

Figure 18

The first mode shape of the central structure without both the bracing members and the steam generator (f_1 = 0.4299 Hz).

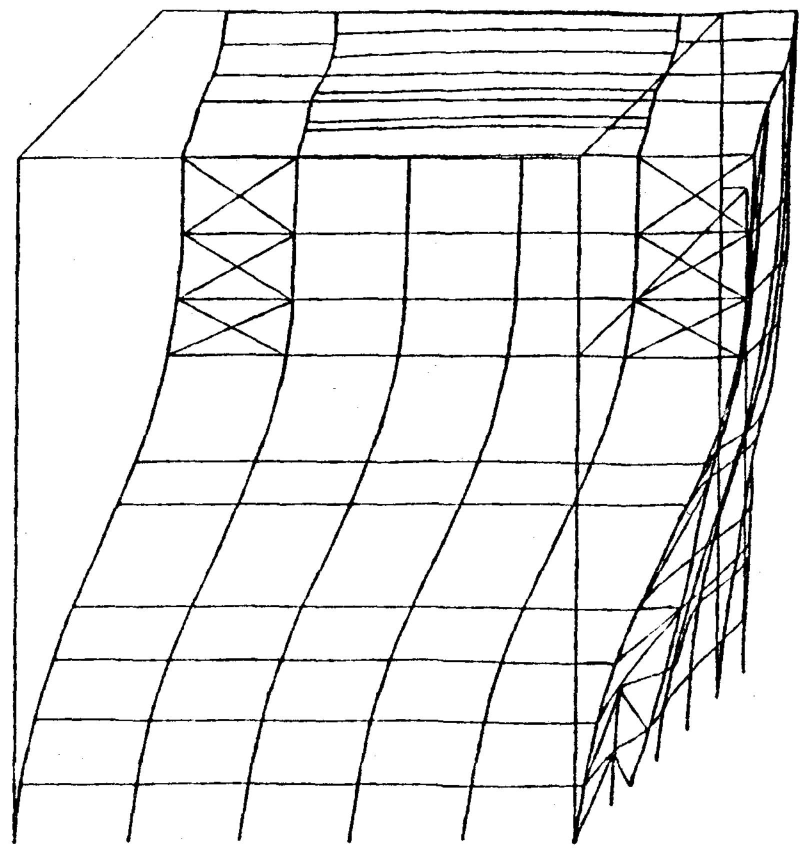

Figure 19

The first mode shape of the central structure without the steam generator but with the bracing members (f_1 = 0.5517 Hz).

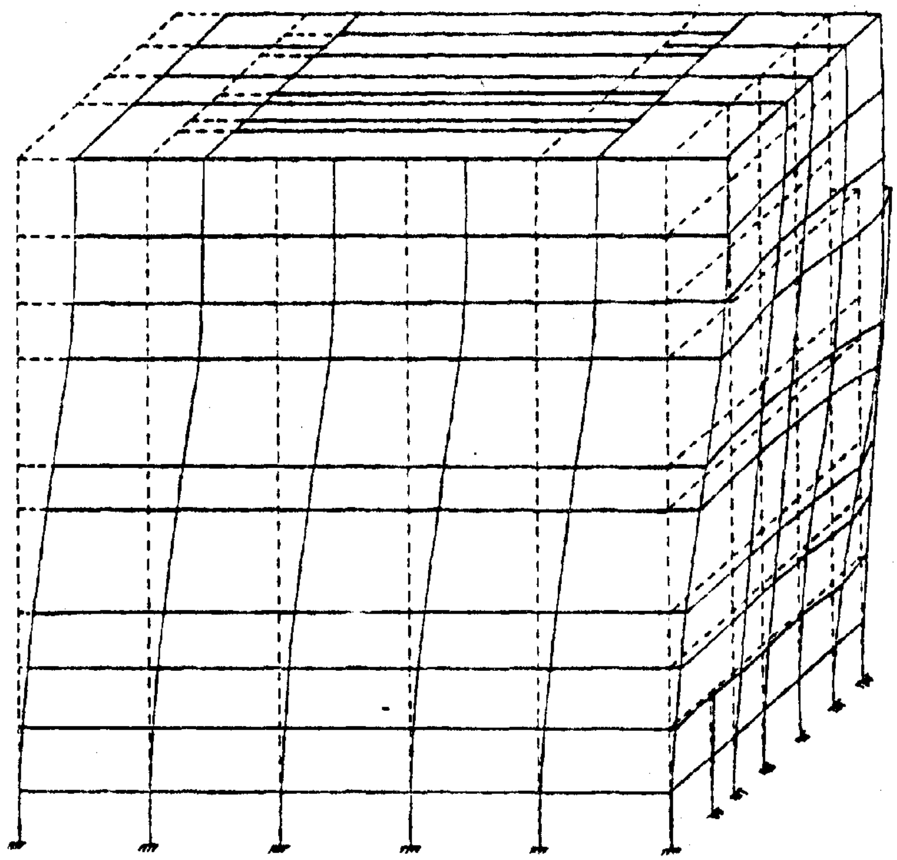

Figure 20

The first mode shape of the central structure with the steam generator but without the bracing members (f_1 = 0.1556 Hz).

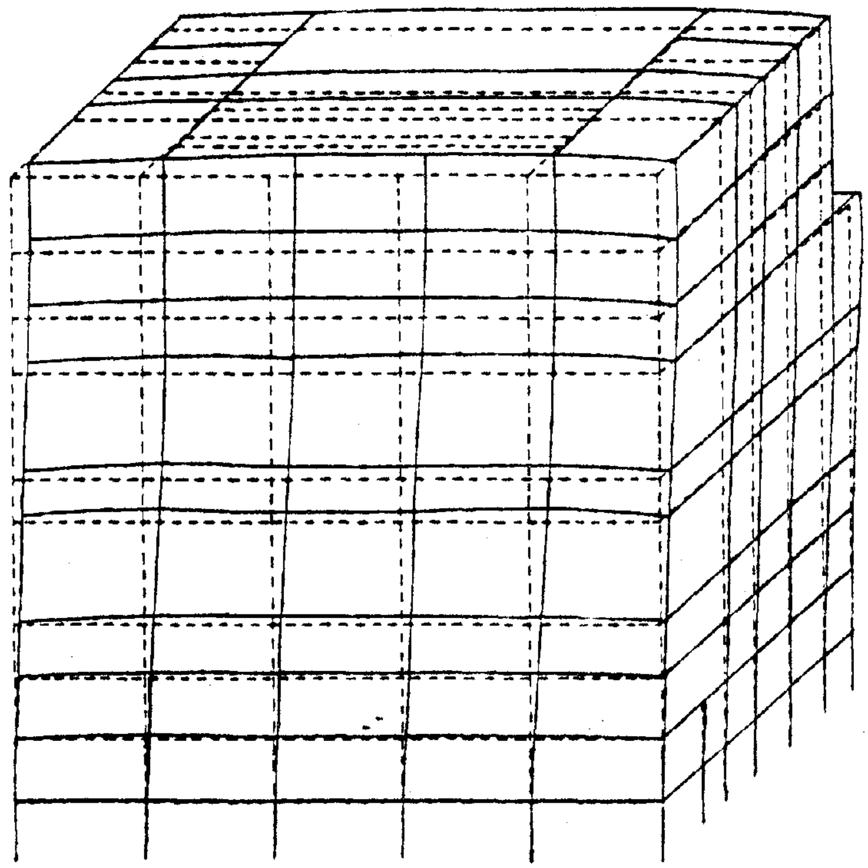

Figure 21

The second mode shape of the central structure with the steam generator but without the bracing members (f_2 = 0.1987 Hz).

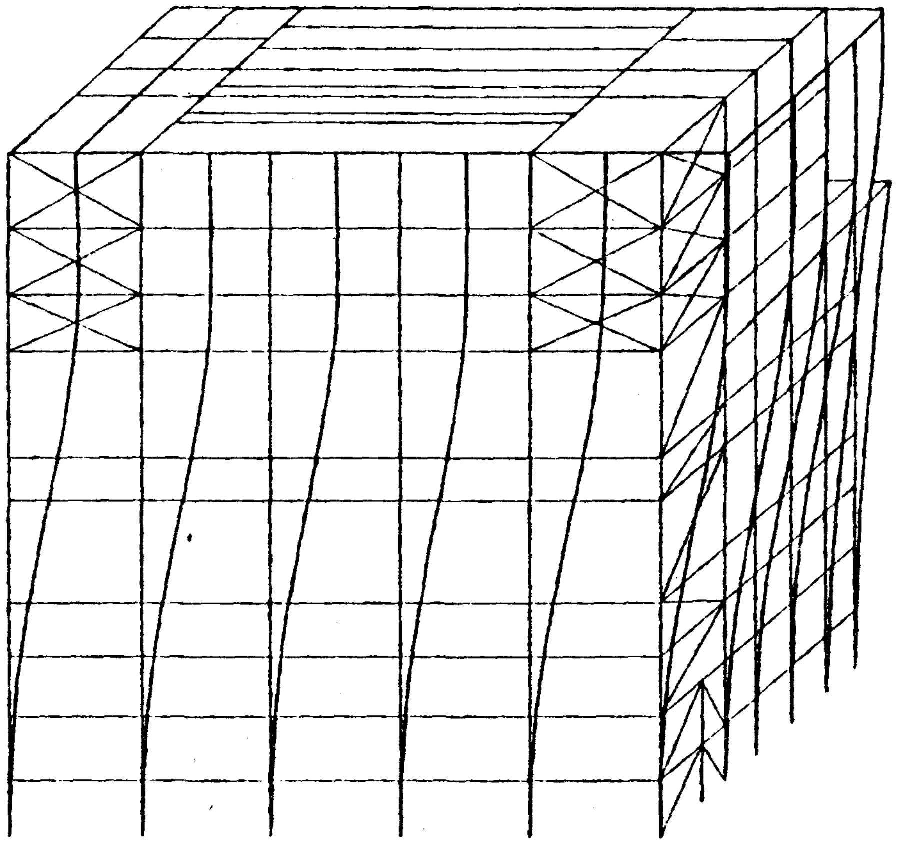

Figure 22

The first mode shape of the central structure with both the steam generator and the bracing members (f_1 = 0.2060 Hz).

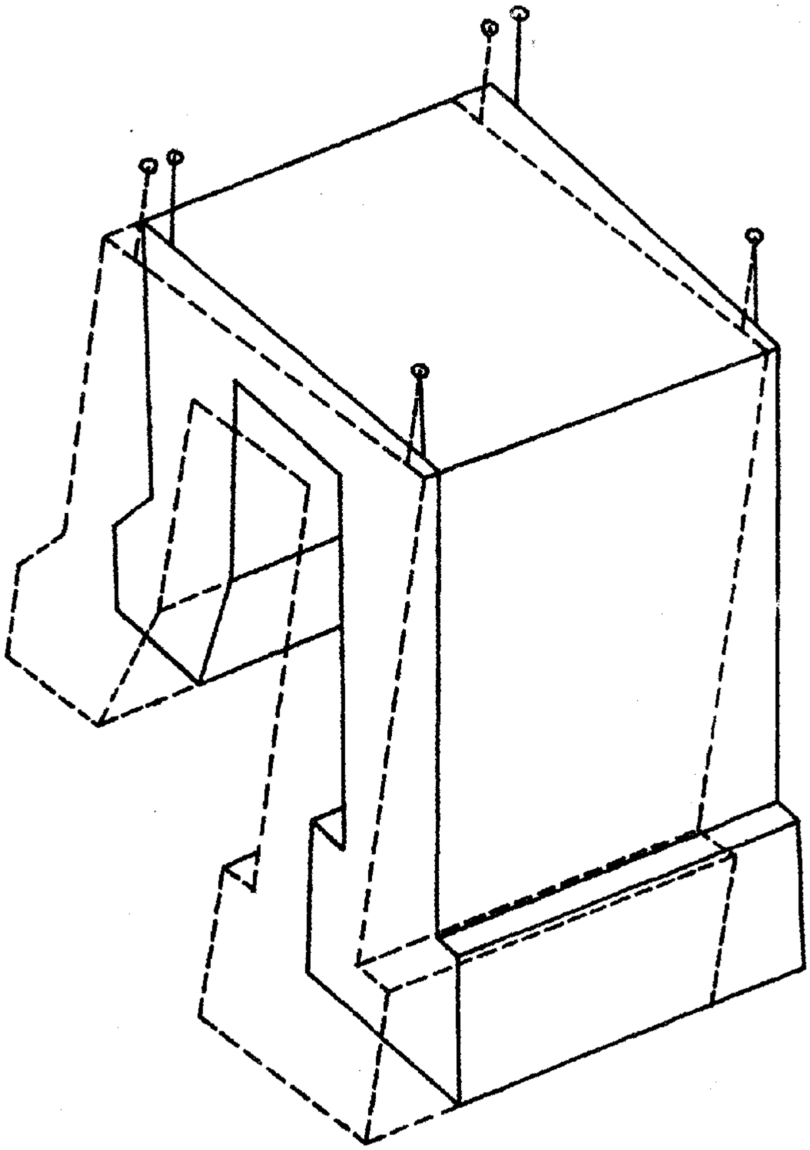

Figure 23
The first mode shape of the steam generator supported by the central structure with the bracing members.

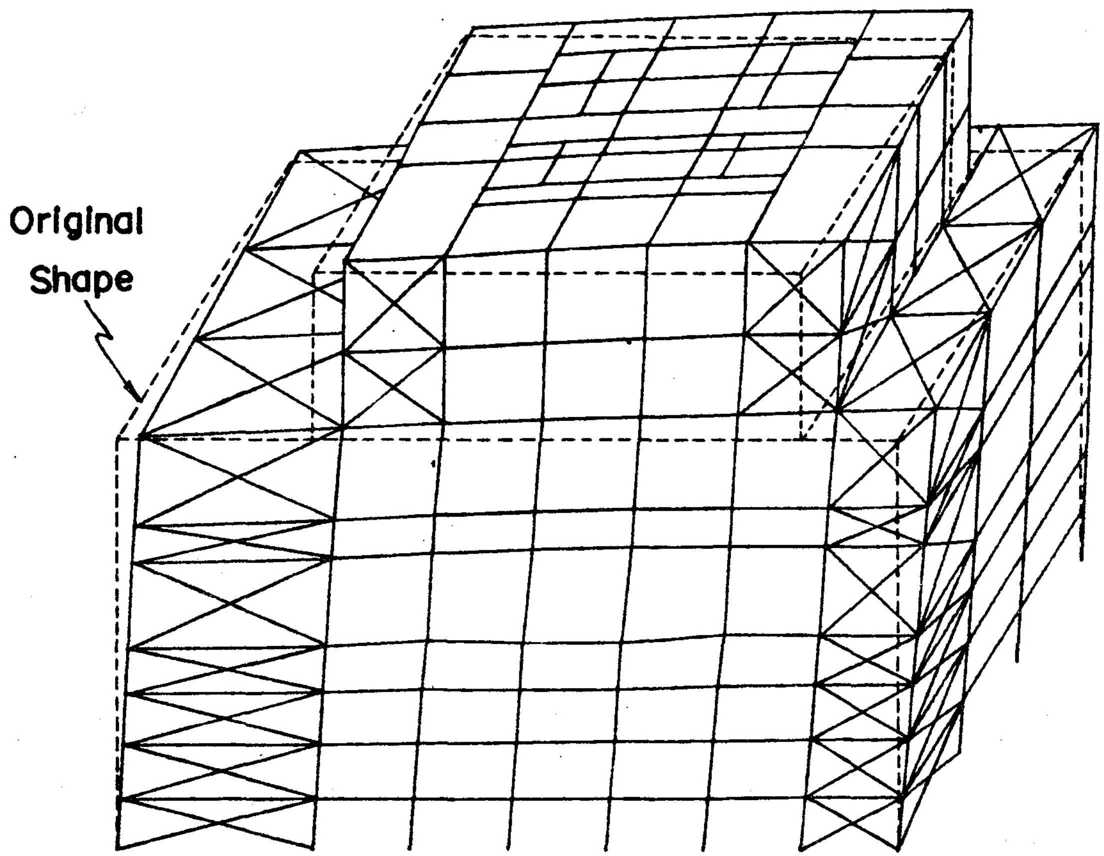

Figure 24

The first mode shape of system No. 1 in a three-dimensional view.

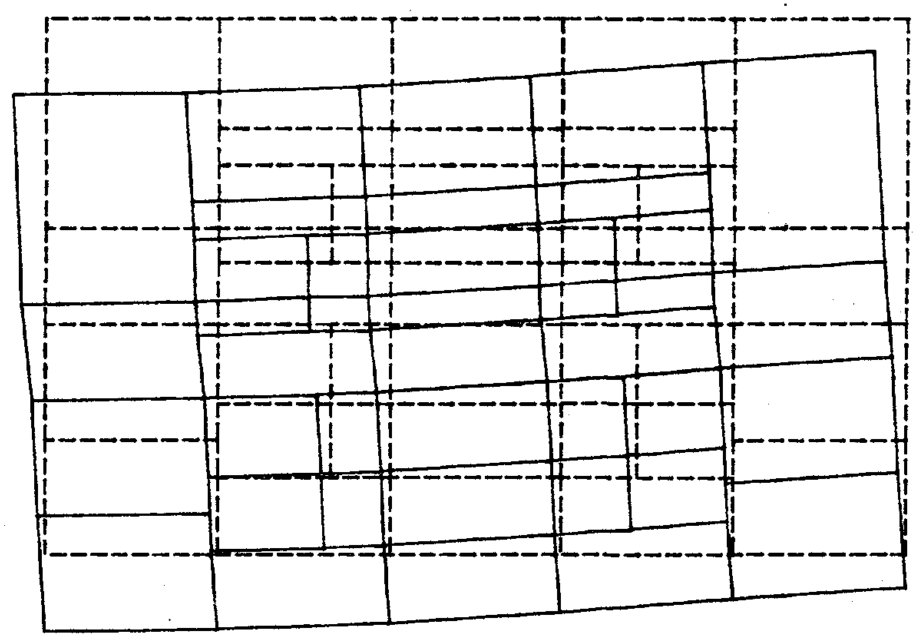

Figure 25

The first mode shape of system No. 1 in a plane view.

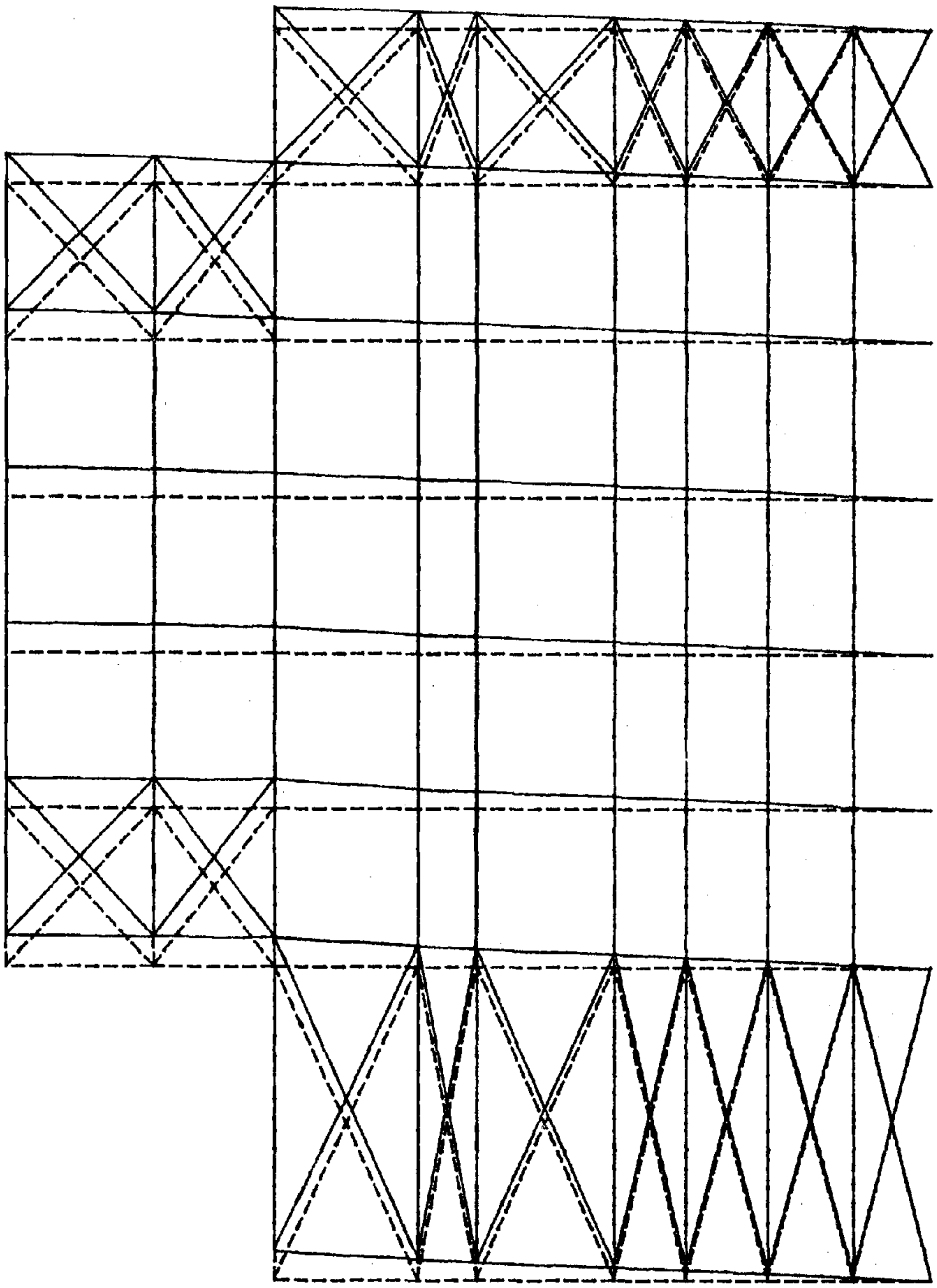

Figure 26

The first mode shape of system No. 1 in an elevation view.

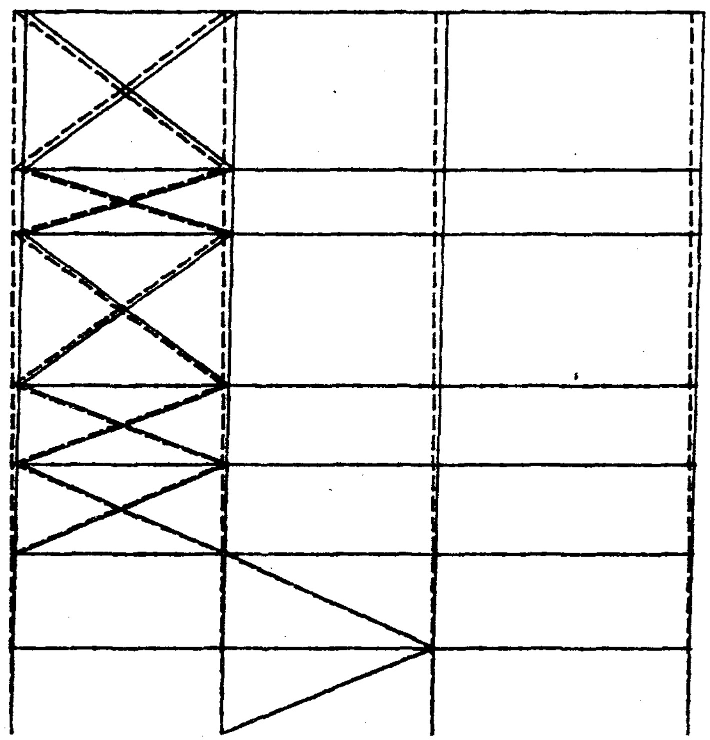

Figure 27

The first mode shape of system No. 1 in a side view.

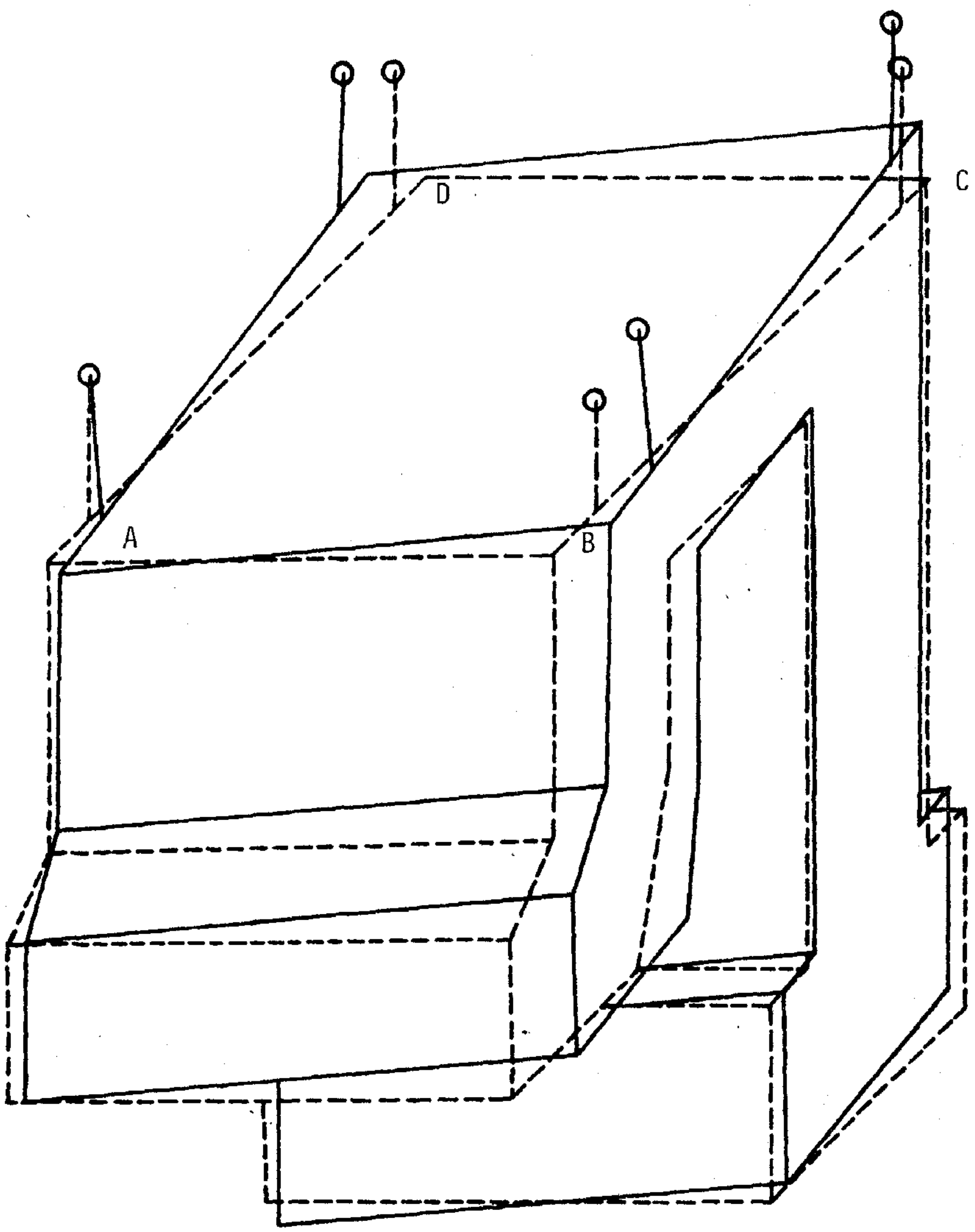

Figure 28

A three-dimensional view of the steam generator of system No. 1 vibrating in the first mode.

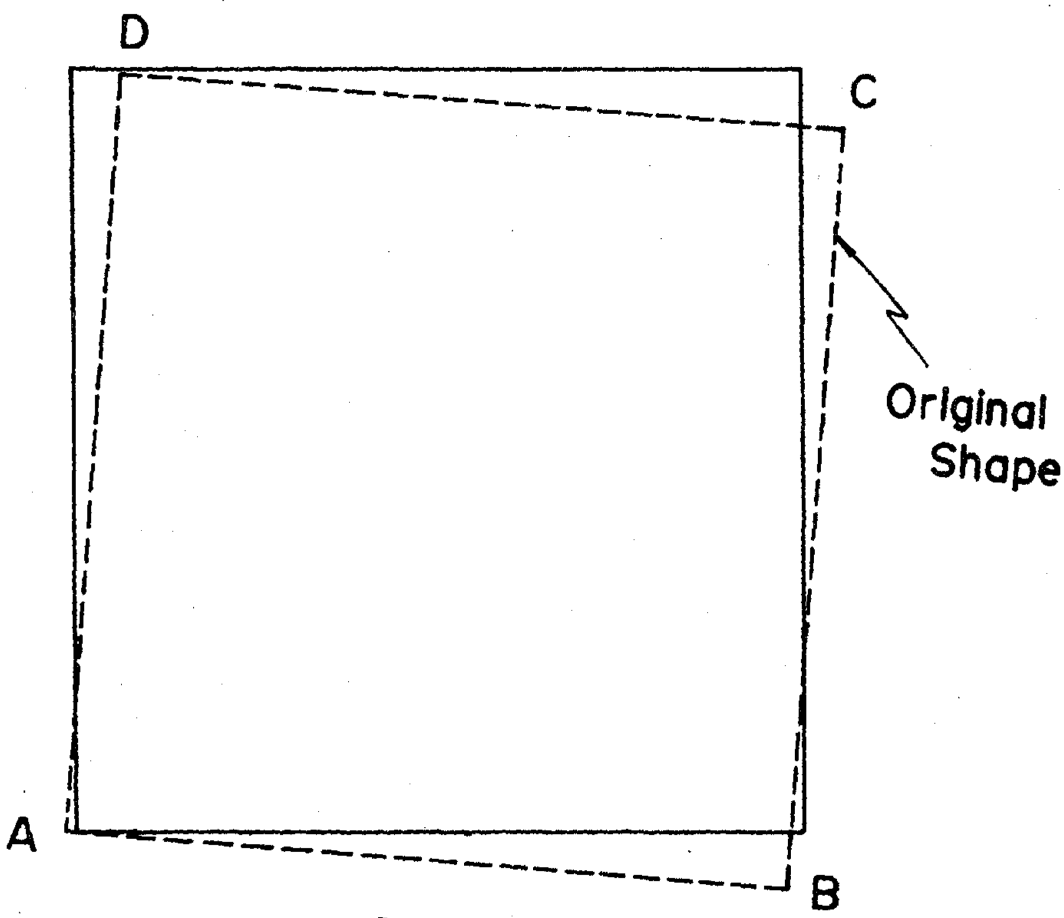

Figure 29

A plan view of the horizontal section at the top of the steam generator of system No. 1 vibrating in the first mode.

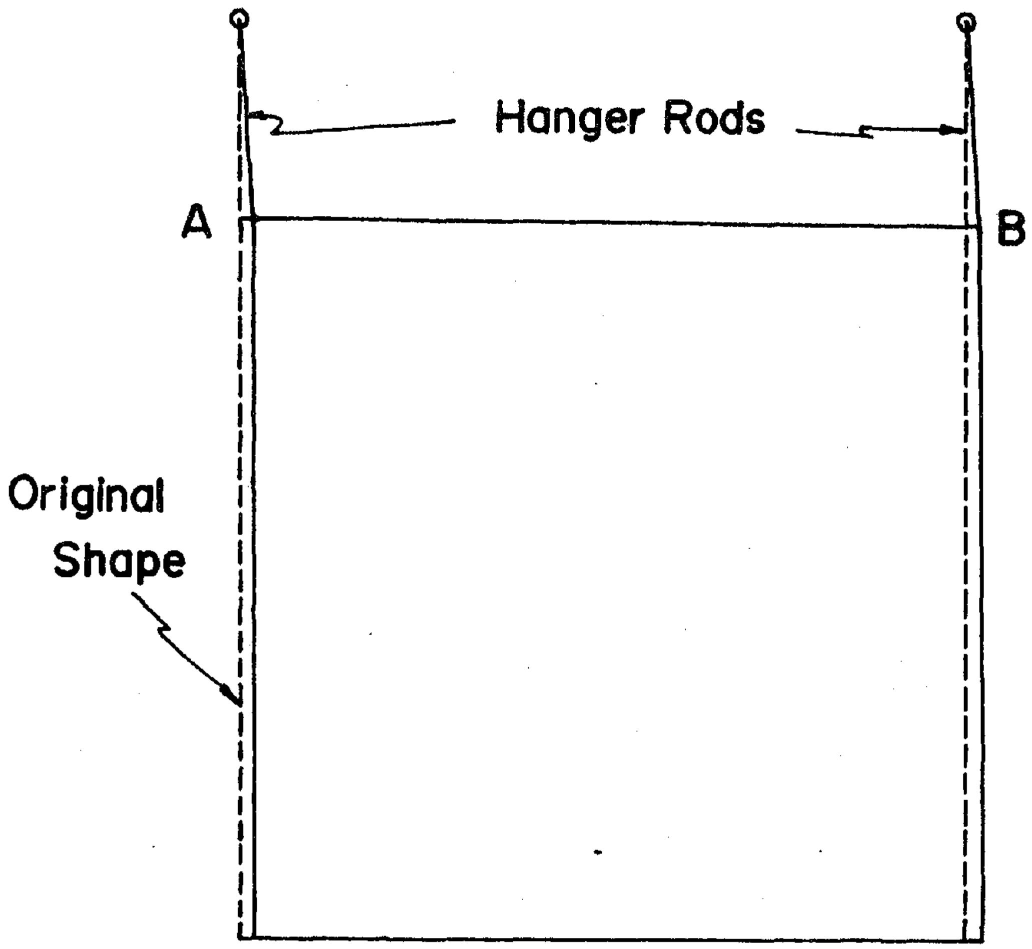

Figure 30

A side view of the steam generator wall along line AB vibrating in the first mode.

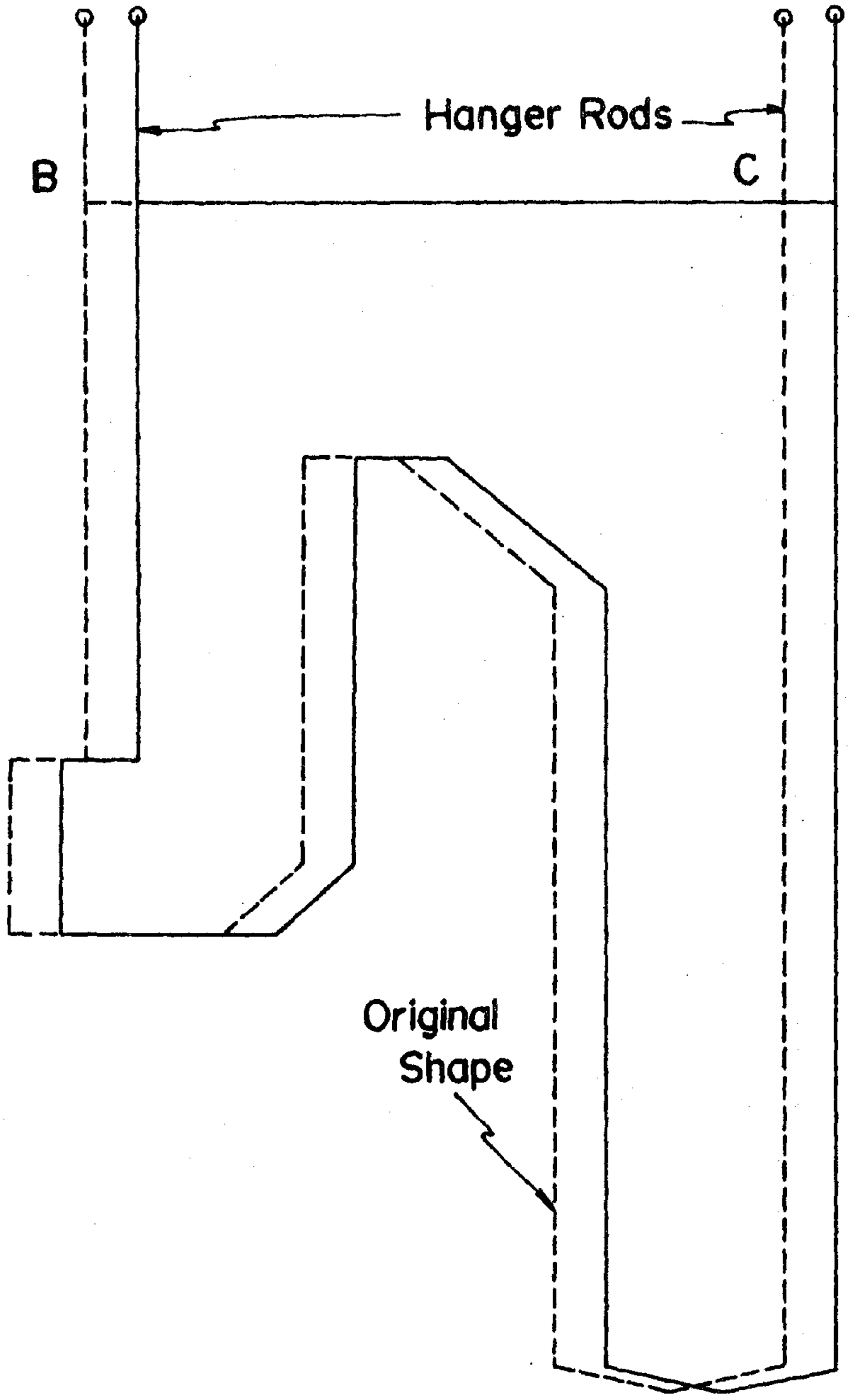

Figure 31

A side view of the steam generator wall along line BC vibrating in the first mode.

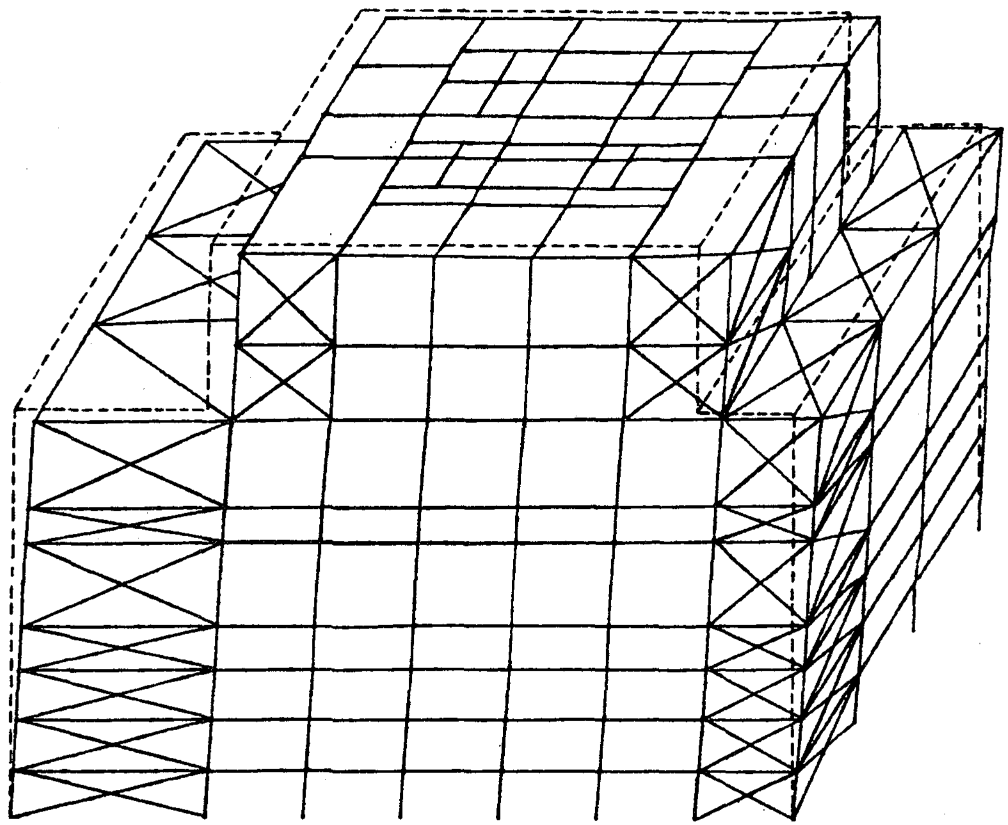

Figure 32

The second mode shape of system No. 1 in a three-dimensional view.

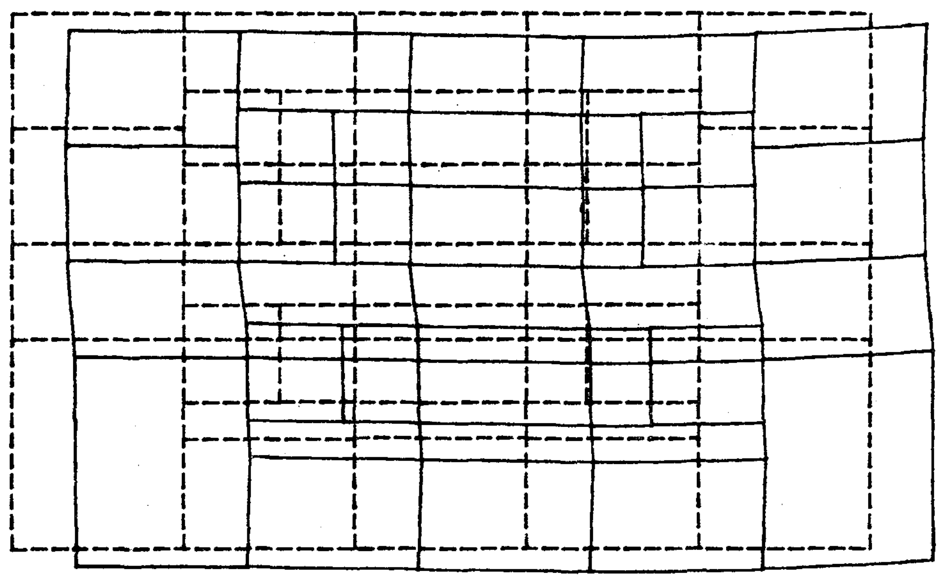

Figure 33

The second mode shape of system No. 1 in a plan view.

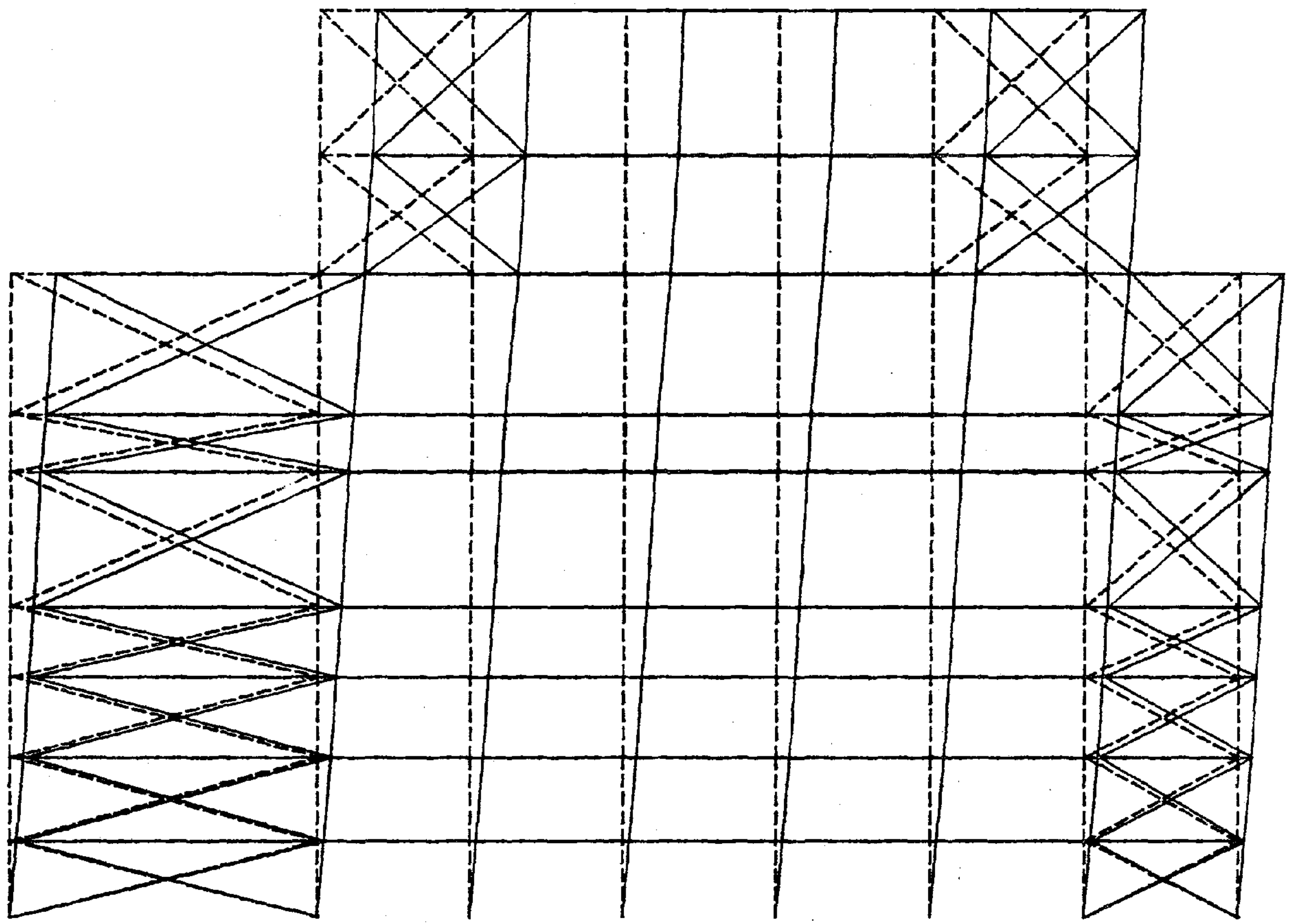

Figure 34

The second mode shape of system No. 1 in an elevation view.

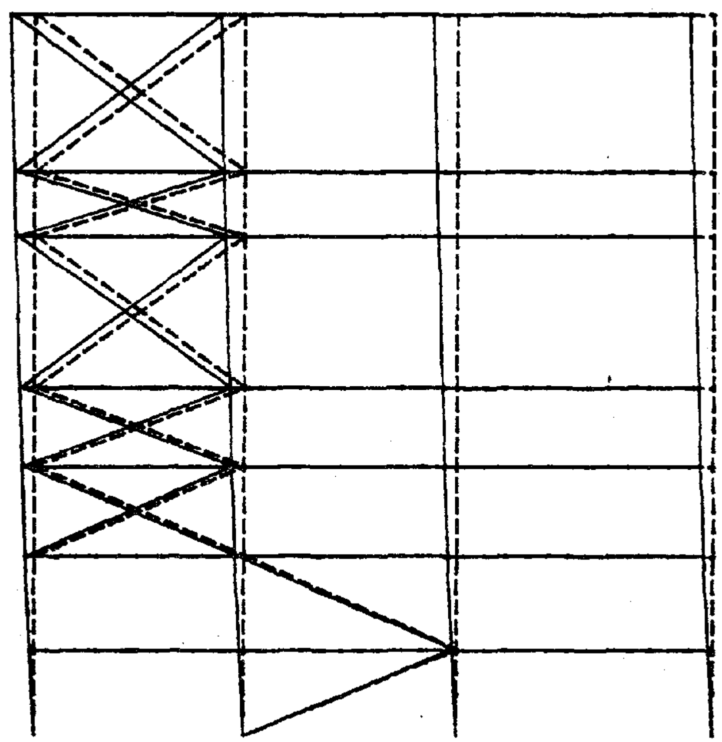

Figure 35

The second mode shape of system No. 1 in a side view.

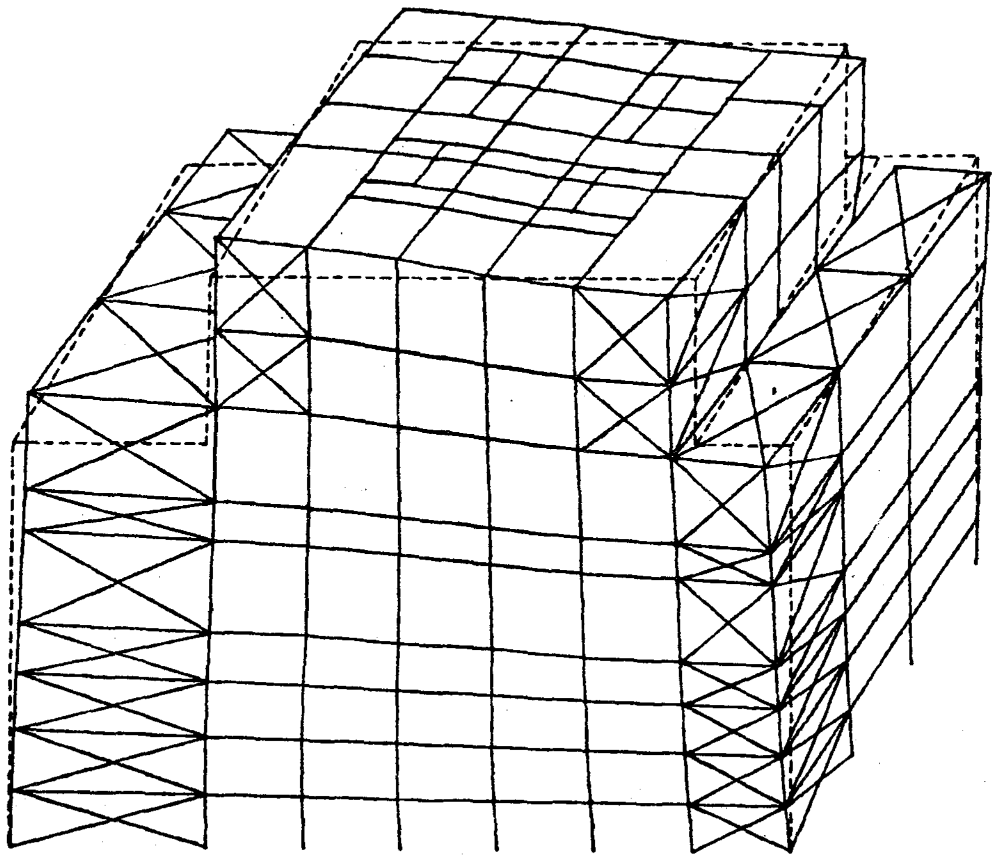

Figure 36

The third mode shape of system No. 1 in a three-dimensional view.

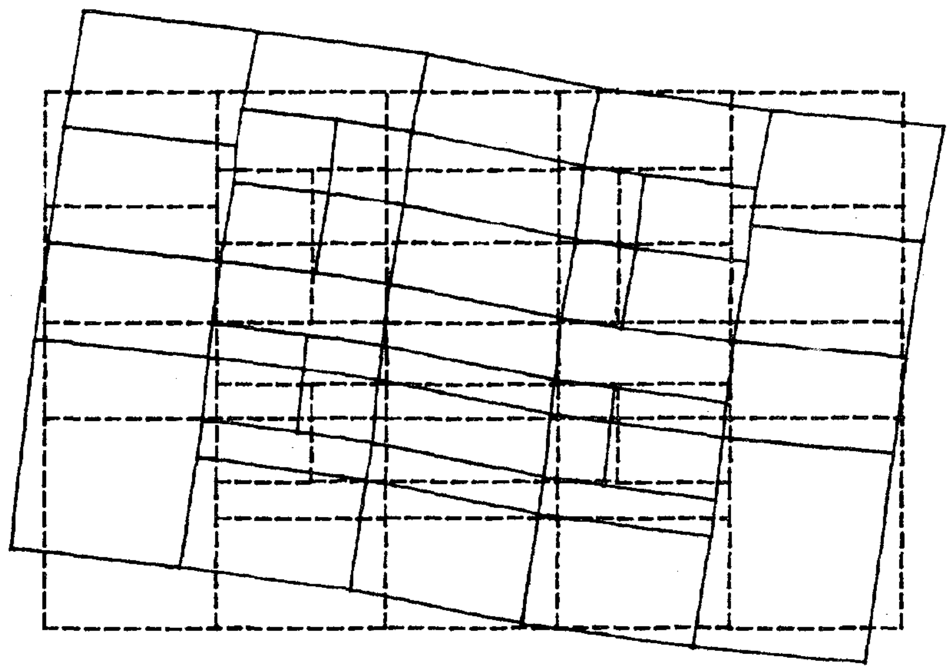

Figure 37

The third mode shape of system No. 1 in a plan view.

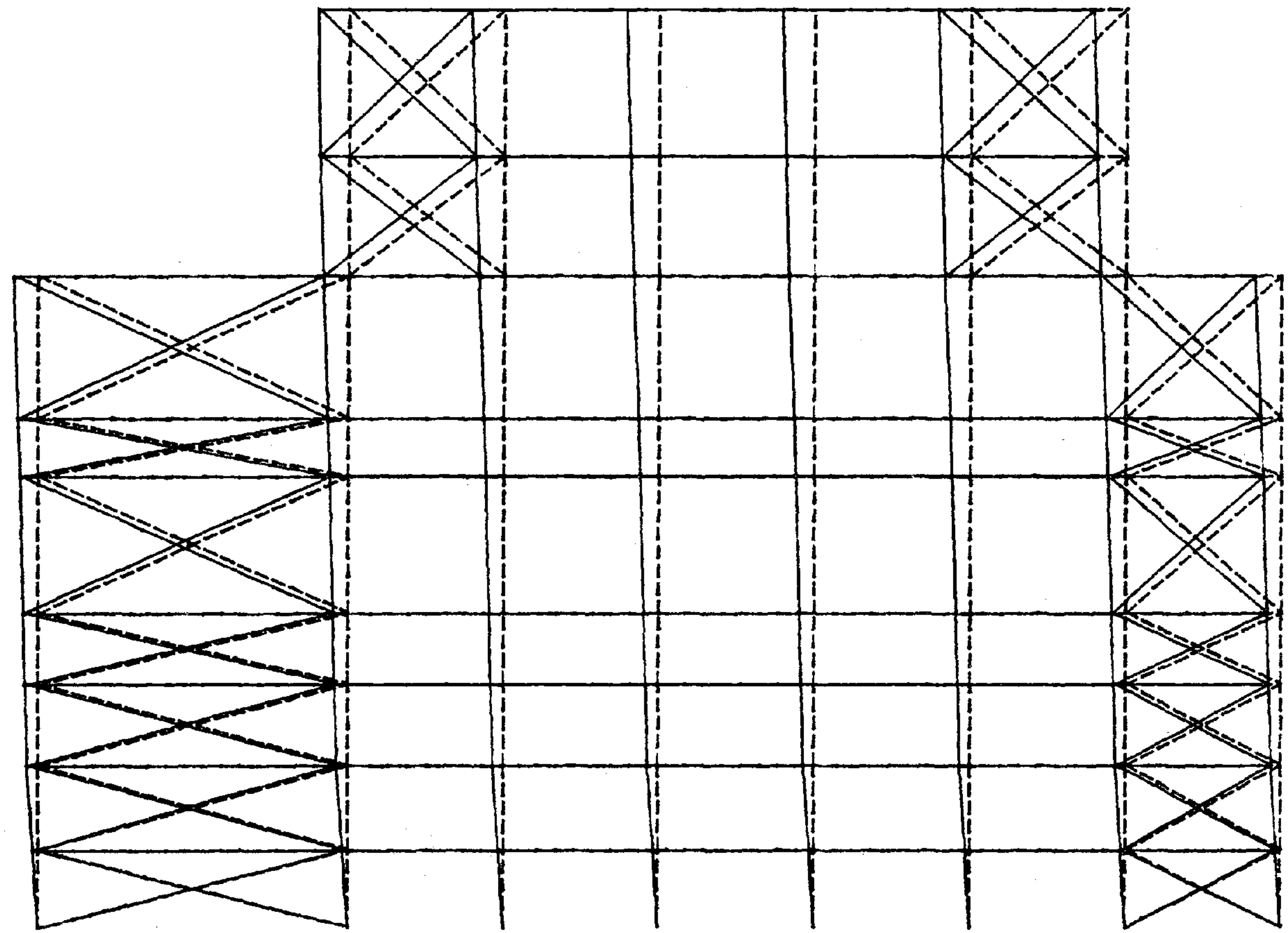

Figure 38

The third mode shape of system No. 1 in an elevation view.

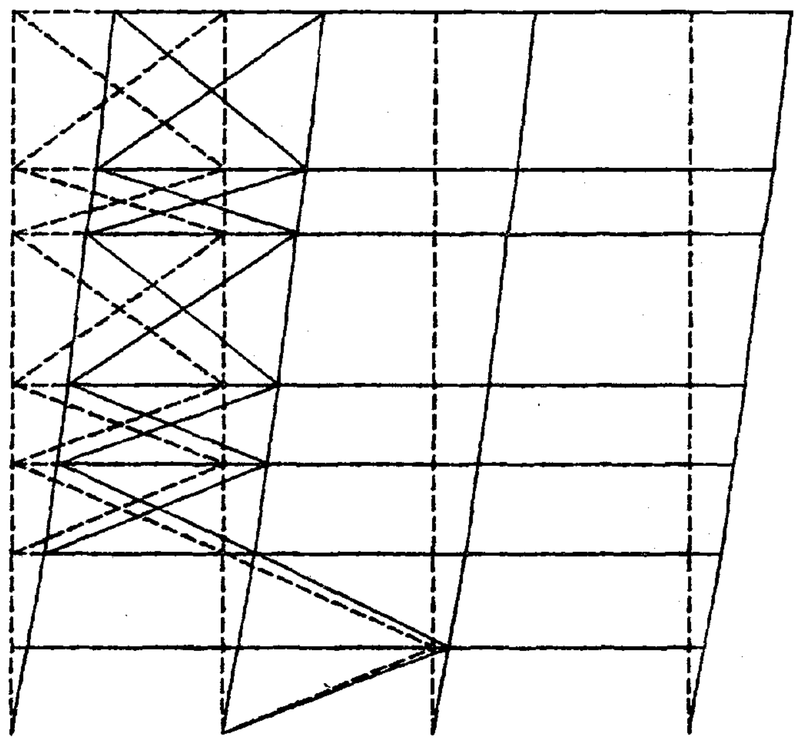

Figure 39

The third mode shape of system No. 1 in a side view.

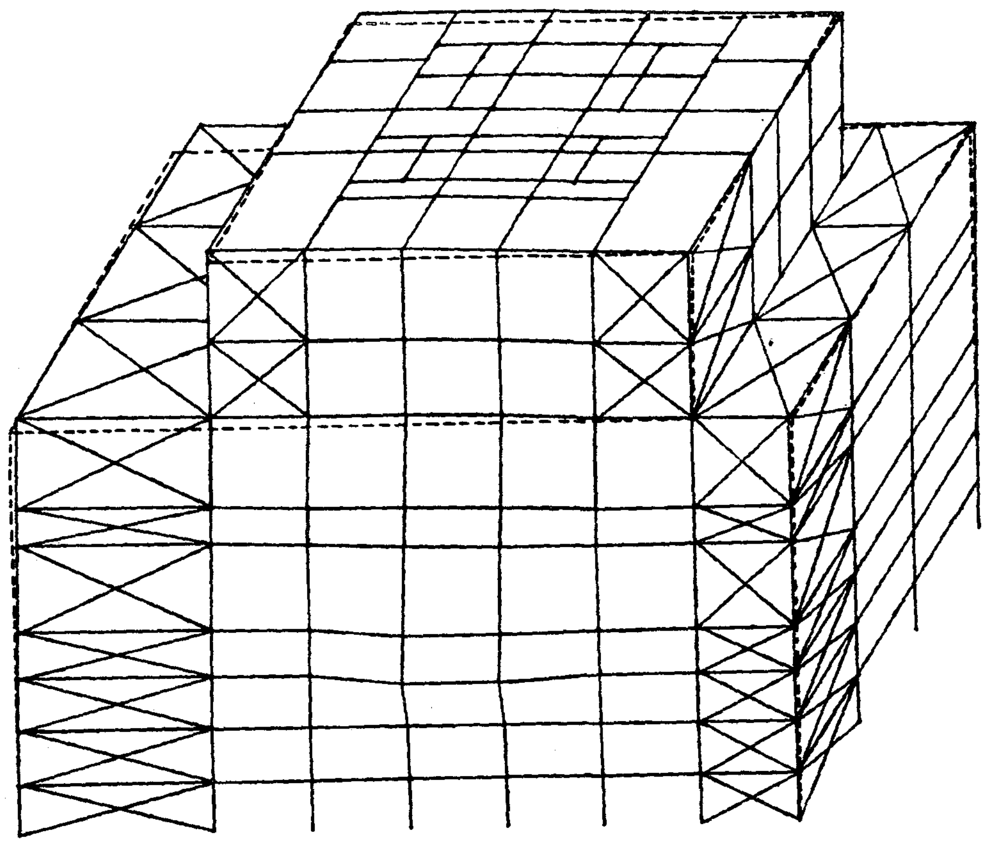

Figure 40

The fourth mode shape of system No. 1 in a three-dimensional view.

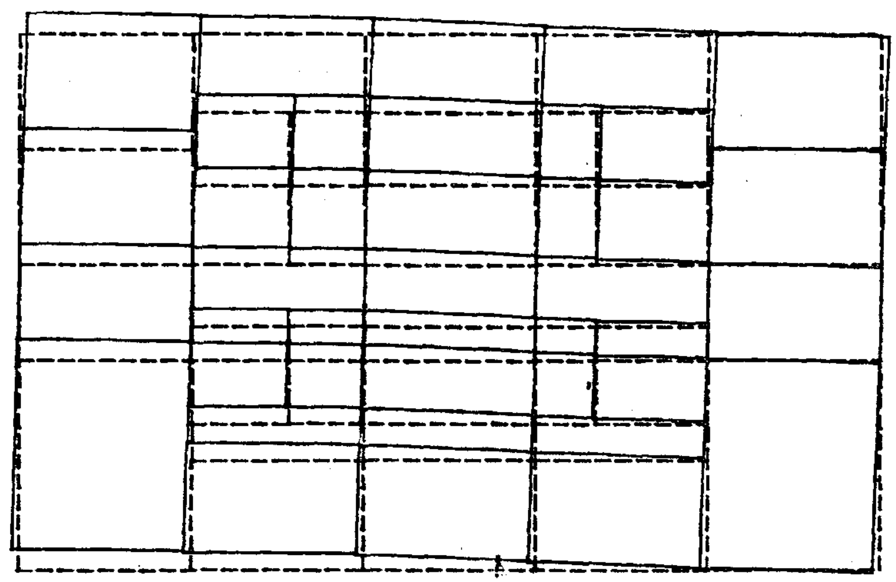

Figure 41

The fourth mode shape of system No. 1 in a plan view.

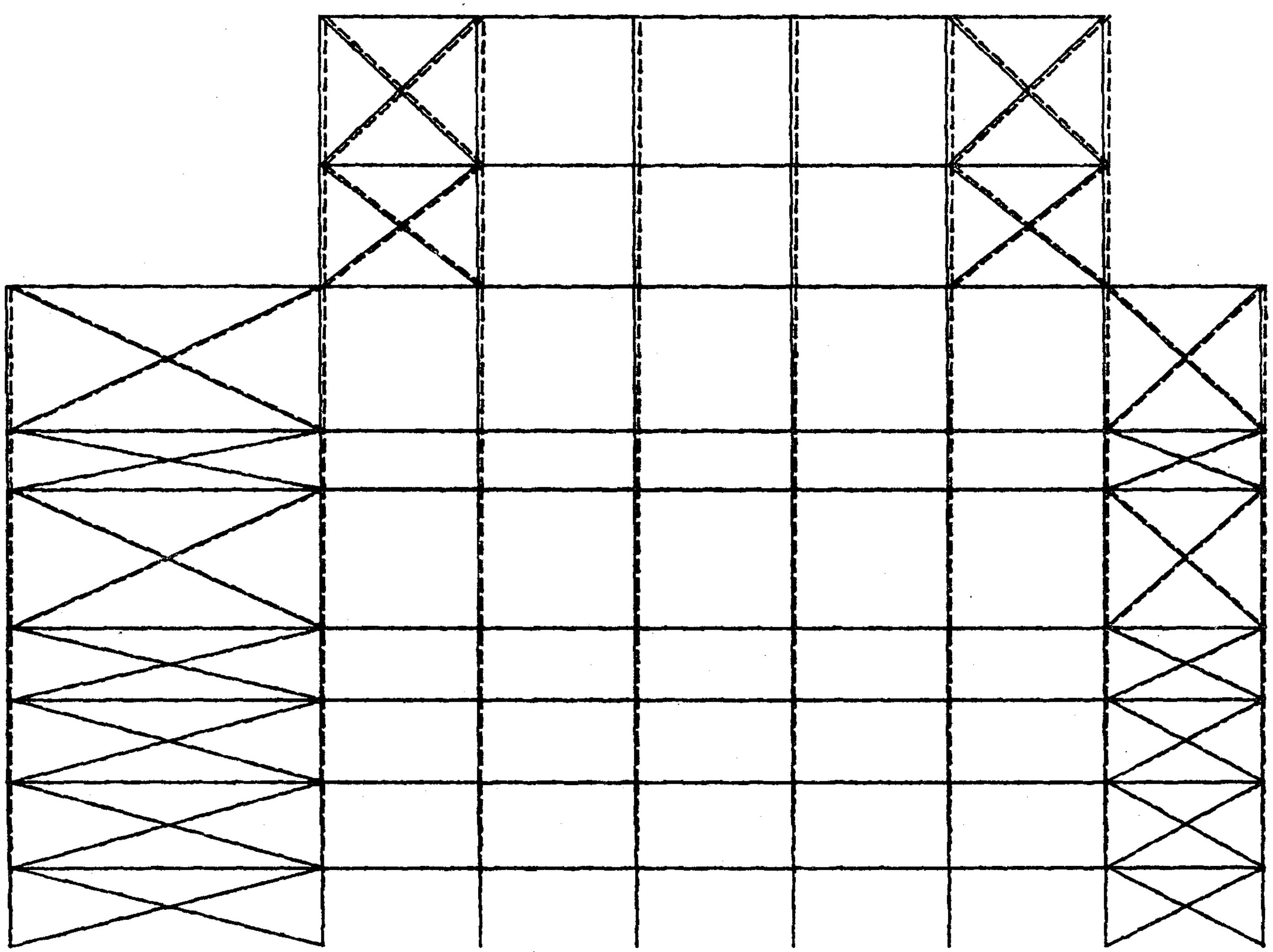

Figure 42

The fourth mode shape of system No. 1 in an elevation view.

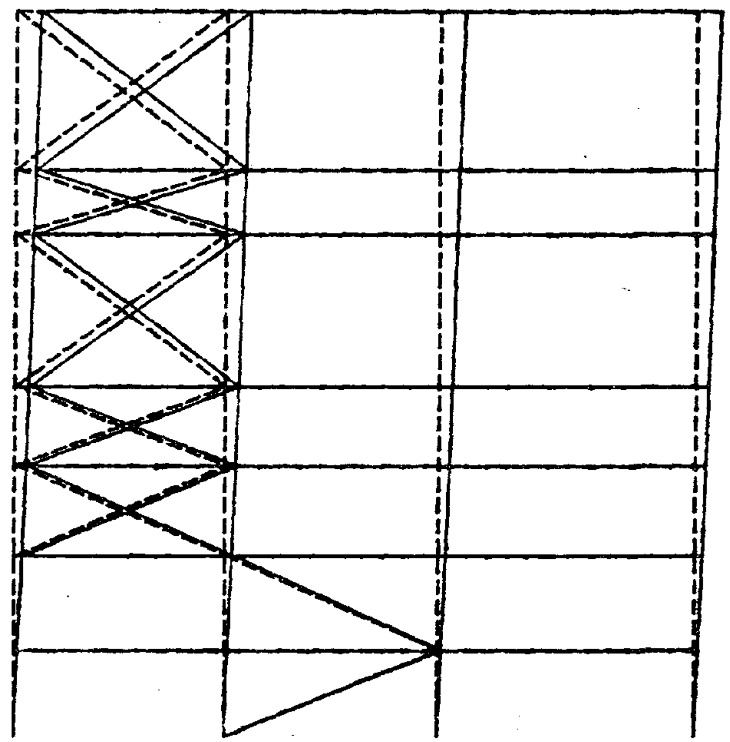

Figure 43

The fourth mode shape of system No. 1 in a side view.

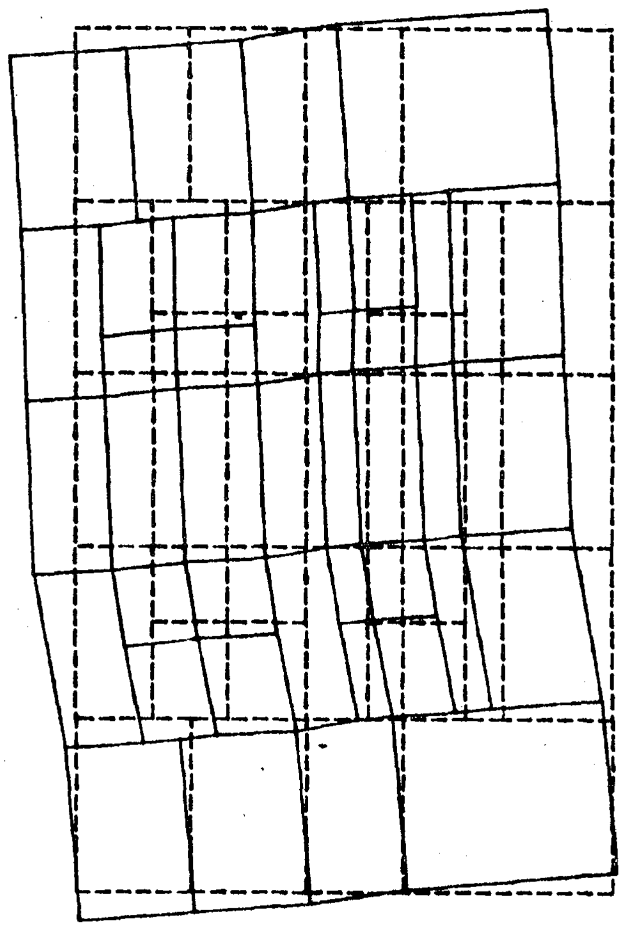

Figure 44

The fifth mode shape of system No. 1 in a plan view.

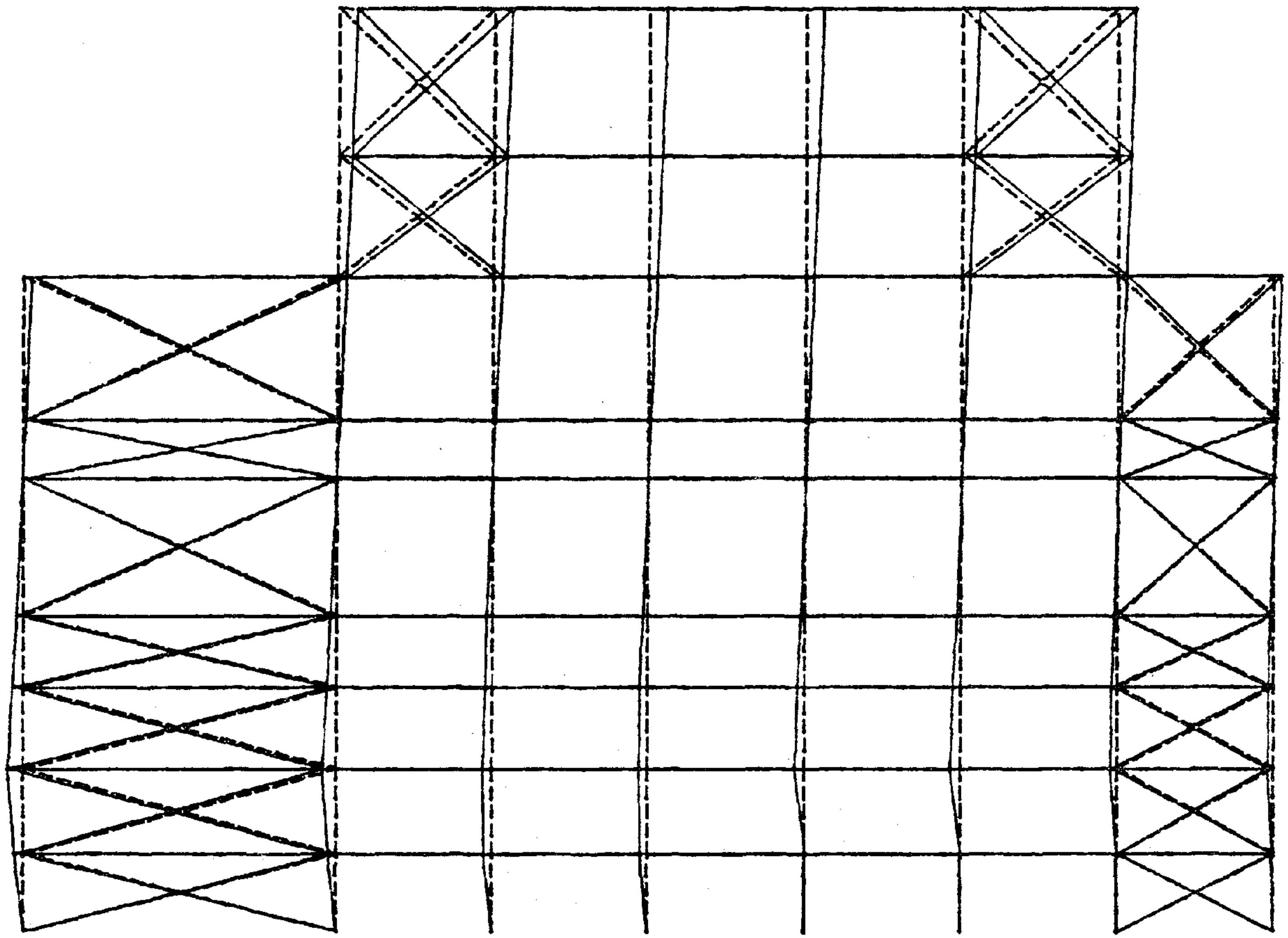

Figure 45

The fifth mode shape of system No. 1 in an elevation view.

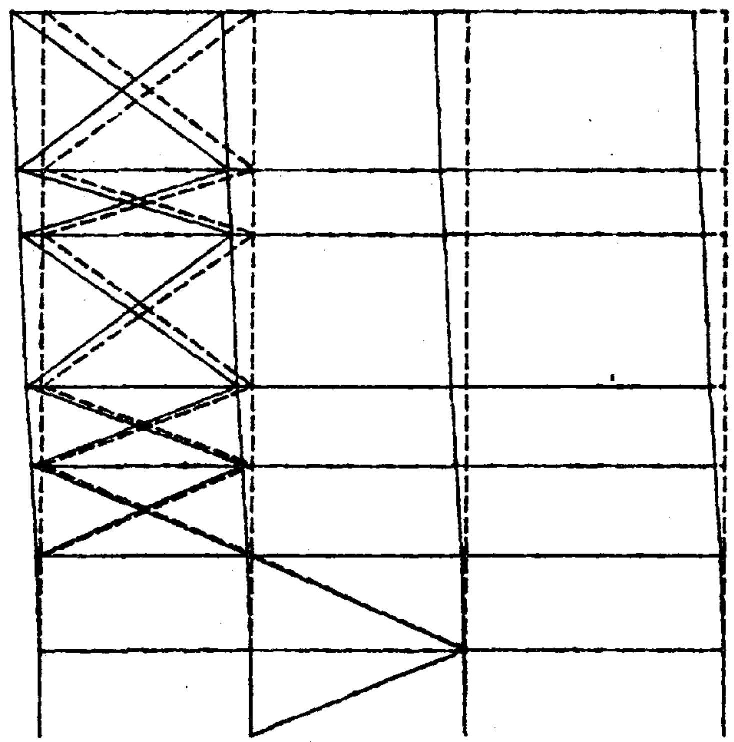

Figure 46

The fifth mode shape of system No. 1 in a side view.

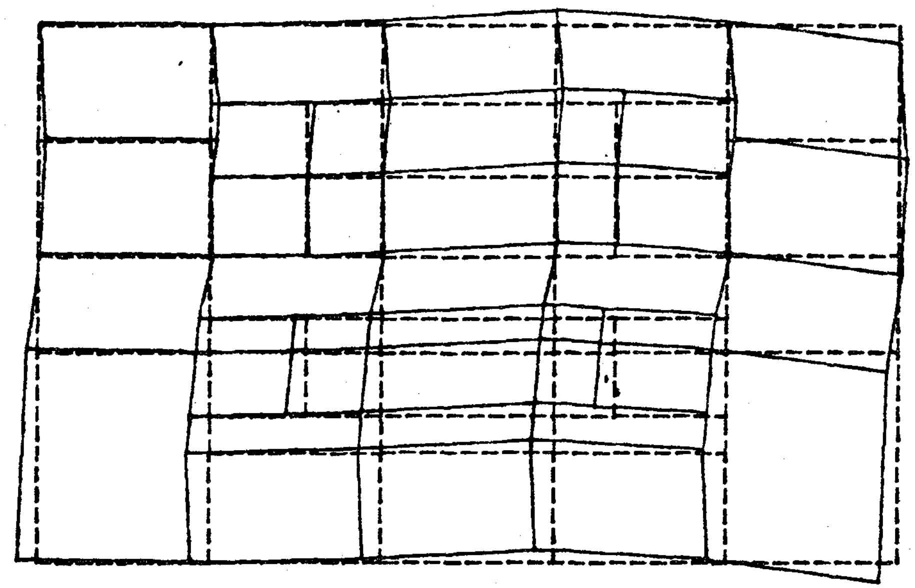

Figure 47

The sixth mode shape of system No. 1 in a plan view.

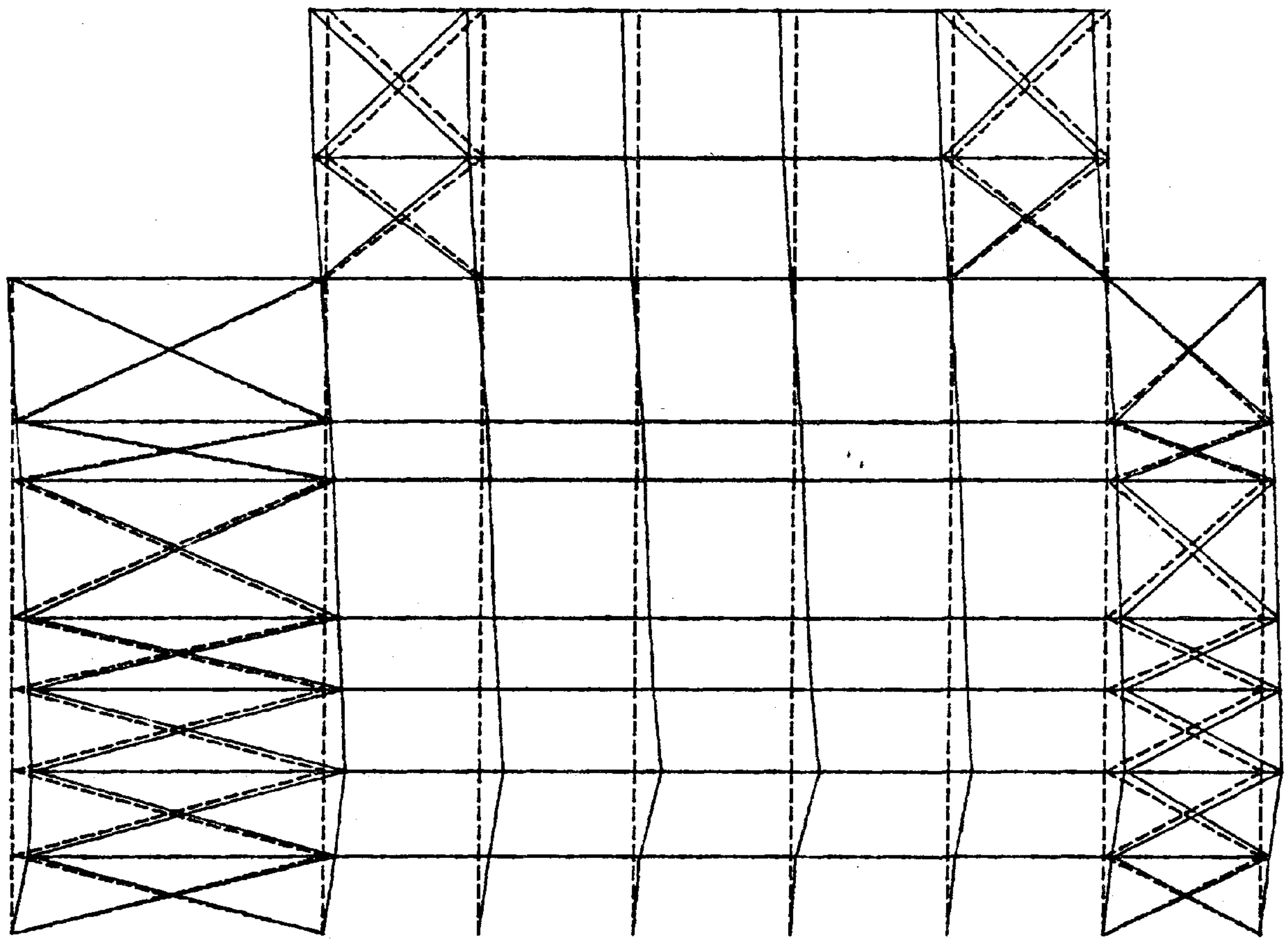

Figure 48

The sixth mode shape of system No. 1 in an elevation view.

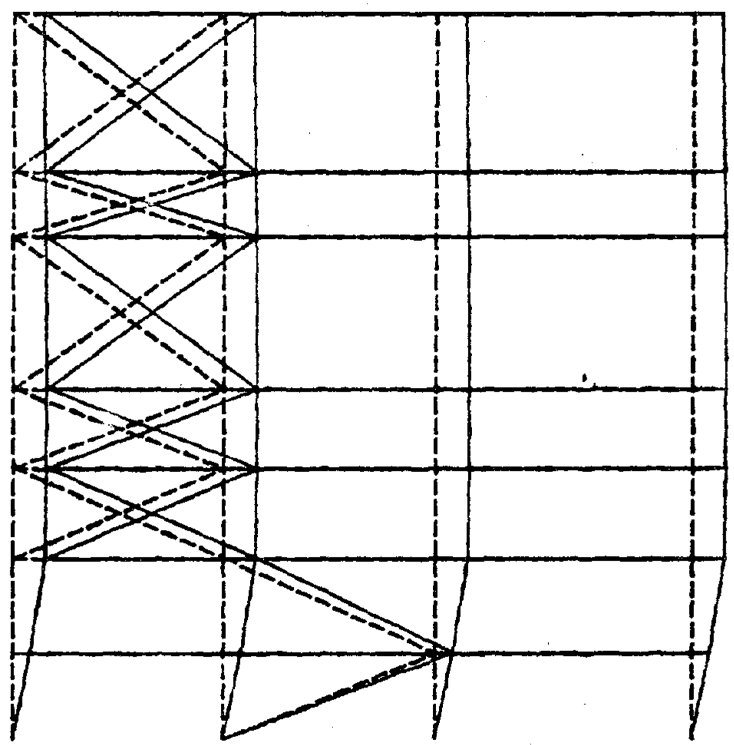

Figure 49

The sixth mode shape of system No. 1 in a side view.

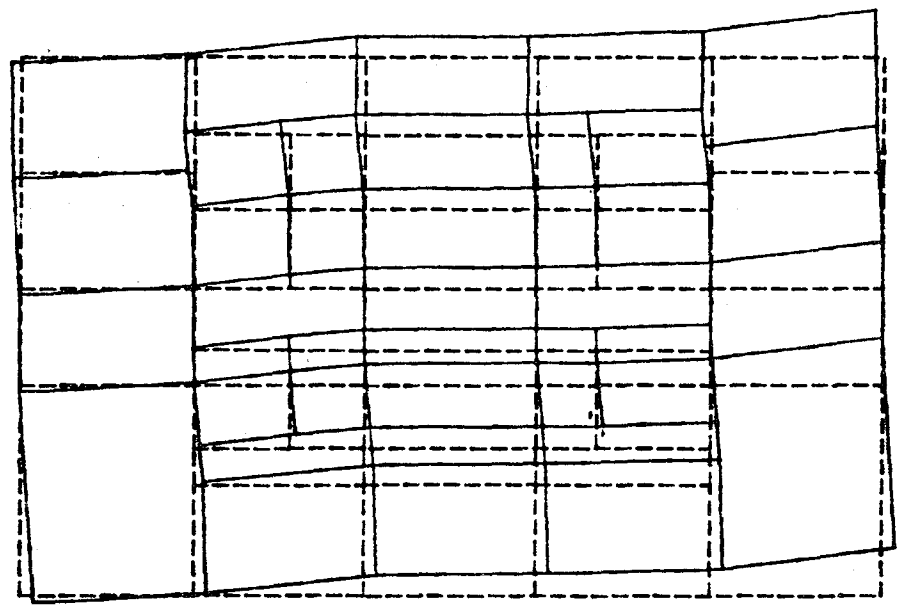

Figure 50

The seventh mode of system No. 1 in a plan view.

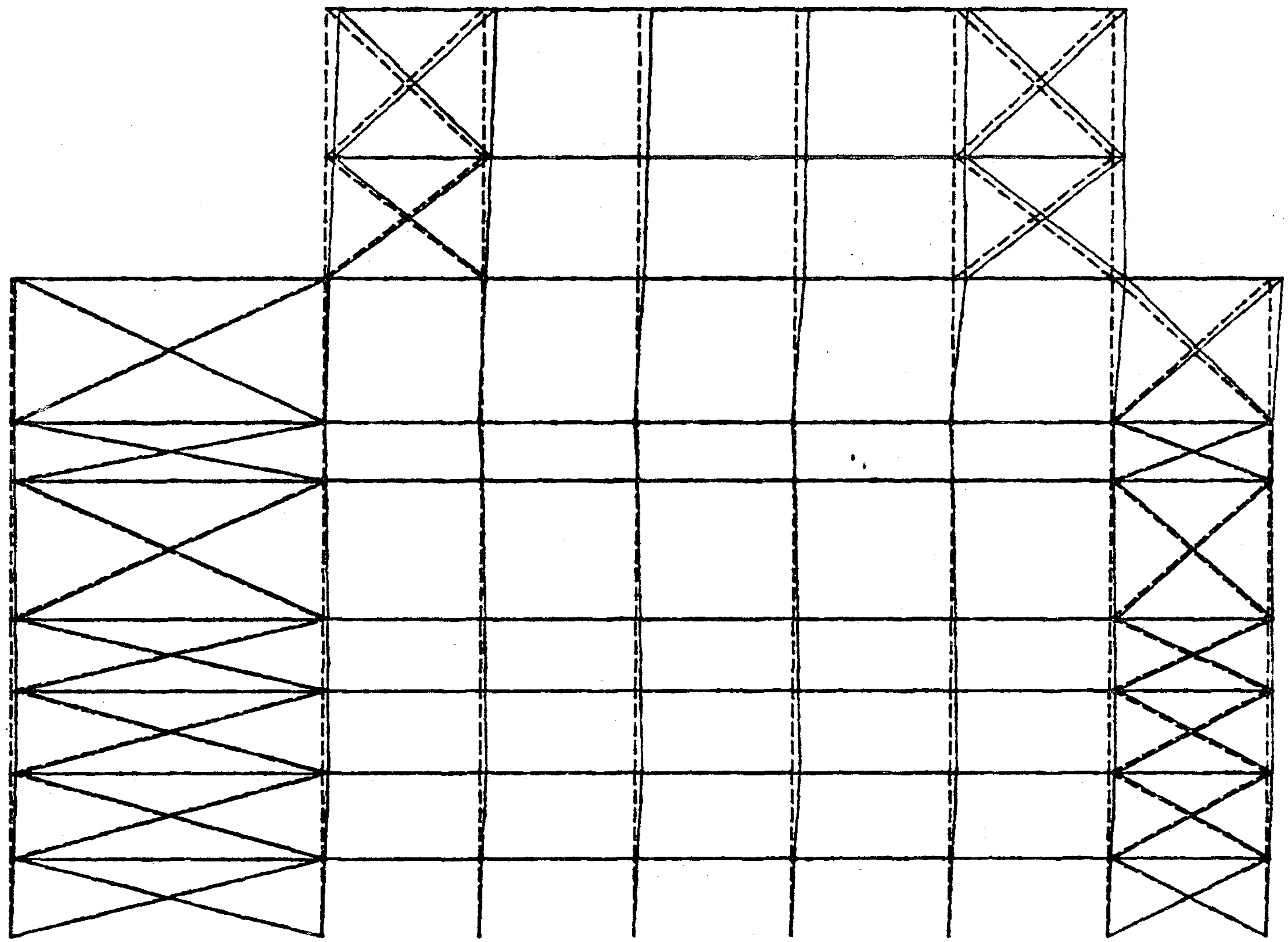

Figure 51

The seventh mode of system No. 1 in an elevation view.

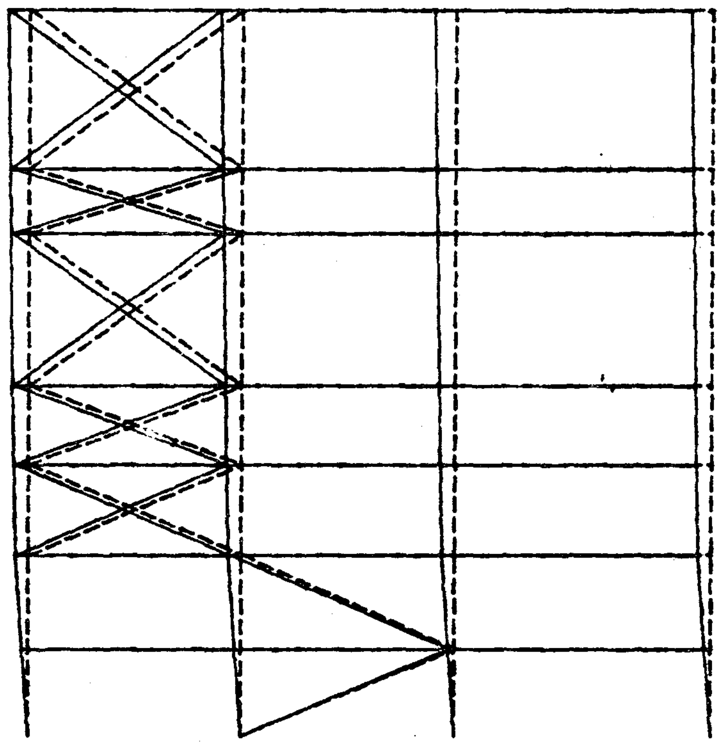

Figure 52

The seventh mode of system No. 1 in a side view.

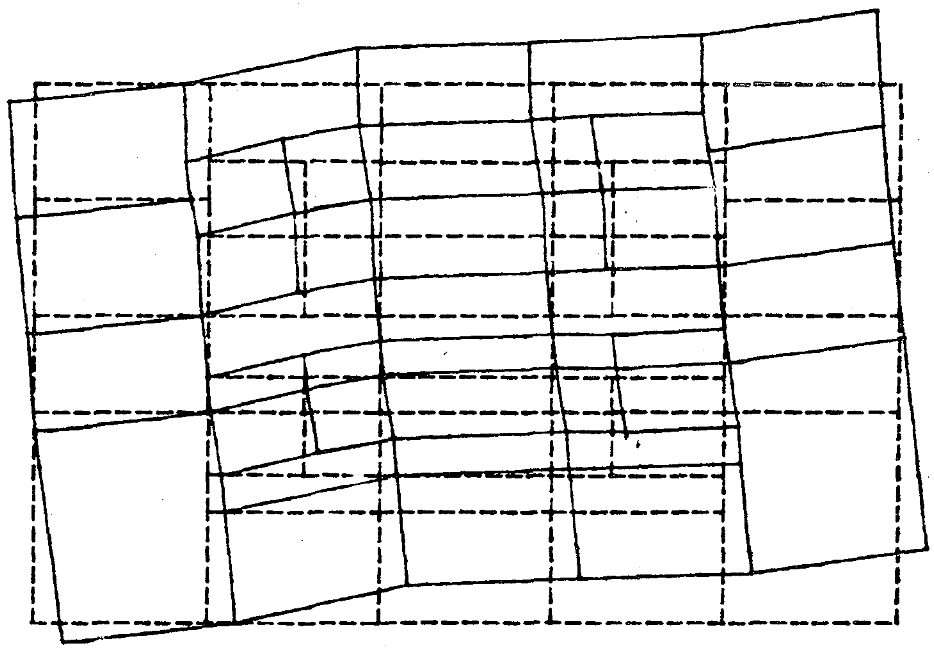

Figure 53

The eighth mode of system No. 1 in a plan view.

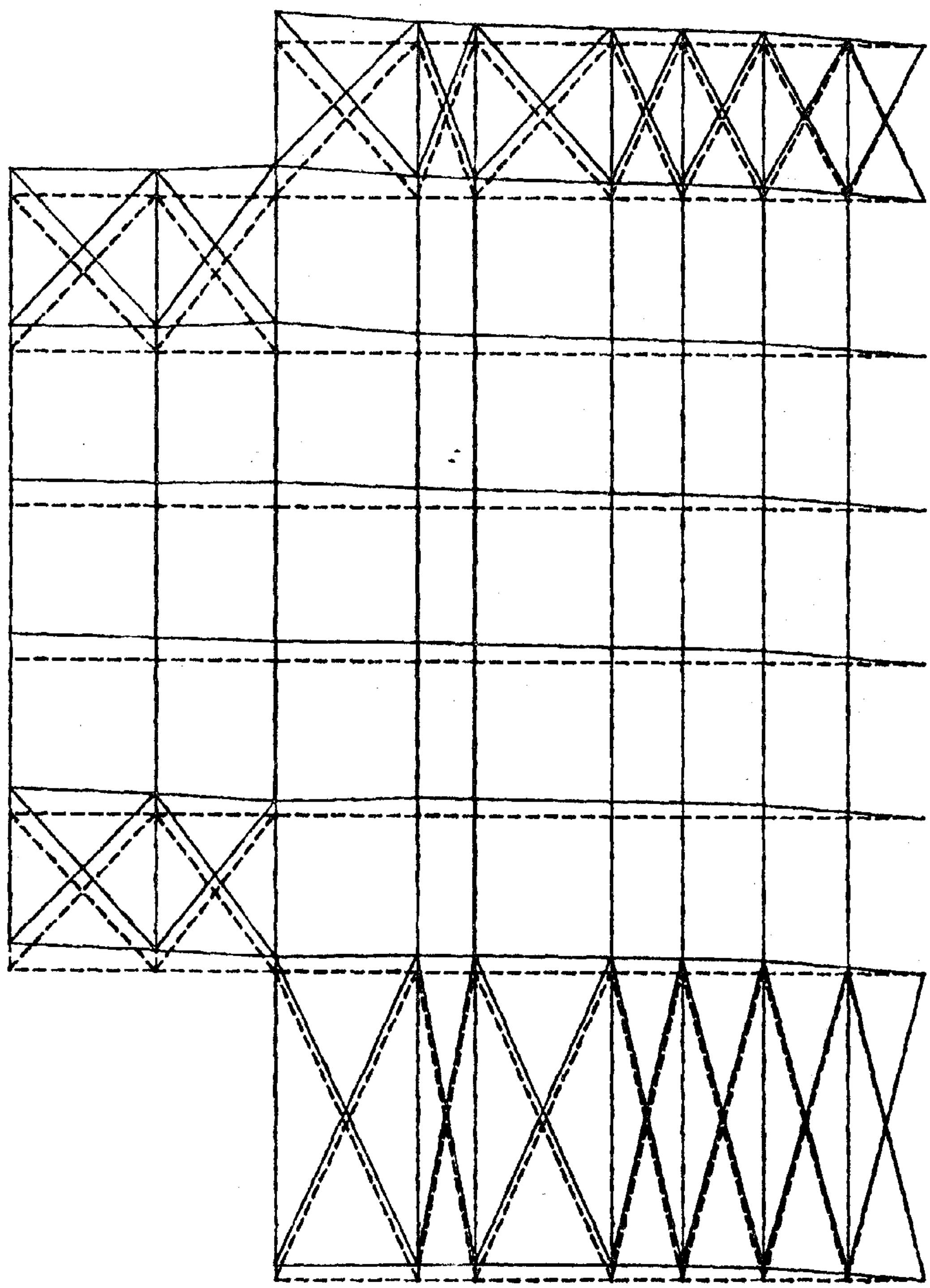

Figure 54

The eighth mode of system No. 1 in an elevation view.

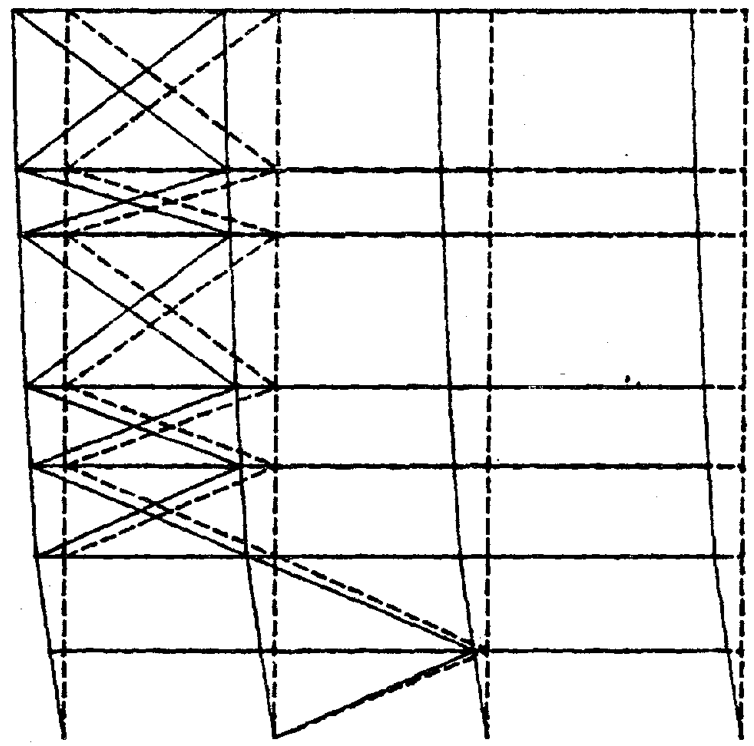

Figure 55

The eighth mode of system No. 1 in a side view.

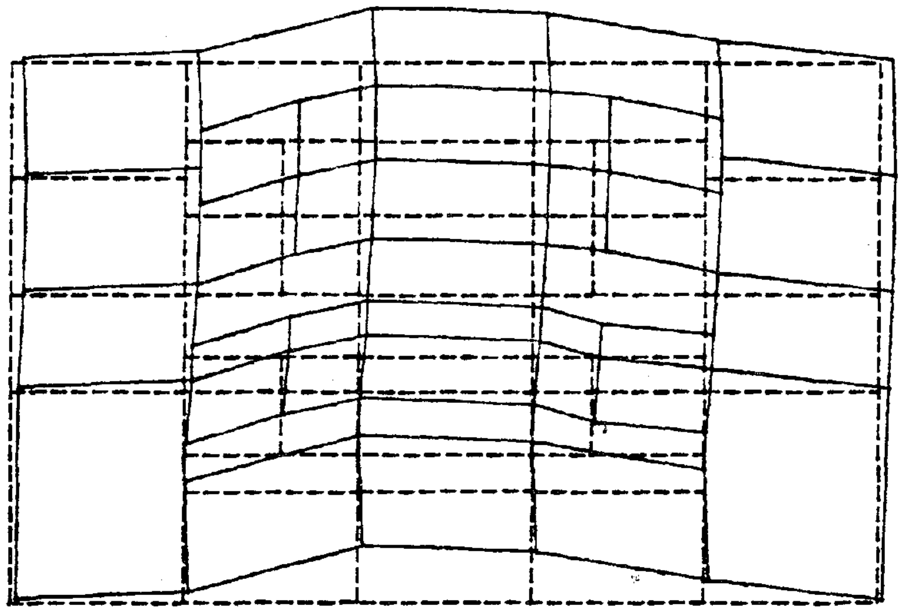

Figure 56

The ninth mode of system No. 1 in a plan view.

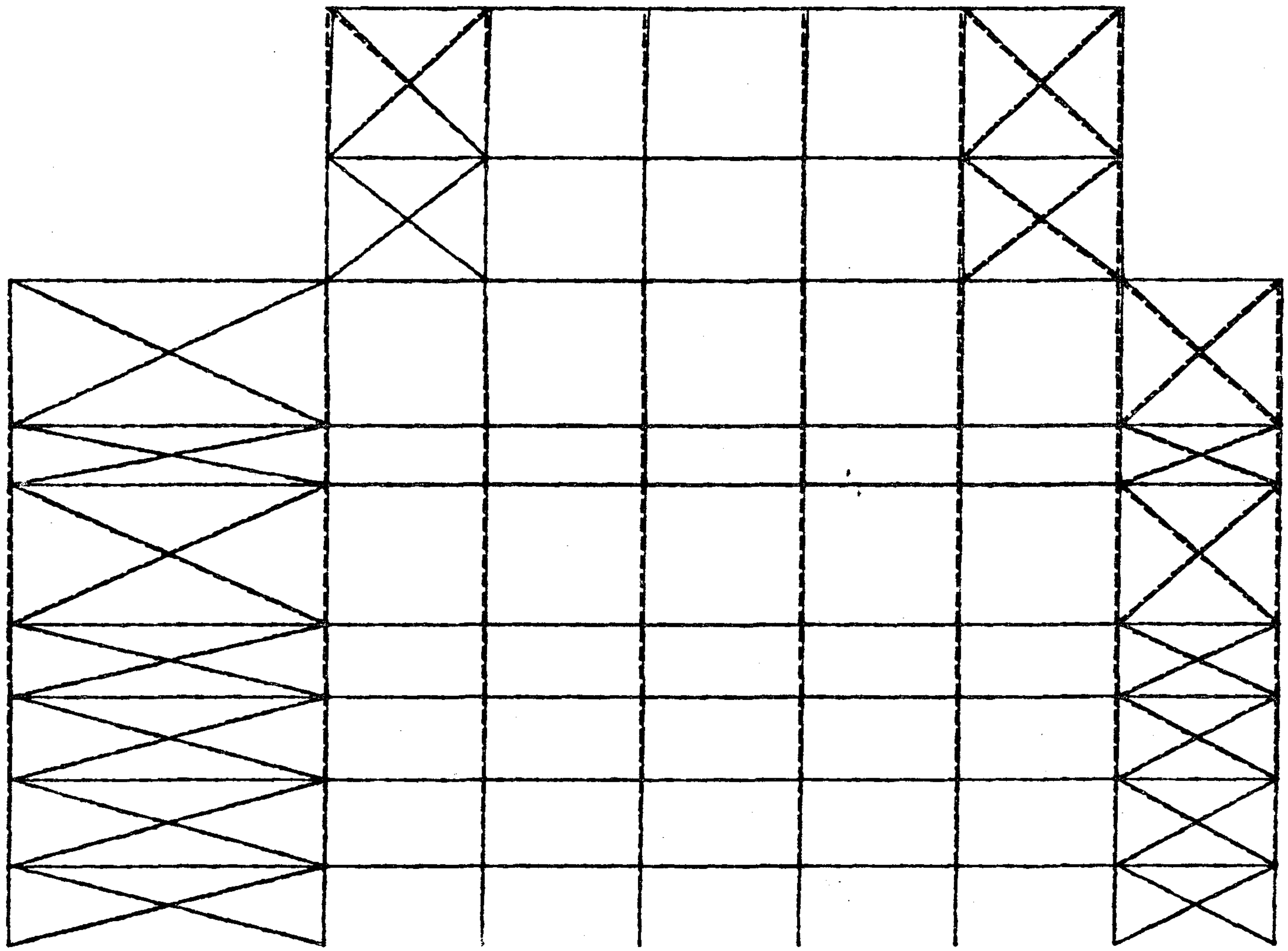

Figure 57

The ninth mode of system No. 1 in an elevation view.

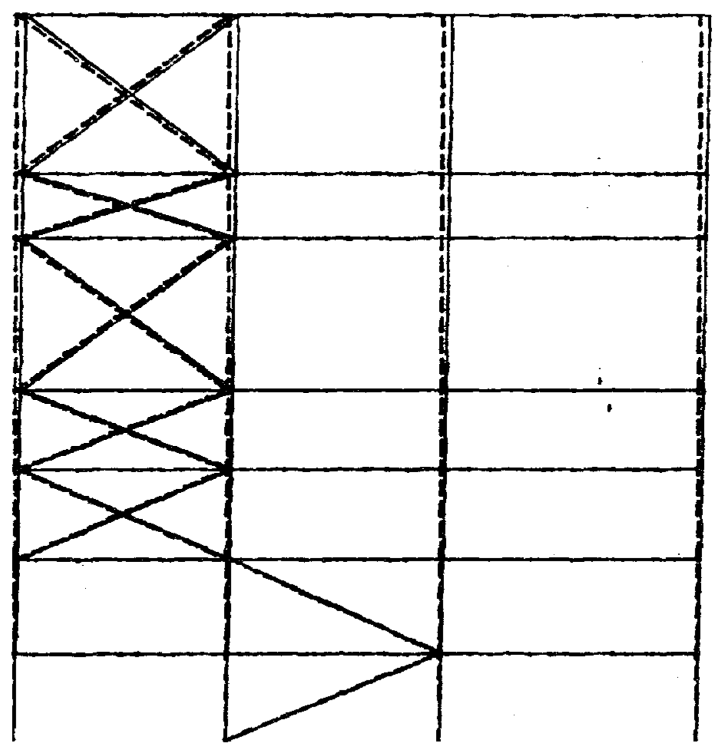

Figure 58

The ninth mode of system No. 1 in a side view.

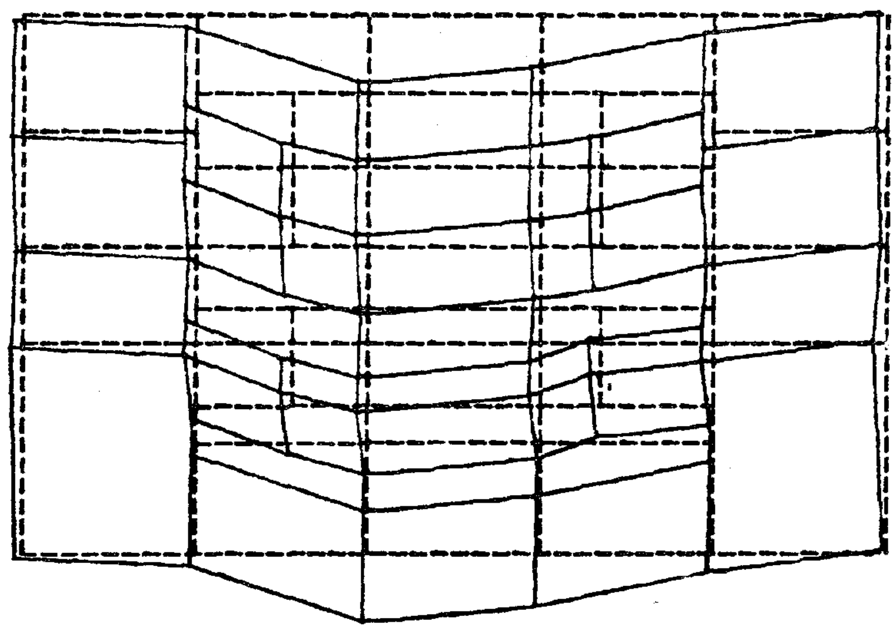

Figure 59

The tenth mode of system No. 1 in a plan view.

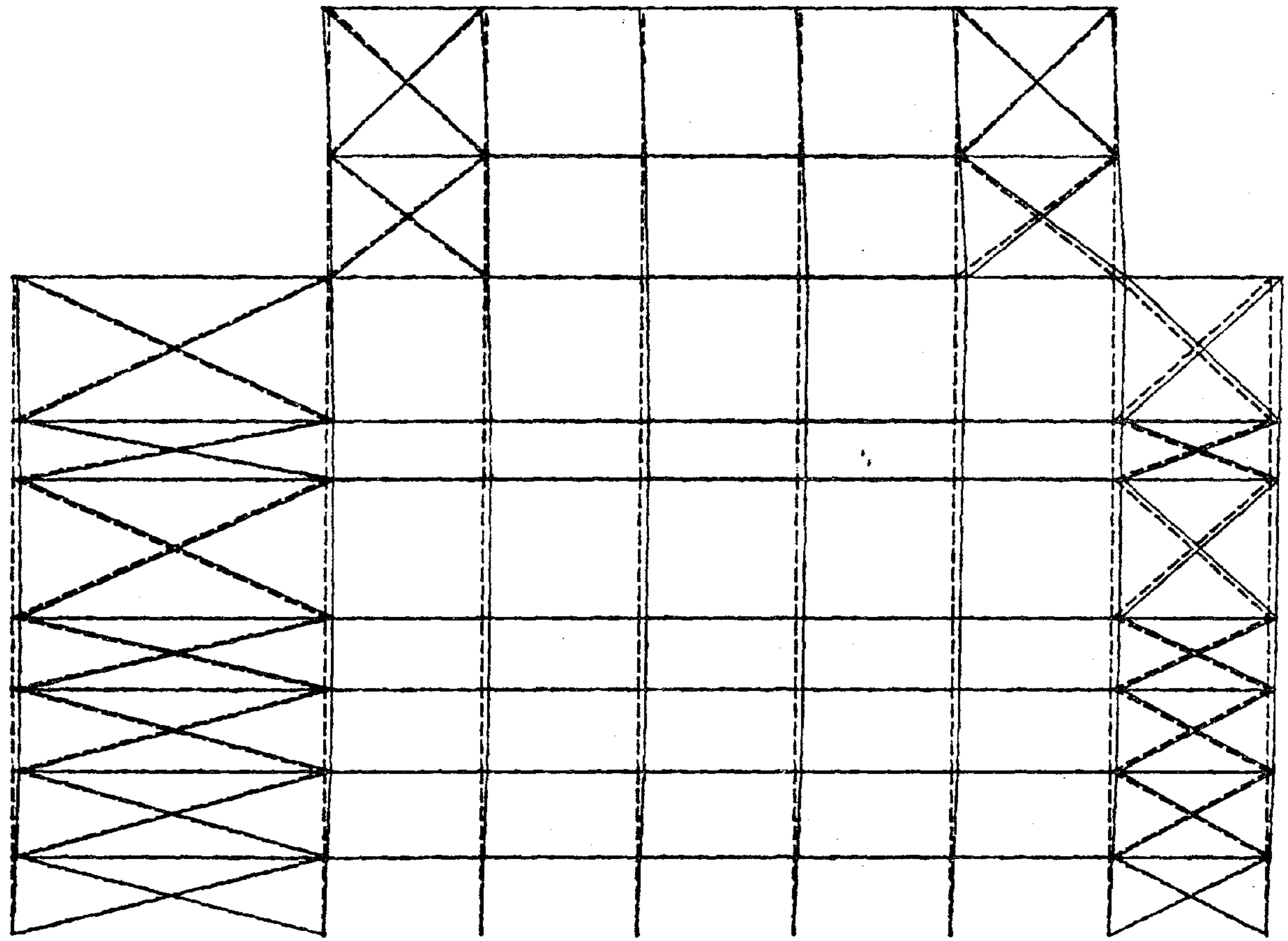

Figure 60

The tenth mode of system No. 1 in an elevation view.

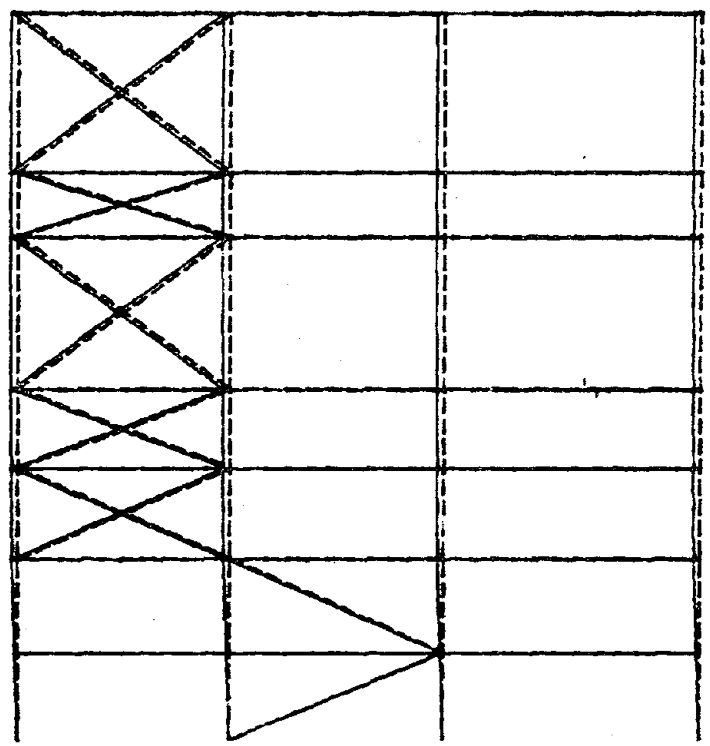

Figure 61

The tenth mode of system No. 1 in a side view.

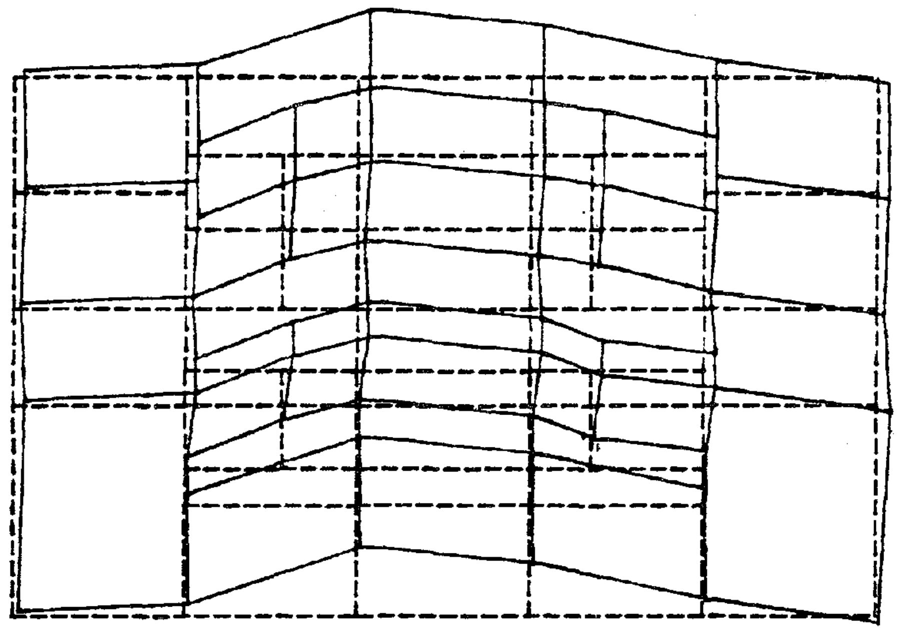

Figure 62

The eleventh mode of system No. 1 in a plan view.

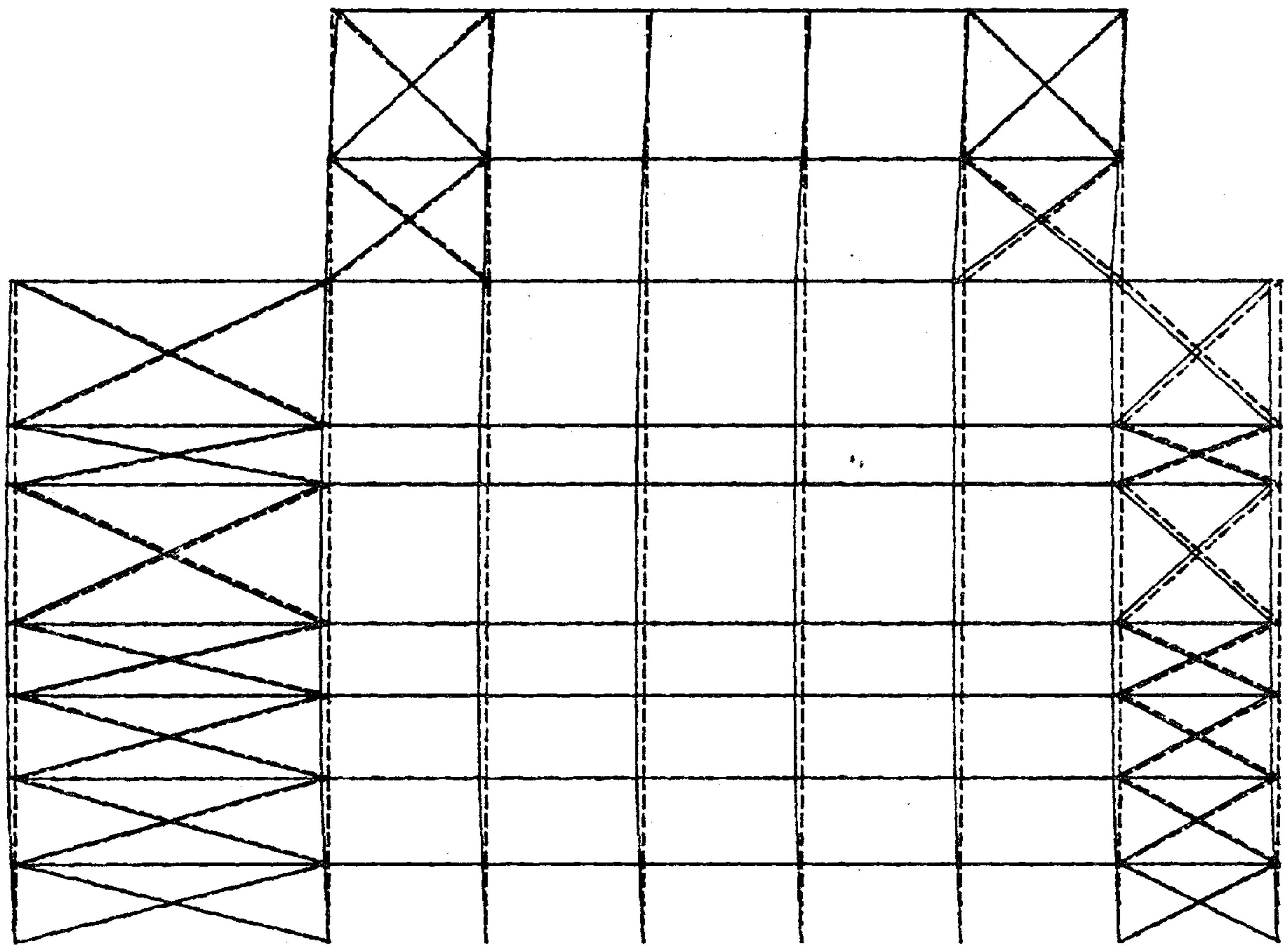

Figure 63

The eleventh mode of system No. 1 in an elevation view.

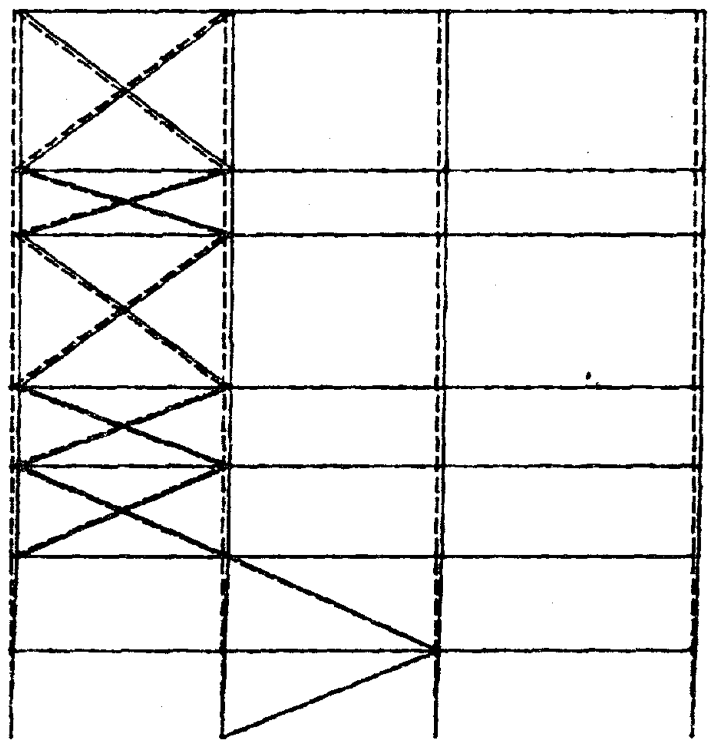

Figure 64

The eleventh mode of system No. 1 in a side view.

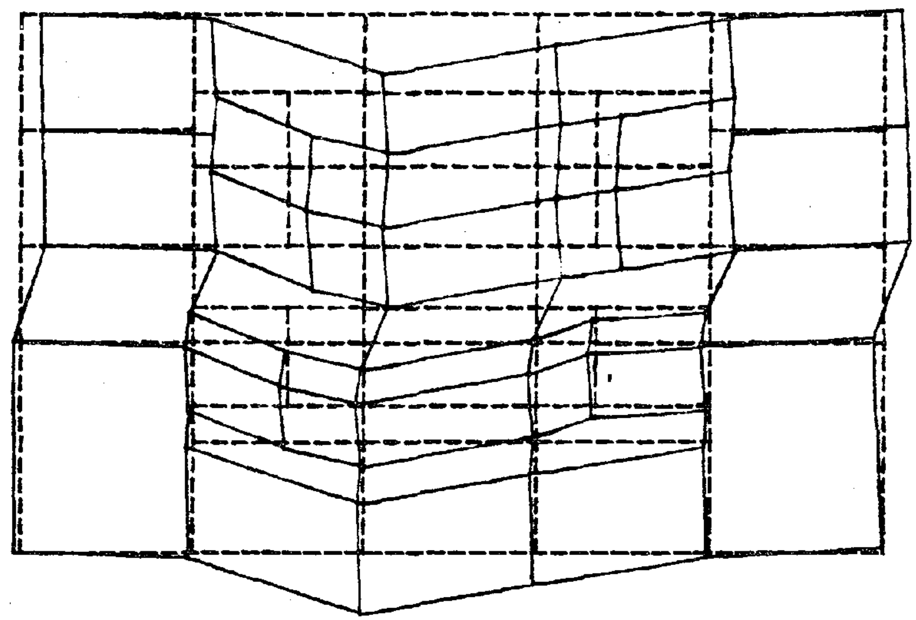

Figure 65

The twelfth mode of system No. 1 in a plan view.

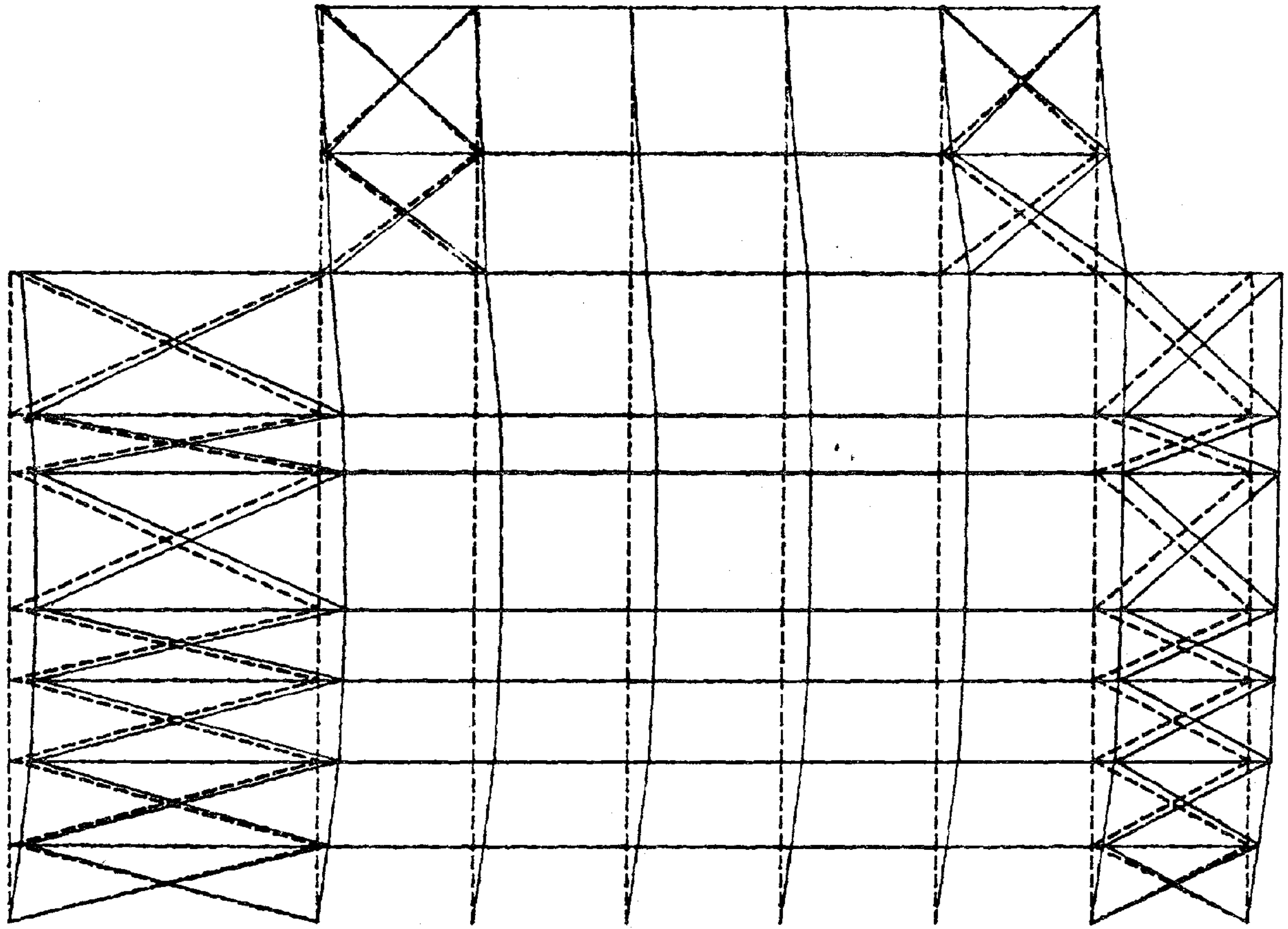

Figure 66

The twelfth mode of system No. 1 in an elevation view.

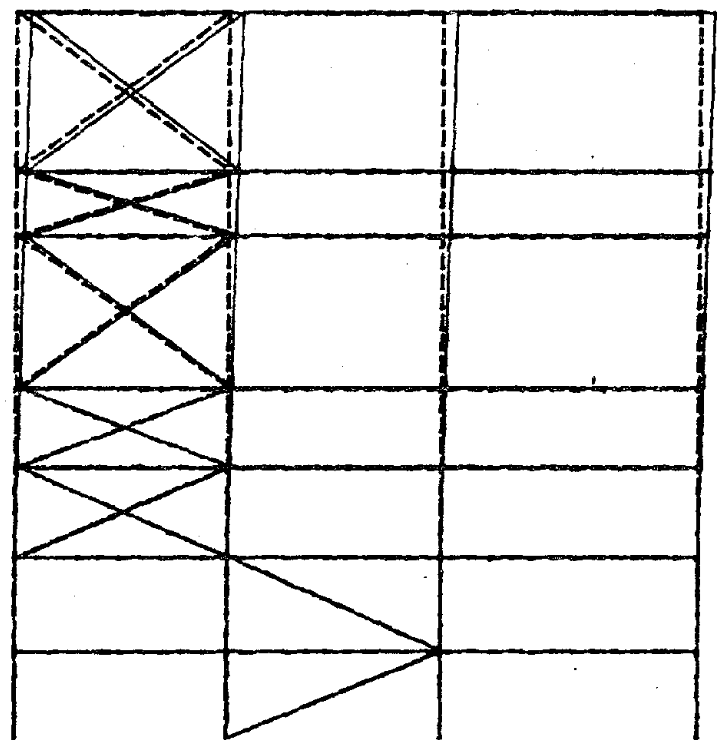

Figure 67

The twelfth mode of system No. 1 in a side view.

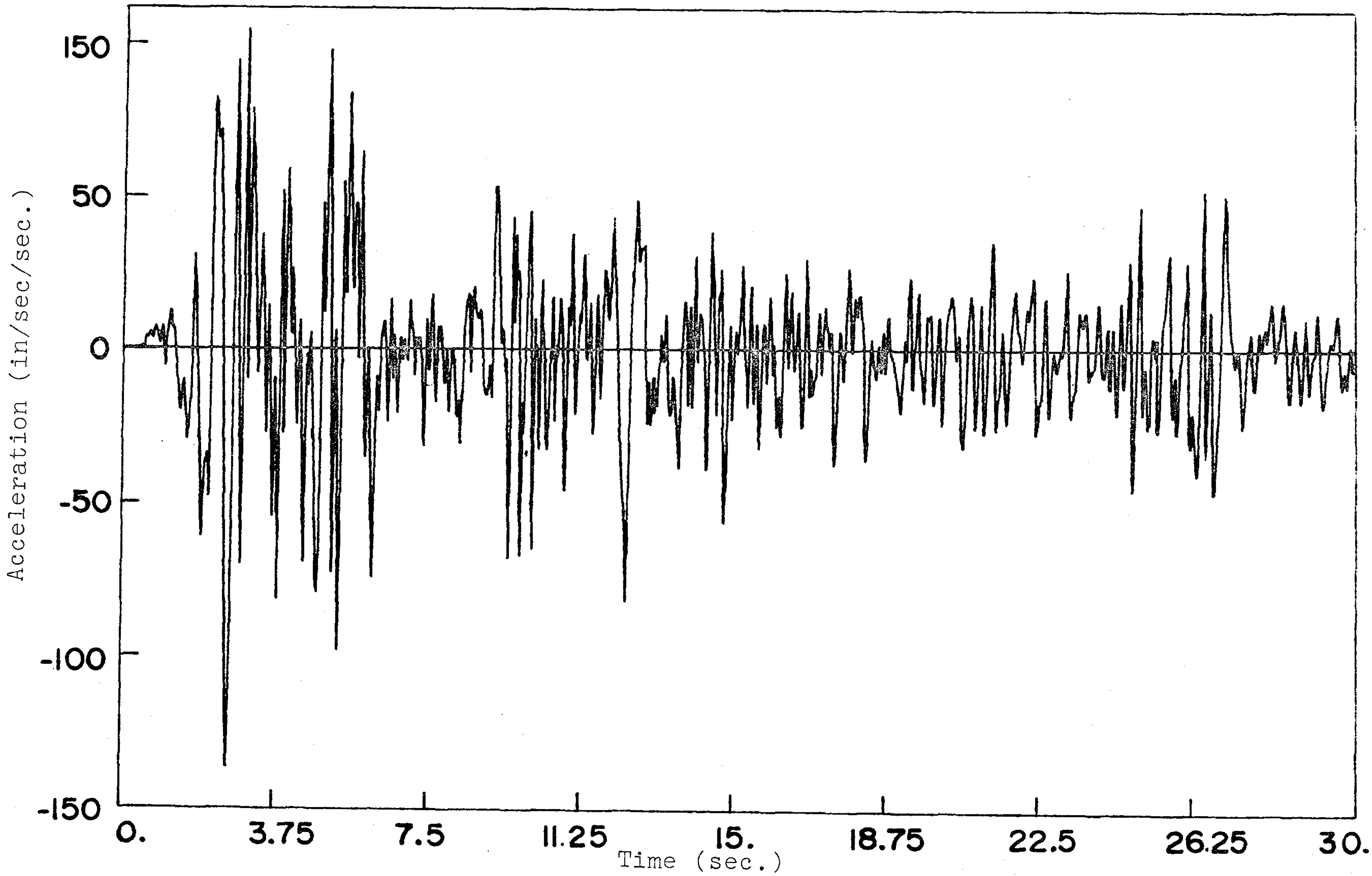

Figure 68

The North-South component of the ground acceleration of the El Centro earthquake of May 18, 1940.

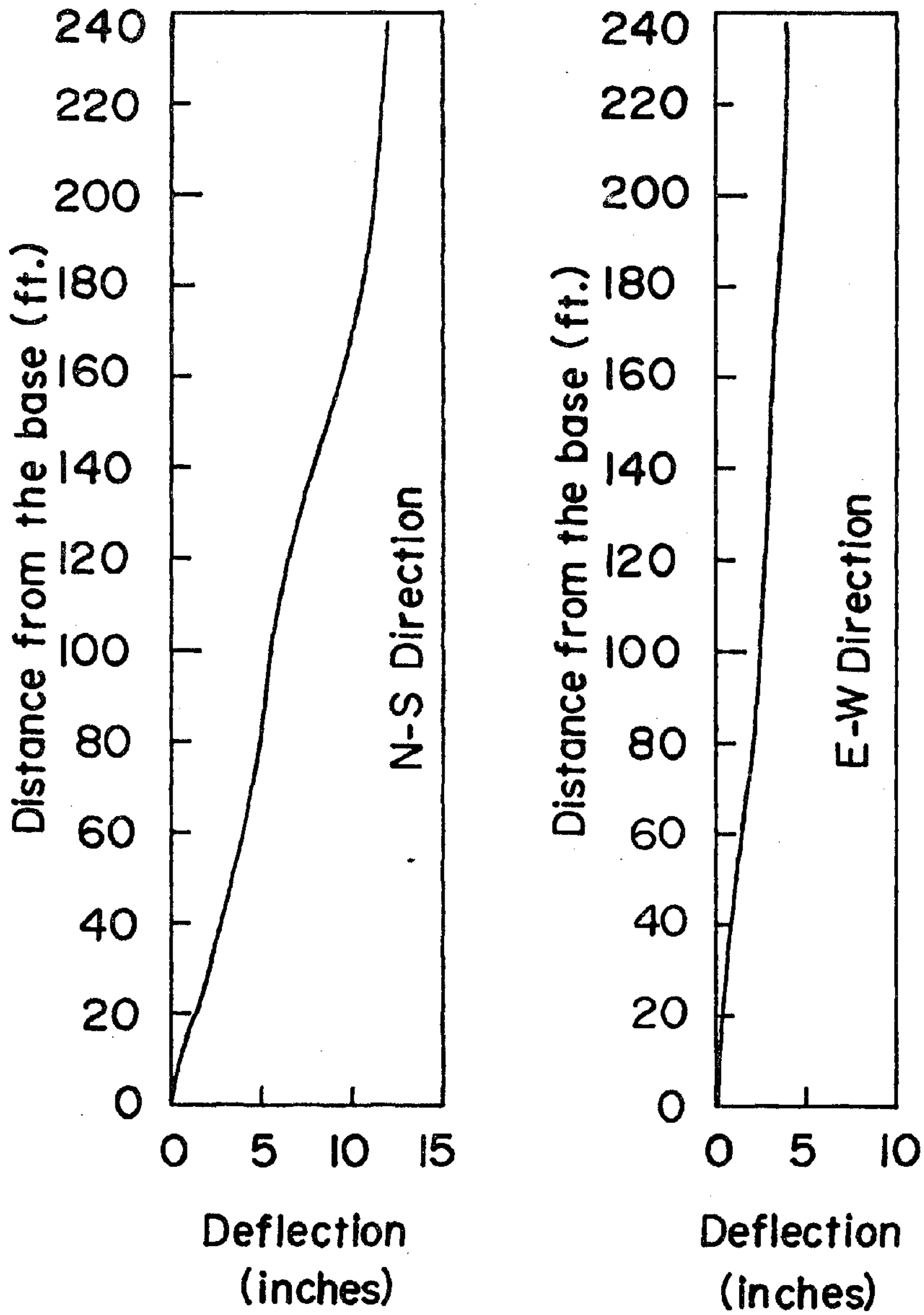

Figure 69

Components of the maximum deflection of the column $23N_z$ of system No. 1 in two orthogonal directions.

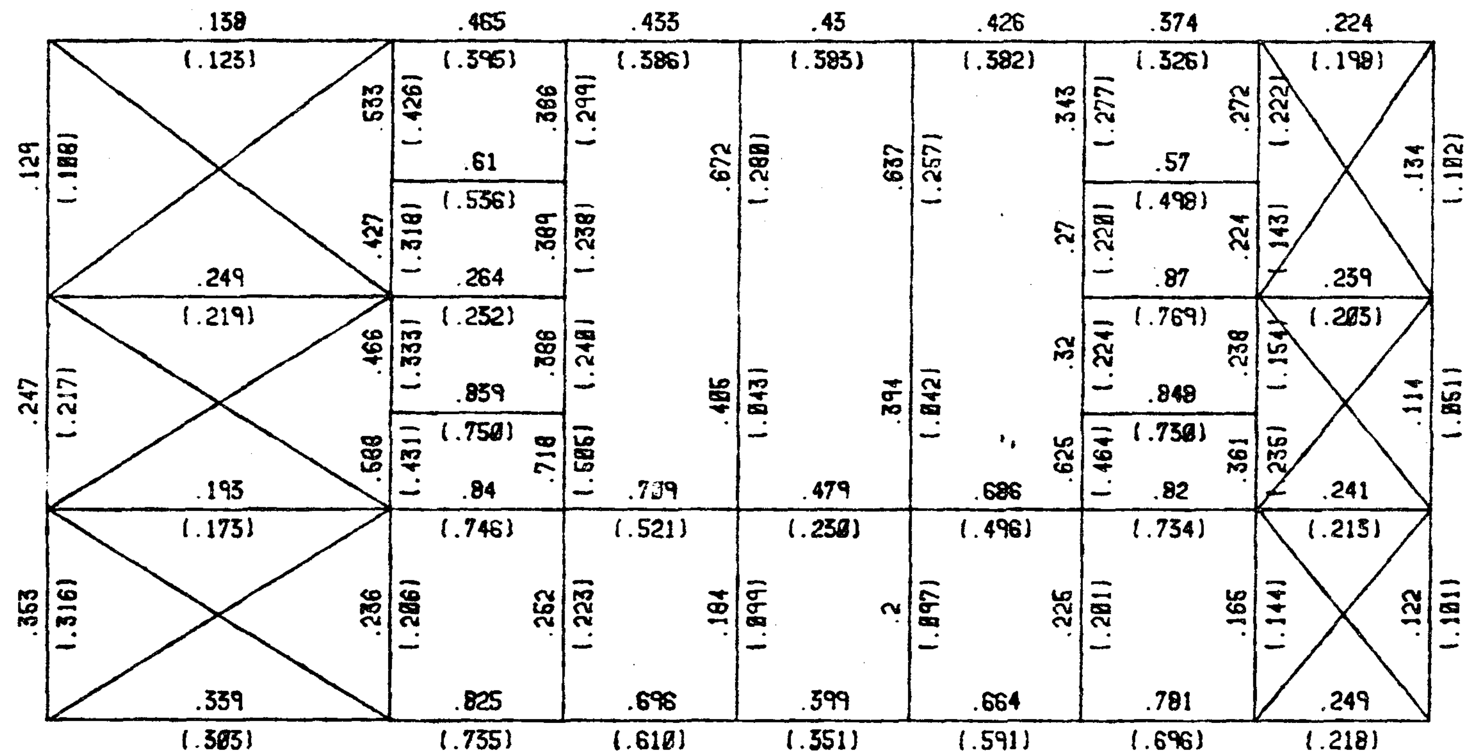

Figure 70

Ratios of the stresses in the beam members of system No. 1 located at EL 400.

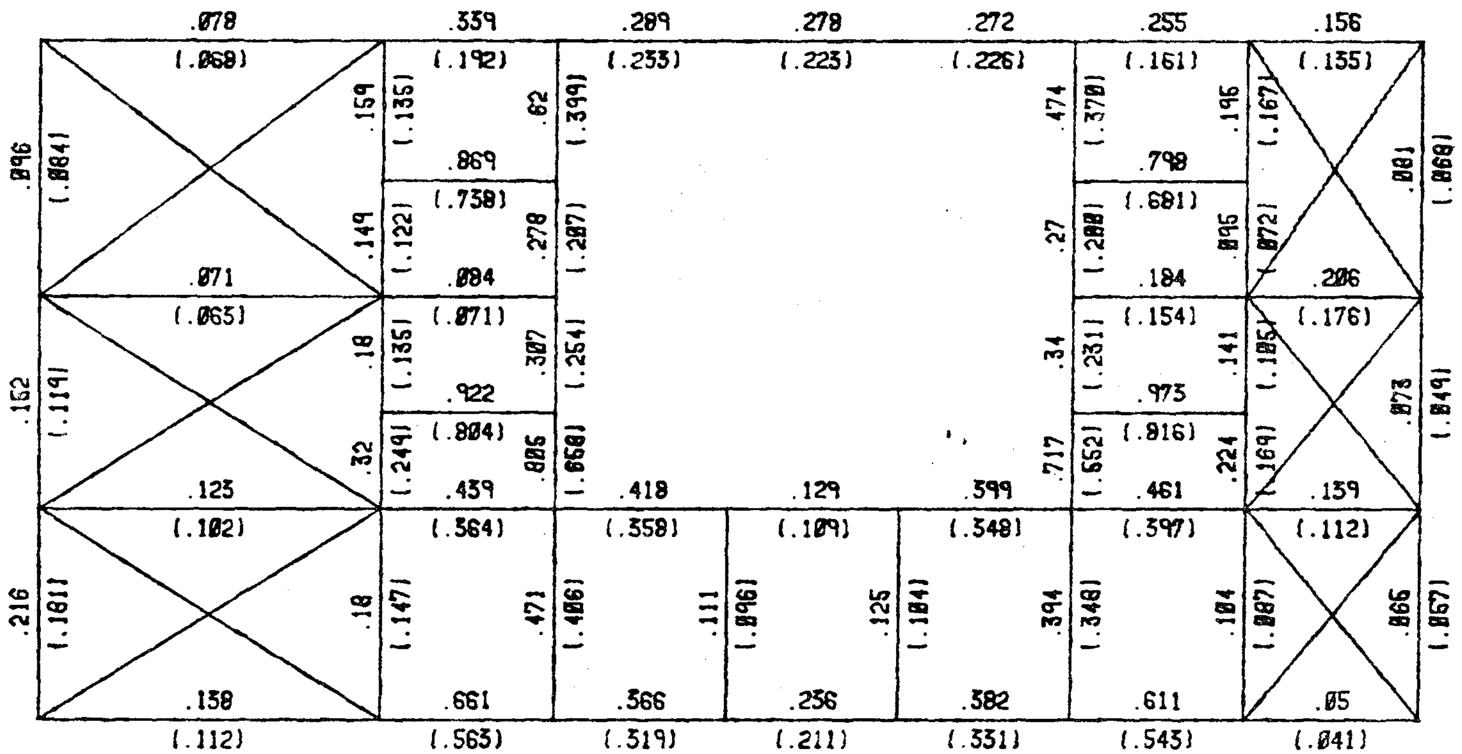

Figure 71

Ratios of the stresses in the beam members of system No. 1 located at EL 422.

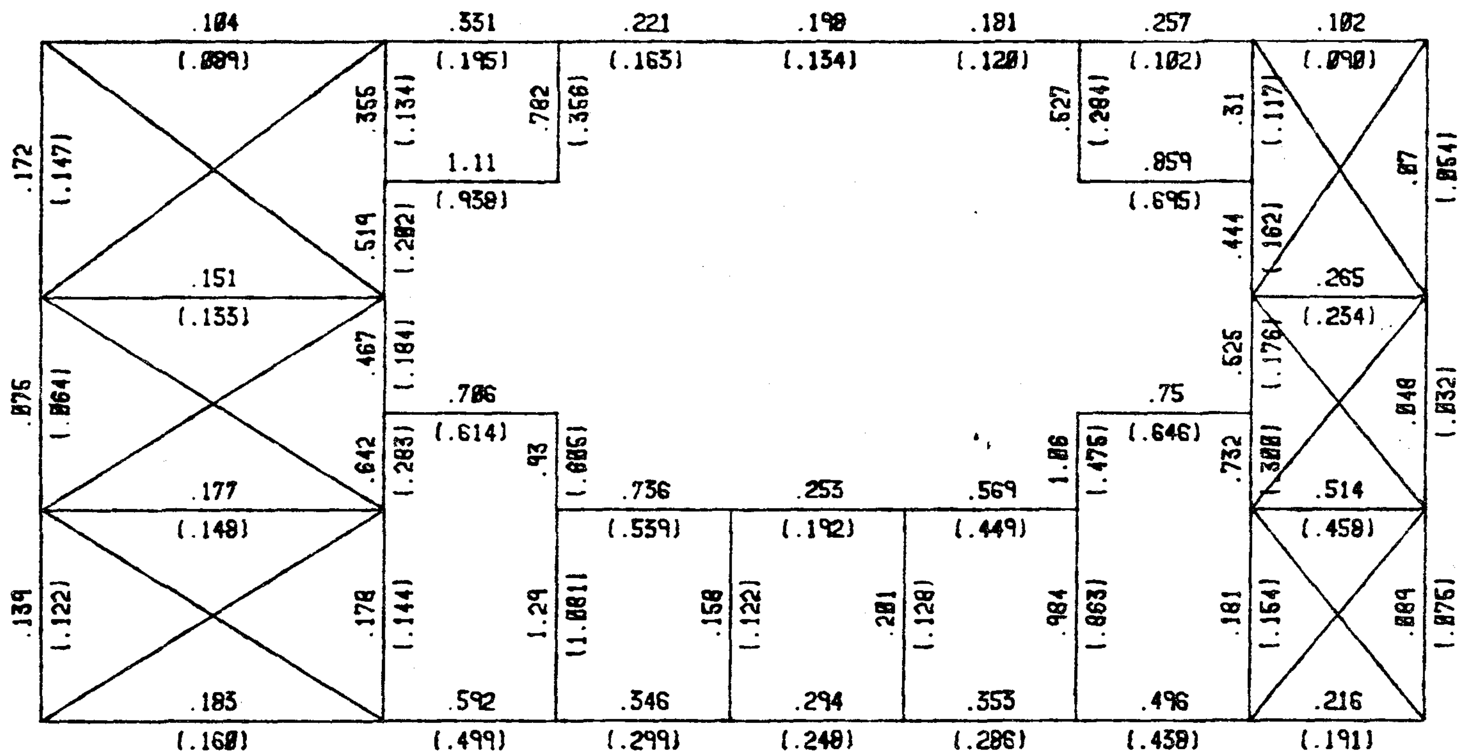

Figure 72

Ratios of the stresses in the beam members of system No. 1 located at EL 443.

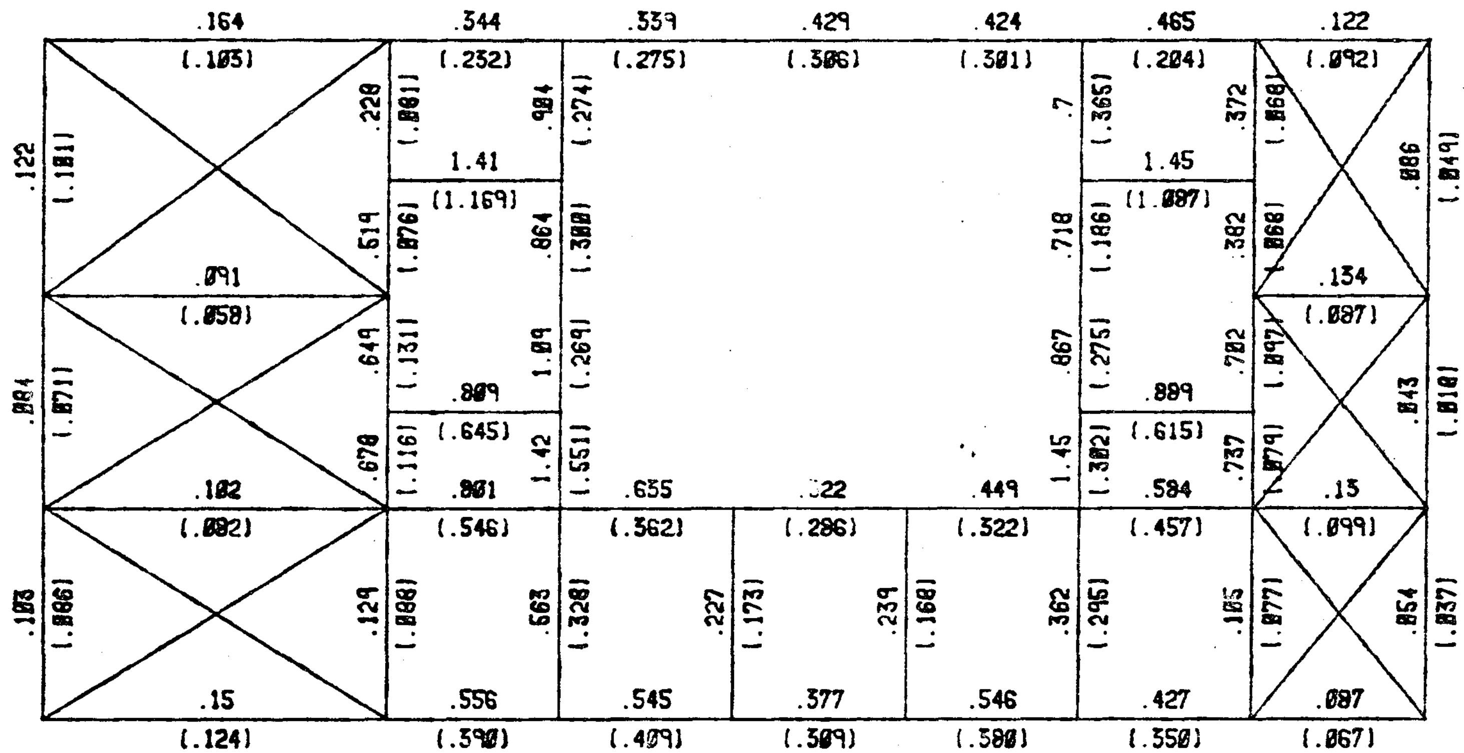

Figure 73

Ratios of the stresses in the beam members of system No. 1 located at EL 461.5.

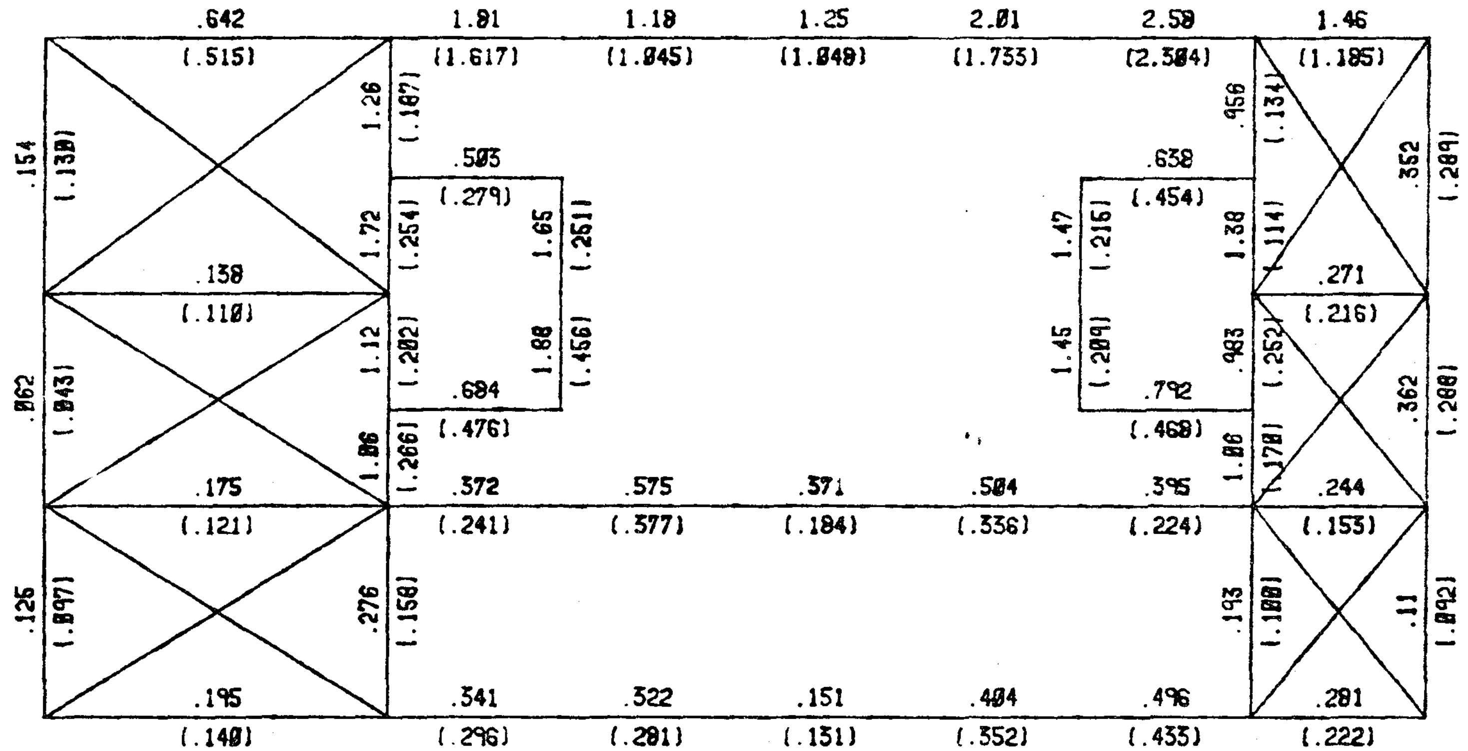

Figure 74

Ratios of the stresses in the beam members of system No. 1 located at EL 497.

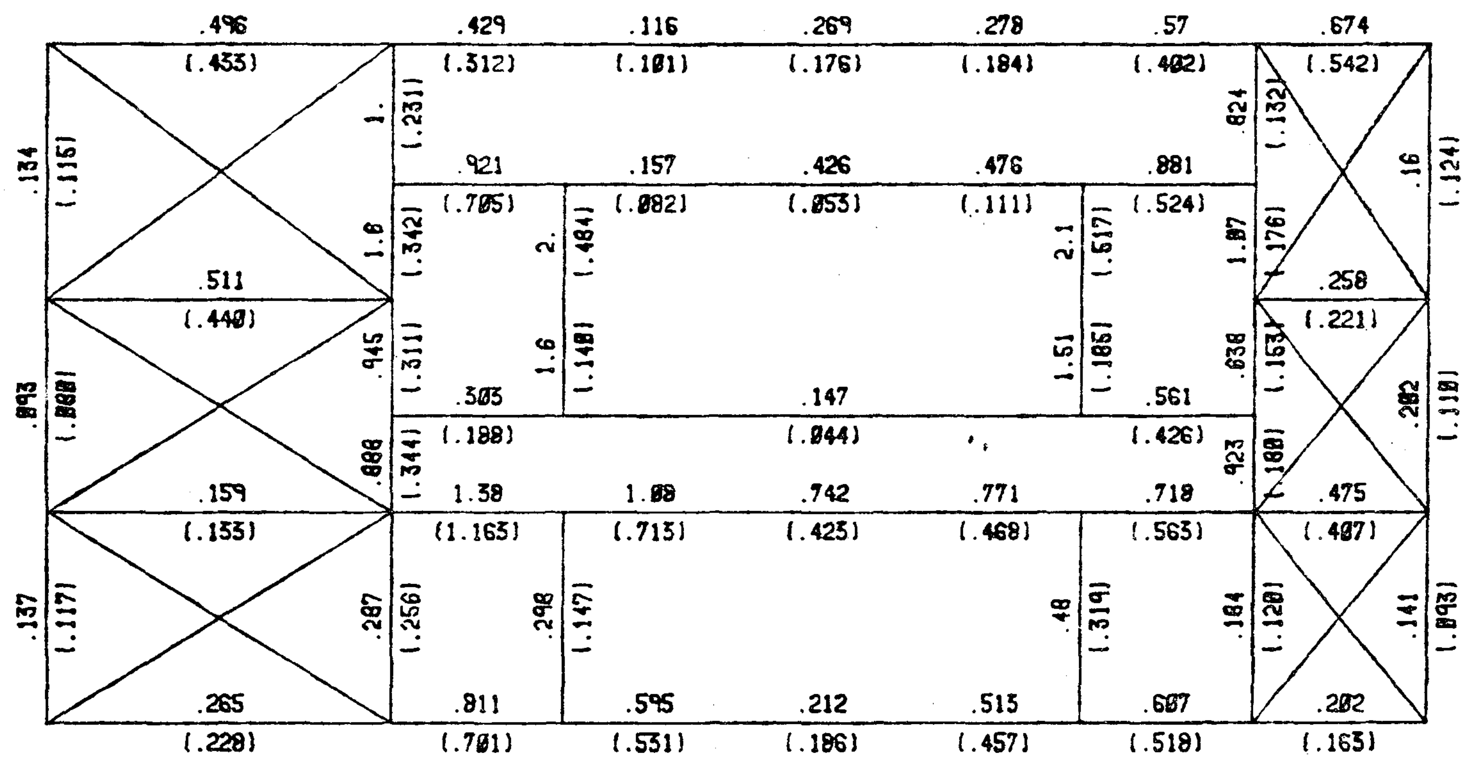

Figure 75

Ratios of the stresses in the beam members of system No. 1 located at EL 512.

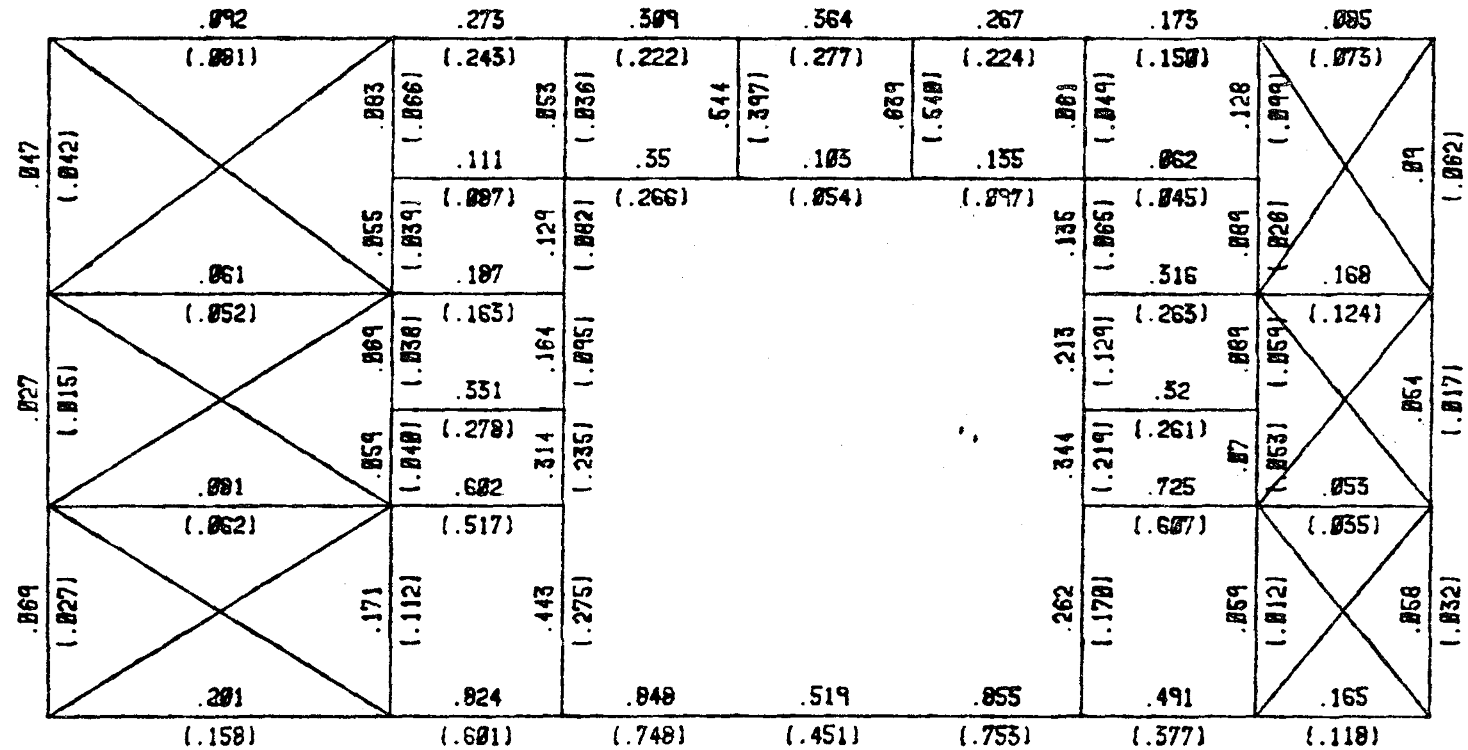

Figure 76

Ratios of the stresses in the beam members of system No. 1 located at EL 549.

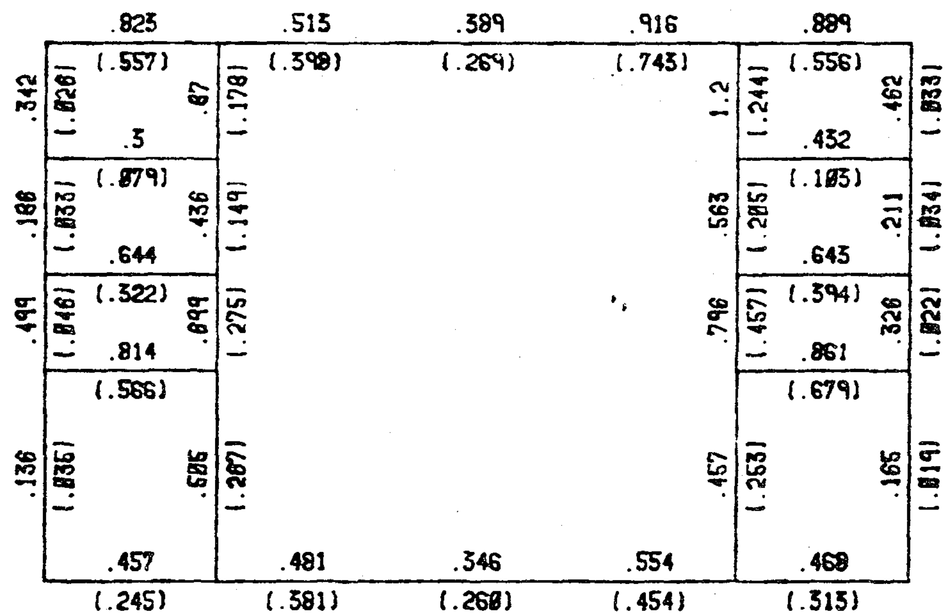

Figure 77

Ratios of the stresses in the beam members of system No. 1 located at EL 580.

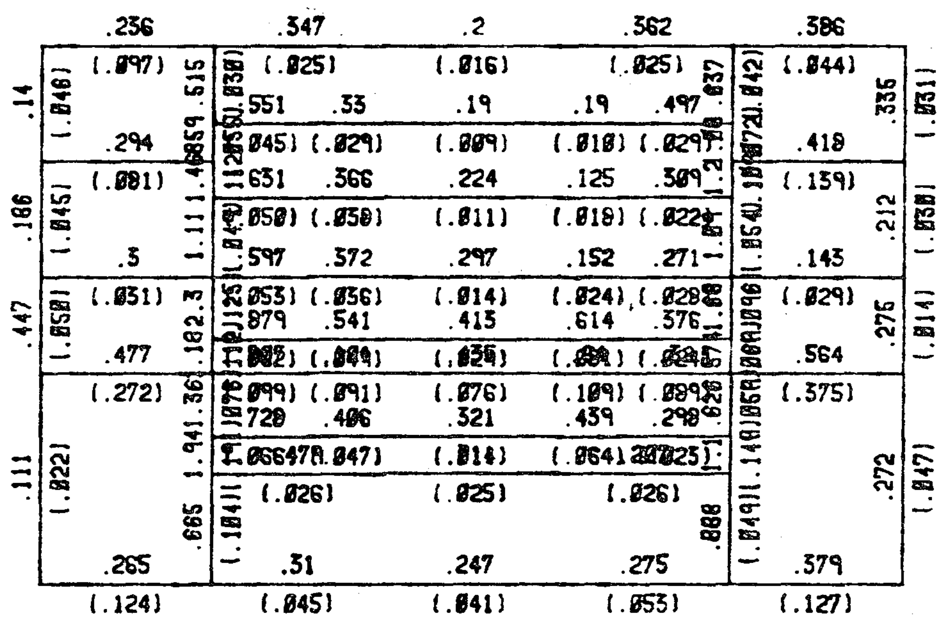

Figure 78

Ratios of the stresses in the beam members of system No. 1 located at EL 618.

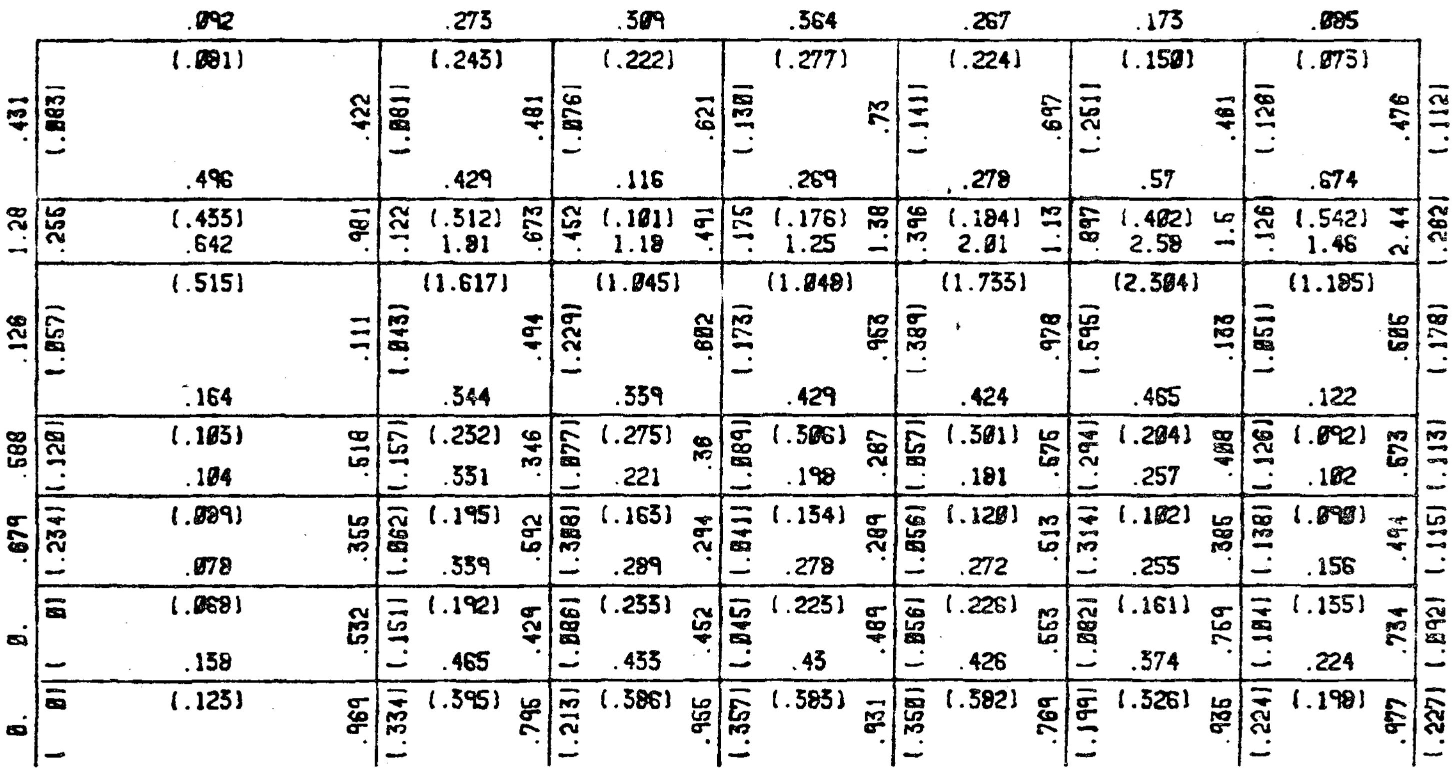

Figure 79

Ratios of the stresses in the beam members of system No. 1 located on a vertical plane at line E.

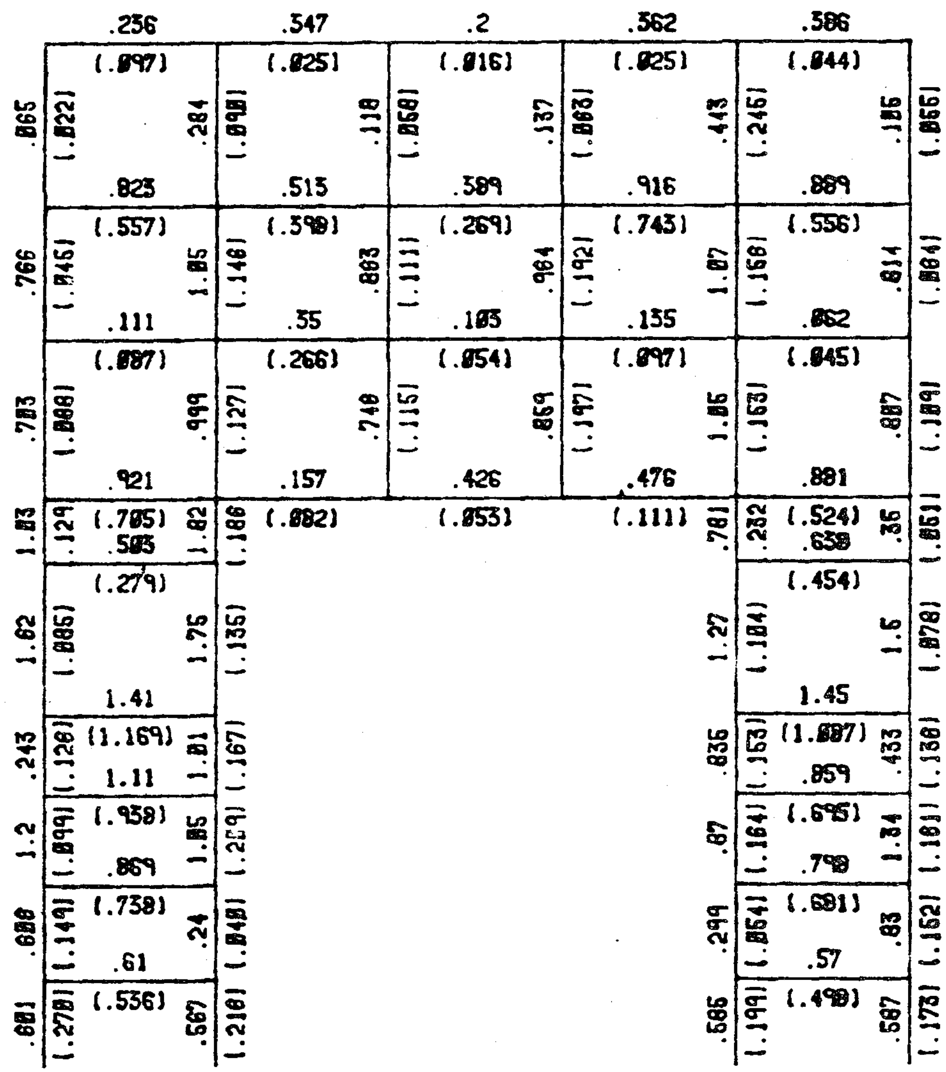

Figure 80

Ratios of the stresses in the beam members of system No. 1 located on a vertical plane at line GV.

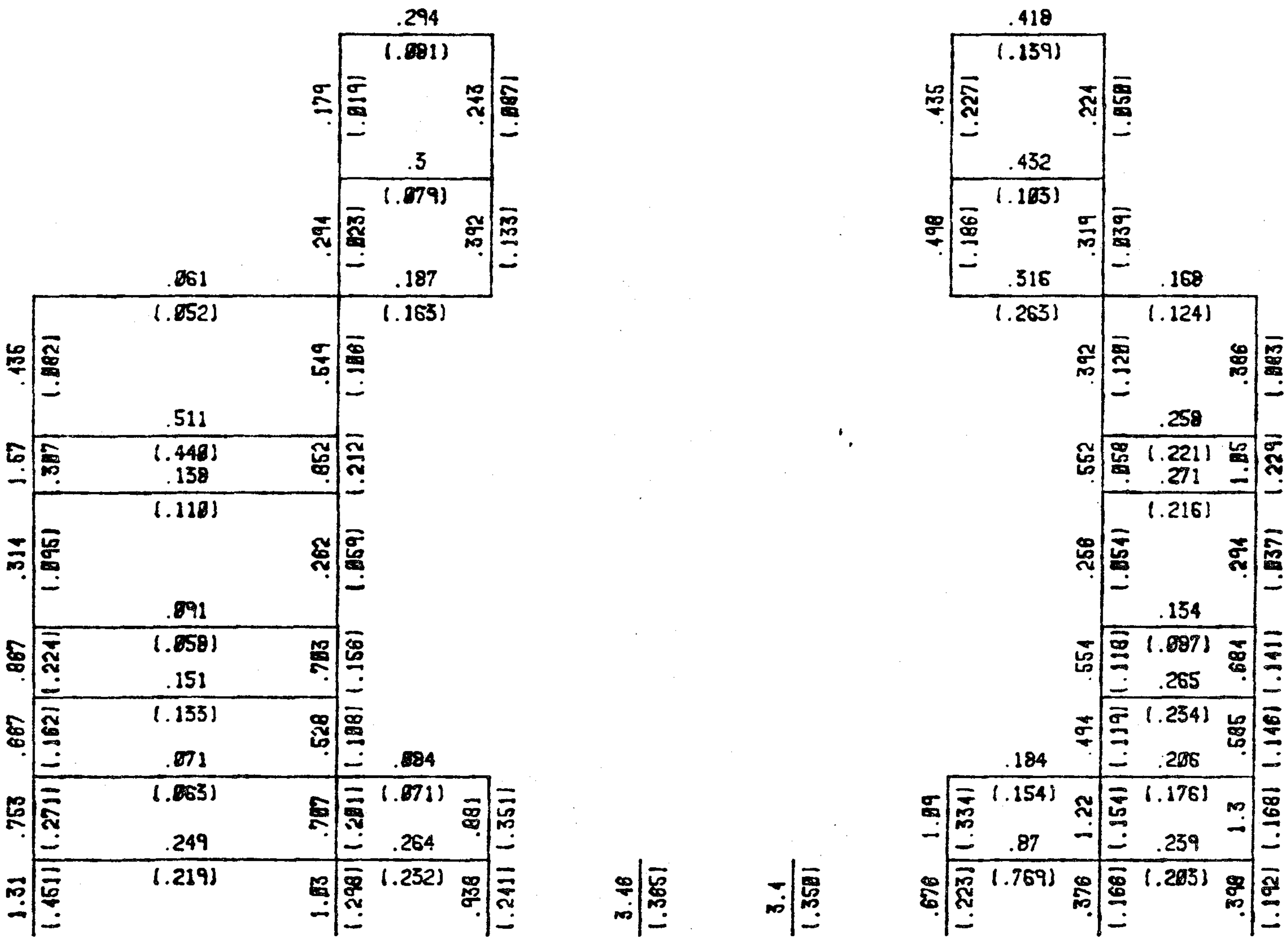

Figure 81

Ratios of the stresses in the beam members of system No. 1 located on a vertical plane at line Hv.

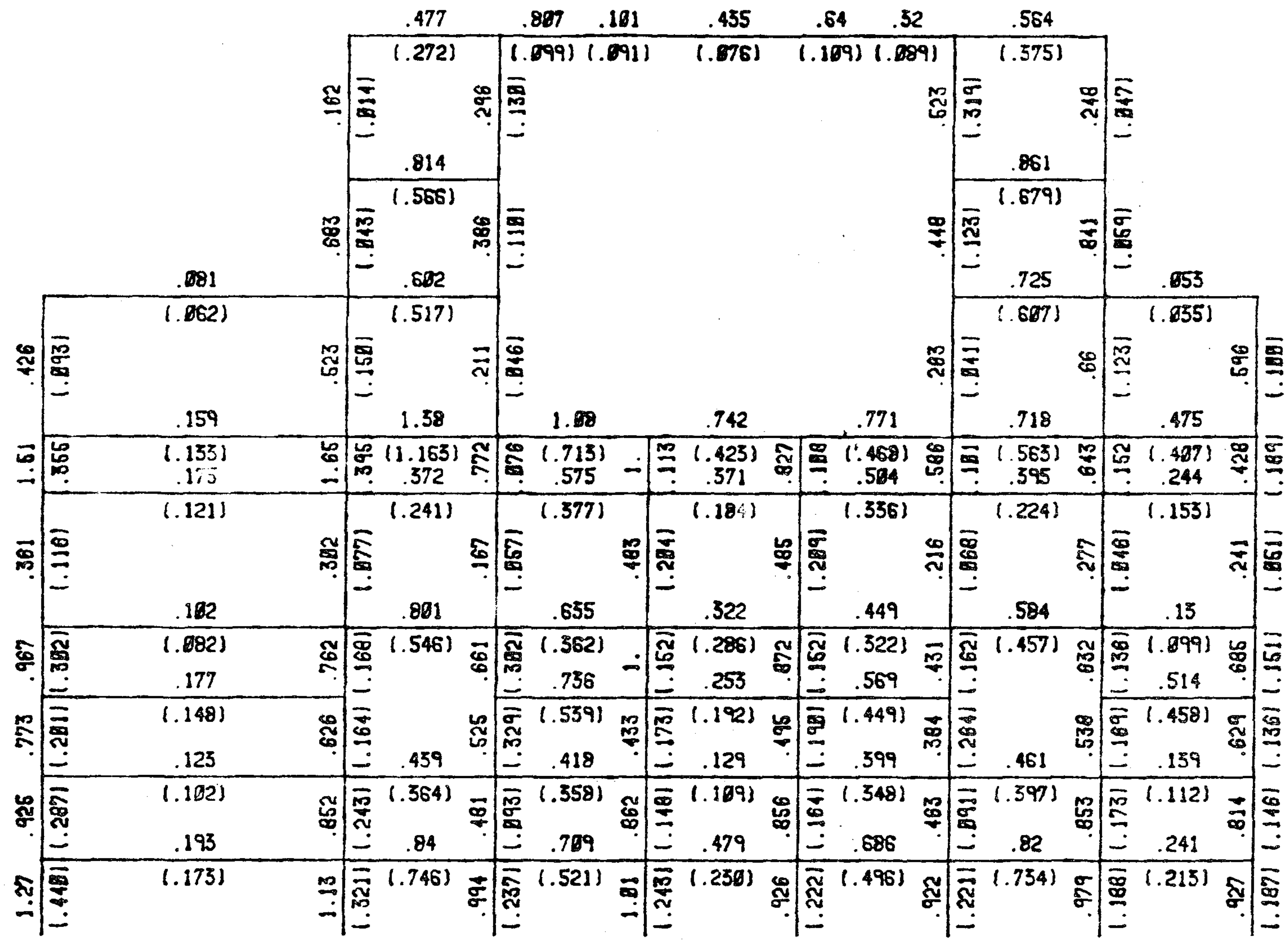

Figure 82

Ratios of the stresses in the beam members of system No. 1 located on a vertical plane at line Kv.

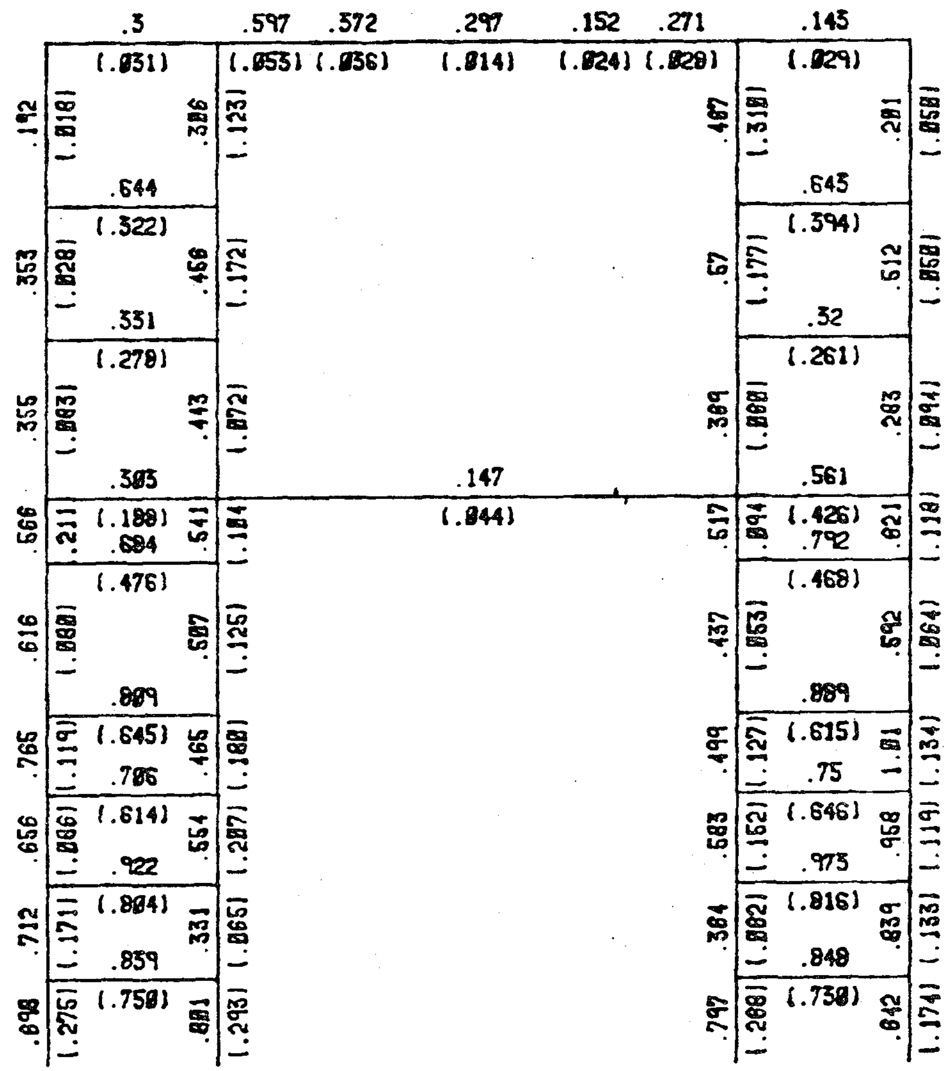

Figure 83

Ratios of the stresses in the beam members of system No. 1 located on a vertical plane at line Jv.

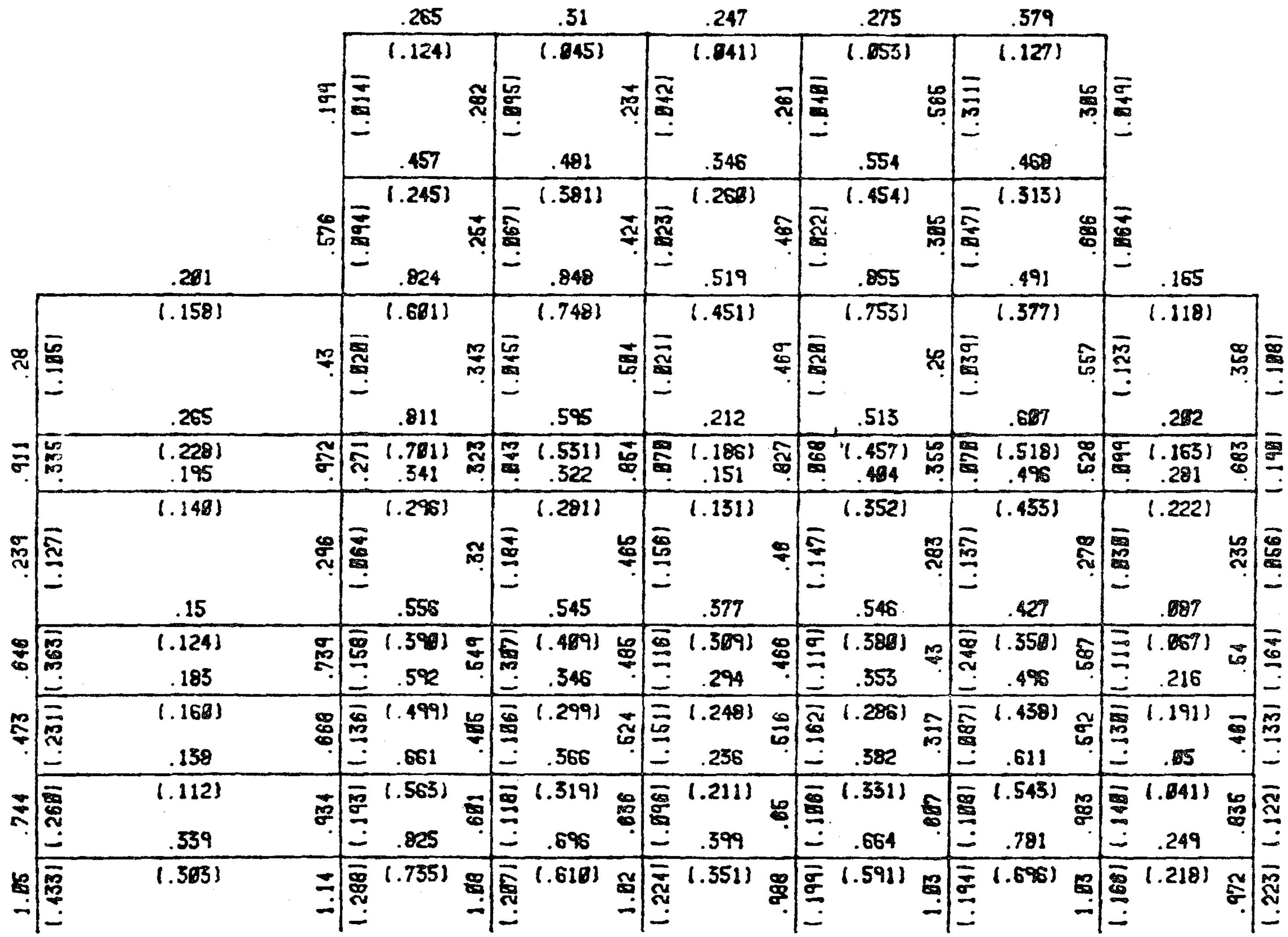

Figure 84

Ratios of the stresses in the beam members of system No. 1 located on a vertical plane at line Nz.

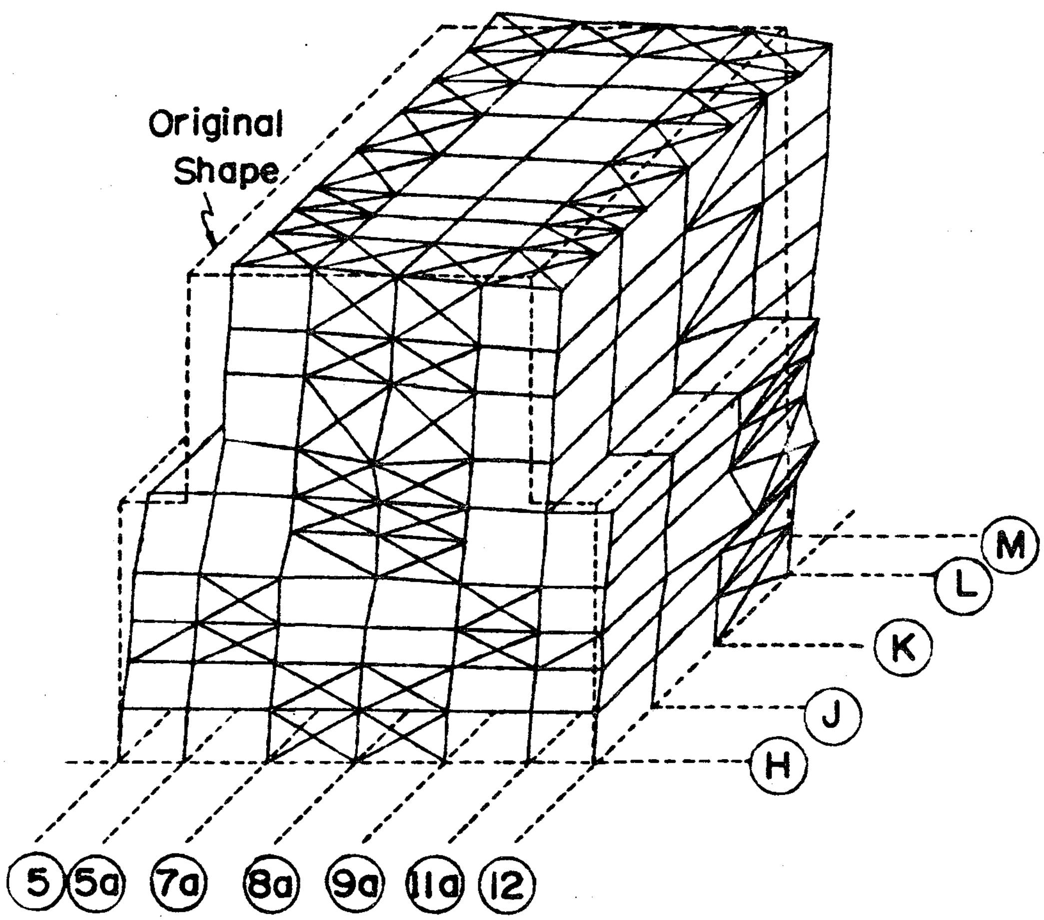

Figure 85

The first mode shape of system No. 2 in a three-dimensional view.

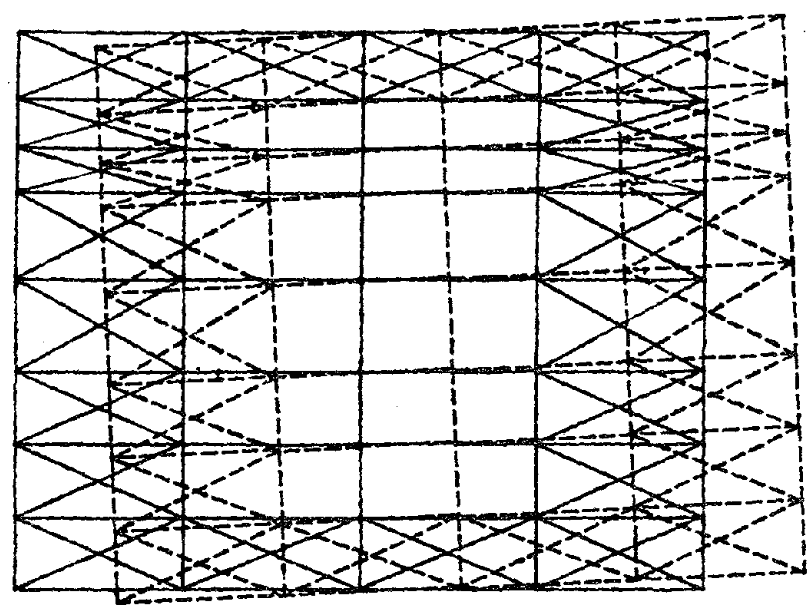

Figure 86

The first mode shape of system No. 2 in a plan view.

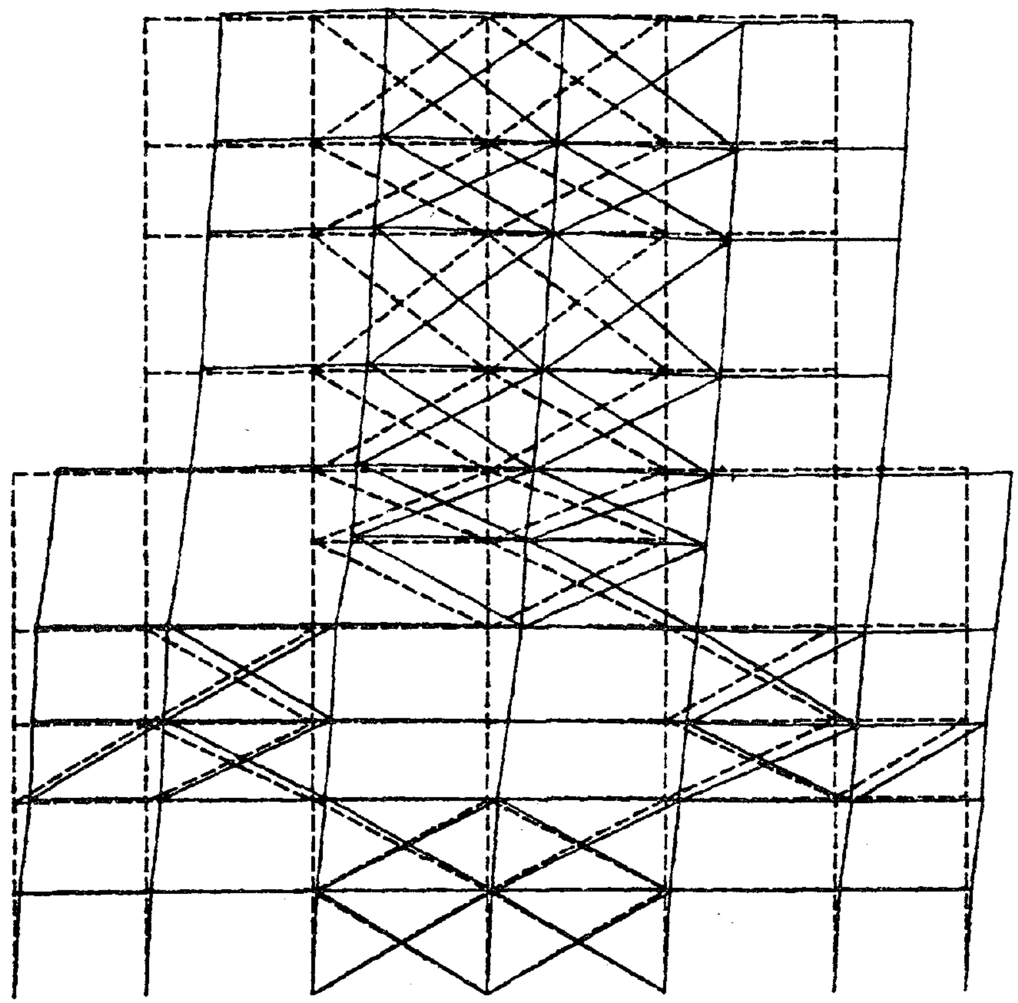

Figure 87

The first mode shape of system No. 2 in an elevation view.

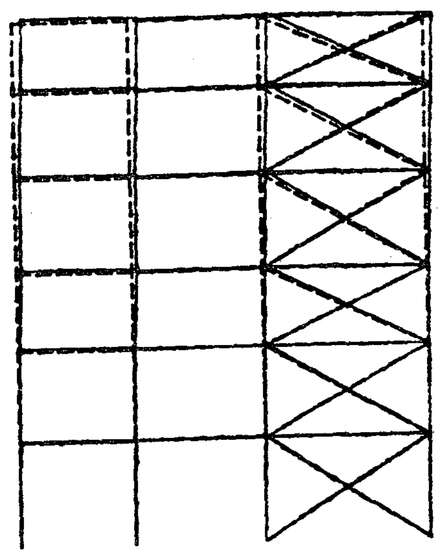

Figure 88

The first mode shape of system No. 2 in a side view.

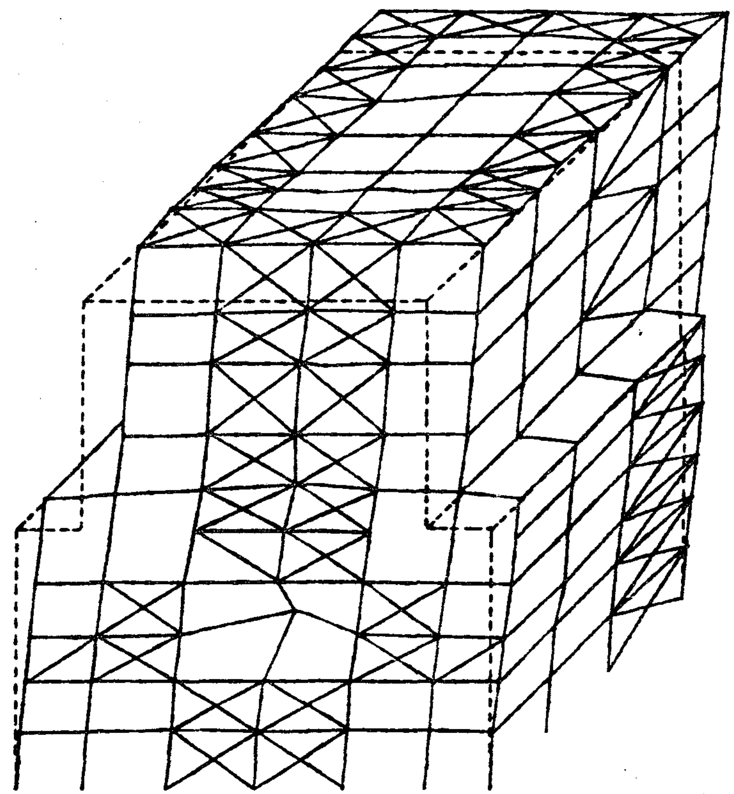

Figure 89

The second mode shape of system No. 2 in a three-dimensional view.

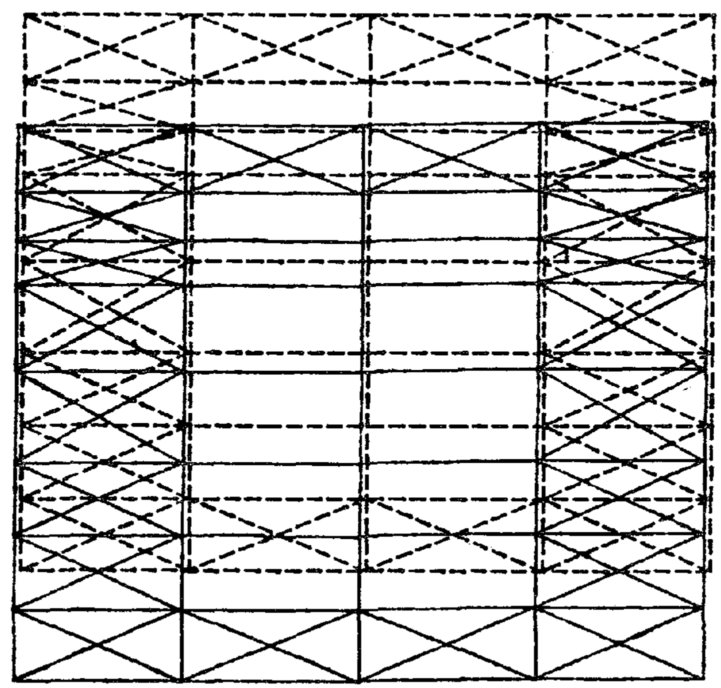

Figure 90

The second mode shape of system No. 2 in a plan view.

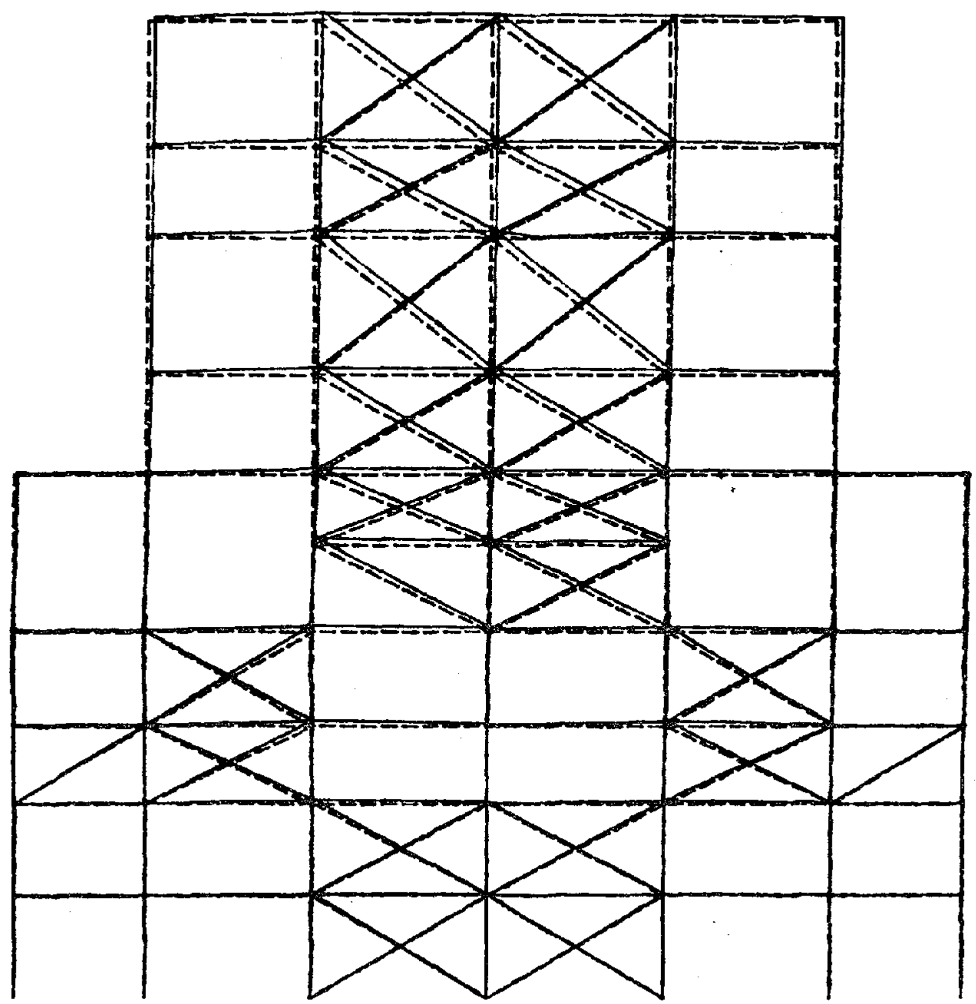

Figure 91

The second mode shape of system No. 2 in an elevation view.

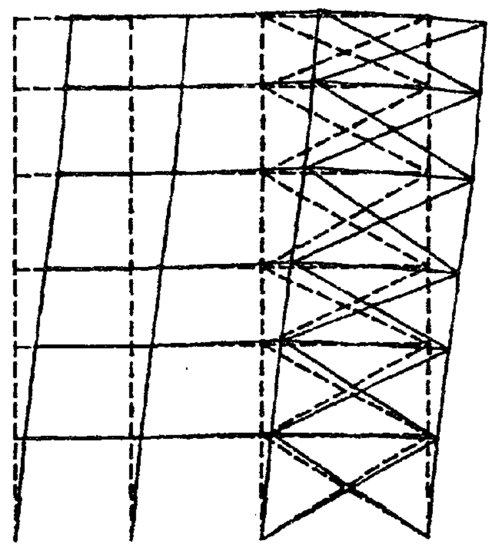

Figure 92

The second mode shape of system No. 2 in a side view.

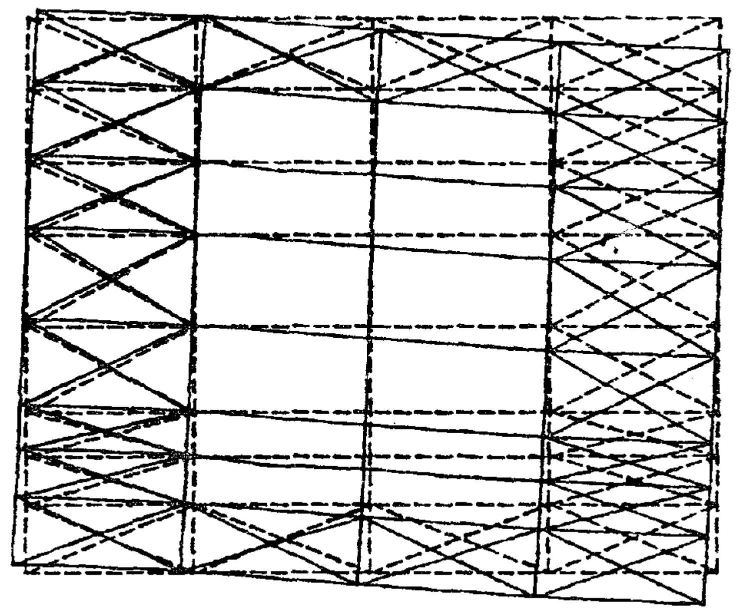

Figure 93

The third mode shape of system No. 2 in a plan view.

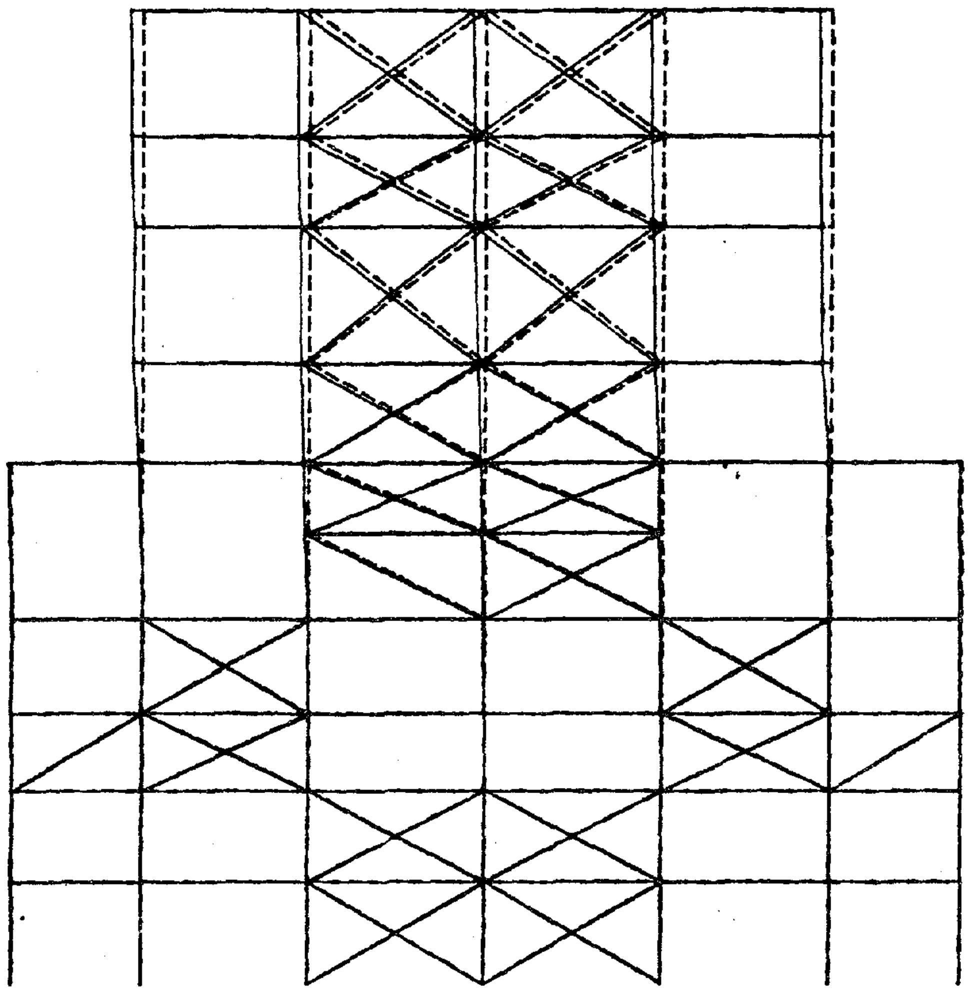

Figure 94

The third mode shape of system No. 2 in an elevation view.

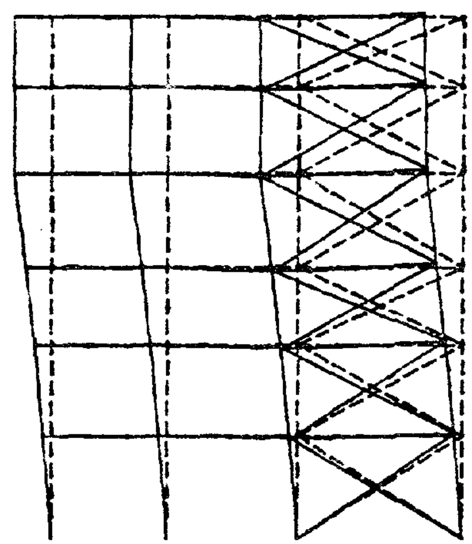

Figure 95

The third mode shape of system No. 2 in a side view.

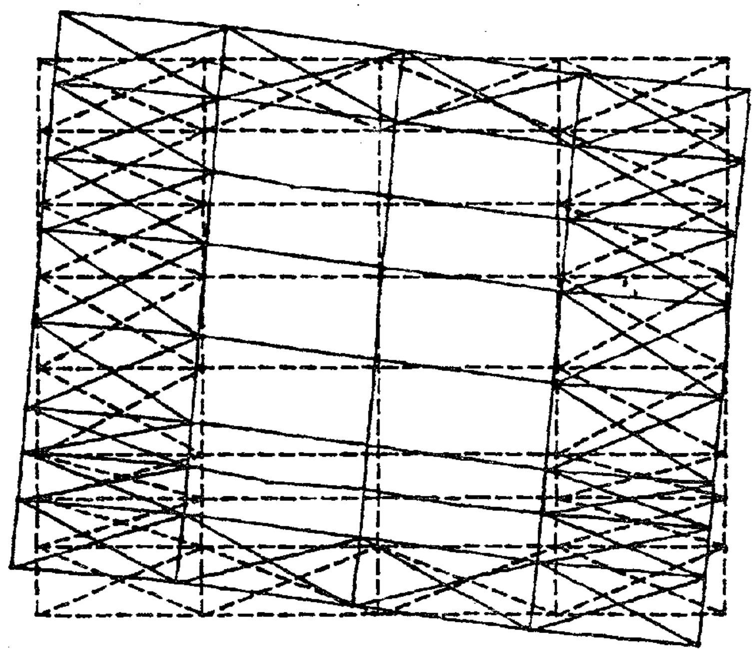

Figure 96

The fourth mode shape of system No. 2 in a plan view.

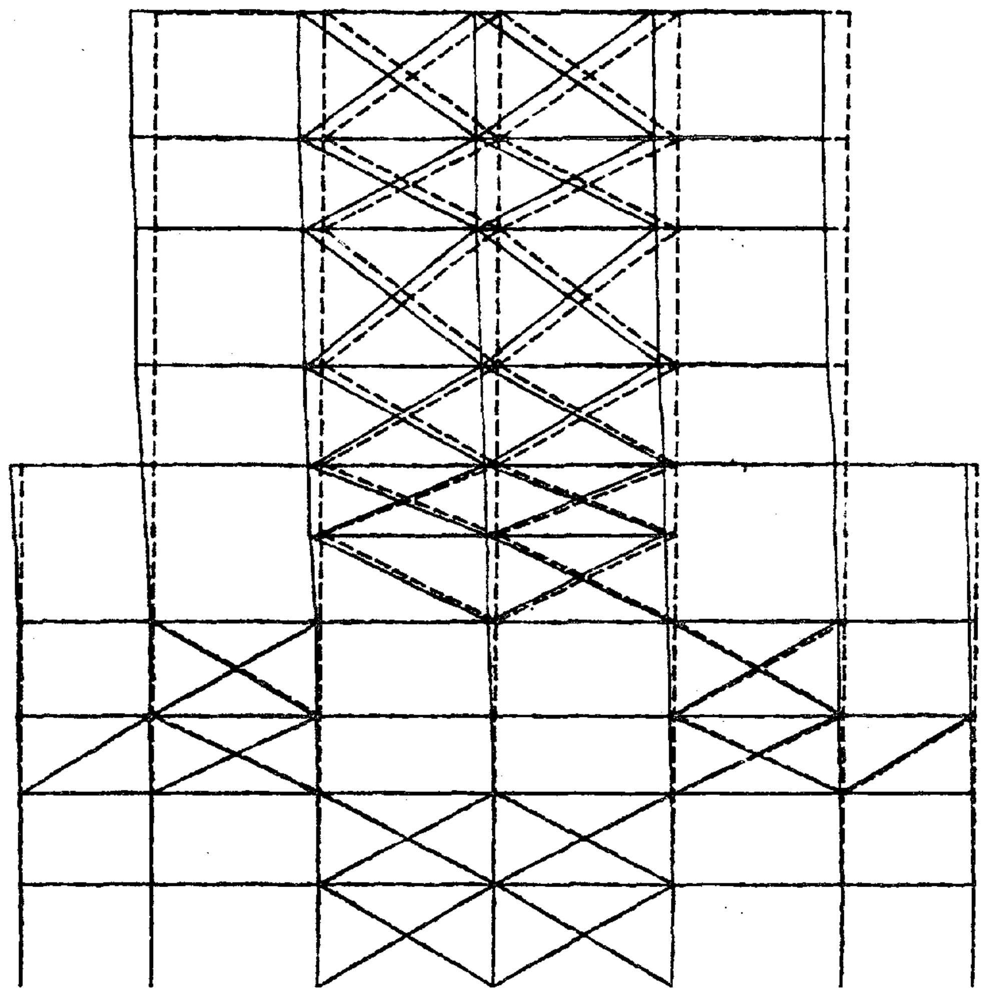

Figure 97

The fourth mode shape of system No. 2 in an elevation view.

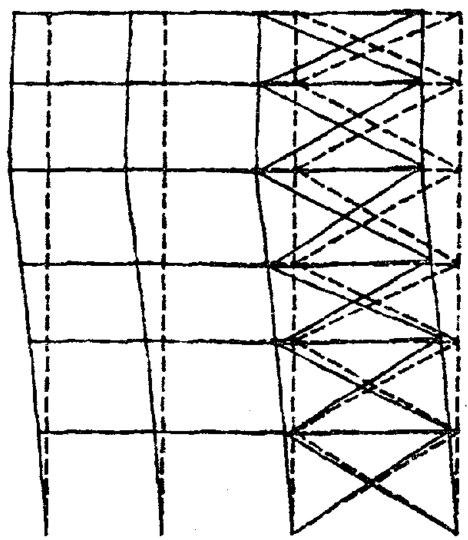

Figure 98

The fourth mode shape of system No. 2 in a side view.

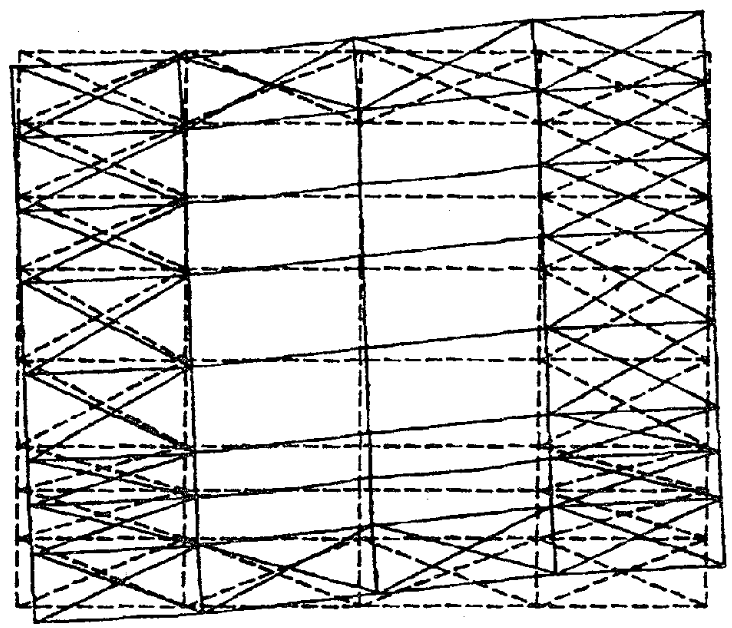

Figure 99

The fifth mode shape of system No. 2 in a plan view.

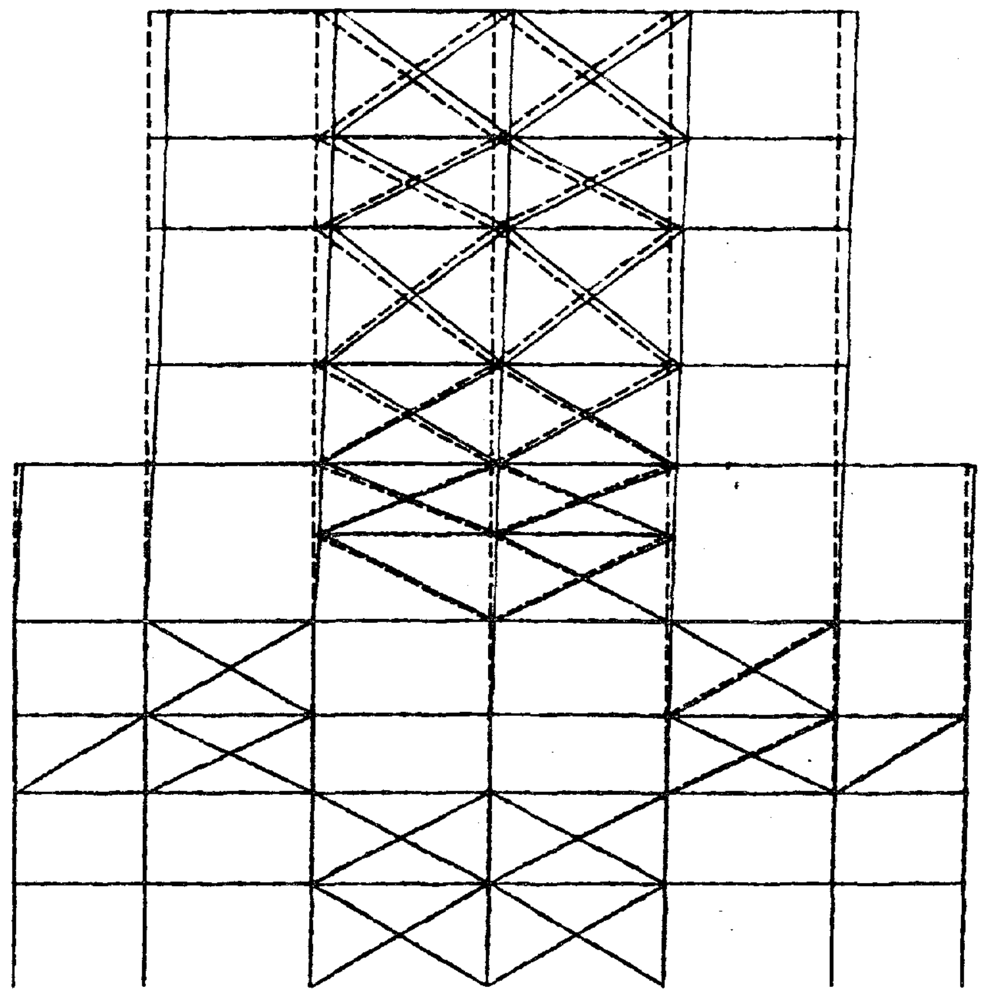

Figure 100

The fifth mode shape of system No. 2 in an elevation view.

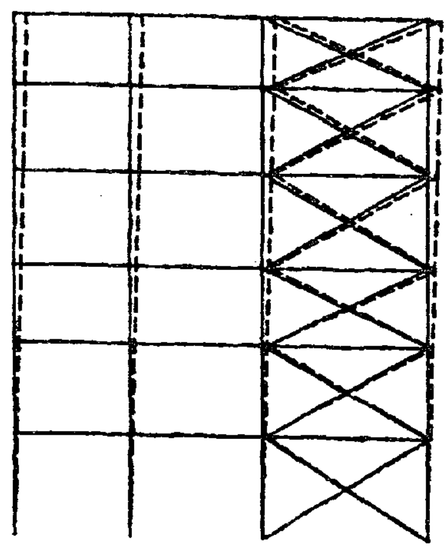

Figure 101

The fifth mode shape of system No. 2 in a side view.

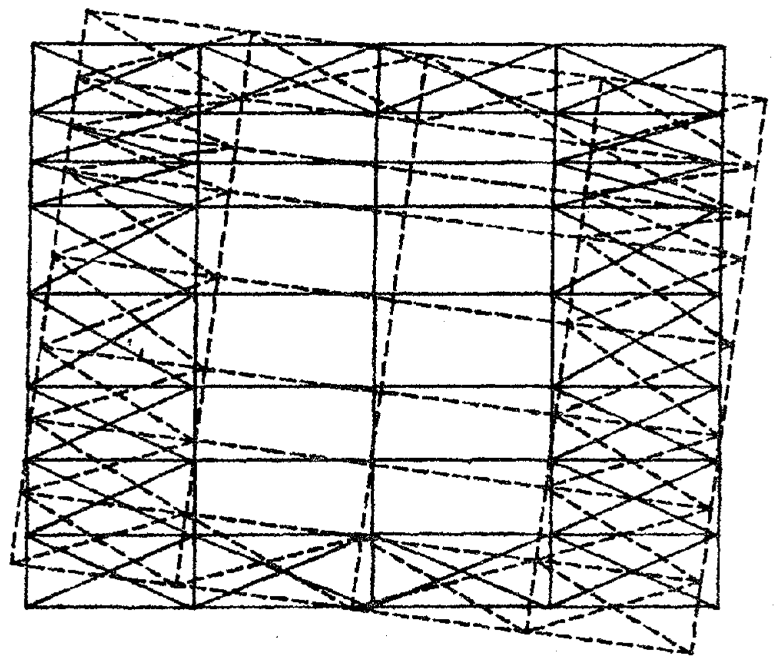

Figure 102
The sixth mode shape of system No. 2 in a plan view.

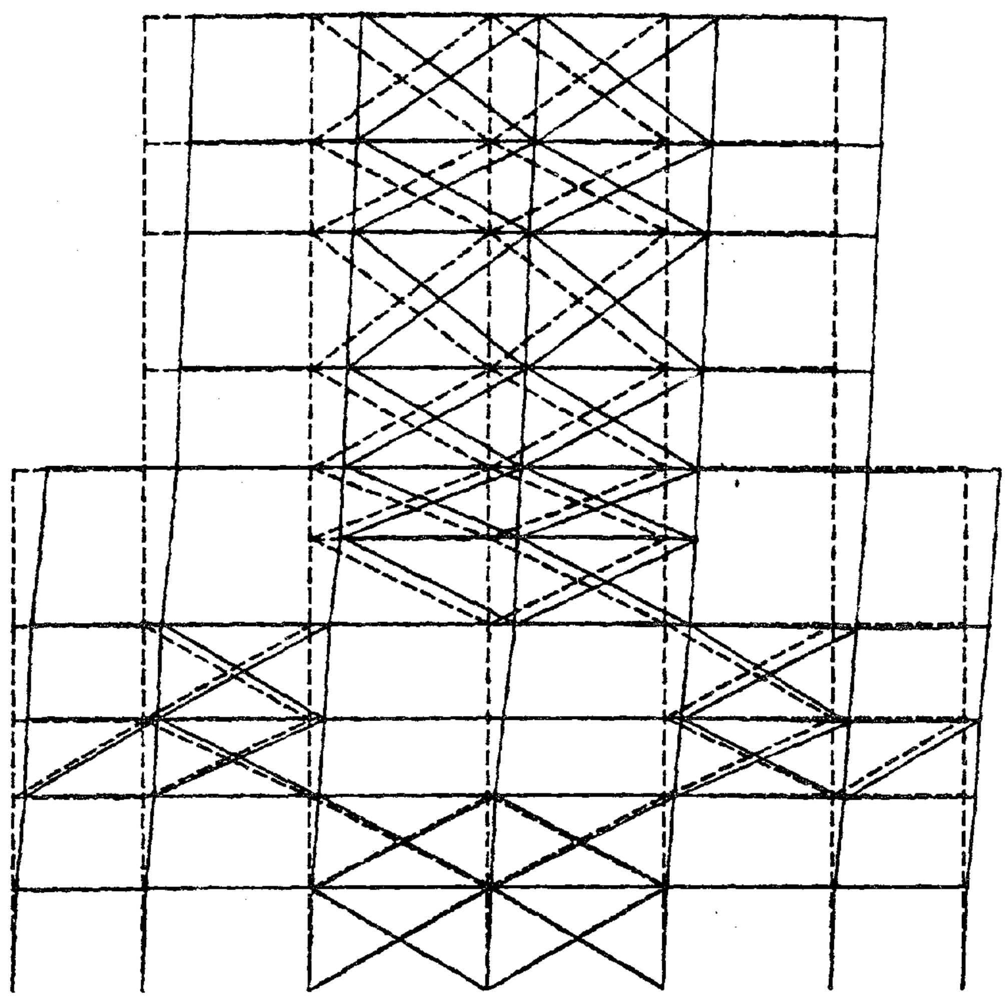

Figure 103

The sixth mode shape of system No. 2 in an elevation view.

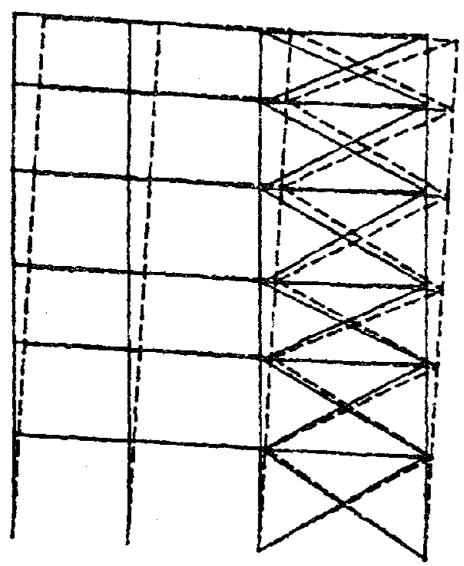

Figure 104

The sixth mode shape of system No. 2 in a side view.

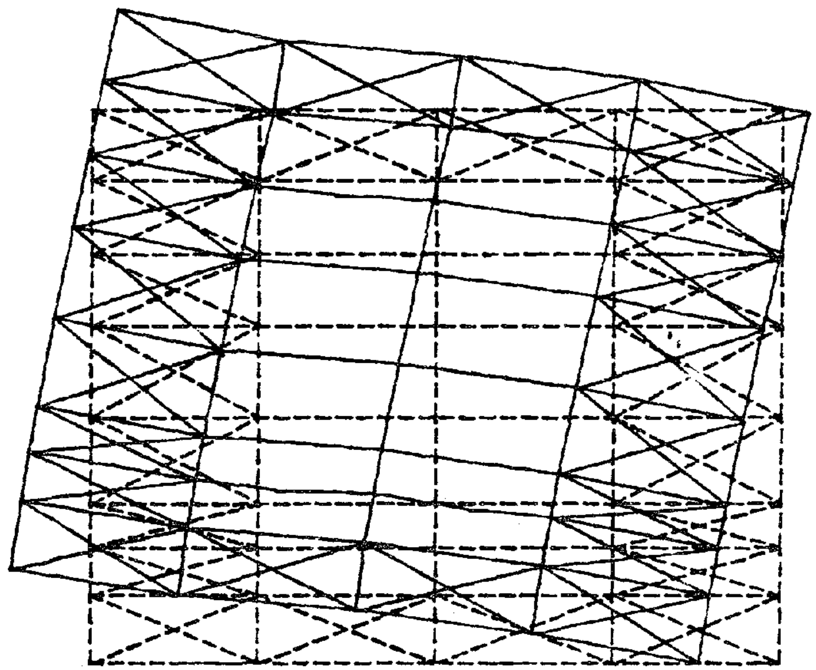

Figure 105

The seventh mode shape of system No. 2 in a plan view.

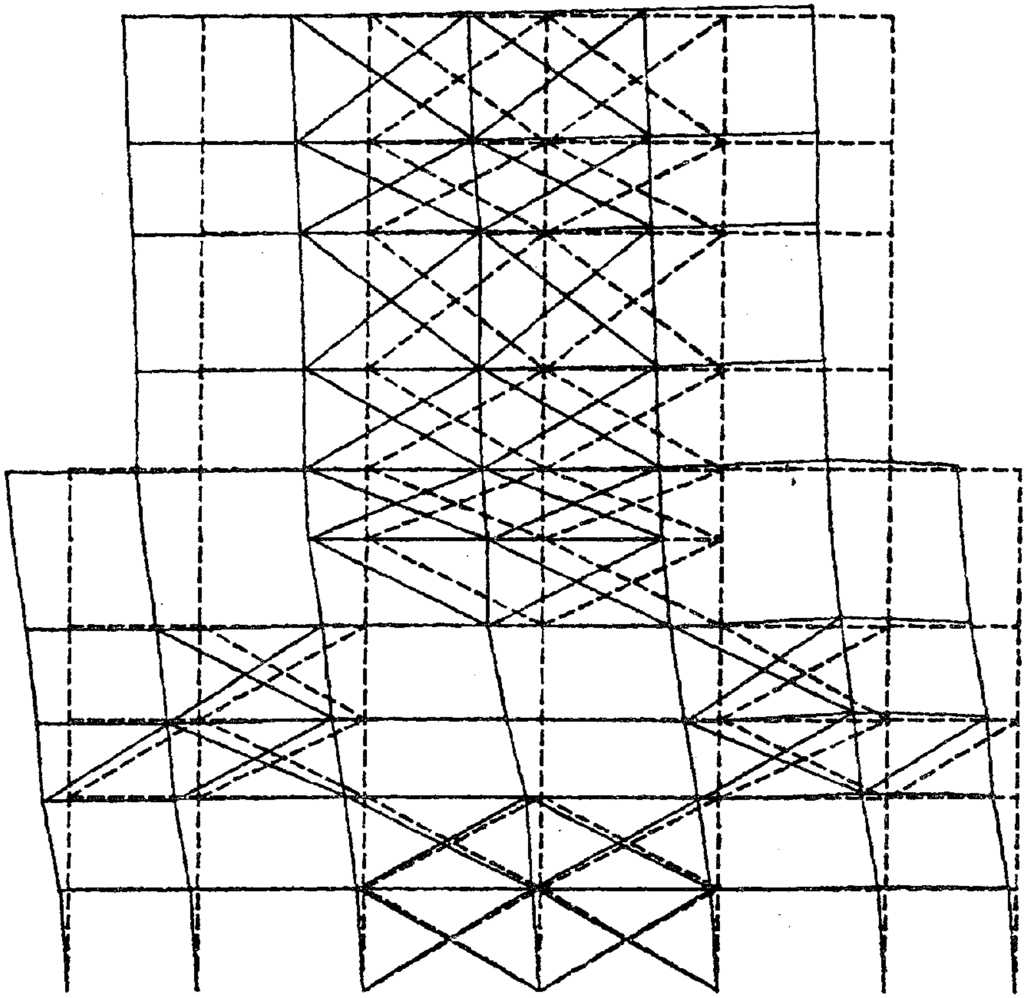

Figure 106

The seventh mode shape of system No. 2 in an elevation view.

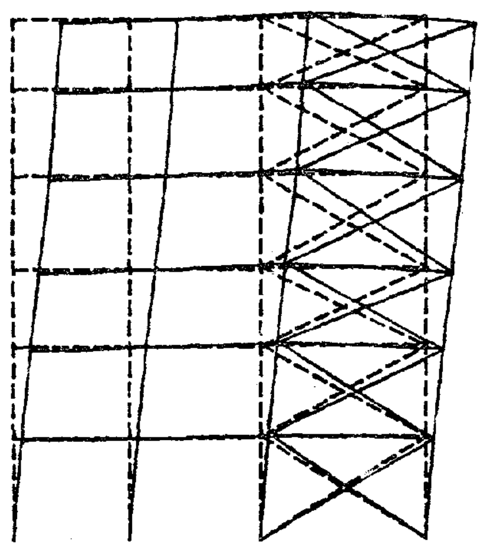

Figure 107

The seventh mode shape of system No. 2 in a side view.

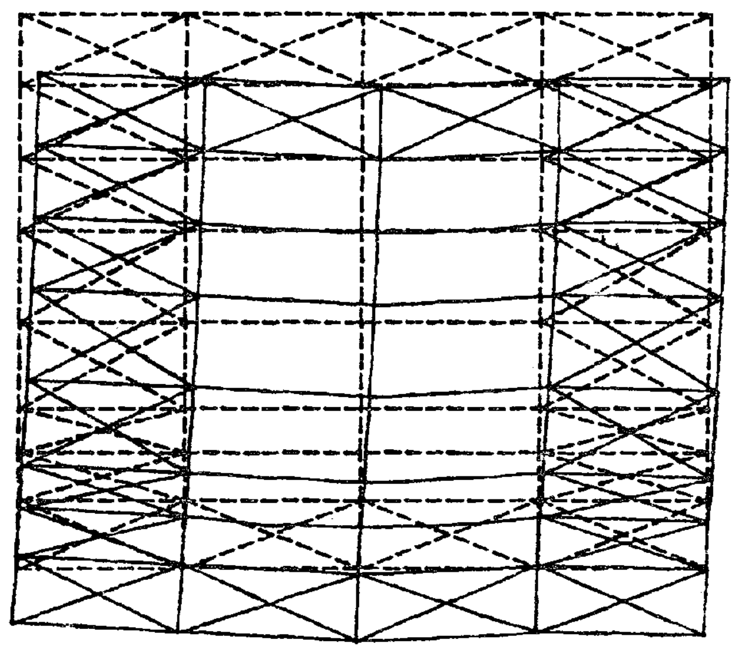

Figure 108

The eighth mode shape of system No. 2 in a plan view.

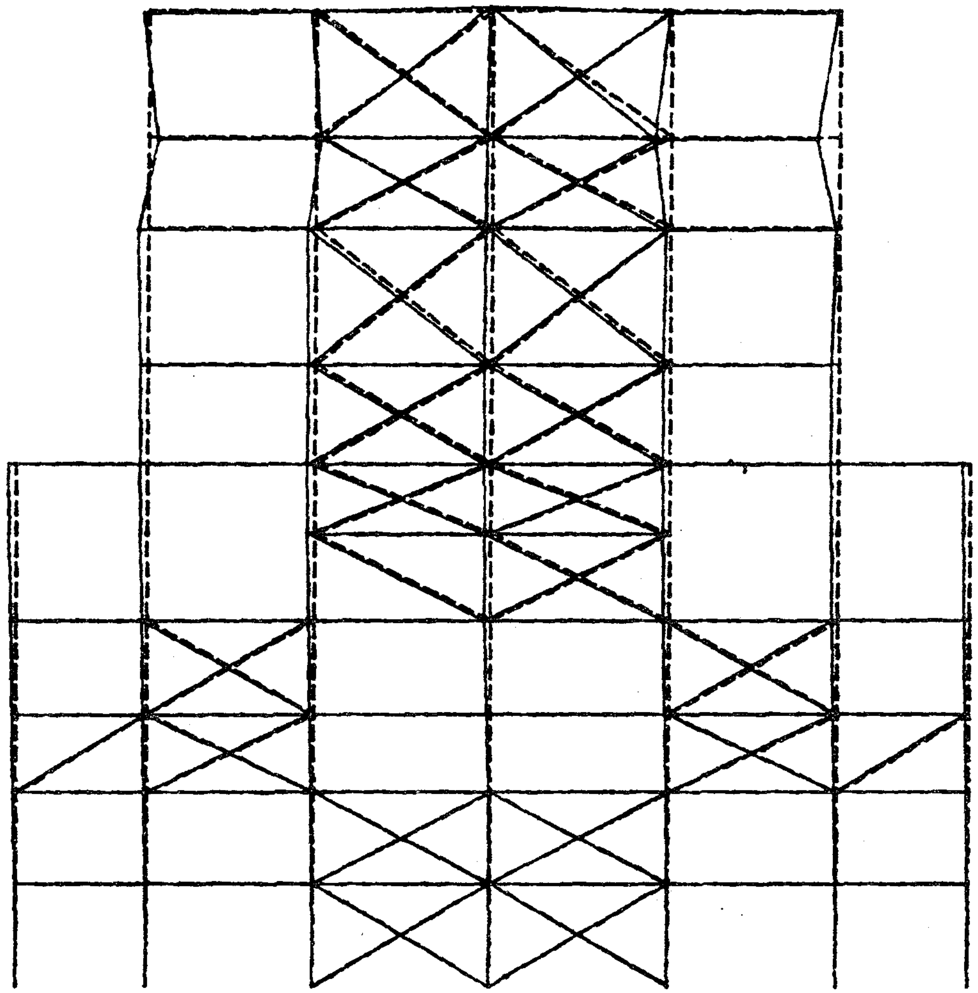

Figure 109

The eighth mode shape of system No. 2 in an elevation view.

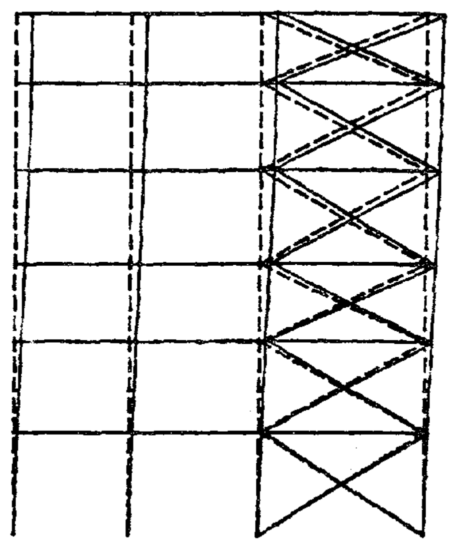

Figure 110

The eighth mode shape of system No. 2 in a side view.

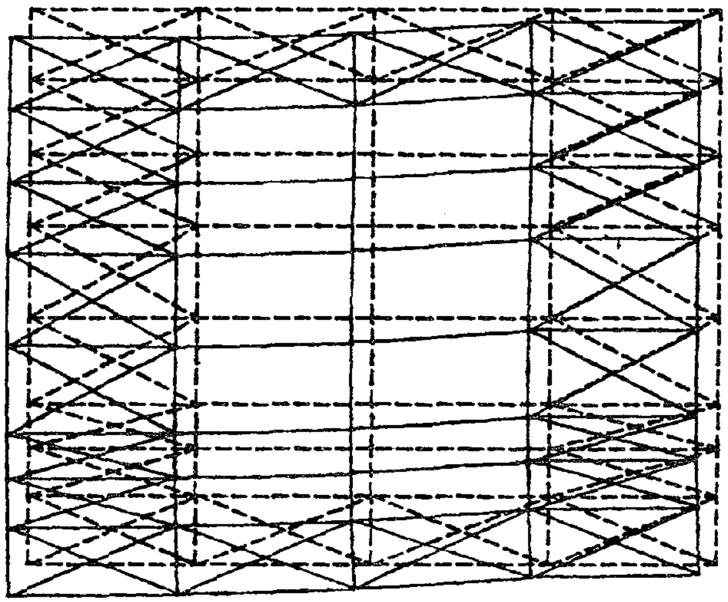

Figure 111

The ninth mode shape of system No. 2 in a plan view.

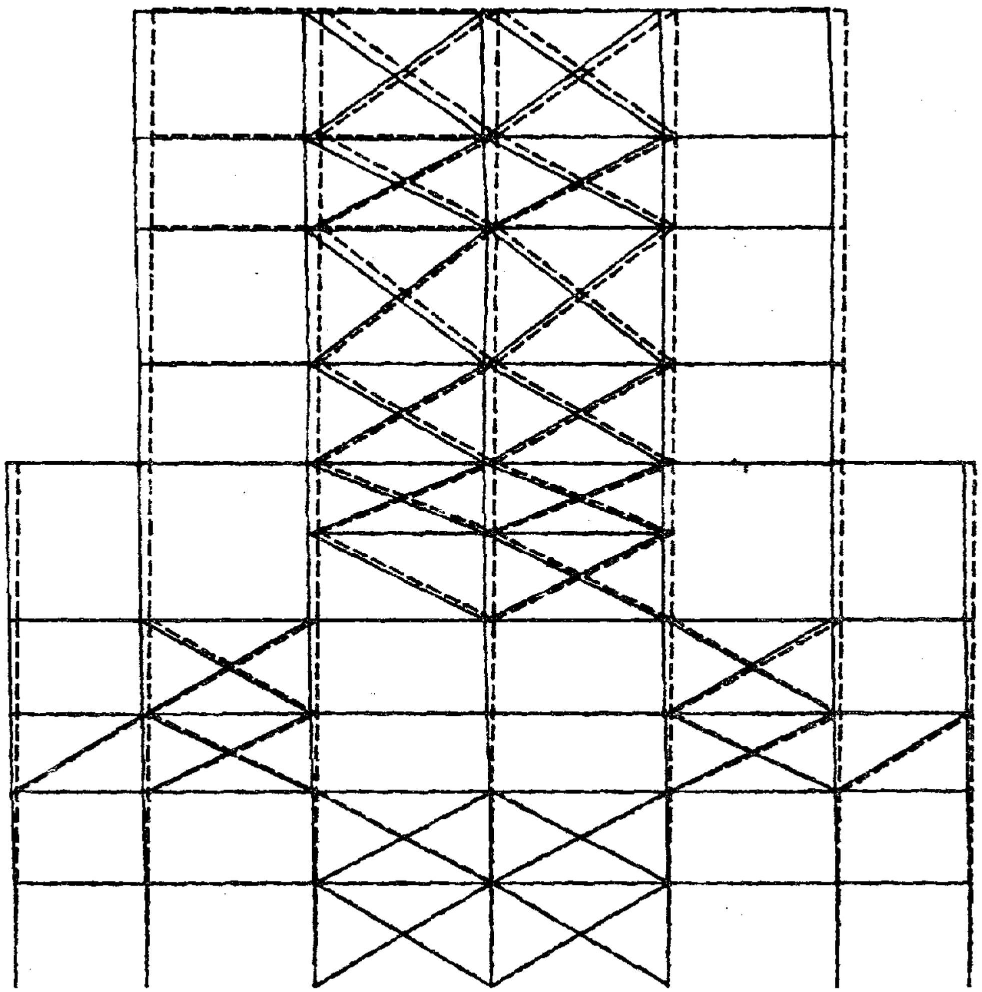

Figure 112

The ninth mode shape of system No. 2 in an elevation view.

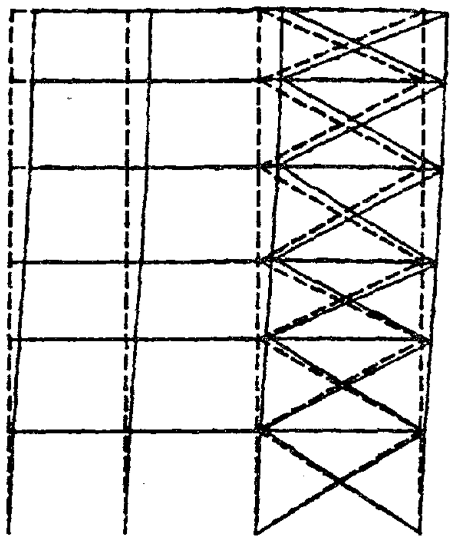

Figure 113

The ninth mode shape of system No. 2 in a side view.

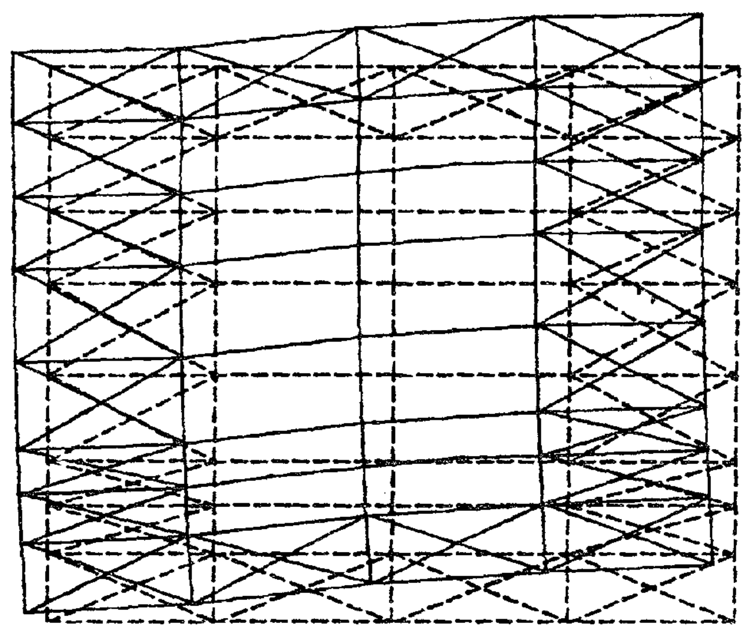

Figure 114

The tenth mode shape of system No. 2 in a plan view.

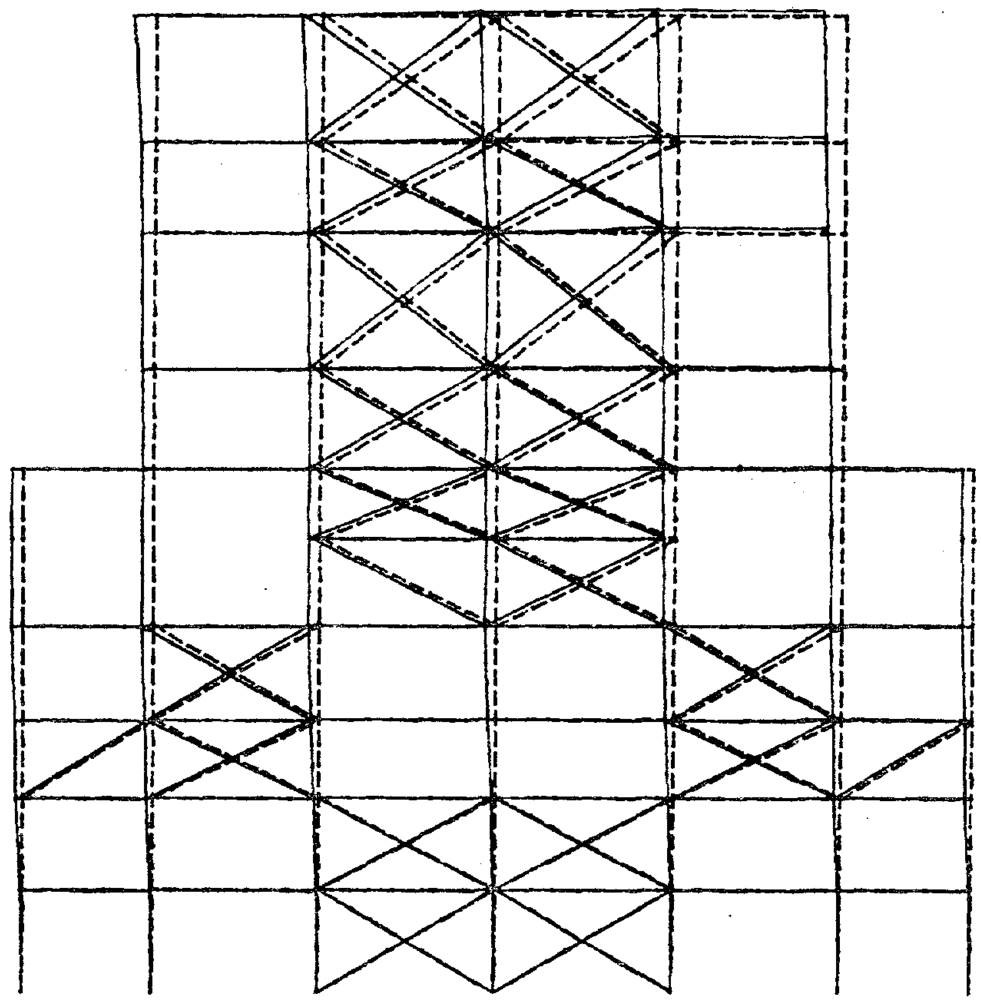

Figure 115

The tenth mode shape of system No. 2 in an elevation view.

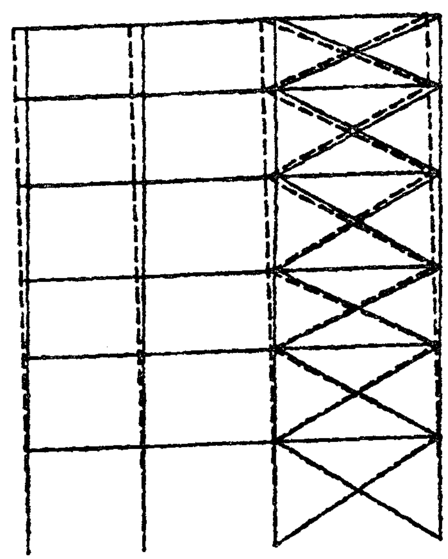

Figure 116

The tenth mode shape of system No. 2 in an elevation view.

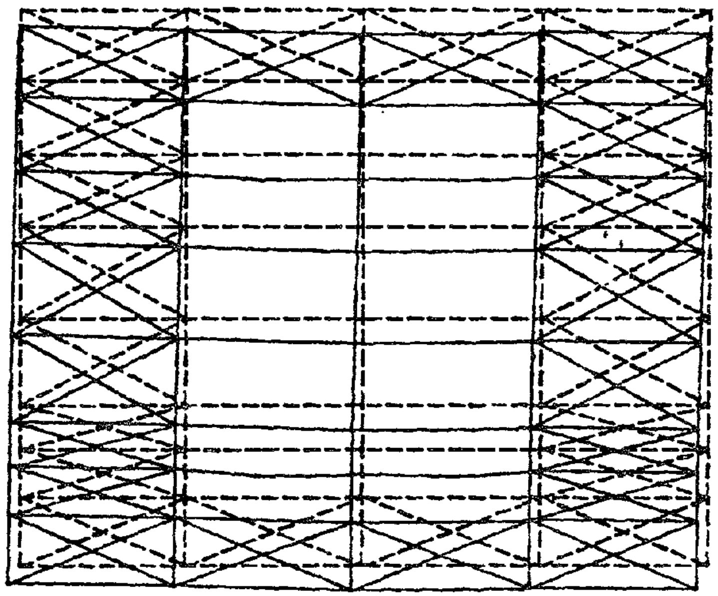

Figure 117

The eleventh mode shape of system No. 2 in a plan view.

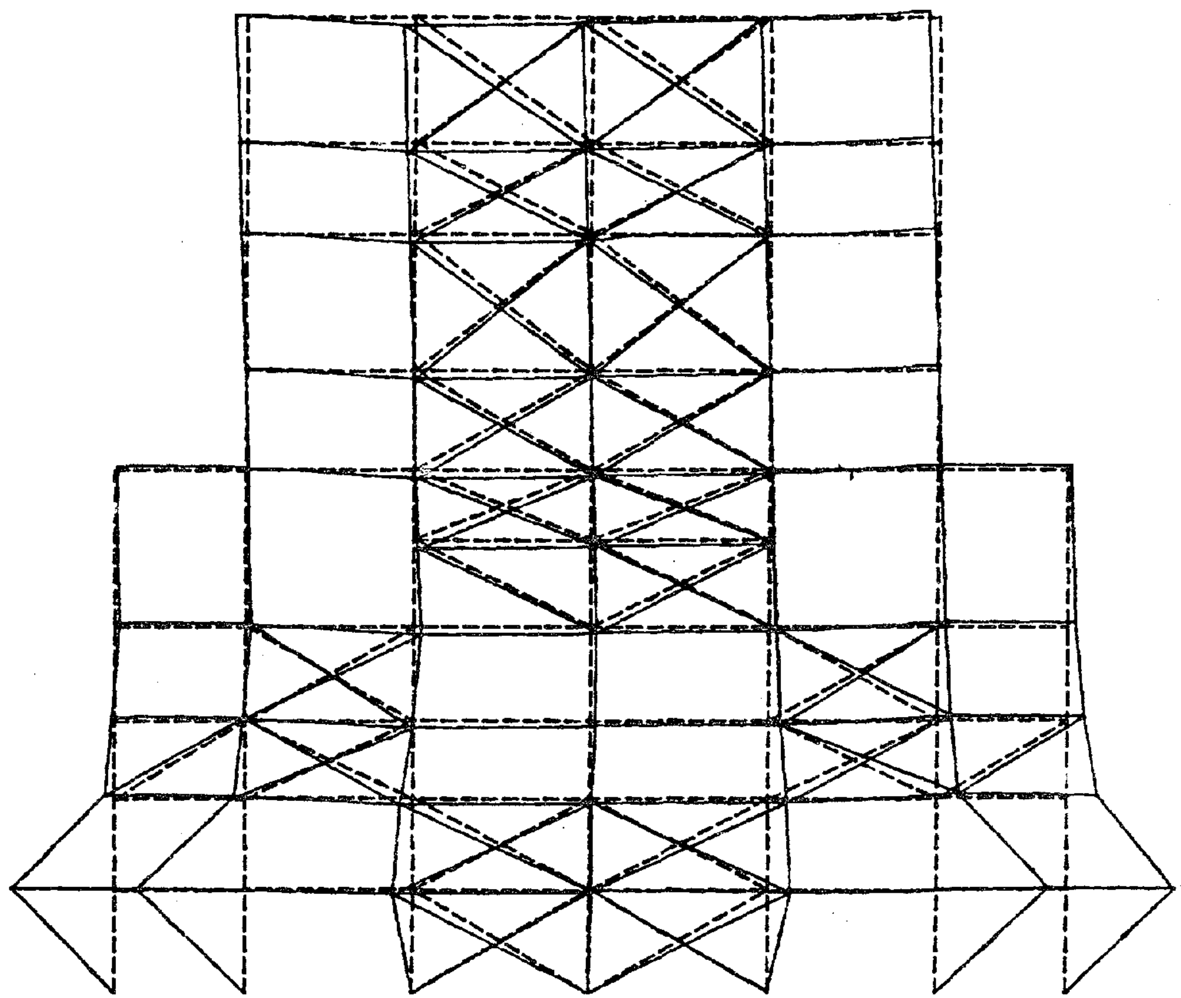

Figure 118

The eleventh mode shape of system No. 2 in an elevation view.

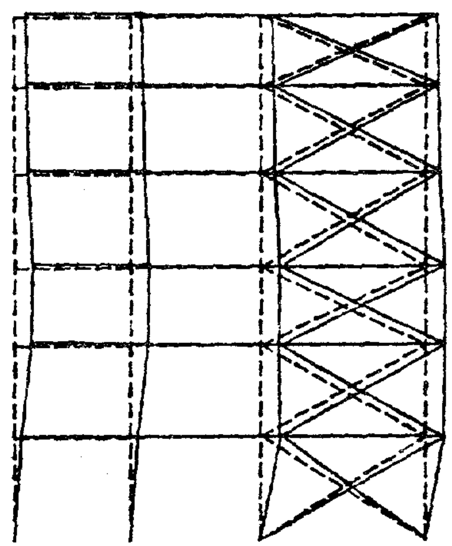

Figure 119

The eleventh mode shape of system No. 2 in a side view.

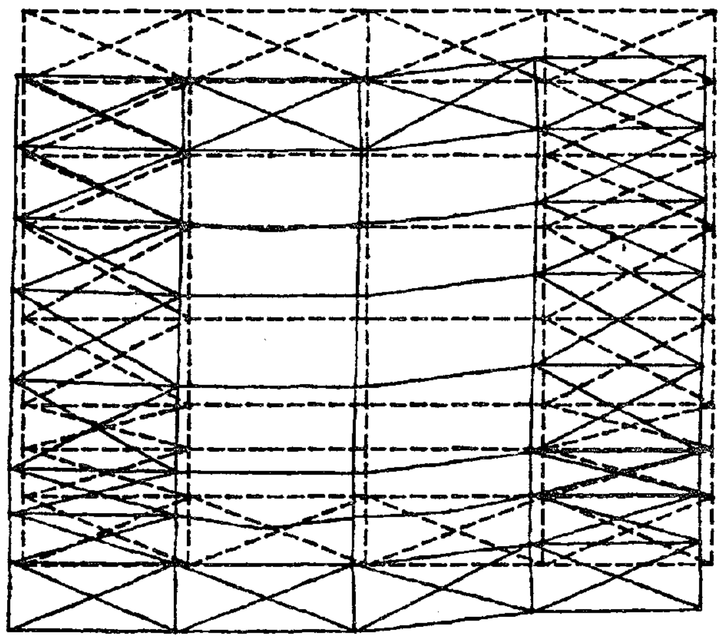

Figure 120

The twelfth mode shape of system No. 2 in a plan view.

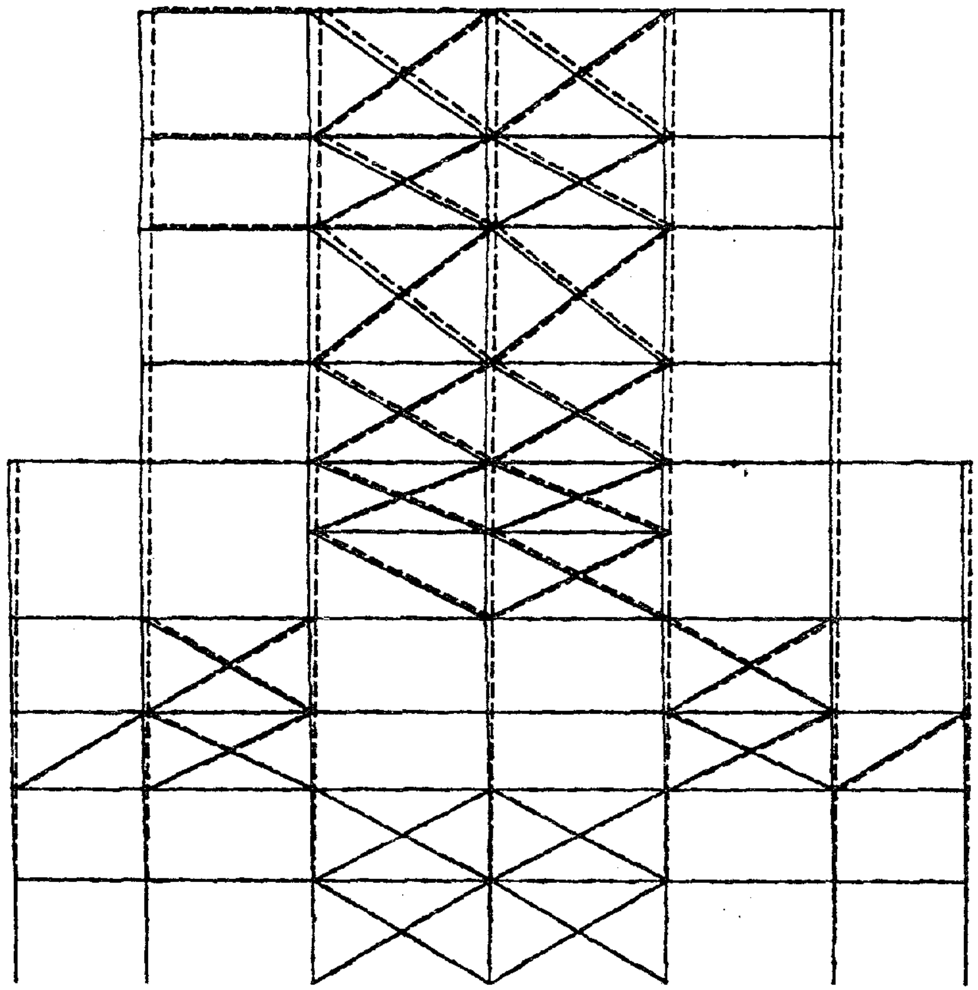

Figure 121

The twelfth mode shape of system No. 2 in an elevation view.

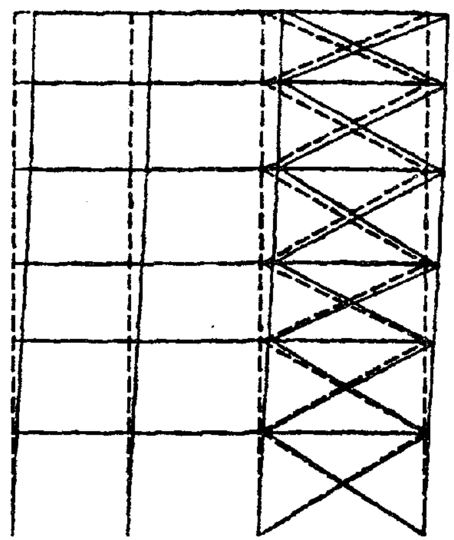

Figure 122

The twelfth mode shape of system No. 2 in a side view.

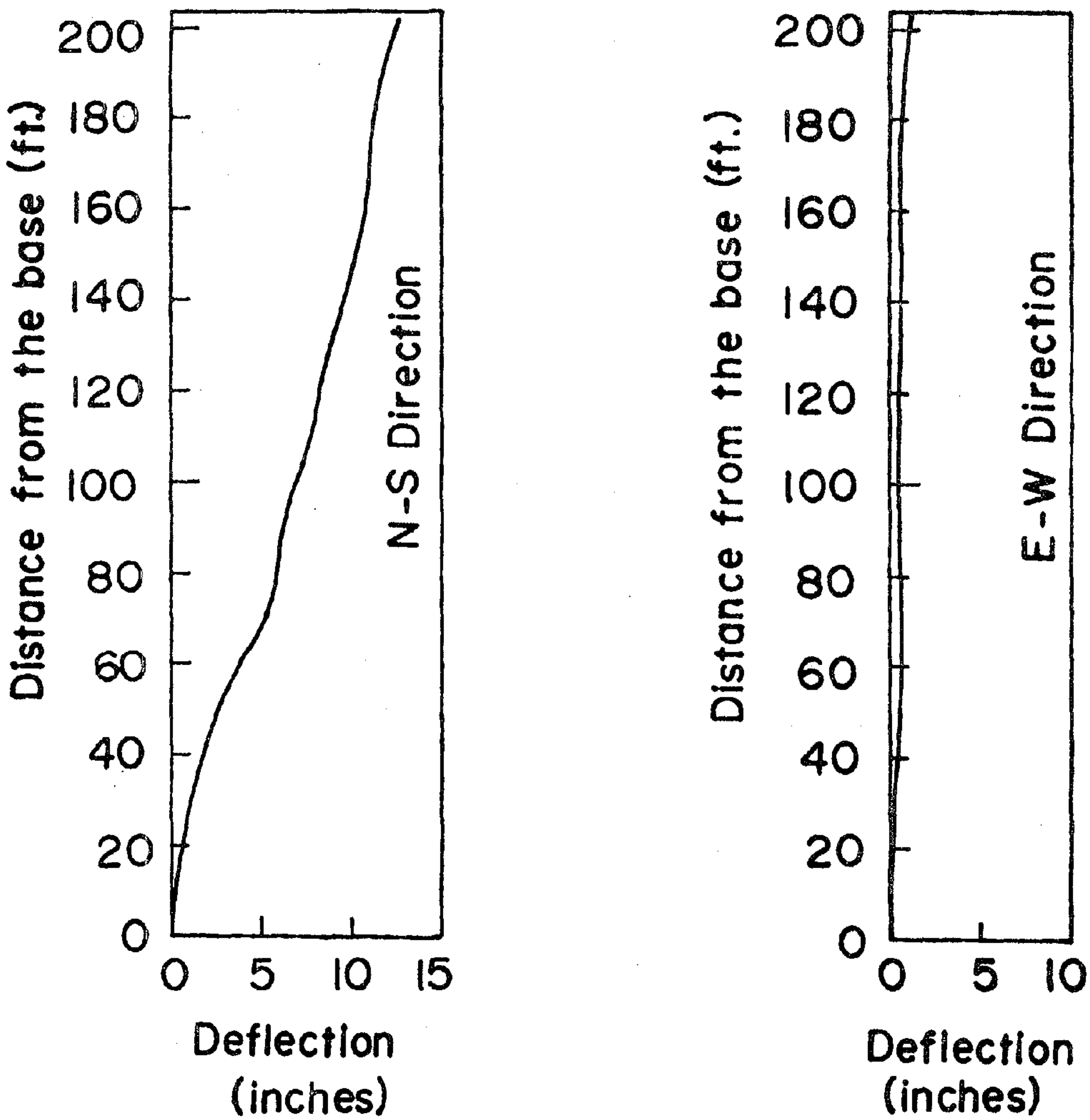

Figure 123

Components of the maximum deflection of the column H4 of system No. 2 in two orthogonal directions.

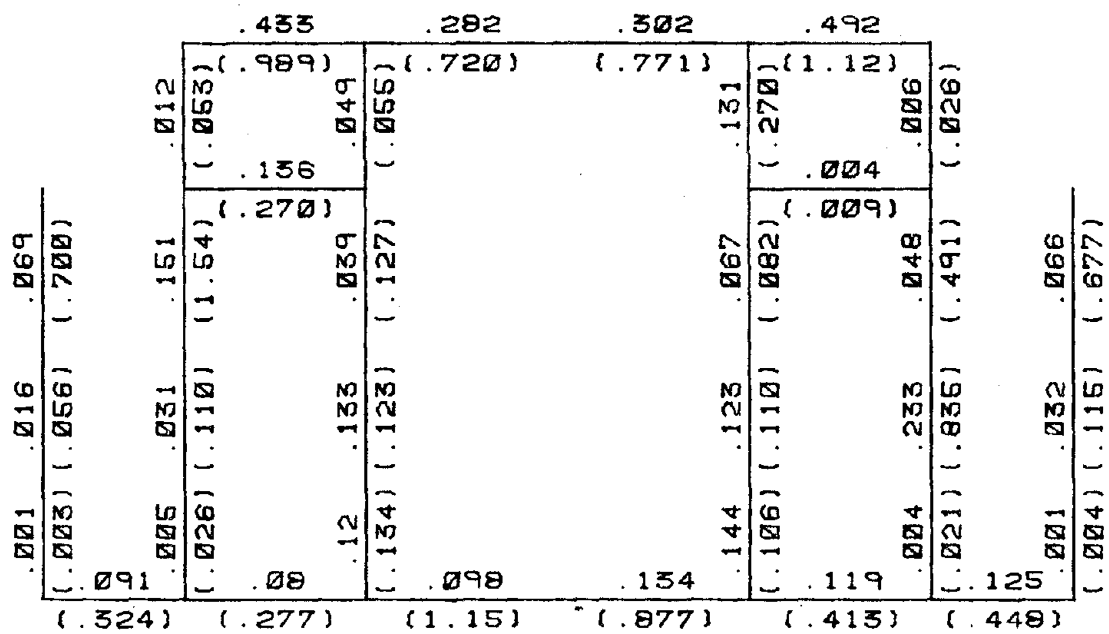

Figure 124

Ratios of the stresses in the members of system No. 2 located at EL 317.

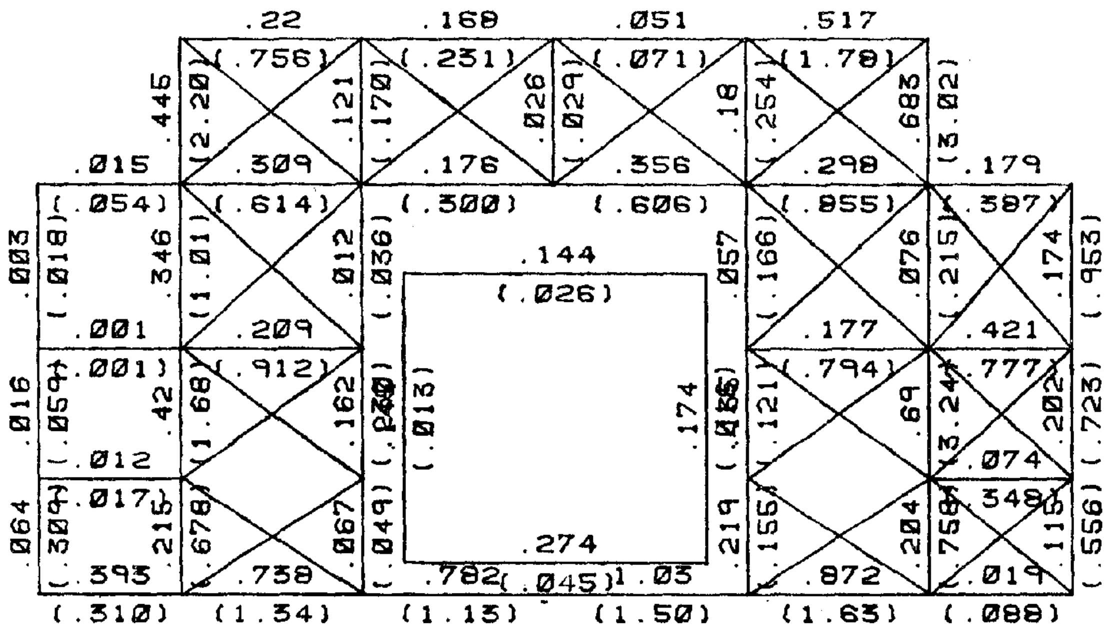

Figure 125

Ratios of the stresses in the members of system No.2 located at EL 336.

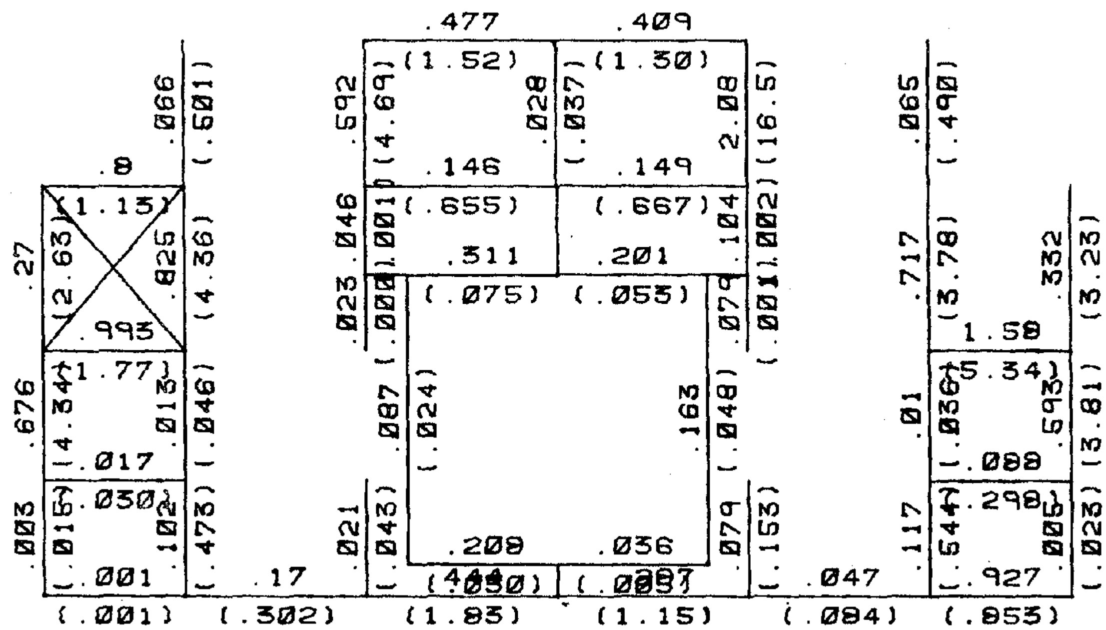

Figure 126

Ratios of the stresses in the members of system No. 2 located at EL 352.

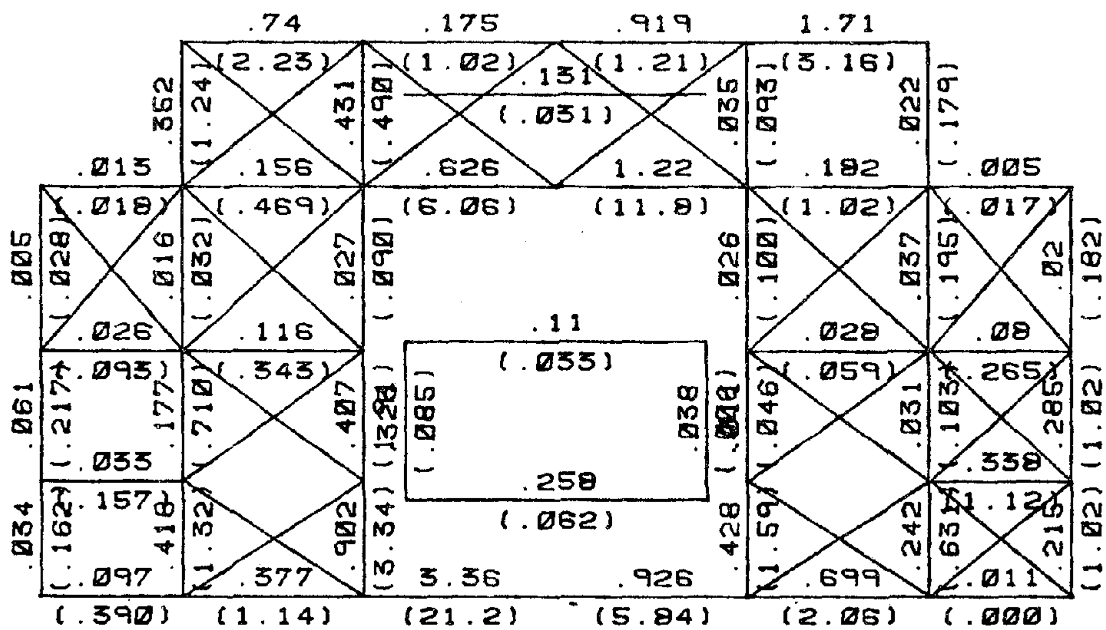

Figure 127

Ratios of the stresses in the members of system No. 2 located at EL 371.5.

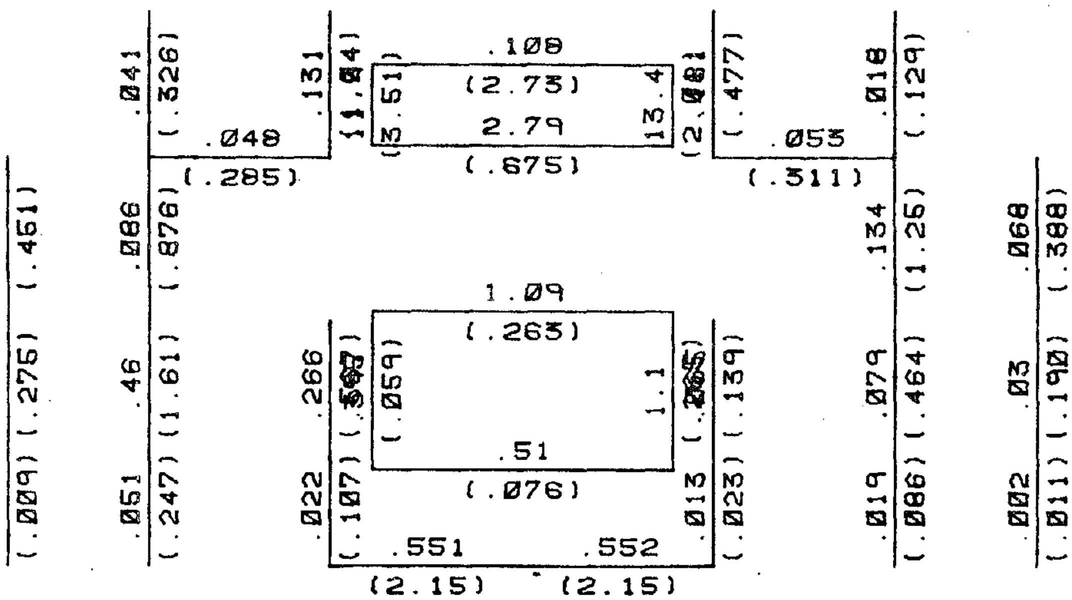

Figure 128

Ratios of the stresses in the members of system No. 2 located at EL 389.5.

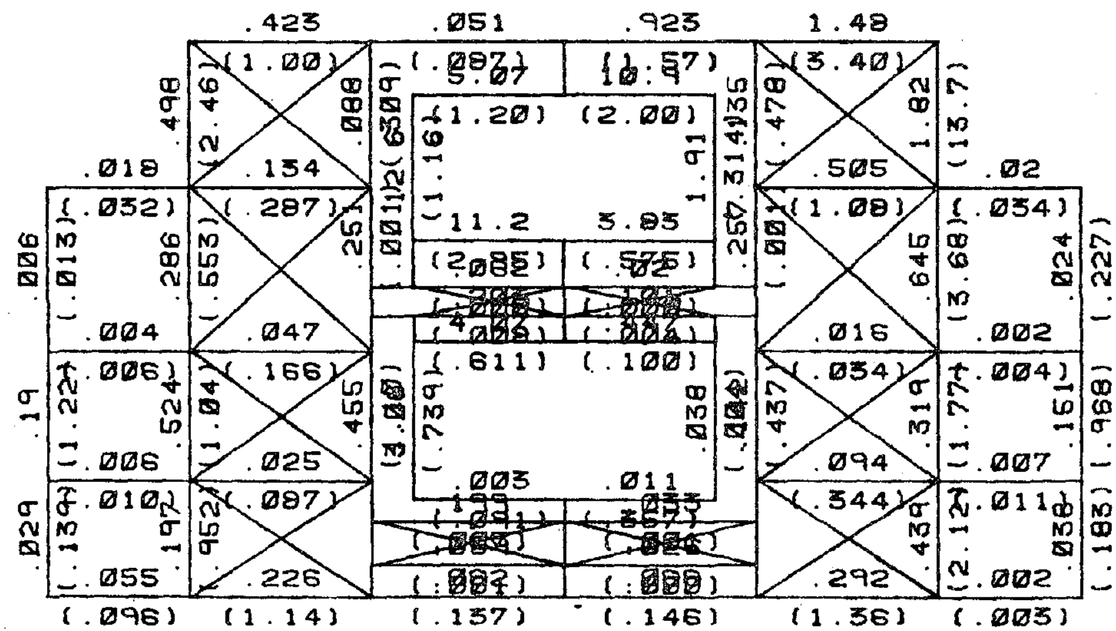

Figure 129

Ratios of the stresses in the members of system No. 2 located at EL 404.

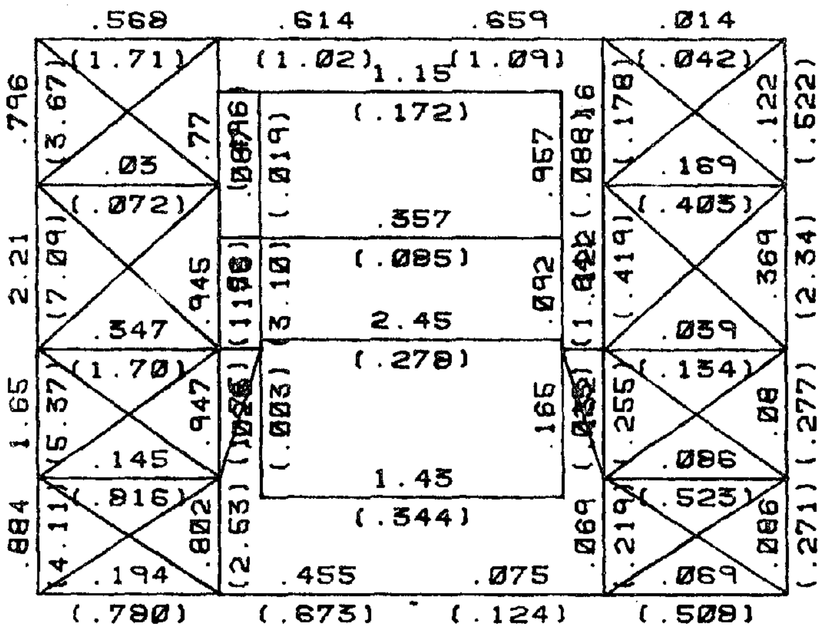

Figure 130

Ratios of the stresses in the members of system No. 2 located at EL 424.75.

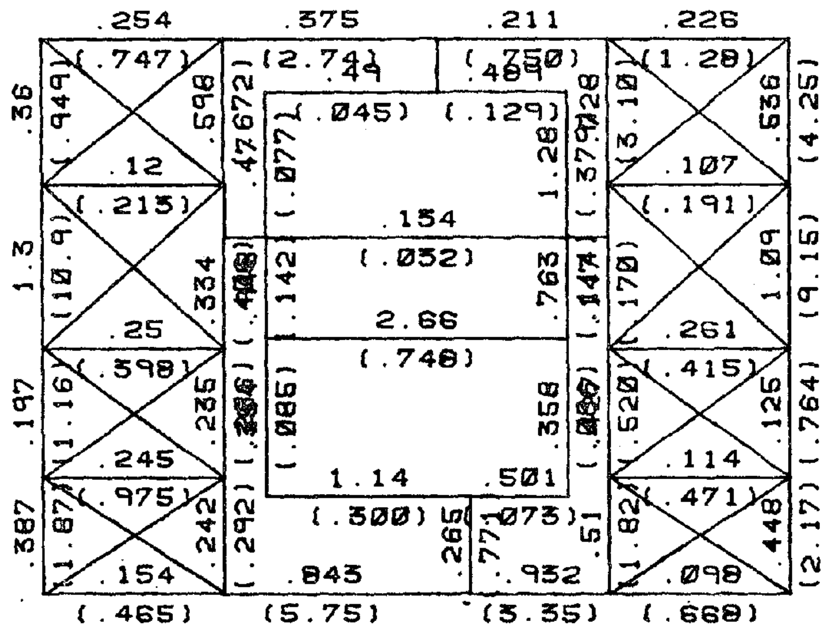

Figure 131

Ratios of the stresses in the members of system No. 2 located at EL 453.

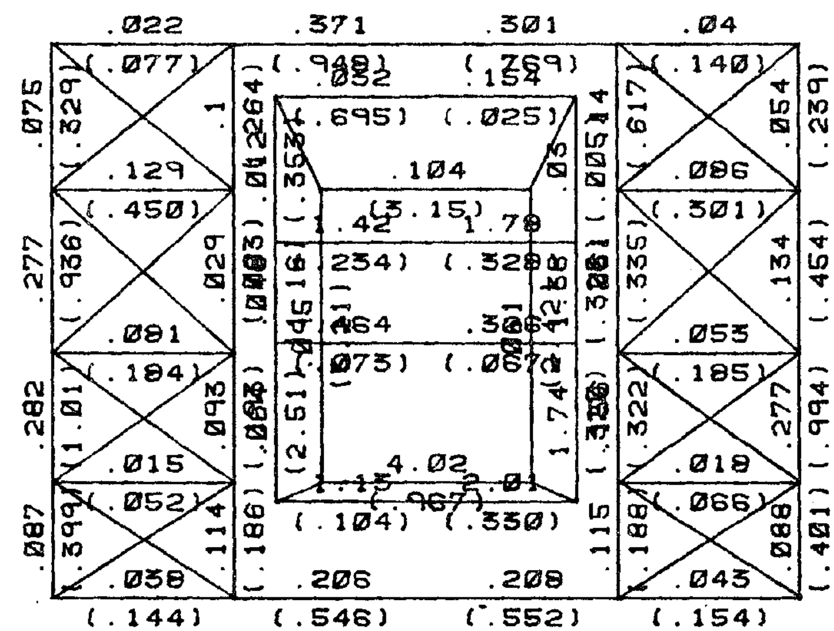

Figure 132

Ratios of the stresses in the members of system No. 2 located at EL 471.75.

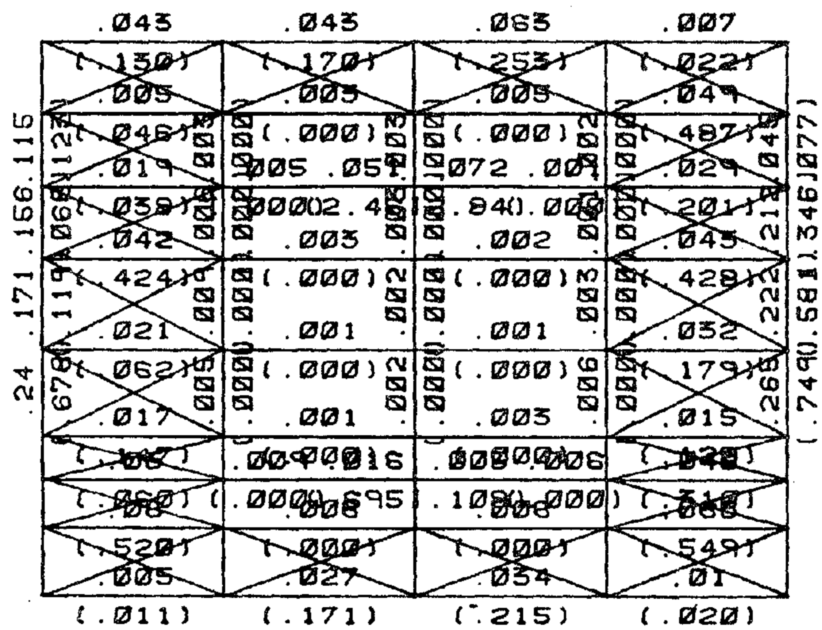

Figure 133

Ratios of the stresses in the members of system No. 2 located at EL 498.

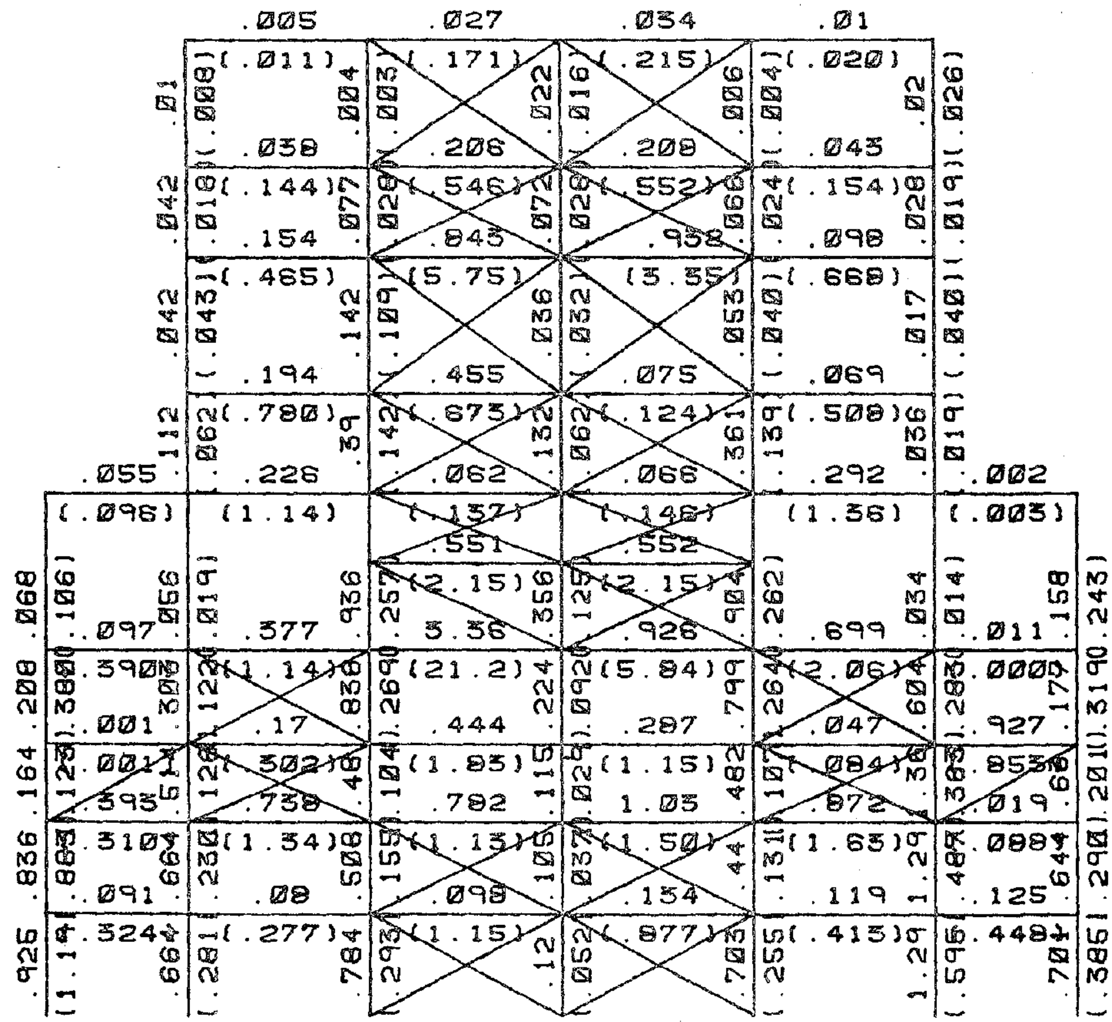

Figure 134

Ratios of the stresses in the members of system No. 2 located on a vertical plane at line II.

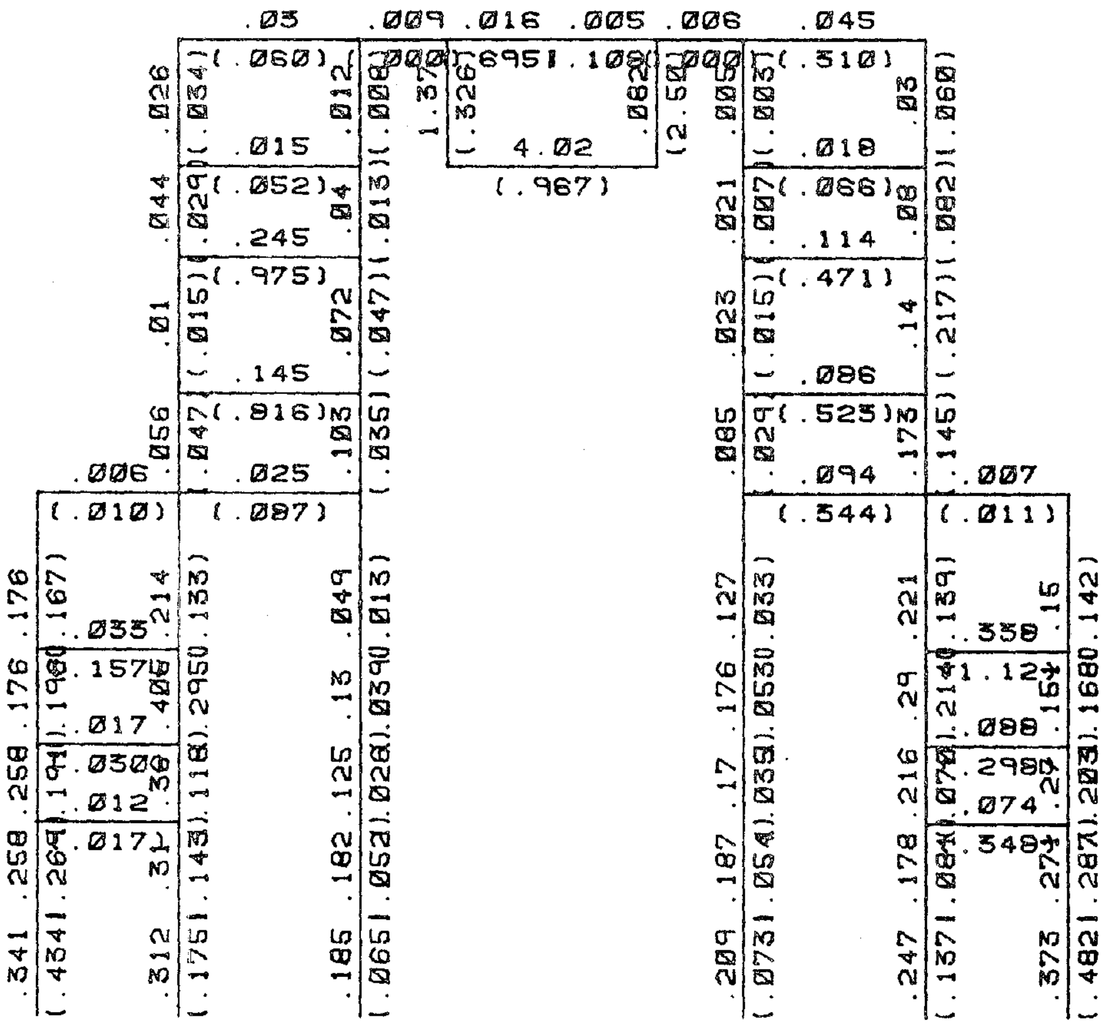

Figure 135

Ratios of the stresses in the members of system No. 2 located on a vertical plane at line J.

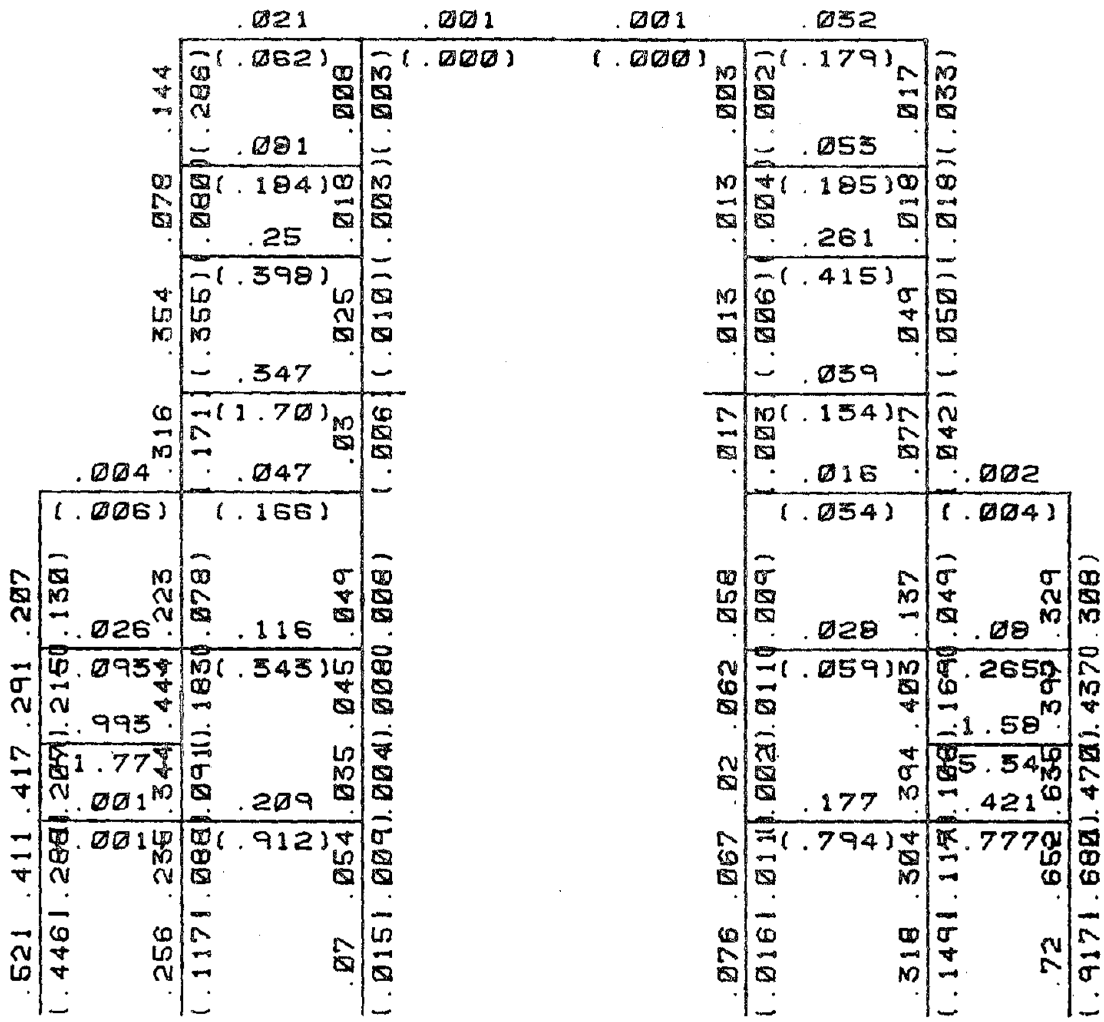

Figure 136

Ratios of the stresses in the members of system No. 2 located on a vertical plane at line K.

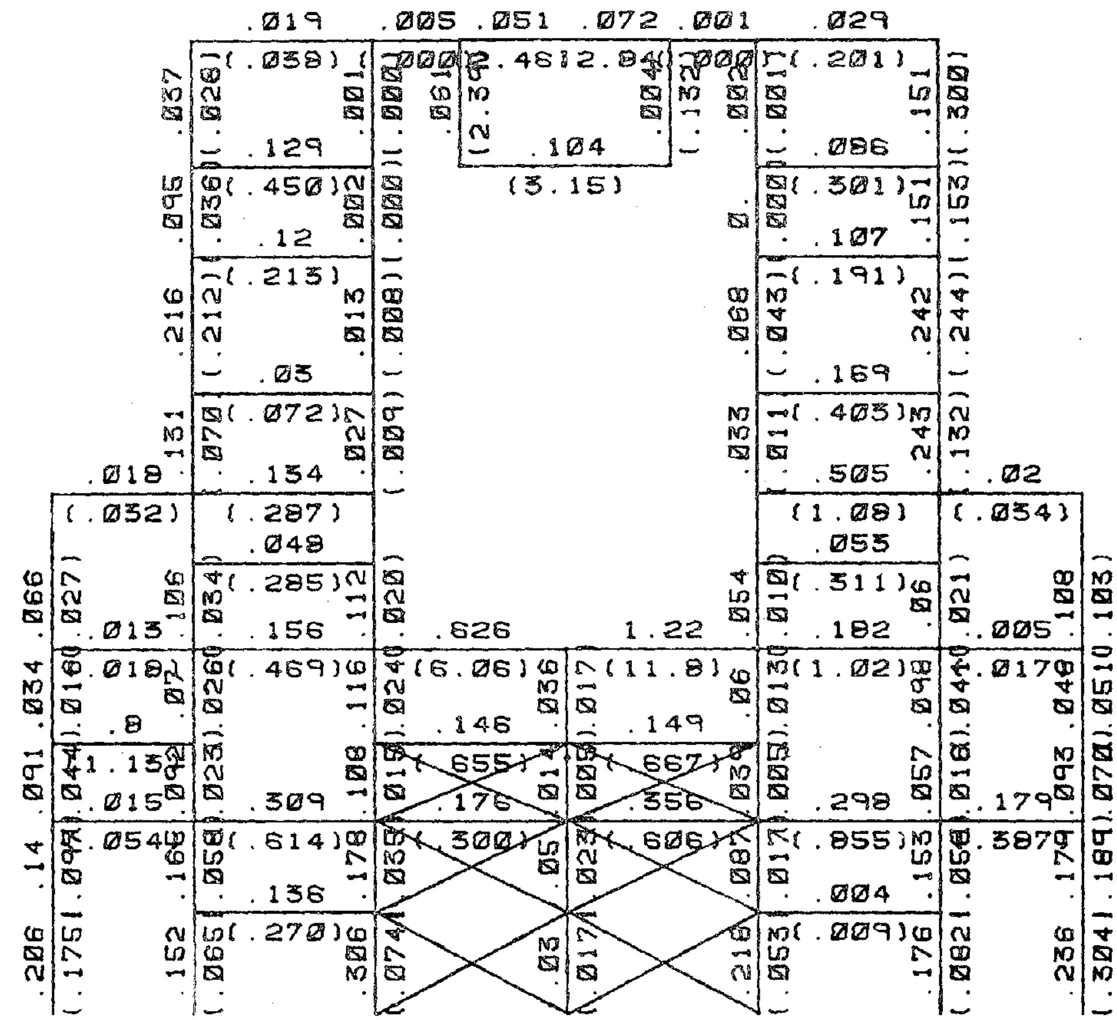

Figure 137

Ratios of the stresses in the members of system No. 2 located on a vertical plane at line L.

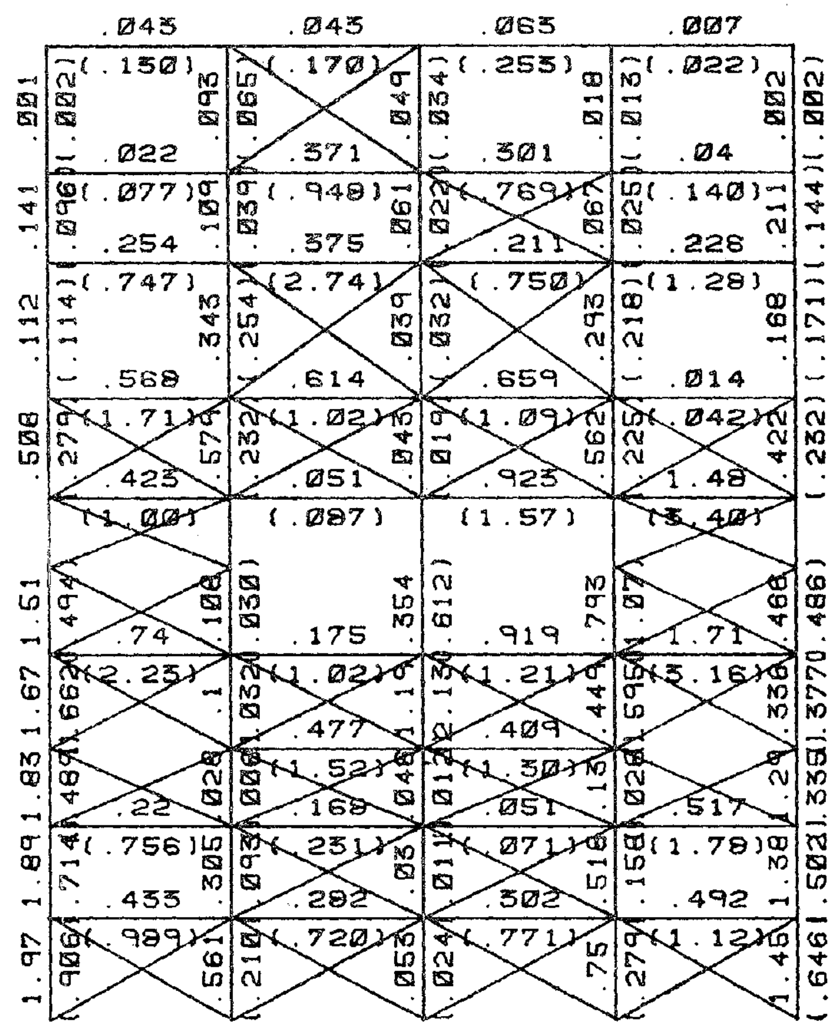

Figure 138

Ratios of the stresses in the members of system in No. 2 located on a vertical plane at line M.

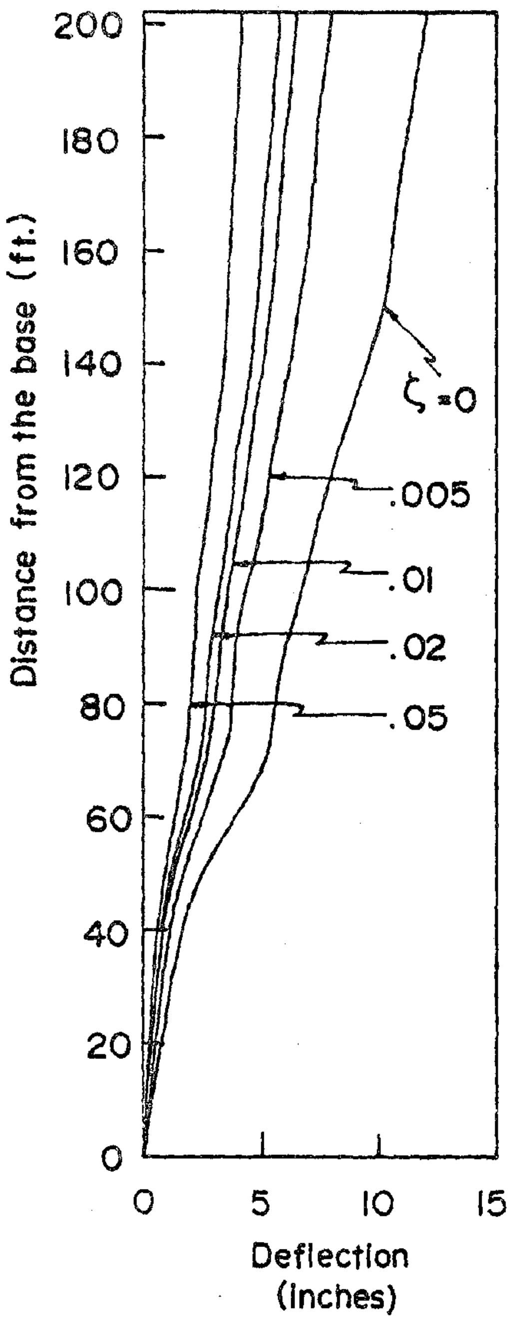

Figure 139

Maximum displacements of column H4 of system No. 2 for various damping ratios.

Appendix 1

Evaluation of Earthquake Displacement Spectrum

The Spectral Displacement of an earthquake is defined in eqn. (2.2.16) as:

$$Sd_n = [\frac{1}{\omega_n}\int_0^t \ddot{x}_k(\tau)\ \exp\{-\ \zeta_n\omega_n(t-\tau)\}\ \sin\{\omega_n(t-\tau)\}d\tau]_{max} \qquad (A1.1)$$

A plot of Sd_n versus the period ($= \frac{2\pi}{\omega_n}$) is referred as Earthquake Displacement Spectrum. To plot this spectrum, the Duhamel integral defined above must be evaluated for various frequencies ω_n over a wide time interval, the maximum value of which yields the ordinate of displacement spectrum. The data of earthquake ground acceleration of El Centro earthquake of May 18, 1940 is available at intervals of 0.02 sec. If the ground acceleration is assumed to vary linearly between this interval, we may write

$$\ddot{x}_k(\tau) = a + b\tau \qquad (A1.2)$$

where, $a = \ddot{x}_k(t_1)$ and $b = \frac{\ddot{x}_k(t_1 + 0.02) - \ddot{x}_k(t_1)}{0.02}$ (A1.3)

The value of integral defined by eqn. (A1.1) may be evaluated discreetly in various segment of interval 0.02 sec. A summation of the values in segments till time t would, therefore, give $Sd_n(t)$ for various values of t. The maximum value of Sd_n may be searched from these values. Use of eqn. (A1.2) in the Duhamel integral yields:

$$Sd_n(t) = \frac{1}{\omega_n}\int_0^t (a + b\tau)\exp\{-\zeta_n\omega_n(t-\tau)\}\sin\ \omega_n(t-\tau)d\tau \qquad (A1.4)$$

As the limits of integral in eqn. (A1.4) is from zero to t. It will be convenient to rearrange the terms in this integral for ease of computation. We may write

$$Sd_n(t) = \frac{1}{\omega_n}\sum_{i=1}^{M}\int_{0.02(i-1)}^{0.02i} (a_1+b_i\tau)\exp\{-\zeta_n\omega_n(0.02M-\tau)\}\sin\ \omega_n(0.02M-\tau)d\tau\} (A1.5)$$

where M = t/0.02.

$$Sd_n(t) = \frac{1}{\omega_n} \sum_{i=1}^{M} \exp(-\zeta_n\omega_n x0.02M)[\sin(\omega_n x0.02M) a_i \int_{0.02(i-1)}^{0.02i} \exp(\zeta_n\omega_n\tau)\cos(\omega_n\tau)d\tau$$

$$- \cos(\omega_n x0.02M)\ a_i \int_{0.02(i-1)}^{0.02i} \exp(\zeta_n\omega_n\tau)(\sin\ \omega_n\tau)d\tau$$

$$+ \sin(\omega_n x0.02M)\ b_i \int_{0.02(i-1)}^{0.02i} \tau \exp(\zeta_n\omega_n\tau)\cos(\omega_n\tau)d\tau$$

$$- \cos(\omega_n x0.02M)\ b_i \int_{0.02(i-1)}^{0.02i} \tau \exp(\zeta_n\omega_n\tau)\sin(\omega_n\tau)d\tau \qquad (A1.6)$$

$$Sd_n(t) = \frac{1}{\omega_n} \exp(-\zeta_n\omega_n x0.02M)[\sin(\omega_n x0.02M) \sum_{i=1}^{M} (a_i I_{1_i} + b_i I_{2_i})$$

$$- \cos(\omega_n x0.02M) \sum_{i=1}^{M} (a_i I_{3_i} + b_i I_{4_i})] \qquad (A1.7)$$

where

$$I_{1_i} = \int_{0.02(i-1)}^{0.02i} \exp(\zeta_n\omega_n\tau)\ \cos(\omega_n\tau)d\tau$$

$$I_{2_i} = \int_{0.02(i-1)}^{0.02i} \exp(\zeta_n\omega_n\tau)\ \sin(\omega_n\tau)d\tau$$

$$I_{3_i} = \int_{0.02(i-1)}^{0.02i} \exp(\zeta_n\omega_n\tau)\ \cos(\omega_n\tau)d\tau \qquad (A1.8)$$

$$I_{4_i} = \int_{0.02(i-1)}^{0.02i} \exp(\zeta_n\omega_n\tau)\ \sin(\omega_n\tau)d\tau$$

The quantities defined by eqn. (A1.8) may be evaluated for each segment. The eqn. (A1.7) can easily be programmed. The maximum value of $Sd_n(t)$ between the interval 0 and 30 secs is obtained. Evaluation of $(Sd_n)_{max}$ for various values of ω_n results in the plot of displacement spectrum.

APPENDIX 2

PROGRAM FOR PLOTTING THE STRUCTURAL SYSTEMS

```
C     ************************************************************************
C     *                                                                      *
C     *    PLOT IS THE PROGRAM TO PLOT THE STRUCTURE IN DIFFERENT VIEWS, VIZ. *
      *  PLAN/ ELEVATION/ SIDE VIEW/ 3-D ORTHOGONAL VIEW/ ORTHOGONAL VIEW   OF *
C     *  THE BOILER ALONE. THIS PROGRAM USES THE PUNCH OUTPUT DATA FROM MODI- *
C     *  FIED SAP4. THE PROGRAM CAN PLOT EITHER A PARTICULAR VIEW FOR ALL THE *
C     *  MODES OR ALL THE VIEWS FOR A PARTICULAR MODE.                        *
C     *                                                                      *
C     ************************************************************************
C
      PROGRAM PLOT (INPUT,OUTPUT,PLOT,DATA12,TAPE5=INPUT,TAPE6=OUTPUT,TA
     1PE1=DATA12)
      COMMON /ABC/ X(650),Y(650),Z(650),MI(2000),MJ(2000),M
      COMMON /BAC/ XD(650),YD(650),ZD(650)
      DIMENSION AMULT(20)
C
C     AMULT(I) IS MULTIPLICATION FACTOR FOR I-TH EIGENVECTOR.
C
      DATA (AMULT(I),I=1,12)/500.,500.,500.,1000.,400000.,200000.,3000.,
     1250.,100.,500.0,500.0,200./
C
C     READ NODE NUMBERS AND THEIR COORDINATES.
C
  101 READ (5,110) N,SX,SY,SZ
      IF (N.EQ.0) GO TO 102
      X(N)=SX
      Y(N)=SY
      Z(N)=SZ
      GO TO 101
  102 CONTINUE
      DO 103 I=1,650
         XD(I)=X(I)
         YD(I)=Y(I)
  103 ZD(I)=Z(I)
C
C     READ ELEMENT NUMBERS AND THEIR END NODAL NUMBERS.
C     FORM ARRAY OF END NODES FOR EACH ELEMENT.
C
  104 READ (5,111) N,MIS,MJS
      IF (N.EQ.0) GO TO 105
      MI(N)=MIS
      MJ(N)=MJS
      GO TO 104
  105 CONTINUE
      CALL USTART
      CALL UDIMEN (11.,9.5)
      CALL UDAREA (0.,11.,1.,9.5)
      CALL UPSET (≠SETDASH≠,32.)
      DO 109 M=1,1
         REWIND 1
  106    CONTINUE
C
C     READ THE DISPLACEMENTS OF EACH NODE IN M-TH MODE.
C
         IF (M.EQ.1) READ (1,112) N,SX,SY,SZ
         IF (M.EQ.2) READ (1,113) N,SX,SY,SZ
         IF (M.EQ.3) READ (1,114) N,SX,SY,SZ
         IF (M.EQ.4) READ (1,115) N,SX,SY,SZ
         IF (M.EQ.5) READ (1,116) N,SX,SY,SZ
         IF (M.EQ.6) READ (1,117) N,SX,SY,SZ
         IF (M.EQ.7) READ (1,118) N,SX,SY,SZ
         IF (M.EQ.8) READ (1,119) N,SX,SY,SZ
         IF (M.EQ.9) READ (1,120) N,SX,SY,SZ
         IF (M.EQ.10) READ (1,121) N,SX,SY,SZ
         IF (M.EQ.11) READ (1,122) N,SX,SY,SZ
```

```
         IF (M.EQ.12) READ (1,123) N,SX,SY,SZ
         IF (N.EQ.0) GO TO 107
C
C     FORM THE ARRAY OF DISPLACED COORDINATES FOR EACH NODE.
C
         XD(N)=X(N)+AMULT(M)*SX
         YD(N)=Y(N)+AMULT(M)*SY
         ZD(N)=Z(N)+AMULT(M)*SZ
         GO TO 106
  107    CONTINUE
         DO 108 I=1,1
            IF (I.EQ.1) CALL PLAN
            IF (I.EQ.2) CALL ELVTN
            IF (I.EQ.3) CALL SDVIW
            IF (I.EQ.4) CALL PLOT3D
            IF (I.EQ.5) CALL BOILER
  108    CONTINUE
  109 CONTINUE
      CALL UEND
      STOP
C
  110 FORMAT (I5,3F10.0)
  111 FORMAT (3I5)
  112 FORMAT (I4,4X,3E12.4///////////)
  113 FORMAT (/,I4,4X,3E12.4//////////)
  114 FORMAT (//,I4,4X,3E12.4/////////)
  115 FORMAT (///,I4,4X,3E12.4////////)
  116 FORMAT (////,I4,4X,3E12.4///////)
  117 FORMAT (/////,I4,4X,3E12.4//////)
  118 FORMAT (//////,I4,4X,3E12.4/////)
  119 FORMAT (///////,I4,4X,3E12.4////)
  120 FORMAT (////////,I4,4X,3E12.4///)
  121 FORMAT (/////////,I4,4X,3E12.4//)
  122 FORMAT (//////////,I4,4X,3E12.4/)
  123 FORMAT (///////////,I4,4X,3E12.4)
C
      END


      SUBROUTINE PLAN
C
C     SUBROUTINE PLAN PLOTS THE BEAM OR TRUSS MEMBERS OF THE STRUCTURE
C     IN THE PLAN VIEW.
C
      COMMON /ABC/ X(650),Y(650),Z(650),MI(2000),MJ(2000),M
      COMMON /BAC/ XD(650),YD(650),ZD(650)
      DIMENSION EL(10)
C
C     EL(I) REPRESENTS THE ELEVATION AT WHICH PLAN VIEW IS DESIRED.
C
      EL(1)=20.0
      EL(2)=42.0
      EL(3)=63.0
      EL(4)=81.5
      EL(5)=117.0
      EL(6)=132.0
      EL(7)=169.0
      EL(8)=200.0
      EL(9)=238.0
      EL(10)=238.0
C
C     DEFINE THE PLOTTING SURFACE.
C
      XMIN=-60.
      XMAX=380.
      YMIN=-100.
      YMAX=240.
      CALL UWINDO (XMIN,XMAX,YMIN,YMAX)
      DO 102 I=9,9,1
         DO 101 J=1,1290
```

```
C
C     FOR J-TH MEMBER FIND THE END COORDINATES OF BOTH ORIGINAL SHAPE
C     AND THE DISPLACED SHAPE.
C
            IP=MI(J)
            JP=MJ(J)
            ZI=Z(IP)
            ZJ=Z(JP)
            IF (ZI.NE.ZJ) GO TO 101
            IF (ZI.NE.EL(I)) GO TO 101
C
C     CHECK WHETHER THE MEMBER LIES ON THE DESIRED ELEVATION.
C
            XI=X(IP)
            YI=Y(IP)
            XJ=X(JP)
            YJ=Y(JP)
            XID=XD(IP)
            YID=YD(IP)
            XJD=XD(JP)
            YJD=YD(JP)
C
C     PLOT ORIGINAL SHAPE OF THE MEMBER BY DOTTED LINE.
C
            CALL USET (≠DASHED≠)
            CALL UMOVE (XI,YI)
            CALL UPEN (XJ,YJ)
C
C     PLOT DISPLACED SHAPE OF THE MEMBER BY SOLID LINE.
C
            CALL USET (≠LINES≠)
            CALL UMOVE (XID,YID)
            CALL UPEN (XJD,YJD)
  101     CONTINUE
C
C     PRINT THE LABEL ON THE PLOT.
C
          CALL USET (≠ACENTERING≠)
          CALL USET (≠MEDIUM≠)
          CALL UPRINT (160.,-65.,≠TVA PLANT¬≠)
          IF (I.EQ.1) CALL UPRINT (160.,-75.,≠PLAN VIEW ON EL400.0¬≠)
          IF (I.EQ.2) CALL UPRINT (160.,-75.,≠PLAN VIEW ON EL422.0¬≠)
          IF (I.EQ.3) CALL UPRINT (160.,-75.,≠PLAN VIEW ON EL443.0¬≠)
          IF (I.EQ.4) CALL UPRINT (160.,-75.,≠PLAN VIEW ON EL461.5¬≠)
          IF (I.EQ.5) CALL UPRINT (160.,-75.,≠PLAN VIEW ON EL497.0¬≠)
          IF (I.EQ.6) CALL UPRINT (160.,-75.,≠PLAN VIEW ON EL512.0¬≠)
          IF (I.EQ.7) CALL UPRINT (160.,-75.,≠PLAN VIEW ON EL549.0¬≠)
          IF (I.EQ.8) CALL UPRINT (160.,-75.,≠PLAN VIEW ON EL580.0¬≠)
          IF (I.EQ.9) CALL UPRINT (160.,-75.,≠PLAN VIEW ON EL618.0¬≠)
          IF (I.EQ.10) CALL UPRINT (160.,-75.,≠PLAN VIEW ON EL618.0¬≠)
          IF (M.EQ.1) CALL UPRINT (160.,-85.,≠FIRST MODE¬≠)
          IF (M.EQ.2) CALL UPRINT (160.,-85.,≠SECOND MODE¬≠)
          IF (M.EQ.3) CALL UPRINT (160.,-85.,≠THIRD MODE¬≠)
          IF (M.EQ.4) CALL UPRINT (160.,-85.,≠FOURTH MODE¬≠)
          IF (M.EQ.5) CALL UPRINT (160.,-85.,≠FIFTH MODE¬≠)
          IF (M.EQ.6) CALL UPRINT (160.,-85.,≠SIXTH MODE¬≠)
          IF (M.EQ.7) CALL UPRINT (160.,-85.,≠SEVENTH MODE¬≠)
          IF (M.EQ.8) CALL UPRINT (160.,-85.,≠EIGHTH MODE¬≠)
          IF (M.EQ.9) CALL UPRINT (160.,-85.,≠NINETH MODE¬≠)
          IF (M.EQ.10) CALL UPRINT (160.,-85.,≠TENTH MODE¬≠)
          IF (M.EQ.11) CALL UPRINT (160.,-85.,≠ELEVENTH MODE¬≠)
          IF (M.EQ.12) CALL UPRINT (160.,-85.,≠TWELVTH MODE¬≠)
          CALL UOUTLN
          CALL UERASE
  102 CONTINUE
      RETURN
C
      END
```

```
      SUBROUTINE ELVTN
C
C     SUBROUTINE ELVTN PLOTS THE BEAM OR TRUSS MEMBER OF THE STRUCTURE
C     IN THE ELEVATION VIEW.
C
      COMMON /ABC/ X(650),Y(650),Z(650),MI(2000),MJ(2000),M
      COMMON /BAC/ XD(650),YD(650),ZD(650)
      DIMENSION EL(7)
C
C     EL(I) REPRESENTS THE LOCATION OF THE I-TH ELEVATION VIEW.
C
      EL(1)=0.0
      EL(2)=49.0
      EL(3)=71.5
      EL(4)=98.5
      EL(5)=125.5
      EL(6)=148.0
      EL(7)=158.0
C
C     DEFINE THE PLOTTING SURFACE.
C
      XMIN=-60.
      XMAX=380.
      YMIN=-60.
      YMAX=240.
      CALL UWINDO (XMIN,XMAX,YMIN,YMAX)
      DO 102 I=1,1,1
         DO 101 J=1,1290
            IP=MI(J)
            JP=MJ(J)
            XI=X(IP)
            YI=Y(IP)
            YJ=Y(JP)
            IF (YI.NE.YJ) GO TO 101
            IF (YI.NE.EL(I)) GO TO 101
C
C      CHECK WHETHER THE MEMBER LIES ON THE DESIRED LOCATION.
C
            ZI=Z(IP)
            XJ=X(JP)
            ZJ=Z(JP)
            XID=XD(IP)
            ZID=ZD(IP)
            XJD=XD(JP)
            ZJD=ZD(JP)
C
C     PLOT ORIGINAL SHAPE OF THE MEMBER BY DOTTED LINE.
C
            CALL USET (≠DASHED≠)
            CALL UMOVE (XI,ZI)
            CALL UPEN (XJ,ZJ)
C
C     PLOT DISPLACED SHAPE OF THE MEMBER BY SOLID LINE.
C
            CALL USET (≠LINES≠)
            CALL UMOVE (XID,ZID)
            CALL UPEN (XJD,ZJD)
  101    CONTINUE
C
C     PRINT THE LABEL ON THE PLOT.
C
         CALL USET (≠ACENTERING≠)
         CALL USET (≠MEDIUM≠)
         CALL UPRINT (160.,-25.,≠TVA PLANT¬≠)
         IF (I.EQ.1) CALL UPRINT (160.,-35.,≠ELEVATION VIEW ON LINE NZ¬≠
         IF (I.EQ.2) CALL UPRINT (160.,-35.,≠ELEVATION VIEW ON LINE KV¬≠
         IF (I.EQ.3) CALL UPRINT (160.,-35.,≠ELEVATION VIEW ON LINE JV¬≠
         IF (I.EQ.4) CALL UPRINT (160.,-35.,≠ELEVATION VIEW ON LINE HV¬≠
         IF (I.EQ.5) CALL UPRINT (160.,-35.,≠ELEVATION VIEW ON LINE GV¬≠
         IF (I.EQ.6) CALL UPRINT (160.,-35.,≠ELEVATION VIEW ON LINE FV¬≠
```

```
         IF (I.EQ.7) CALL UPRINT (160.,-35.,≠ELEVATION VIEW ON LINE E¬≠)
         IF (M.EQ.1) CALL UPRINT (160.,-45.,≠FIRST MODE¬≠)
         IF (M.EQ.2) CALL UPRINT (160.,-45.,≠SECOND MODE¬≠)
         IF (M.EQ.3) CALL UPRINT (160.,-45.,≠THIRD MODE¬≠)
         IF (M.EQ.4) CALL UPRINT (160.,-45.,≠FOURTH MODE¬≠)
         IF (M.EQ.5) CALL UPRINT (160.,-45.,≠FIFTH MODE¬≠)
         IF (M.EQ.6) CALL UPRINT (160.,-45.,≠SIXTH MODE¬≠)
         IF (M.EQ.7) CALL UPRINT (160.,-45.,≠SEVENTH MODE¬≠)
         IF (M.EQ.8) CALL UPRINT (160.,-45.,≠EIGHTH MODE¬≠)
         IF (M.EQ.9) CALL UPRINT (160.,-45.,≠NINETH MODE¬≠)
         IF (M.EQ.10) CALL UPRINT (160.,-45.,≠TENTH MODE¬≠)
         IF (M.EQ.11) CALL UPRINT (160.,-45.,≠ELEVENTH MODE¬≠)
         IF (M.EQ.12) CALL UPRINT (160.,-45.,≠TWELVTH MODE¬≠)
         CALL UOUTLN
         CALL UERASE
  102 CONTINUE
      RETURN
C
      END

      SUBROUTINE SDVIW
C
C     SUBROUTINE SDVIW PLOTS THE SIDE VIEW OF THE STRUCTURE.
C
      COMMON /ABC/ X(650),Y(650),Z(650),MI(2000),MJ(2000),M
      COMMON /BAC/ XD(650),YD(650),ZD(650)
      DIMENSION EL(11)
      EL(1)=0.0
      EL(2)=40.0
      EL(3)=80.0
      EL(4)=120.0
      EL(5)=160.0
      EL(6)=200.0
      EL(7)=240.0
      EL(8)=280.0
      EL(9)=320.0
      EL(10)=130.33
      EL(11)=226.00
      XMIN=-141.
      XMAX=299.
      YMIN=-60.
      YMAX=280.
      CALL UWINDO (XMIN,XMAX,YMIN,YMAX)
      DO 102 I=1,1,1
         DO 101 J=1,1290
            IP=MI(J)
            JP=MJ(J)
            XI=X(IP)
            XJ=X(JP)
            IF (XI.NE.XJ) GO TO 101
            IF (XI.NE.EL(I)) GO TO 101
C
C     CHECK WHETHER THE MEMBER LIES ON THE DESIRED LOCATION.
C
            YI=Y(IP)
            ZI=Z(IP)
            YJ=Y(JP)
            ZJ=Z(JP)
            YID=YD(IP)
            ZID=ZD(IP)
            YJD=YD(JP)
            ZJD=ZD(JP)
C
C     PLOT ORIGINAL SHAPE OF THE MEMBER BY DOTTED LINE.
C
            CALL USET (≠DASHED≠)
            CALL UMOVE (YI,ZI)
            CALL UPEN (YJ,ZJ)
C
```

```
C     PLOT DISPLACED SHAPE OF THE MEMBER BY SOLID LINE.
C     PLOT DISPLACED SHAPE OF THE MEMBER BY SOLID LINE.
C
            CALL USET (≠LINES≠)
            CALL UMOVE (YID,ZID)
            CALL UPEN (YJD,ZJD)
  101     CONTINUE
C
C     PRINT THE LABEL ON THE PLOT.
C
         CALL USET (≠ACENTERING≠)
         CALL USET (≠MEDIUM≠)
         CALL UPRINT (79.,-25.,≠TUA PLANT¬≠)
         IF (I.EQ.1) CALL UPRINT (79.,-35.,≠SIDE VIEW ON LINE 20¬≠)
         IF (I.EQ.2) CALL UPRINT (79.,-35.,≠SIDE VIEW ON LINE 21¬≠)
         IF (I.EQ.3) CALL UPRINT (79.,-35.,≠SIDE VIEW ON LINE 22¬≠)
         IF (I.EQ.4) CALL UPRINT (79.,-35.,≠SIDE VIEW ON LINE 23¬≠)
         IF (I.EQ.5) CALL UPRINT (79.,-35.,≠SIDE VIEW ON LINE 24¬≠)
         IF (I.EQ.6) CALL UPRINT (79.,-35.,≠SIDE VIEW ON LINE 25¬≠)
         IF (I.EQ.7) CALL UPRINT (79.,-35.,≠SIDE VIEW ON LINE 26¬≠)
         IF (I.EQ.8) CALL UPRINT (79.,-35.,≠SIDE VIEW ON LINE 27¬≠)
         IF (I.EQ.9) CALL UPRINT (79.,-35.,≠SIDE VIEW ON LINE 28¬≠)
         IF (M.EQ.1) CALL UPRINT (79.,-45.,≠FIRST MODE¬≠)
         IF (M.EQ.2) CALL UPRINT (79.,-45.,≠SECOND MODE¬≠)
         IF (M.EQ.3) CALL UPRINT (79.,-45.,≠THIRD MODE¬≠)
         IF (M.EQ.4) CALL UPRINT (79.,-45.,≠FOURTH MODE¬≠)
         IF (M.EQ.5) CALL UPRINT (79.,-45.,≠FIFTH MODE¬≠)
         IF (M.EQ.6) CALL UPRINT (79.,-45.,≠SIXTH MODE¬≠)
         IF (M.EQ.7) CALL UPRINT (79.,-45.,≠SEVENTH MODE¬≠)
         IF (M.EQ.8) CALL UPRINT (79.,-45.,≠EIGHTH MODE¬≠)
         IF (M.EQ.9) CALL UPRINT (79.,-45.,≠NINETH MODE¬≠)
         IF (M.EQ.10) CALL UPRINT (79.,-45.,≠TENTH MODE¬≠)
         IF (M.EQ.11) CALL UPRINT (79.,-45.,≠ELEVENTH MODE¬≠)
         IF (M.EQ.12) CALL UPRINT (79.,-45.,≠TWELVTH MODE¬≠)
         CALL UOUTLN
         CALL UERASE
  102 CONTINUE
      RETURN
C
      END
```

```
      SUBROUTINE PLOT3D
C
C     SUBROUTINE PLOT3D PLOTS THE STRUCTURE IN 3-D ORTHOGONAL VIEW.
C
      COMMON /ABC/ X(650),Y(650),Z(650),MI(2000),MJ(2000),M
      COMMON /BAC/ XD(650),YD(650),ZD(650)
C
C     DEFINE THE PLOTTING SURFACE.
C
      XMIN=-120.
      XMAX=540.
      YMIN=-90.
      YMAX=420.
      CALL UWINDO (XMIN,XMAX,YMIN,YMAX)
      DO 107 I=1,1290
         IP=MI(I)
         JP=MJ(I)
         XI=X(IP)
         YI=Y(IP)
         ZI=Z(IP)
         XJ=X(JP)
         YJ=Y(JP)
         ZJ=Z(JP)
C
C     SORT OUT THE MEMBERS WHICH SHOW IN 3-D ORTHOGONAL VIEW.
C
         IF (YI.NE.0.) GO TO 101
         IF (YJ.NE.0.) GO TO 101
```

```
      GO TO 106
101   IF (XI.NE.320.) GO TO 102
      IF (XJ.NE.320.) GO TO 102
      GO TO 106
102   IF (ZI.NE.238.) GO TO 103
      IF (ZJ.NE.238.) GO TO 103
      GO TO 106
103   IF (ZI.NE.169.) GO TO 105
      IF (ZJ.NE.169.) GO TO 105
      IF (XI.GT.80.) GO TO 104
      IF (XJ.GT.80.) GO TO 105
      GO TO 106
104   IF (XI.LT.280.) GO TO 105
      IF (XJ.LT.280.) GO TO 105
      GO TO 106
105   IF (ZI.LT.169.) GO TO 107
      IF (ZJ.LT.169.) GO TO 107
      IF (XI.NE.280.) GO TO 107
      IF (XJ.NE.280.) GO TO 107
106   CONTINUE
      IF ((I.EQ.402).OR.(I.EQ.408).OR.(I.EQ.417).OR.(I.EQ.452).OR.(I.
     1EQ.440).OR.(I.EQ.454).OR.(I.EQ.455).OR.(I.EQ.456).OR.(I.EQ.457)
     2.OR.(I.EQ.425).OR.(I.EQ.431).OR.(I.EQ.436).OR.(I.EQ.441).OR.(I.
     3EQ.446)) GO TO 107
C
C     EVALUATE THE COORDINATES OF THE PROJECTION OF MEMBERS IN 3-D
C     ORTHOGONAL VIEW.
C
      XID=XD(IP)
      YID=YD(IP)
      ZID=ZD(IP)
      XXID=XID+(1.-0.1*YID/158.)*YID*COS(45.)
      YYID=YID+(1.-0.1*YID/158.)*YID*SIN(45.)
      XJD=XD(JP)
      YJD=YD(JP)
      ZJD=ZD(JP)
      XXJD=XJD+(1.-0.1*YJD/158.)*YJD*COS(45.)
      YYJD=ZJD+(1.-0.1*YJD/158.)*YJD*SIN(45.)
C
C     PLOT THE MEMBERS
C
      CALL USET (≠LINES≠)
      CALL UMOVE (XXID,YYID)
      CALL UPEN (XXJD,YYJD)
  107 CONTINUE
C
C     PRINT THE LABEL ON THE PLOT.
C
      CALL USET (≠ACENTERING≠)
      CALL USET (≠MEDIUM≠)
      CALL UPRINT (210.,-30.,≠TVA PLANT¬≠)
      IF (M.EQ.1) CALL UPRINT (210.,-45.,≠FIRST MODE¬≠)
      IF (M.EQ.2) CALL UPRINT (210.,-45.,≠SECOND MODE¬≠)
      IF (M.EQ.3) CALL UPRINT (210.,-45.,≠THIRD MODE¬≠)
      IF (M.EQ.4) CALL UPRINT (210.,-45.,≠FOURTH MODE¬≠)
      IF (M.EQ.5) CALL UPRINT (210.,-45.,≠FIFTH MODE¬≠)
      IF (M.EQ.6) CALL UPRINT (210.,-45.,≠SIXTH MODE¬≠)
      IF (M.EQ.7) CALL UPRINT (210.,-45.,≠SEVENTH MODE¬≠)
      IF (M.EQ.8) CALL UPRINT (210.,-45.,≠EIGHTH MODE¬≠)
      IF (M.EQ.9) CALL UPRINT (210.,-45.,≠NINETH MODE¬≠)
      IF (M.EQ.10) CALL UPRINT (210.,-45.,≠TENTH MODE¬≠)
      IF (M.EQ.11) CALL UPRINT (210.,-45.,≠ELEVENTH MODE¬≠)
      IF (M.EQ.12) CALL UPRINT (210.,-45.,≠TWELVTH MODE¬≠)
      CALL UOUTLN
      CALL UERASE
      RETURN
C
      END
```

```
      SUBROUTINE BOILER
C
C      SUBROUTINE BOILER PLOTS THE 3-D ORTHOGONAL VIEW OF THE BOILER.
C
      COMMON /ABC/ X(650),Y(650),Z(650),MI(2000),MJ(2000),M
      COMMON /BAC/ XD(650),YD(650),ZD(650)
C
C     COORDINATES OF BOILER NODES ARE EVALUATED WITH RESPECT TO
C     NODAL POINT NO. 284.
C
      X1=XD(284)-X(284)
      Y1=YD(284)-Y(284)
      Z1=ZD(284)-Z(284)
      DO 101 I=1,611
         XD(I)=XD(I)-X1
         YD(I)=YD(I)-Y1
  101 ZD(I)=ZD(I)-Z1
C
C     DEFINE THE PLOTTING SURFACE.
C
      XMIN=48.
      XMAX=378.
      YMIN=65.
      YMAX=320.
      CALL UWINDO (XMIN,XMAX,YMIN,YMAX)
      DO 103 I=1,1290
         IP=MI(I)
         JP=MJ(I)
         XI=X(IP)
         YI=Y(IP)
         ZI=Z(IP)
C
C      SORT OUT THE MEMBERS WHICH SHOW IN 3-D ORTHOGONAL VIEW.
C
         IF ((XI.EQ.130.33).OR.(XJ.EQ.130.33)) GO TO 102
         IF ((XI.EQ.226.).OR.(XJ.EQ.226.)) GO TO 102
         GO TO 103
  102    IF ((XI.LT.130.33).OR.(XJ.LT.130.33)) GO TO 103
         IF ((XI.GT.226.).OR.(XJ.GT.226.)) GO TO 103
         IF ((YI.LT.3.5).OR.(YJ.LT.3.5)) GO TO 103
         IF ((ZI.EQ.238.).AND.(ZJ.EQ.238.)) GO TO 103
         IF ((YI.GT.115.).OR.(YJ.GT.115.)) GO TO 103
         XXI=XI+0.707*YI
         YYI=ZI+0.707*YI
         XJ=X(JP)
         YJ=Y(JP)
         ZJ=Z(JP)
         XXJ=XJ+0.707*YJ
         YYJ=ZJ+0.707*YJ
         XID=XD(IP)
         YID=YD(IP)
         ZID=ZD(IP)
         XXID=XID+0.707*YID
         YYID=ZID+0.707*YID
         XJD=XD(JP)
         YJD=YD(JP)
         ZJD=ZD(JP)
         XXJD=XJD+0.707*YJD
         YYJD=ZJD+0.707*YJD
C
C     PLOT ORIGONAL SHAPE OF THE MEMBER BY DOTTED LINE.
C
         CALL USET (≠DASHED≠)
         CALL UMOVE (XXID,YYID)
         CALL UPEN (XXJD,YYJD)
C
C     PLOT DISPLACED SHAPE OF THE MEMBER BY SOLID LINE.
C
         CALL USET (≠LINES≠)
         CALL UMOVE (XXI,YYI)
```

```
         CALL UPEN (XXJ,YYJ)
  103 CONTINUE
C
C     PRINT THE LABEL ON THE PLOT.
C
      CALL USET (≠ACENTERING≠)
      CALL USET (≠MEDIUM≠)
      CALL UPRINT (213.,95.,≠TVA BOILER¬≠)
      IF (M.EQ.1) CALL UPRINT (213.,80.,≠FIRST MODE¬≠)
      IF (M.EQ.2) CALL UPRINT (213.,80.,≠SECOND MODE¬≠)
      IF (M.EQ.3) CALL UPRINT (213.,80.,≠THIRD MODE¬≠)
      IF (M.EQ.4) CALL UPRINT (213.,80.,≠FOURTH MODE¬≠)
      IF (M.EQ.5) CALL UPRINT (213.,80.,≠FIFTH MODE¬≠)
      IF (M.EQ.6) CALL UPRINT (213.,80.,≠SIXTH MODE¬≠)
      IF (M.EQ.7) CALL UPRINT (213.,80.,≠SEVENTH MODE¬≠)
      IF (M.EQ.8) CALL UPRINT (213.,80.,≠EIGHTH MODE¬≠)
      IF (M.EQ.9) CALL UPRINT (213.,80.,≠NINETH MODE¬≠)
      IF (M.EQ.10) CALL UPRINT (213.,80.,≠TENTH MODE¬≠)
      IF (M.EQ.11) CALL UPRINT (213.,80.,≠ELEVENTH MODE¬≠)
      IF (M.EQ.12) CALL UPRINT (213.,80.,≠TWELVTH MODE¬≠)
      CALL UOUTLN
      CALL UERASE
      RETURN
C
      END
```